



Enamides and ynamides to generate molecular complexity

Yongxiang Zheng

► To cite this version:

Yongxiang Zheng. Enamides and ynamides to generate molecular complexity. Organic chemistry. Université de Strasbourg, 2021. English. NNT: 2021STRAF057 . tel-04271877

HAL Id: tel-04271877

<https://theses.hal.science/tel-04271877>

Submitted on 6 Nov 2023

HAL is a multi-disciplinary open access archive for the deposit and dissemination of scientific research documents, whether they are published or not. The documents may come from teaching and research institutions in France or abroad, or from public or private research centers.

L'archive ouverte pluridisciplinaire **HAL**, est destinée au dépôt et à la diffusion de documents scientifiques de niveau recherche, publiés ou non, émanant des établissements d'enseignement et de recherche français ou étrangers, des laboratoires publics ou privés.

ÉCOLE DOCTORALE DES SCIENCES CHIMIQUES

UMR 7177

THÈSE présentée par :

Yongxiang ZHENG

soutenue le : **28 Septembre 2021**

pour obtenir le grade de : **Docteur de l'université de Strasbourg**

Discipline/ Spécialité : Chimie Organique

**Des énamides et des ynamides pour la
synthèse
d'hétérocycles fonctionnalisés**

THÈSE dirigée par :

Madame MIESCH Laurence

Docteur, Université de Strasbourg

RAPPORTEURS :

Madame Fanny Roussi

Docteur, Université Paris-Saclay

Monsieur Erwan Poupon

Professeur, Université Paris-Saclay

AUTRES MEMBRES DU JURY :

Madame Emilie Moulin

Docteur, Université de Strasbourg

ACKNOWLEDGEMENT FOR THE THESIS	5
ABBREVIATIONS	6
GENERAL INTRODUCTION.....	8
I. CHAPTER 1 TERTIARY ENAMIDE-PROMOTED DIASTEROSELECTIVE DOMINO/<i>N</i>-ACYLIUM ION TRAPPING AND NAZAROV CYCLIZATION	10
I.1. I. Reactivity of tertiary enamides	10
I.1.1. Enamides - Definition	10
I.1.2. Tertiary enamide nucleophilic addition reactions	11
I.2. The Nazarov cyclization	31
I.2.1. Introduction.....	31
I.2.2. Directed Nazarov reactions	33
I.2.3. Polarized Nazarov cyclizations:	37
I.2.4. Asymmetric Nazarov reactions.....	39
I.2.5. Application of the Nazarov reaction in the total synthesis of natural products	44
I.2.6. Recent trends for the Nazarov reaction	48
I.2.7. Tertiary enamide/enamine promoted Nazarov cyclizations	49
I.3. Tertiary Enamide-Promoted Diastereoselective Domino: <i>N</i>-Acyliminium Ion Trapping and Nazarov Cyclization.....	55
I.3.1. The aim of our project	55
I.3.2. Previous work	56
I.3.3. New route to the synthesis cyclopenta-diazepine motifs	57
I.3.4. Mechanistic studies of the domino: <i>N</i> -acyliminium ion trapping and Nazarov cyclization	73
I.4. Conclusion	78
II. CHAPTER 2 SYNTHESIS OF CF₂H-SUBSTITUTED 2-AMIDOFURANS VIA COPPER-CATALYZED ADDITION OF α-DIFLUORINATED-DIAZOACETONE TO YNAMIDES.....	79
II.1. Introduction.....	79
II.2. Synthesis of amino-/amidofurans.....	79
II.2.1. By using nitriles	80
II.2.2. Three-component coupling of isocyanides, alkynes, and carbonyl compounds	81
II.2.3. Synthesis of 2-aminofurans from 2-haloketones	83
II.2.4. Amino-/amidofuran synthesis using enamines	84
II.2.5. Synthesis of amidofurans using ynamides	85
II.2.6. Synthesis of furans via homoallenyl amides	88

II.2.7. Copper-catalyzed direct amidation of furans	90
II.3. Synthesis of CF₂H-substituted furans	90
II.3.1. Difluorination of furans via CF ₂ CO ₂ Et functionalization	90
II.3.2. Difluoromethylation of aryl iodides.....	91
II.3.3. Palladium-catalyzed difluoromethylation of aryl boronic acids.....	91
II.3.4. Direct C-H difluoromethylation <i>via</i> organic photoredox catalysis	92
II.4. Synthesis of CF₂H-Substituted 2-Amidofurans via Copper-Catalyzed Addition of α-Difluorinated Diazoacetone to Ynamides.....	93
II.4.1. Previous results	93
II.4.2. Addition of diazo-carbonyl compounds to ynamides.....	94
II.4.3. Synthesis of CF ₂ H-substituted 2-amidofurans.....	98
II.4.4. Difluorinated amido-furans as platforms to synthesize more complex heterocycles.....	105
II.4.5. Mechanistic studies.....	108
II.5. Conclusion	110
II.6. Perspectives.....	111
III. CHAPTER 3 COPPER-CATALYZED SYNTHESIS OF TERMINAL VS. FLUORINE SUBSTITUTED N-ALLENAMIDES VIA ADDITION OF DIAZO-COMPOUNDS TO TERMINAL YNAMIDES.....	112
III.1. Introduction : <i>N</i>-allenamines vs <i>N</i>-Allenamides	112
III.2. Synthesis of <i>N</i>-allenamides.....	113
III.3. Copper-catalyzed synthesis of terminal vs. fluorine substituted <i>N</i>-allenamides <i>via</i> addition of diazo-compounds to terminal ynamides.....	117
III.3.1. Previous work	117
III.3.2. Objective	117
III.3.3. State of the art : Addition of TMS-diazomethane to alkynes	117
III.3.4. Copper-catalyzed addition of TMS-diazomethane to terminal ynamides.....	118
III.3.5. Batiste Moegle's contribution	118
III.4. Synthesis of fluorinated <i>N</i>-allenamides	120
III.4.1. Blanchard's work	120
III.4.2. Our results	121
III.5. Plausible reaction mechanism	123
III.6. Conclusion	123
IV. GENERAL CONCLUSION.....	125
Tertiary enamide-promoted diastereoselective domino/ <i>N</i>-acyliminium ion trapping and Nazarov cyclization.	125

Synthesis of CF₂H-substituted 2-amidofurans <i>via</i> copper-catalyzed addition of a-difluorinated-diazoacetone to ynamides.....	125
Copper-catalyzed synthesis of terminal vs. fluorine substituted <i>N</i>-allenamides <i>via</i> addition of diazo-compounds to terminal ynamides	126
V. RÉSUMÉ DE THÈSE EN FRANÇAIS.....	127
V.1. Introduction	127
V.1.1. Les énamides tertiaires	127
V.1.2. Les ynamides	129
V.2. Résultats et discussions.....	130
V.2.1. Réaction DOMINO au départ d'énamides tertiaires substitués par un ion <i>N</i> -acyliminium	130
V.2.2. Synthèse d'amido-furanes difluorés par addition de difluorodiazoacétone sur des ynamides vrais	133
V.2.3. Synthèse cupro-catalysées de <i>N</i> -allèniamides terminaux ou fonctionnalisés par addition de composés diazo sur des ynamides terminaux.....	135
V.3. Conclusion Générale.....	137
V.4. Références	138
VI. EXPERIMENTAL PART	139

ACKNOWLEDGEMENT FOR THE THESIS

Time flies, three years of happy time in the SOPhy group pass by. I am grateful to my motherland-China and China Scholarship Council for providing me with financial support.

Firstly, I am honored to study under the supervision of Dr. Laurence Miesch during my PhD at the University of Strasbourg. Thanks to my tutor for her helping in the experiment and the training of the presentation. Her passion for research and patience with students inspired me.

Secondly, I would like to thanks the jury, Dr. Fanny Roussi, University of Paris-Saclay, Prof. Erwan Poupon, University of Paris-Saclay and Dr. Emilie Moulin, University of Strasbourg. Thank you for reviewing my thesis and defense

Thanks to the members of my lab.

Dr. Philippe Geoffroy, Thanks for your helping in the experiments and please stop the "17euro 50 cents" charge.

Dr. Lucile Andna, Thanks for your helping on the experiment notebook and supporting information.

Dr. Santanu Ghosh, Thanks for the interesting sharing about the reactions and Indian culture.

Maxime Hourtoule, Now the bar is open, after one day of experiment, we can meet in the bar.

Baptiste Moegle, Miss the afternoons of smoking with you.

Clément Gommenginger, The new PhD of the SOPhy group, and an old acquaintance of our group, my Two fume hoods" now they are yours" will bring you good luck. I will remember those moments when I discussed the mechanism with you.

Pauline Lebrun, Quentin Buck, Miss the time with you.

Thanks to the test teams, The NMR team, Lionel Allouche, Maurice Coppe, Bruno Vincent. The Mass team, Hélène Nierengarten Stéphanie Cou as well as Nathalie Gruber for the X-ray structures.

Thanks to my friends from the University of Strasbourg, Wenzhi Wang, Haijun Peng, Jing Zhang, Yiming Liang, Jing Luo, Jing Sun, Jing Wang, Yulin Zhou, Chuan Gao, Yaowei Hu, Ning Jiang and so on, my unforgettable time in Strasbourg. Also, Thanks to my friends and teachers in Bordeaux, Hongwei Li, Fangyu Fu, Qi Wang, Yun Wang, Yue He, Minlei Jing, Meiyu Jia and so on.

Finally, Thanks my parents upbringing. To my wife, thank you for your care and staying with me for so long, Even though I'm thousands of miles away, I can still feel your deeply love.

I won't forget that happiest moment of my life when we were together!

Best regards

Merci, a tous.

ABBREVIATIONS

% mol : molar percentage
°C : degrees Celsius
1-10 phen. : 1-10 phenanthroline
Å : Ångström
Ac : acetyl
APC : chiral phosphoric acid
aq : aqueous
atm : atmosphere
Bn : benzyl
Boc : *tert*-butoxycarbonyl
BTAC : benzyltrimethylammonium chloride
C : carbon
c. : concentration
cat. : catalyst
Cbz : carboxybenzoyl
cHex, Cy : cyclohexyl
cPent : cyclopentyl
cPr : cyclopropyl
CV : cyclic voltammetry
DABCO : 1,4-diazabicyclo[2.2.2]octane
DBU : 1,8-Diazabicyclo[5.4.0]undec-7-ene
DCC : *N,N*-dicyclohexylcarbodiimide
DCE : 1,2-dichloroethane
DDQ : 2,3-Dichloro-5,6-dicyano-1,4-benzoquinone
DFT : Density Functional Theory
DIBAL : diisobutylaluminum hydride
DMAP : 4-dimethylaminopyridine
DME : dimethoxyethane
DMF : *N,N*-dimethylformamide
DMSO : dimethyl sulfoxide
d : days
dr : diastereomeric ratio
DTBP : di-*tert*-butyl peroxide
E⁺ : electrophile
ee : enantiomeric excess
eq. : equivalent(s)
et al. : and collaborators
Et : ethyl
EWG : electron withdrawing group
h : hour(s)
HFIP : 1,1,1,3,3-Hexafluoro-2-propanol
HMPA : hexamethylphosphoramide
iPr : isopropyl
IMDAF : Intramolecular Diels–Alder Cycloaddition of Furans
LDA : lithium diisopropylamide

LiHMDS : lithium bis (trimethylsilyl) amide, lithium hexamethyldisilazane
mol : molar
Me : methyl
min : minute(s)
MS : molecular sieve
Ms : mesyl, methane sulfonyl
NAI : *N*-acyliminium ion
NBS : *N*-bromosuccinimide
nBu : *n*-butyl
NFSI : *N*-Fluorobenzenesulfonimide
NIS : *N*-iodosuccinimide
nm : nanometer(s)
NME : *N*-methylephedrine
NMM : *N*-methylmorpholine
nOct : *n*-octyl
npent : *n*-pentyl
nPr : *n*-propyl
Ns : nosyl, nitrobenzene sulfonyl
Nu⁻ : nucleophile
p-ABSA : 4-Acetamidobenzenesulfonyl azide
Ph : phenyl
PMB : para-methoxybenzyl
PMP : para-methoxyphenyl
p-TsOH : *p*-Toluenesulfonic Acid
NMR : nuclear magnetic resonance
SEAr : Aromatic electrophilic substitution reaction
rt : ambient temperature
T : temperature
TBA : tetrabutylammonium
TBAF : Tetrabutylammonium fluoride
TBS : TBDMS, *tert*- butyldimethylsilyl
t-Bu : *tert*-butyl
TEMPO : (2,2,6,6-tetramethylpiperidin-1-yl) oxyl
tet : tetragonal
Tf : triflate, trifluoromethane sulfonate
TFA : trifluoroacetic acid
TFP : tris(2-furyl)phosphine
THF : tetrahydrofuran
TIPS : triisopropylsilyl
TMG : tetramethylguanidine
TMS : trimethylsilyl
trig: trigonal
Triton B : tetrabutylammonium hydroxide
Ts : tosyl, toluene sulfonyl

GENERAL INTRODUCTION

One of the main tasks of the organic chemist is the synthesis of new materials and compounds. Amongst all compounds and materials one can imagine, organic molecules have outstanding position as all life is build upon and around organic molecules.

Organic molecules are used in nature for various functions in all forms of life. These molecules, often highly bioactive, can be isolated only in small amounts from nature in most cases. Therefore, their synthesis as well as their analogues are of great importance in order to understand their effects and find possible applications.

In particular, polyheterocyclic frameworks are of great interest. On that account, numberless laboratories worldwide work on the total synthesis of such compounds and on the development of new methodologies needed for the construction of the building blocks involved.

Based on this precedence, numerous laboratories worldwide are ever and anon attracted to develop innovative methodologies to achieve this goal.

In this context, our laboratory is interested to take advantage of the reactivity of ynamides, and tertiary enamides as privileged intermediates for the construction of nitrogen containing frameworks.

The objectiv of my work during my PhD time consisted in further explore the reactivity of ynamides and tertiary enamides.

We first set our focus on the reactivity of tertiary enamides towards the construction of polyheterocyclic frameworks. Within the laboratory, it has been shown that in acidic medium tertiary enamide add to the *N*-acyliminium species to form diazepine drug substructures. Various imides, different spacer lengths, as well as different substituents on the ynamide were tolerated. In the first chapter of my PhD thesis, to extend the chemical space of this concept, special attention was drawn on a domino reaction involving *N*-acyliminium ion trapping followed by a Nazarov cyclization.

In the second part of my work, as ynamides constitute a selected field in our team, we became interested in the reactivity of those substrates towards diazo-compounds. We prepared a new fluorinated diazo-compound and achieved the synthesis of amido-difluorinated furans in this way.

The unique reactivity of ynamides towards diazo-compounds brought us to investigate a new area in our team concerning the chemistry of *N*-allenamides. Using the requisite diazo-compound, we developed not only a new synthesis of terminal *N*-allenamides but also a new access to fluorinated *N*-allenamides.

All our results will be described in the following three chapters:

-Chapter 1 : Tertiary enamide promoted diastereoselective domino : *N*-acyliminium ion trapping and Nazarov Cyclization.

-Chapter 2 : Direct synthesis of CF₂H-substituted 2-amido-furans via copper-catalyzed addition of difluorinated diazoactenone to ynamides.

- Chapter 3 : Copper-catalyzed synthesis of terminal vs. fluorine substituted *N*-allenamides via addition of diazo-compounds to terminal ynamides.

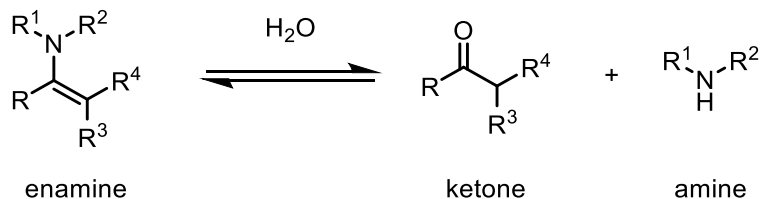
I. CHAPTER 1 TERTIARY ENAMIDE-PROMOTED DIASTEREOSELECTIVE DOMINO/*N*-ACYLIMINIUM ION TRAPPING AND NAZAROV CYCLIZATION

In this first chapter, tertiary enamides will be defined, and a focus will be placed on their reactivity as nucleophiles. The Nazarov cyclization will subsequently be presented using suitable examples, highlighting different concepts that characterize this reaction by showcasing recent trends and current advances. This overview is by no means exhaustive, and only highlights a limited number of representative papers. A description of the project that places the research contextually within field and the state-of-the-art will also be presented.

I.1. I. Reactivity of tertiary enamides

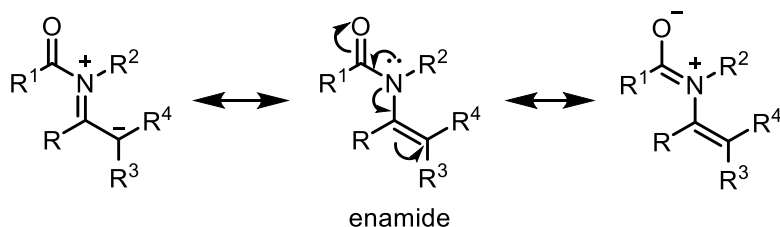
I.1.1. Enamides - Definition

Since their description by Stork in 1953, enamines characterized by a double bond substituted by an amine have widely been used for the formation of C-C bonds.¹ The delocalization of the nitrogen lone pair through the double bond makes enamines more electron-rich than simple enol ethers or silylated enols, giving them their enaminic, nucleophilic reactivity.² However, enamines are unstable because they are highly sensitive to hydrolysis and therefore difficult to handle, isolate and store



Scheme 1: Enamine hydrolysis

To increase the stability of these enamines, the nitrogen atom can be substituted by an electron-withdrawing group, such as is found in enamides. In this case, the nitrogen lone pair can delocalize through the electron-withdrawing group in addition to the double bond (**Scheme 2**). Enamides are therefore more stable than enamines, but have reduced enamidic reactivity compared to enamines.



Scheme 2: Schematic representation of the mesomeric forms of enamides

¹ G. Stork, S. R. Dowd, *J. Am. Chem. Soc.* **1963**, *85*, 2178–2180.

² B. Kempf, N. Hampel, A. R. Oftal, H. Mayr, *Chem. Eur. J.* **2003**, *9*, 2209–2218.

Depending on the nature of the electron-withdrawing group, three main classes of enamides can be distinguished (**Figure 1**). Enamides where the double bond is substituted by an amide group, those wherein the electron-withdrawing group is an ester, and finally enesulfonamides carrying a sulfonyl group at the nitrogen atom.

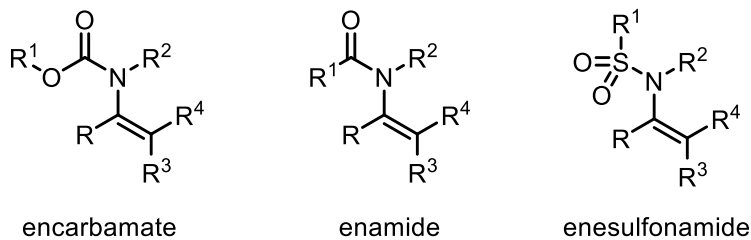


Figure 1. Schematic representation of the different classes of enamides

In this chapter, the focus will be exclusively on tertiary enamides, i.e., enamides trisubstituted on the nitrogen atom as opposed to secondary enamides, which are disubstituted on the nitrogen atom.³ Tertiary enamides have long been considered “inert” species and have seen growing interest since early research by Wang.⁴

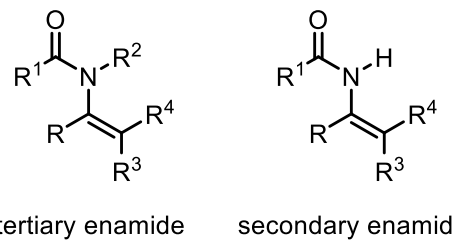


Figure 2. Schematic representation of secondary and tertiary enamides

Over the last years, tertiary enamides have emerged as powerful synthetic intermediates, and a diversified range of new reactions has been developed for the synthesis of nitrogen-containing compounds.⁵ The enaminic activity of tertiary enamides will be outlined in the next section.

I.1.2. Tertiary enamide nucleophilic addition reactions

I.1.2.1. Nucleophilic addition of tertiary enamides to epoxides

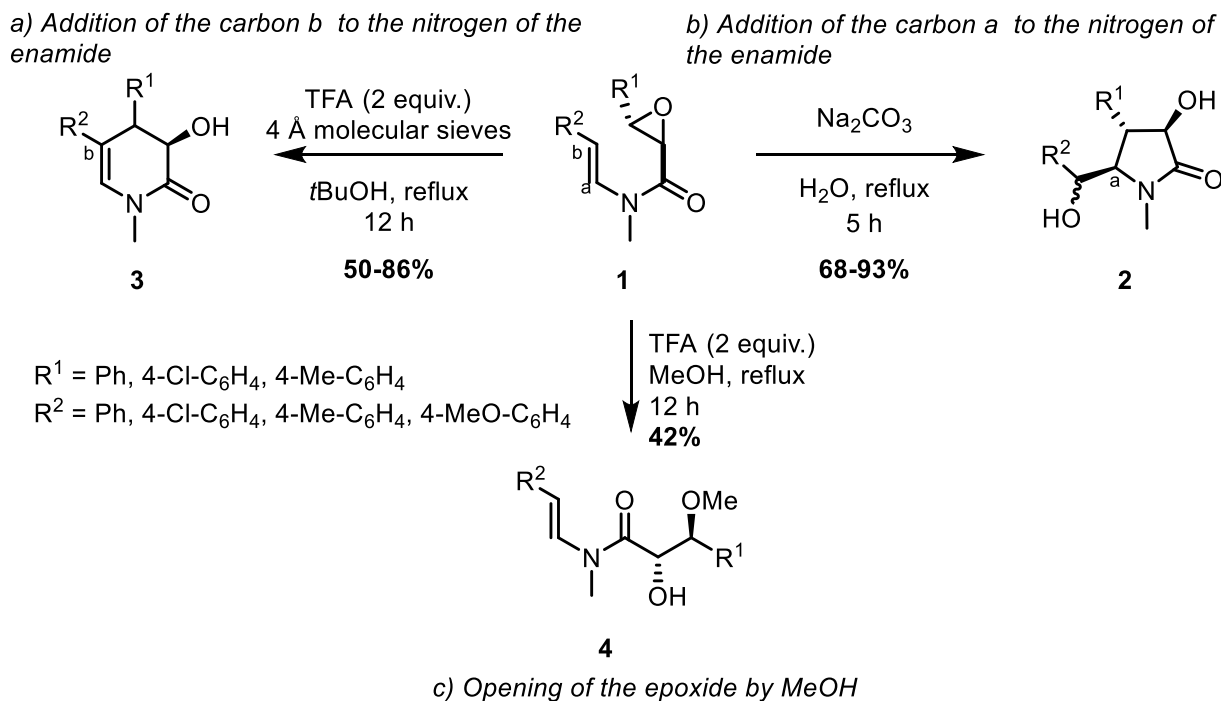
Wang *et al.* began their study of the reactivity of tertiary enamides as nucleophiles on epoxides. Thus, starting from tertiary enamides **1** bearing an epoxide, the neoclausenamides **2** can be obtained by 5-*endo*-tet intramolecular reaction in aqueous basic conditions

³ R. Matsubara, S. Kobayashi, *Acc. Chem. Res.* **2008**, *41*, 292–301. D. R. Carbery, *Org. Biomol. Chem.* **2008**, *6*, 3455. X. Cai, M. Yang, H. Guo, *Curr. Org. Synth.* **2019**, *16*, 70–97.

⁴ M.-X. Wang, *Chem. Commun.* **2015**, *51*, 6039–6049.

⁵ X. Cai, M. Yang, H. Guo, *Curr. Org. Synth.* **2019**, *16*, 70–97. F. Beltran, L. Miesch, *Synthesis* **2020**, *52*, A–O

(**Scheme 3**).⁶ However, when the reaction was carried out in acidic medium in methanol, the latter added to the epoxide to afford the open compound **4**.⁷ Furthermore, treatment of these enamides **1** in *tert*-butanol in the presence of trifluoroacetic acid led to the formation of homoclausenamides **3** with good yields.⁸



Scheme 3: Reactivity of tertiary enamides on epoxides

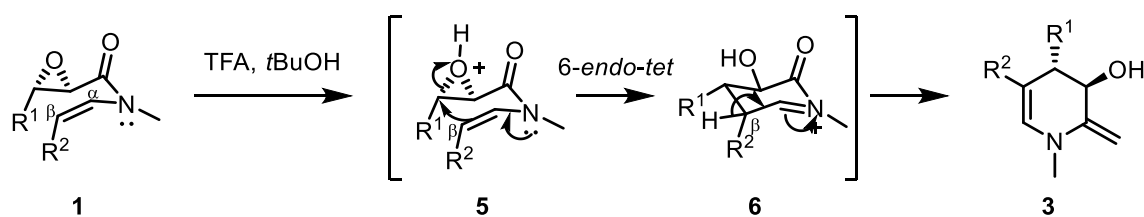
The formation of homoclausenamides **3** can be explained by the activation of epoxide **1** by trifluoroacetic acid (compound **5**) followed by a 6-*endo-tet* addition of the enamide to the epoxide (**Scheme 4**). A simple deprotonation of intermediate **6** leads to homoclausenamides **3**. It should be noted that *tert*-butanol having a weaker nucleophilic character than methanol, must be used as solvent to prevent opening of the epoxide by nucleophilic addition of the solvent to the epoxide as observed with methanol to form compound **4**.

⁶ L. Yang, Q.-Y. Zheng, D.-X. Wang, Z.-T. Huang, M.-X. Wang, *Org. Lett.* **2008**, *10*, 2461–2464.

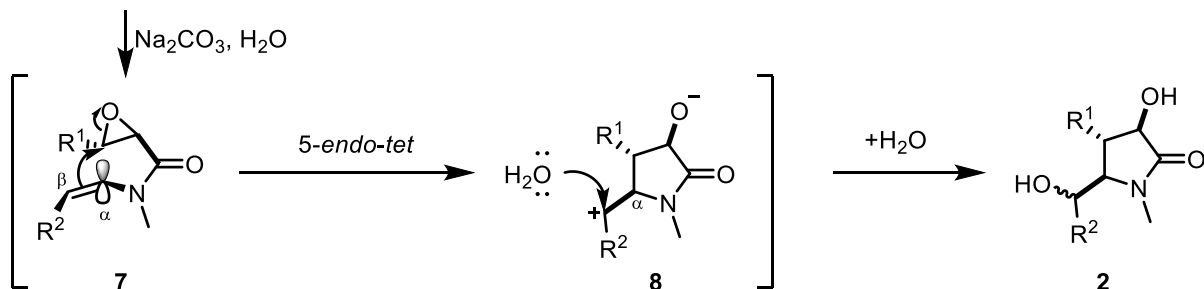
⁷ L. Yang, D.-X. Wang, Q.-Y. Zheng, J. Pan, Z.-T. Huang, M.-X. Wang, *Org. Biomol. Chem.* **2009**, *7*, 2628–2634.

⁸ L. Yang, S. Tong, D.-X. Wang, Z.-T. Huang, J. Zhu, M.-X. Wang, *Synlett* **2011**, *2011*, 927–930.

a) Addition of the β -carbon of the Enamide



b) Addition of the α -carbon of the Enamide



Scheme 4: Mechanism of the synthesis of neoclausenamides **2** and homoclausenamides **3**

The key step for the formation of neoclausenamides **2** in water (**Scheme 4**) is a 5-*endo*-tet cyclization of the enamide on the epoxide. The double bond would be added to the epoxide without assistance from the nitrogen lone pair according to the authors. In water, the initial enamide **1** would adopt a conformation in which the plane of the amide would be perpendicular to the plane of the double bond (conformation **7**), making it impossible to relocate the nitrogen lone pair. Thus, the p orbitals of the carbon α to the nitrogen are located near the benzylic carbon of the epoxide. The carbocation of zwitterion **8** is then trapped by a molecule of water to form the neoclausenamides **2**.

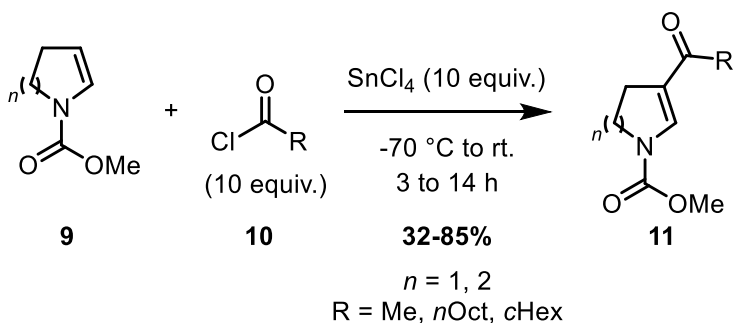
I.1.2.2. Nucleophilic addition of tertiary enamides to carbonyl compounds

Tertiary enamides are also prone to add to a carbonyl group provided the latter are activated by a Lewis acid.

a. Nucleophilic addition of tertiary enamides to acyl chlorides

In 1982, Aoki *et al.* have shown that cyclic tertiary enecarbamates **9** add to acyl chlorides **10** in the presence of tin tetrachloride to form dihydropyrroles **11** (**Scheme 5**).⁹ Activation of acyl chlorides facilitates the nucleophilic addition of enamides. Alkyl acyl chlorides and cyclic acyl chlorides are tolerated in this case.

⁹ T. Shono, Y. Matsumura, K. Tsubata, Y. Sugihara, S. Yamane, T. Kanazawa, T. Aoki, *J. Am. Chem. Soc.* **1982**, *104*, 6697–6703.

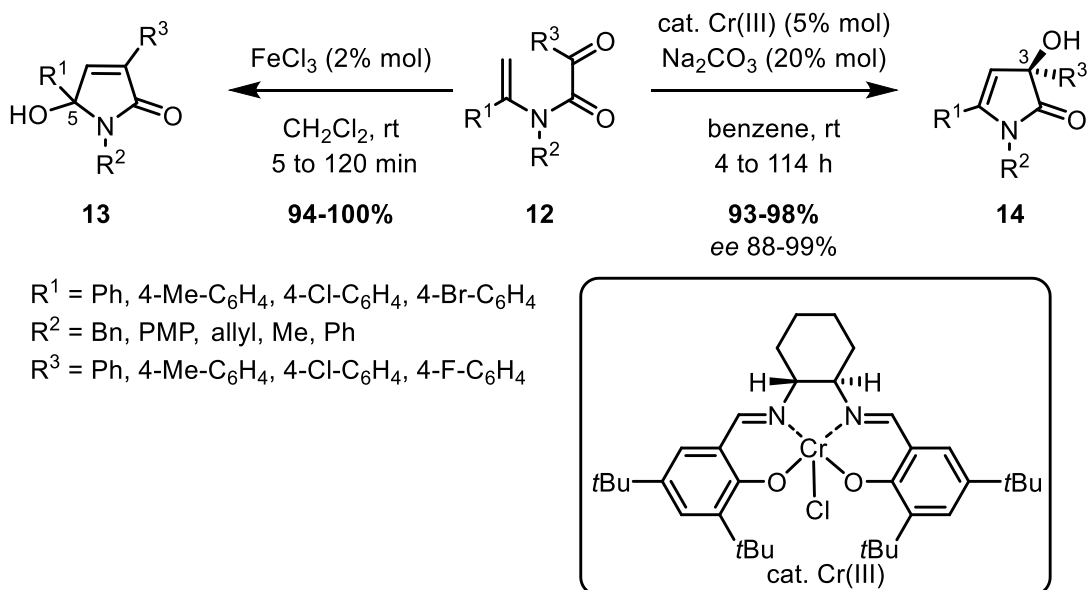


Scheme 5: Reactivity of tertiary enamides on acyl chlorides

b. Nucleophilic addition of tertiary enamides to ketones

Synthesis of dihydropyrroles

Wang *et al.* also studied the reactivity of tertiary enamides as nucleophiles toward ketones. By using a catalytic amount of iron trichloride in dichloromethane at room temperature, the tertiary enamides **12** unsubstituted at the β position led to 5-hydroxypyrrroles **13** (**Scheme 6**).¹⁰ However, starting from the same enamides **12**, in the presence of a chromium(III) metallic complex and sodium carbonate, the 3-hydroxypyrrroles **14** were obtained with yields ranging from 93 to 98% with enantiomeric excesses from 88 to 99%.¹¹ The reaction time is dependent on the electronegativity of the substituents of the aryl groups, but range from 4 to 114 hours for total conversion of the starting enamide **12**.



Scheme 6: Reactivity of tertiary enamides with ketones

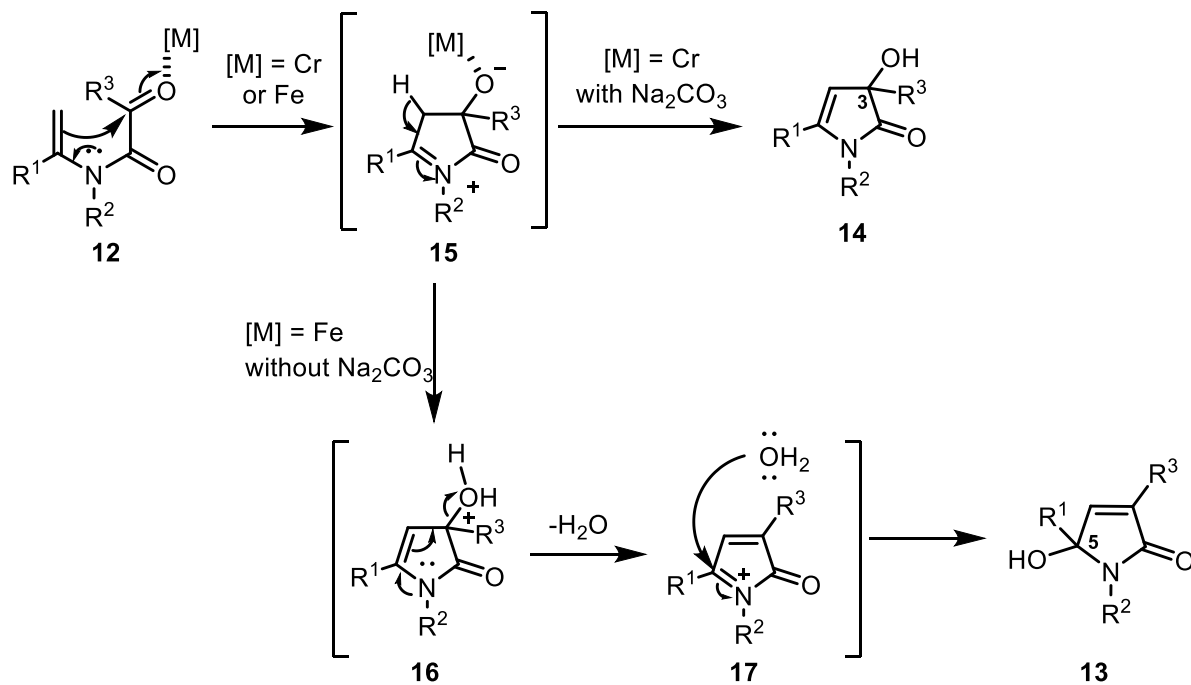
For the formation of hydroxylated pyrroles in position 3, the carbonyl group is activated by the metal complex, allowing the 5-exo-*dig* addition of the tertiary enamide to the activated carbonyl group, providing the 5-membered ring **15** (**Scheme 7**). A deprotonation provides the 3-hydroxypyrrroles **14**. To explain the formation of the hydroxylated pyrroles at position 5

¹⁰ L. Yang, C.-H. Lei, D.-X. Wang, Z.-T. Huang, M.-X. Wang, *Org. Lett.* **2010**, *12*, 3918–3921.

¹¹ L. Yang, D.-X. Wang, Z.-T. Huang, M.-X. Wang, *J. Am. Chem. Soc.* **2009**, *131*, 10390–10391.

(compound **13**), the cyclic intermediate **15** would also be formed, and the deprotonation would also take place. However, without sodium carbonate in the medium to trap the released proton, protonation of the alcohol in position 3 would take place (compound **16**). Tertiary enamide assisted dehydration would provide pyrrolium **17**. Finally, the addition of water to pyrrolium **17** would afford the 5-hydroxypyrrroles **13**.

The use of Na_2CO_3 , therefore makes it possible to trap the proton generated during the formation of **14**, inhibiting dehydration and addition of water to position 5 of the cycle.

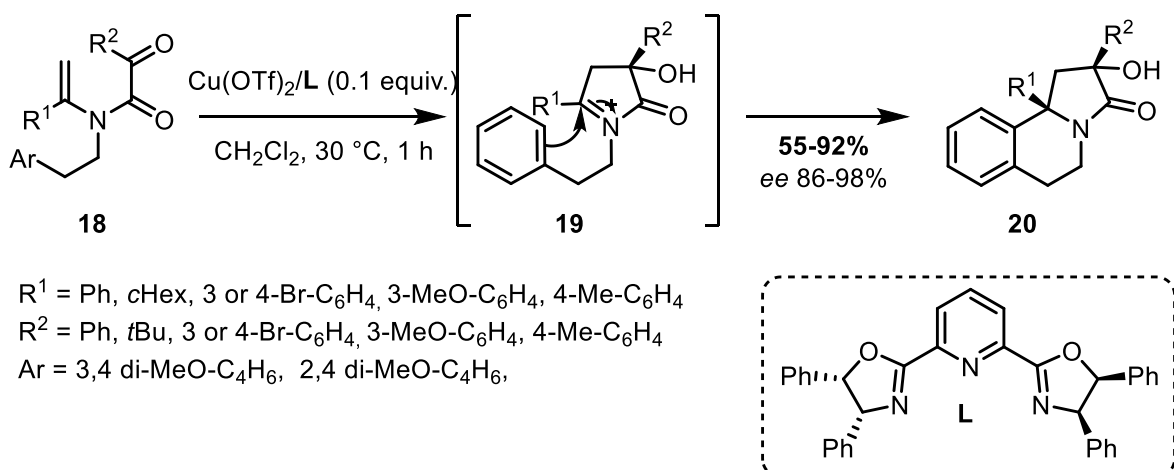


Scheme 7: Mechanism of formation of hydroxypyrrroles

Tandem reaction of tertiary enamides with ketones and subsequent $S_{\text{E}}\text{Ar}$

Finally, these authors subsequently reported a tandem reaction starting with an addition of tertiary enamide on an activated carbonyl group followed by an electrophilic aromatic substitution ($S_{\text{E}}\text{Ar}$) (**Scheme 8**).¹² The cyclic compounds were thus obtained with good yields and also very good selectivities.

¹² X.-M. Xu, L. Zhao, J. Zhu, M.-X. Wang, *Angew. Chem. Int. Ed.* **2016**, *55*, 3799–3803.



Scheme 8: Formation of tricycles **20** by addition of tertiary enamides to a ketone followed by $S_E\text{Ar}$

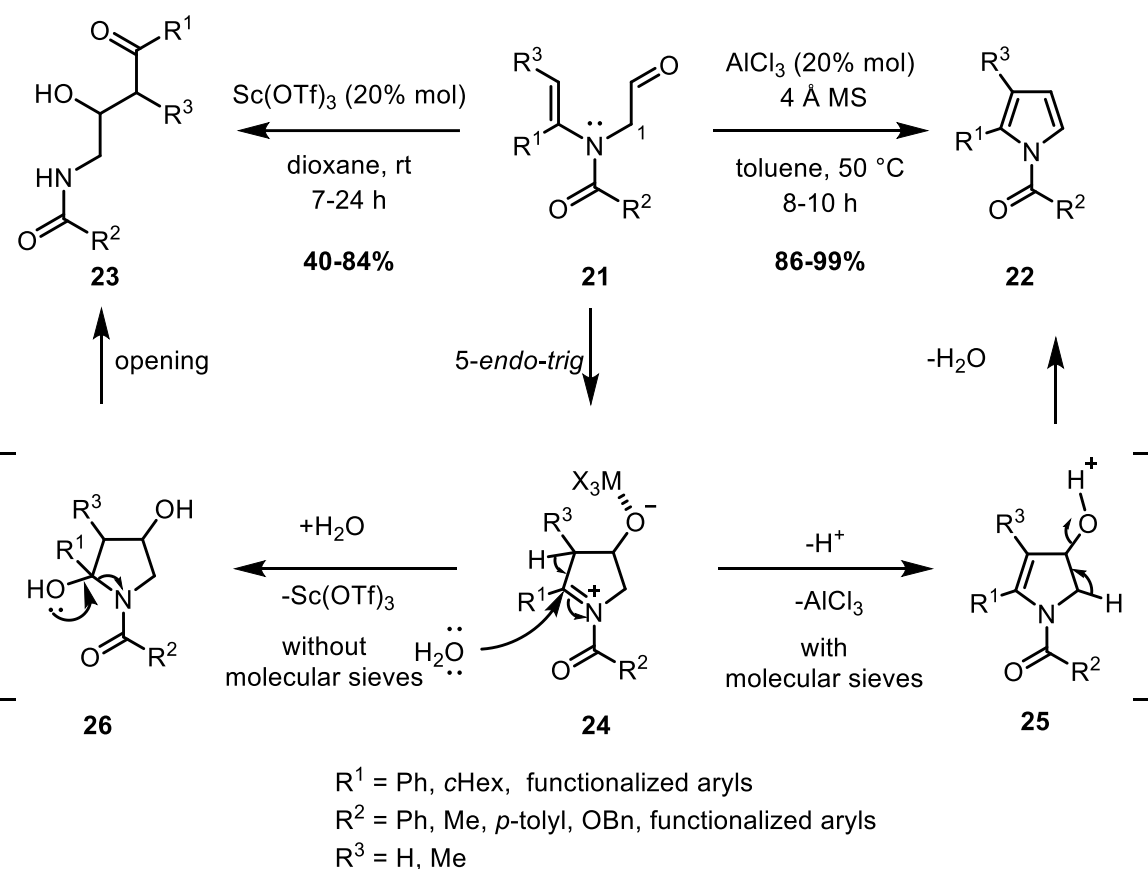
c. Nucleophilic addition of tertiary enamides to aldehydes

Wang's team also studied the enamide reactivity of tertiary enamides with aldehydes in intramolecular and intermolecular processes. The reaction routes varied not only according to the number of methylene units between the nitrogen atom and the aldehyde, but also through tuning of the Lewis acid and using different reaction conditions.

In the case of one methylene unit between the aldehyde and the amide

In the case of a single methylene unit between the aldehyde group and the amide moiety, treatment of tertiary enamide **21** with either aluminium trichloride or scandium triflate led to pyrrolic (compound **22**) or vicinal amino alcohols (compound **23**), respectively (**Scheme 9**).¹³ The 5-*endo-trig* addition of tertiary enamide to the activated aldehyde led to iminium ion **24**, which can evolve two different ways depending on the reaction conditions. When scandium triflate was used without molecular sieves, a molecule of water adds to the *N*-acyliminium ion formed *in situ*, leading to *N*, *O* hemicetal **26**. Subsequent opening of the cycle provided amino vicinal alcohols **23**.

¹³ X.-M. Xu, C.-H. Lei, S. Tong, J. Zhu, M.-X. Wang, *Org. Chem. Front.* **2018**, *5*, 3138–3141.



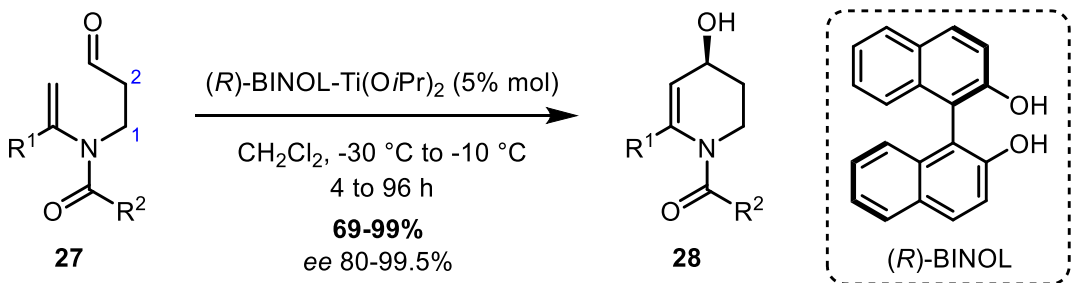
Scheme 9: Enamide reactivity on aldehydes

When aluminium trichloride was used with molecular sieves, the cyclized intermediate **24** resulting from addition of the tertiary enamide to the aldehyde was also formed. However, in the absence of water, deprotonation along with dehydration of **25** ultimately led to the pyrroles **22**.

In the case of two methylene units between the aldehyde and the amide

The reaction of tertiary enamides **27** bearing a two methylene linker chain between the aldehyde and the amide, the presence of a 2 : 1 mixture of (*R*)-BINOL and titanium isopropoxide in cold dichloromethane made it possible to obtain tetrahydropyridines **28** with yields ranging from 69 to 99% with enantiomeric excesses from 80 to 99.5% (**Scheme 10**).¹⁴ Mechanistic studies and theoretical calculations have shown that the active specie was the $[(R)\text{-BINOL-Ti(OiPr)}_2]$ complex, which was able to activate the aldehyde to form the tetrahydropyridines **28** by nucleophilic addition of the enamide to the activated carbonyl.

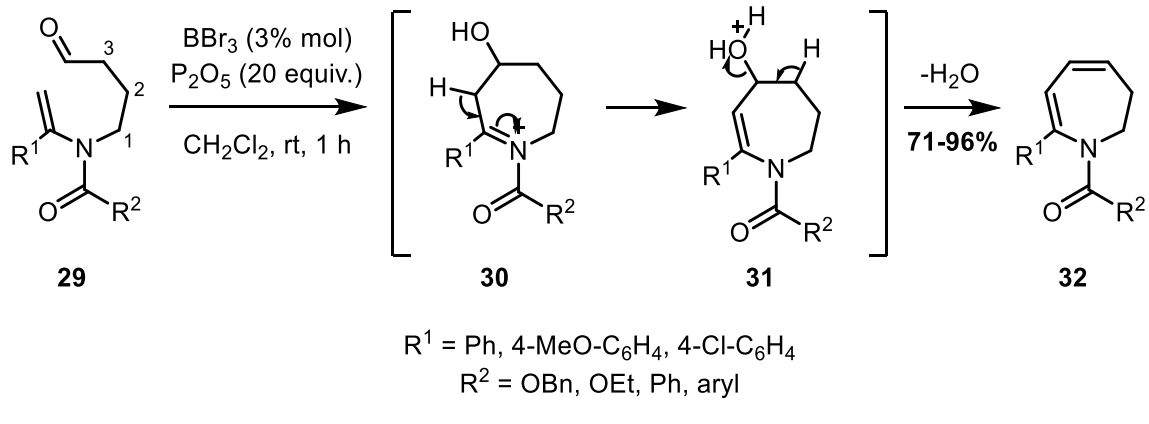
¹⁴ S. Tong, D.-X. Wang, L. Zhao, J. Zhu, M.-X. Wang, *Angew. Chem. Int. Ed.* **2012**, *51*, 4417–4420.



Scheme 10: Formation of tetrahydropyridines

In the case of a chain with three methylene units between the aldehyde and the amide

Finally, in the case of three methylene units between the aldehyde and the amide (compound **29**), treatment with boron tribromide (BBr_3) in the presence of P_2O_5 allows access to dihydroazepinones **32** with good yields (**Scheme 11**).¹⁵ After activation of the aldehyde by BBr_3 addition of the tertiary enamide to the aldehyde, and deprotonation and subsequent dehydration, compound **32** was obtained. Notably, using a Lewis acid bearing a single coordination site, (e.g., BBr_3), is essential to coordinate solely the aldehyde and thereby activate it. Indeed, tertiary enamide **29** could act as a bidentate or tridentate ligand in the presence of a Lewis acid with several coordination sites. Activation of the aldehyde would then compete with other possible chelated forms of the tertiary enamide, inhibiting nucleophilic addition of the tertiary enamide to the activated aldehyde.



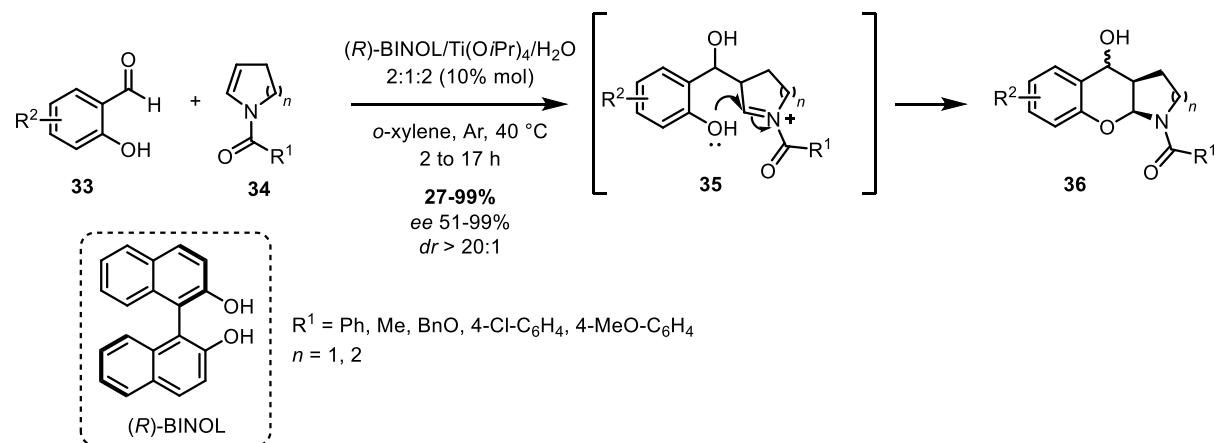
Scheme 11: Synthesis of the dihydroazepinones

Intermolecular nucleophilic addition of tertiary enamides to an aldehyde

Finally, Wang *et al.* also showed that these nucleophilic additions could be carried out in an intermolecular way. During this reaction, chromanols **36** were obtained by treatment of tertiary enamides **34** in the presence of the (R) -BINOL/Ti(O*i*-Pr)₄ with good

¹⁵ W. Zhu, L. Zhao, M.-X. Wang, *J. Org. Chem.* **2015**, *80*, 12047–12057.

enantioselectivities and diastereoselectivities (**Scheme 12**).¹⁶ The mechanism involves the addition of enamide **34** to aldehyde **33**, providing *N*-acyliminium ion **35** that is intermolecularly trapped by the phenolic alcohol present in the latter to form tricycle **36**.



Scheme 12: Synthesis of chromanols

I.1.2.3. Nucleophilic addition of tertiary enamides to activated alkynes

Alkynes can be activated by gold or platinum complexes, thus making them good electrophiles. Numerous examples of nucleophilic additions of tertiary enamides to triple bonds have been reported in the literature.¹⁷ In this part, only selected examples will be discussed to illustrate the nucleophilic reactivity of enamides toward alkynes.

a. Activation of the triple bond by platinum complexes

Dake *et al.* reported that enamides equipped with alkynes **37** and **41** led to spirocyclic compounds **40**, **43** and **45** (**Scheme 13**). Starting with terminal alkynes, the triple bond is activated by a platinum complex, promoting the nucleophilic addition of enamide to the alkyne. The iminium **38** formed is then trapped by methanol, leading to hemiaminal ether **39**. The latter, being not very stable, is reduced in the presence of $\text{BF}_3\text{-OEt}_2$ and Et_3SiH to provide spiro-pyridines **40** with yields from 50 to 93%.¹⁸

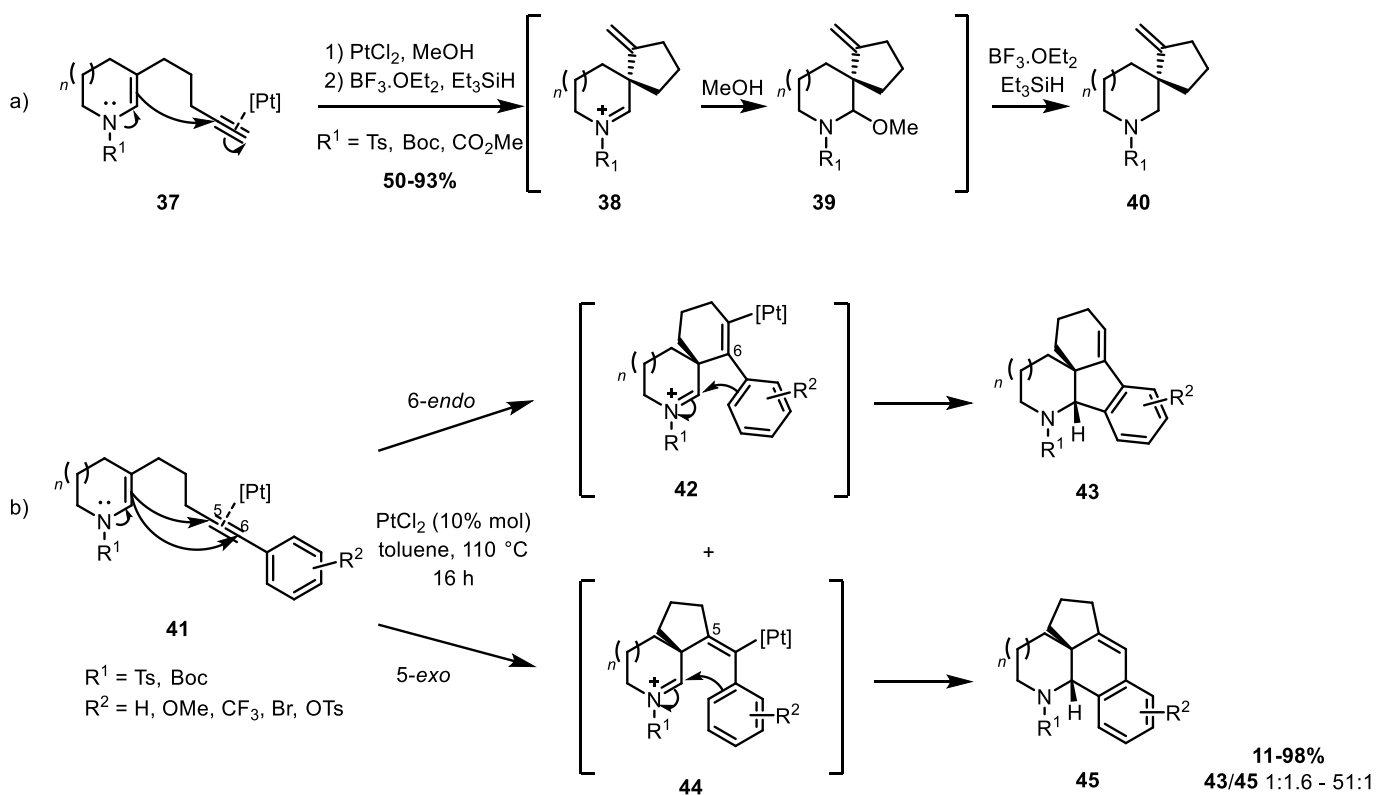
Furthermore, starting from alkynes substituted by an aryl group **41**, after activation of the triple bond by platinum, 6-*endo-dig* addition of the enamide led to cyclized intermediate **42**, whereas 5-*exo-dig* cyclization provided exocyclic compound **44**. The nitrogen-containing tetracycles **43** and **45** were then formed by trapping the iminium ion by a Friedel-Crafts/Pictet-Spengler type transformation followed by protodemetalation.¹⁹

¹⁶ L. He, L. Zhao, D.-X. Wang, M.-X. Wang, *Org. Lett.* **2014**, *16*, 5972–5975.

¹⁷ T. J. Harrison, G. R. Dake, *Org. Lett.* **2004**, *6*, 5023–5026. H. Kim, C. Lee, *J. Am. Chem. Soc.* **2006**, *128*, 6336–6337. J. A. Kozak, B. O. Patrick, G. R. Dake, *J. Org. Chem.* **2010**, *75*, 8585–8590. B. K. Corkey, S. T. Heller, Y.-M. Wang, F. D. Toste, *Tetrahedron* **2013**, *69*, 5640–5646. X.-Y. Ma, X.-T. An, X.-H. Zhao, J.-Y. Du, Y.-H. Deng, X.-Z. Zhang, C.-A. Fan, *Org. Lett.* **2017**, *19*, 2965–2968.

¹⁸ T. J. Harrison, G. R. Dake, *Org. Lett.* **2004**, *6*, 5023–5026.

¹⁹ A. Kozak, J. M. Dodd, T. J. Harrison, K. J. Jardine, B. O. Patrick, G. R. Dake, *J. Org. Chem.* **2009**, *74*, 6929–6935.



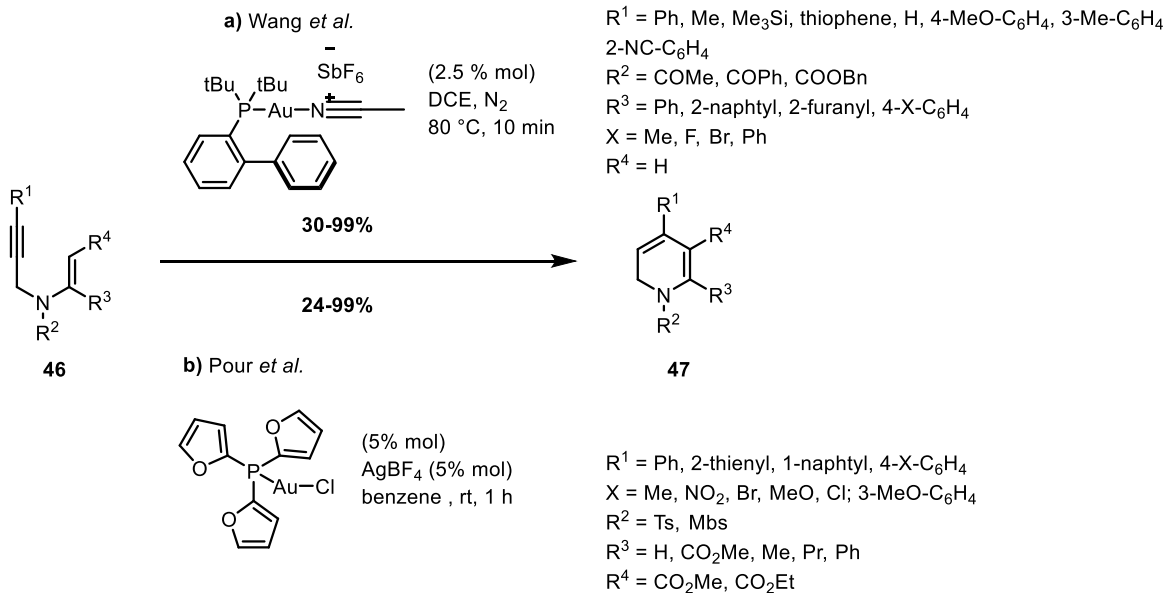
Scheme 13: Spirocyclization by addition of tertiary enamides to activated alkynes

b. Activation of the triple bond by gold complexes

Gold-promoted intramolecular nucleophilic additions of enamides to alkynes have led to functionalized dihydropyridines **47** (**Scheme 14**). Wang *et al.* reported a gold monophosphine complex to activate alkynes, leading to 1,2 dihydropyridines **47** with yields from 30 to 99%.²⁰ In the case of Pour *et al.*'s work, the AuCl gold complex (TFP) in the presence of AgBF_4 allowed the transformation of tertiary enamides **46** into dihydropyridines **47** with yields ranging from 24 to 99%.²¹ Notably, in both cases the authors also described the transformation of functionalized dihydropyridines **47** into the corresponding pyridines either by oxidation using MnO_2 and oxygen for Wang's team, or by deprotection followed by deprotonation for Pour's team.

²⁰ X. Zhang, X.-M. Xu, L. Zhao, J. You, J. Zhu, M.-X. Wang, *Tetrahedron Lett.* **2015**, *56*, 3898–3901.

²¹ J. Mikušek, P. Matouš, E. Matoušová, M. Janoušek, J. Kuneš, M. Pour, *Adv. Synth. Catal.* **2016**, *358*, 2912–2922.



Scheme 14: Synthesis of functionalized dihydropyridines

I.1.2.4. Nucleophilic addition of tertiary enamides to imines

Wang et al. also studied the reactivity of enamides toward imines.^{22,23,24}

a. Intramolecular addition of tertiary enamides to imines

The reaction of tertiary enamides **48** tethered to aldehydes in the presence of a primary amine in dichloromethane at room temperature led to tetrahydropyridines **50** and **52** (**Scheme 15**).²⁵ Two different pathways have to be considered, depending on the primary amine involved. During the reaction of tertiary enamides **48** with anilines, the imine intermediate resulting from the addition of aniline to the aldehyde group **49** is not isolated, and tetrahydropyridines **50** are directly obtained with yields ranging from 81 to 100%. Furthermore, the reaction times are dependent on the substituents of the aniline moiety. For anilines substituted with halogens, several hours or even days are necessary for total conversion of enamide **48**, whereas for enriched anilines, the reaction proceeded in a few minutes.

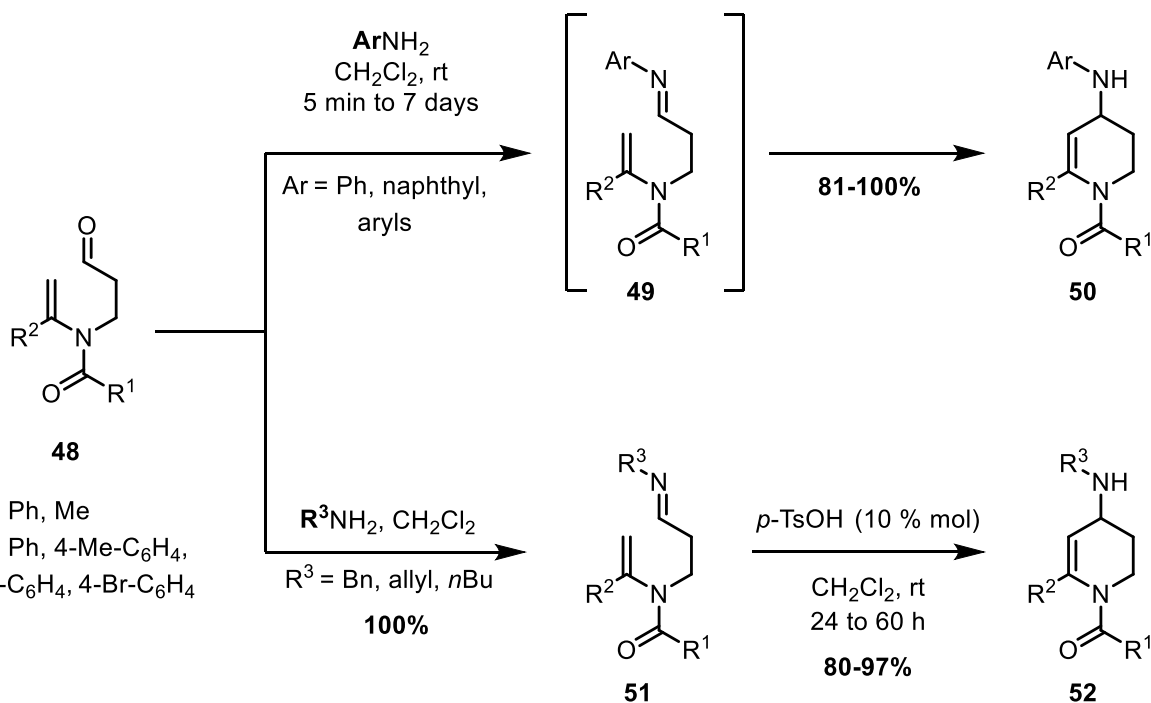
However, when using aliphatic amines, under the same reaction conditions, namely in dichloromethane at room temperature, the reaction stopped at the imine intermediate **51**, being less electrophilic than their non-isolated counterpart **49**. However, activation of the imine **51** by a Brønsted acid, e.g., *para*-toluenesulfonic acid, promotes nucleophilic addition of the tertiary enamide to the activated imine, giving access to tetrahydropyridines **52**.

²² S. Tong, X. Yang, D.-X. Wang, L. Zhao, J. Zhu, M.-X. Wang, *Tetrahedron* **2012**, *68*, 6492–6497.

²³ L. He, H.-B. Liu, L. Zhao, D.-X. Wang, M.-X. Wang, *Tetrahedron* **2015**, *71*, 523–531.

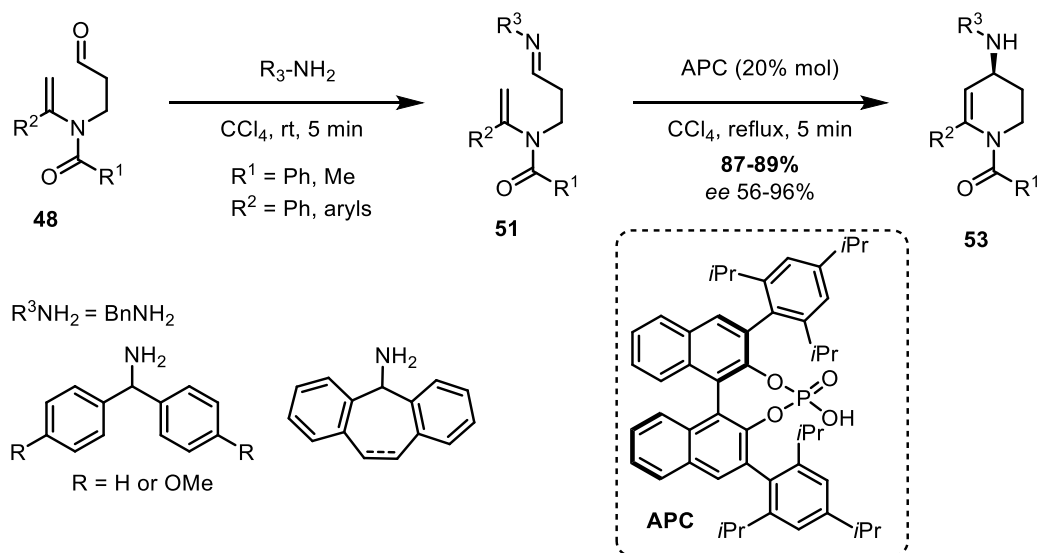
²⁴ S. Tong, M.-X. Wang, *Synlett* **2019**, *30*, 483–487.

²⁵ S. Tong, X. Yang, D.-X. Wang, L. Zhao, J. Zhu, M.-X. Wang, *Tetrahedron* **2012**, *68*, 6492–6497.



Scheme 15: Synthesis of tetrahydropyridines

Recently, the authors extended this reaction to develop an asymmetric version (**Scheme 16**).²⁶ The first step consists in the formation of imine **51** by condensation of the primary amine on the aldehyde. The use of a chiral phosphoric acid (APC) allowed the activation of the imine **51**, making it more electrophilic and thus promoting the formation of dihydropyridines **53** by addition of the enamides to the activated imines.

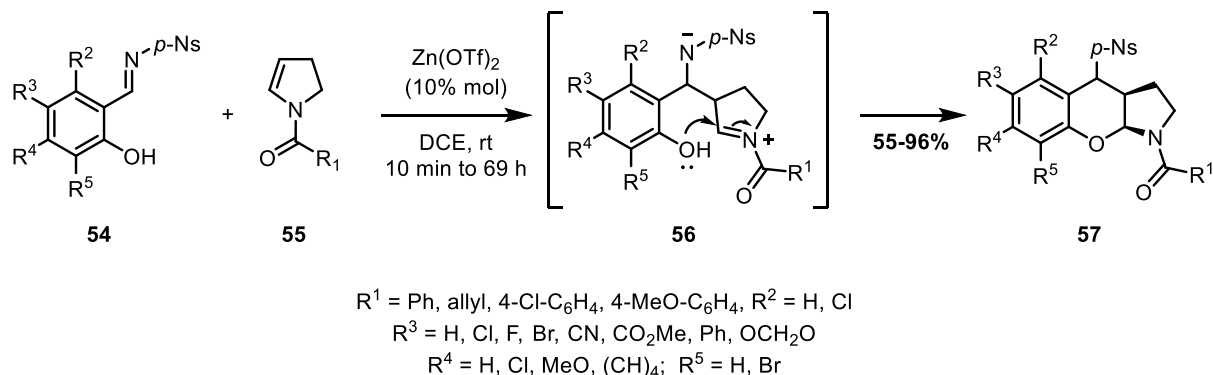


Scheme 16: Synthesis of chiral dihydropyridines

²⁶ S. Tong, M.-X. Wang, *Synlett* **2019**, *30*, 483–487.

b. Intermolecular addition of tertiary enamides to imines

Finally, the addition of tertiary enamides to imines can also be carried out in an intermolecular manner.²⁷ Cyclic enamide **55** reacted with imine **54** activated by zinc triflate, forming the intermediate zwitterion **56**. An intramolecular addition of phenolic alcohol on the formed iminium ion takes place *in situ*, providing chromanols **57** with yields ranging from 55 to 96 % (**Scheme 17**).



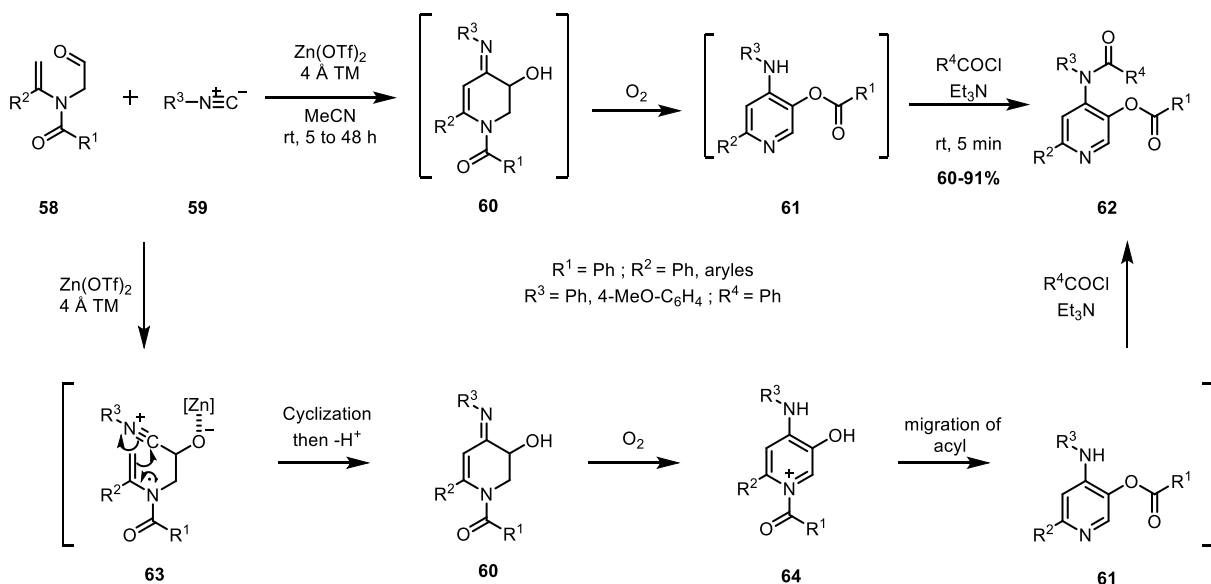
Scheme 17: Synthesis of chromanols

I.1.2.5. Nucleophilic addition of tertiary enamides to nitriliums

The isonitrile carbon possesses both nucleophilic and an electrophilic character. Thus, Wang *et al.* described an Ugi- and Passerini-type reactions involving tertiary enamides and isonitriles. Treatment of enamides tethered to aldehyde **58** with Zn(OTf)₂ under aerobic conditions followed by an acylation step led to substituted pyridines **62** with yields from 60 to 91% (**Scheme 18**).²⁸ After the addition of isonitrile **59** to the aldehyde, the nitrilium ion **63** formed can be trapped by addition of tertiary enamide, thus forming tetrahydropyridine **60** after deprotonation. An oxidative rearomatization makes it possible to obtain pyridinium **64**. A migration of the acyl group of the nitrogen moiety toward the hydroxyl group, provided pyridine **61**. The remaining secondary amine was then acylated to polyfunctionalized pyridines **62**. Numerous polyfunctionalized pyridines **62** with various aryl groups were accessible via this method.

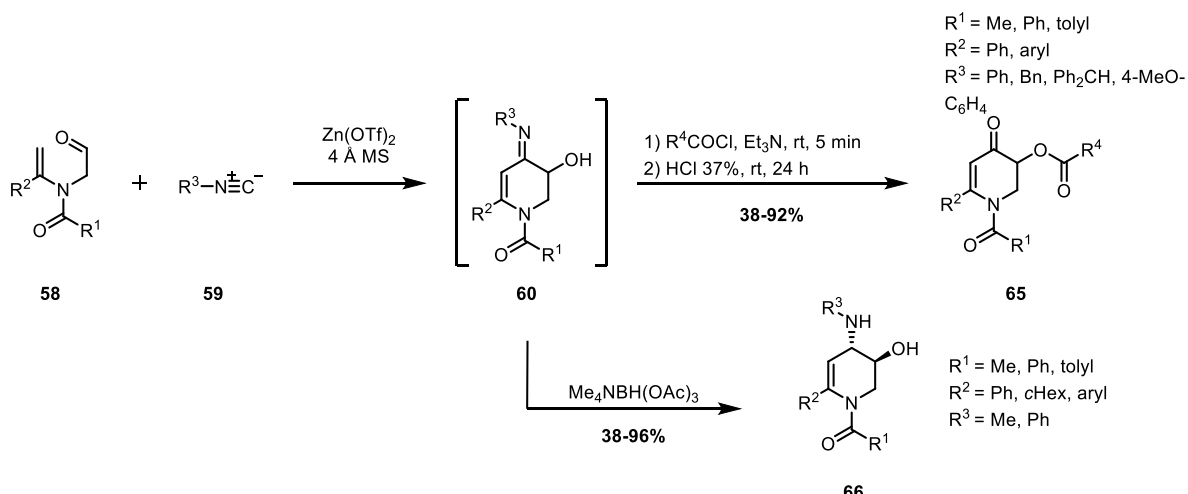
²⁷ L. He, H.-B. Liu, L. Zhao, D.-X. Wang, M.-X. Wang, *Tetrahedron* **2015**, *71*, 523–531.

²⁸ C.-H. Lei, D.-X. Wang, L. Zhao, J. Zhu, M.-X. Wang, *J. Am. Chem. Soc.* **2013**, *135*, 4708–4711.



Scheme 18: Synthesis of polyfunctionalized pyridines under aerobic conditions

The same authors have also shown that under anaerobic conditions, isonitriles **59**, could lead either to tetrahydropyridones **65** or to dihydroaminopyridines **66** (**Scheme 19**).²⁹ In this case, the same starting substrates are used in the presence of $\text{Zn}(\text{OTf})_2$, allowing the formation of intermediate tetrahydropyridine **60** in analogy to the transformation outlined in **Scheme 18**. The dihydroaminopyridines **66** are then obtained stereospecifically by reduction of the imine using tetramethylammonium triacetoxyborohydride, $\text{Me}_4\text{NBH}(\text{OAc})_3$ as a reducing agent.³⁰ Another possible evolution of intermediate **60** is the acylation of the hydroxyl unit followed by the hydrolysis of the imine with hydrochloric acid, leading to formation of tetrahydropyridinones **65**.



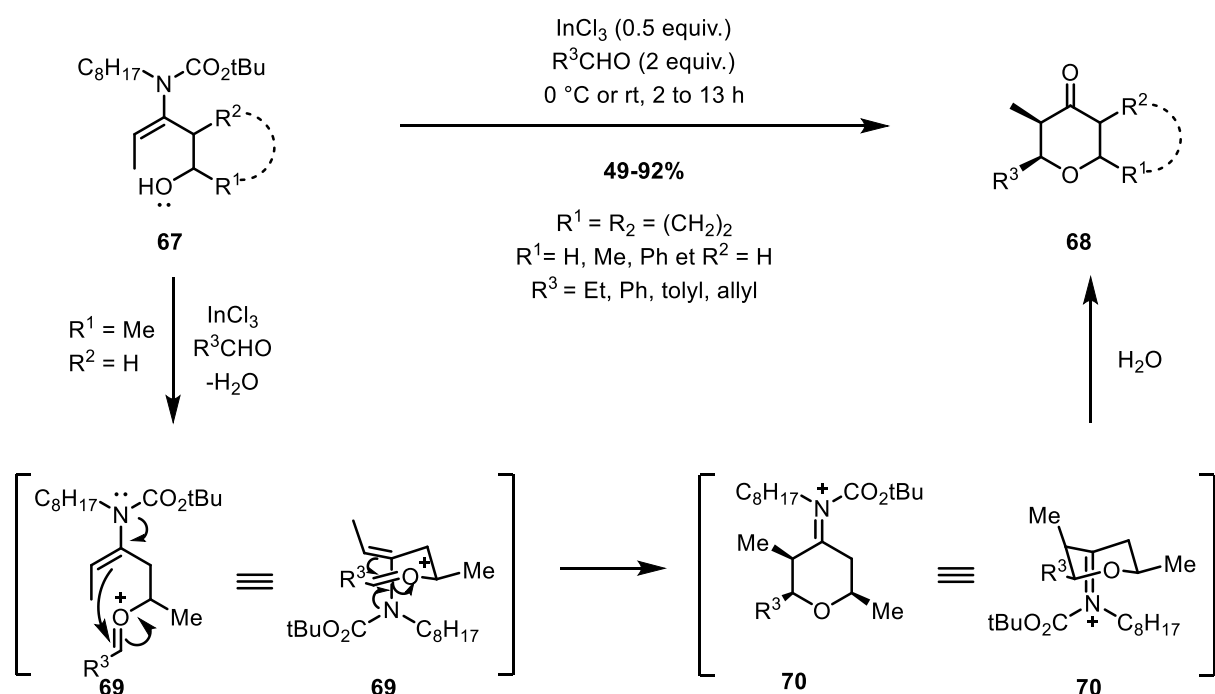
Scheme 19: Synthesis of tetrahydropyridinones **65** and dihydroaminopyridines **66**

²⁹ C.-H. Lei, D.-X. Wang, L. Zhao, J. Zhu, M.-X. Wang, *Chem. - Eur. J.* **2013**, *19*, 16981–16987.

³⁰ D. A. Evans, K. T. Chapman, E. M. Carreira, *J. Am. Chem. Soc.* **1988**, *110*, 3560–3578. A. K. Saksena, P. Mangiaracina, *Tetrahedron Lett.* **1983**, *24*, 273–276.

I.1.2.6. Nucleophilic addition of tertiary enamides to oxocarbeniums

In 2004, Funk *et al.* reported the formation of tetrahydropyranones **68** through a Prins reaction from tertiary enamides **67** in the presence of indium trichloride (InCl_3) and an aldehyde (**Scheme 20**).³¹ The first step consists of the *in situ* formation of oxocarbenium ion **69** by condensation of the alcohol functional group present in the enamide **67** on the aldehyde, releasing a molecule of water. The addition of tertiary enamide to the oxocarbenium ion then led to the formation of tetrahydropyranic intermediate **70** via a chair transition structure, explaining the excellent stereoselectivity control. The water molecule released during the process could then hydrolyze iminium **70** to obtain tetrahydropyranones **68**.



Scheme 20: Synthesis of tetrahydropyranones

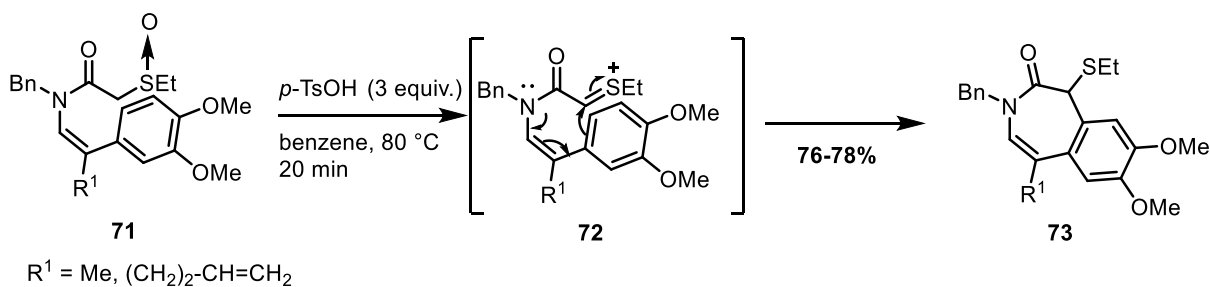
I.1.2.7. Tertiary enamide-assisted reactions

Finally, tertiary enamides can act as nucleophiles indirectly, in the presence of a conjugated system. Pawda *et al.* reported an electrophilic aromatic substitution (S_{EAr}) assisted by the nucleophilic addition of tertiary enamides to thionium ions.³² Starting from tertiary enamide **71** in the presence of *para*-toluenesulfonic acid, azepinones **73** were obtained with good yields (**Scheme 21**).³³ The Brønsted acid allows the activation of the sulfoxide into an electrophilic thionium ion. An S_{EAr} reaction via thionium ion **72** leads to the formation of azepinones **73** after re-aromatization.

³¹ K. N. Cossey, R. L. Funk, *J. Am. Chem. Soc.* **2004**, 126, 12216–12217.

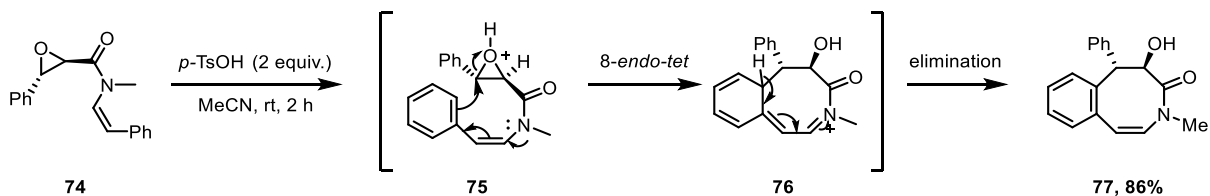
³² A. Padwa, M. D. Danca, *Org. Lett.* **2002**, 4, 715–717.

³³ A. Padwa, M. D. Danca, K. I. Hardcastle, M. S. McClure, *J. Org. Chem.* **2003**, 68, 929–941.



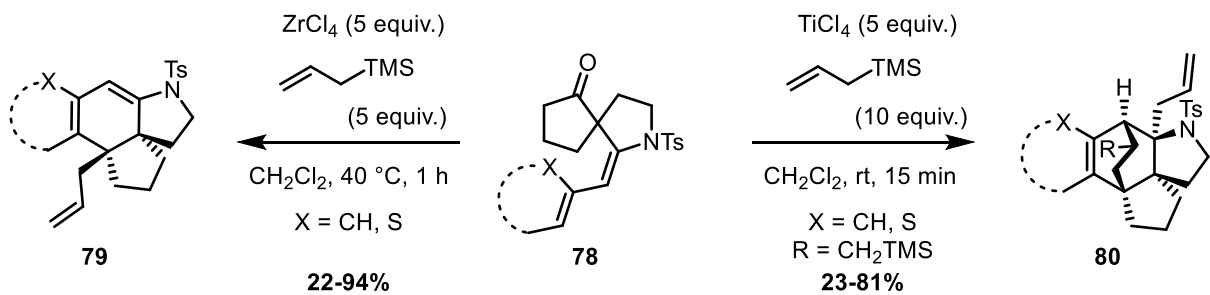
Scheme 21: Electrophilic aromatic substitution assisted by a tertiary enamide on a thionium ion

Wang *et al.* reported a tertiary enamide-assisted intramolecular cyclization of 8-endo-epoxy arene (**Scheme 22**).³⁴ In the presence of *para*-toluenesulfonic acid in acetonitrile for two hours at room temperature, tertiary enamide **74** led to the formation of enantiopure (+)-(5*R*, 6*S*)- ζ -clausenamide **77** in 86% yield. The enamide conjugated to a phenyl group **74** adds to the protonated epoxide by an electrophilic aromatic substitution (S_{EAr}) assisted by the enamide. Then re-aromatization of intermediate **76** makes it possible to generate azabicyclic compound **77**.



Scheme 22: S_{EAr} on an epoxide assisted by a tertiary enamide

More recently, our group has described a tertiary enamide-triggered S_{EAr} involving the delocalization of the tertiary enamide electrons into a benzene ring.³⁵ Depending on the choice of the Lewis acid, the amount of allyltrimethylsilane, and the reaction conditions, the reactivity of the spiroenesulfonamides **78** could be tuned to obtain either tetracyclic fused polycyclic systems **79** or pentacyclic structures **80** in moderate to good yields, with the simultaneous creation of four new well defined stereocenters (**Scheme 23**).

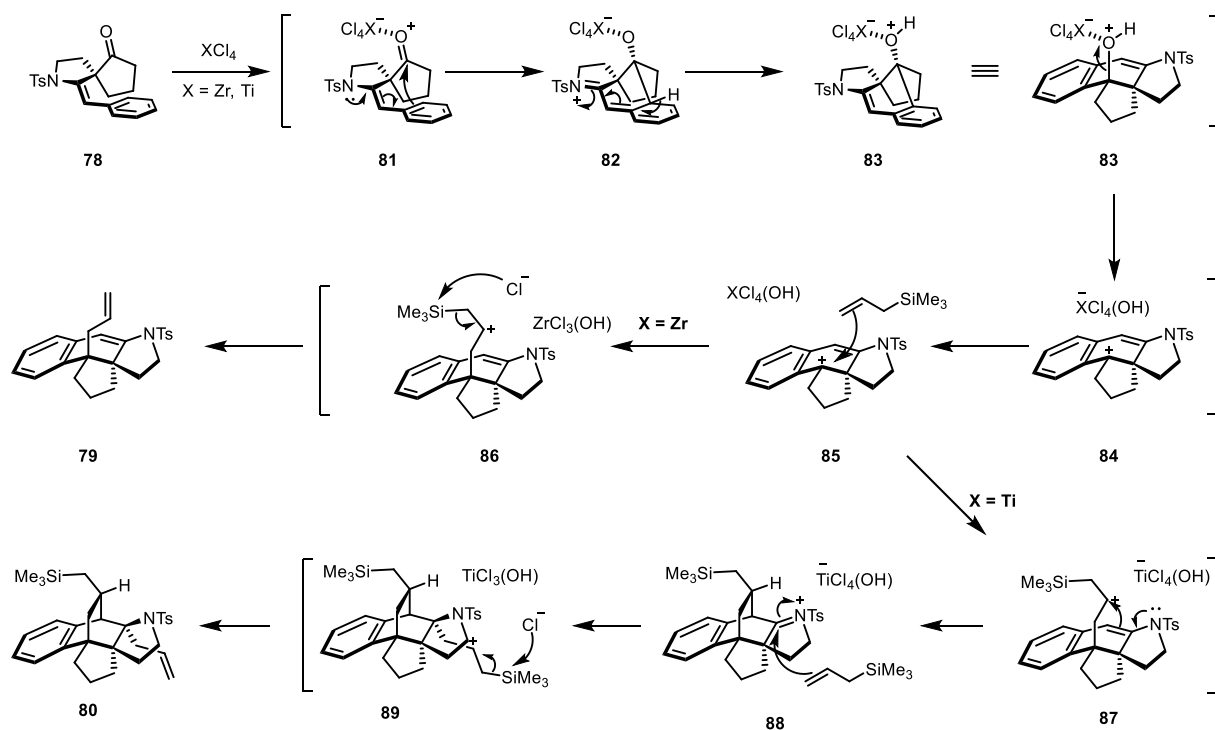


Scheme 23: S_{EAr} assisted by a tertiary enamide on an activated carbonyl

³⁴ L. Yang, G. Deng, D.-X. Wang, Z.-T. Huang, J. Zhu, M.-X. Wang, *Org. Lett.* **2007**, 9, 1387–1390.

³⁵ F. Beltran, L. Miesch, *Org. Lett.* **2019**, 21, 1569–1573.

To explain the formation of these spiro polycyclic-fused ring systems, the mechanism outlined in **Scheme 24** was proposed. Activation of ketone **78** by a Lewis acid provides alkoxide **81**. Subsequent intramolecular electrophilic aromatic substitution assisted by the tertiary spiro-enesulfonamide affords imidium intermediates **82**. Subsequent rearomatization affords **83**. Ionization of the alkoxide/Lewis acid complex **83** leads to tertiary carbocation **84**. At this point, two pathways can be considered, depending on the Lewis acid involved: Addition of allylsilane on the convex face of the molecule provides **86**. Because zirconium(IV) has a much larger ionic radius than titanium(IV), the Zr-Cl bond may be more labile, promoting β -silyl-elimination to form polycyclic system **79**. With $TiCl_4$, allylsilane adds to **85**, providing **87**. In this case, the enamine-like reactivity of **87** is faster than β -elimination of the silicon moiety, thus leading to bridged compound **88**. A second molecule of allylsilane subsequently adds to the iminium ion from the less hindered side of **88**, thus ending with the production of **80** after β -silyl elimination



Scheme 24: Mechanism of the formation of tetracyclic compound **79** and pentacyclic compound **80**

1.1.2.8. Nucleophilic addition of tertiary enamides to N-acyliminium ions

N-Acyliminium ions (NAI) are very reactive electrophiles, widely used for the construction of a wide variety of nitrogen-containing molecules.³⁶ Different types of NAI ions can be distinguished: acyclic NAI ions, endocyclic NAI ions and exocyclic ones (**Figure 3**).³⁷

³⁶ B. E. Maryanoff, H.-C. Zhang, J. H. Cohen, I. J. Turchi, C. A. Maryanoff, *Chem. Rev.* **2004**, *104*, 1431–1628. P. Wu, T. E. Nielsen, *Chem. Rev.* **2017**, *117*, 7811–7856.

³⁷ A. Daïch, A. Ghinet, B. Rigo, in *Comprehensive Organic Synthesis II*, **2014**, 682–742.

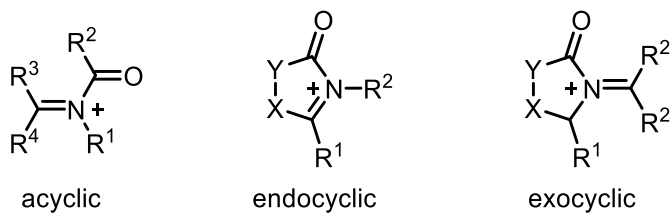


Figure 3. Schematic representation of the classes of *N*-acyliminium ions

Furthermore, depending on the nature of the electron-withdrawing group present on the nitrogen atom, the NAI ions can be classified in several families (**Figure 4**).

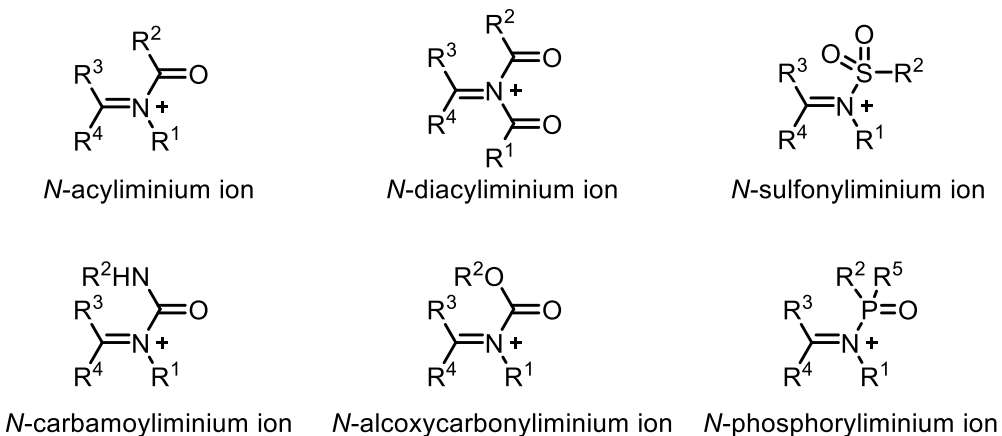


Figure 4. Schematic representation of *N*-iminium ions according to the nature of the electron-withdrawing group of the nitrogen atom

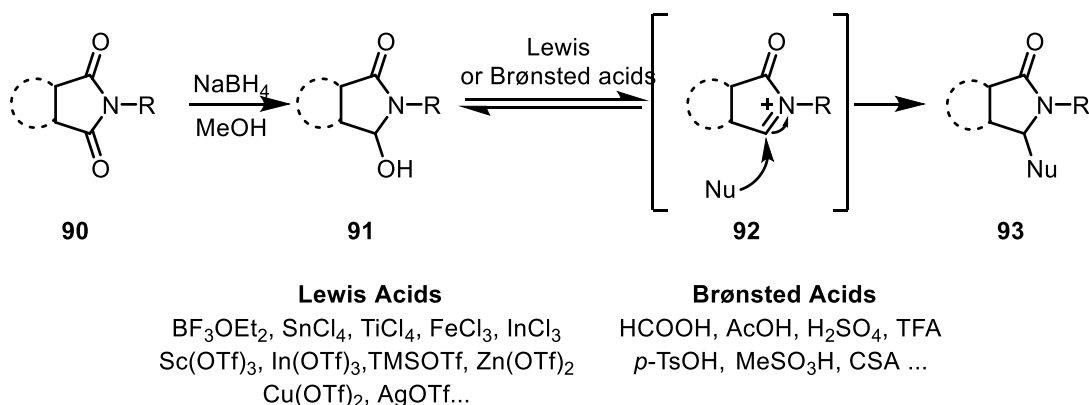
a. Synthesis of *N*-acyliminium ions

Most popular method: using *N*-functionalized α -hydroxylamides

The most widely used method to generate *N*-acyliminium ions consists of removing a leaving group α to the nitrogen atom by reaction with a Lewis or Brønsted acid. The most commonly used leaving group is an activated hydroxyl group. Thus, the reduction of one of the carbonyl functions of a diimide **90** by sodium borohydride (NaBH_4)³⁸ makes it possible to reduce one of the carbonyl groups to generate *N*-functionalized α -hydroxylamide **91**, precursor of an NAI ion (**Scheme 25**).

Among numerous Lewis acids that cause the leaving of the hydroxyl group, boron trifluoride etherate $\text{BF}_3 \cdot \text{OEt}_2$, titanium tetrachloride (TiCl_4), iron trichloride (FeCl_3), or indium trichloride (InCl_3) have been widely exploited. NAI ions can also be formed in the presence of Brønsted acids by protonation of the hydroxyl group, leading to the elimination of water. A nucleophile can then add to the NAI ion formed (**92**) in an intra- or intermolecular way, providing compound **93**.

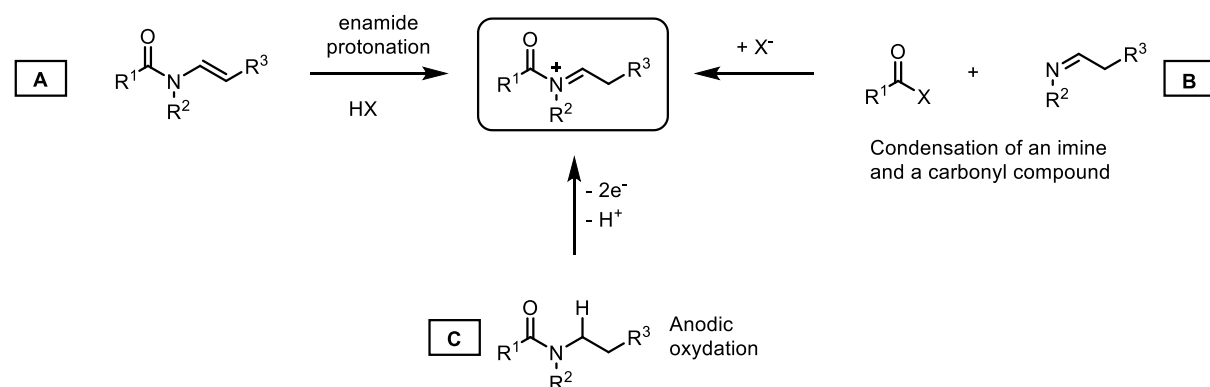
³⁸ J. C. Hubert, J. B. P. A. Wunberg, W. N. Speckamp, *Tetrahedron* **1975**, *31*, 1437–1441.



Scheme 25: Formation and general reactivity of *N*-acyliminium ions

Other methods of accessing NAI ions

To access *N*-acyliminium ions, other synthetic routes are possible (**Scheme 26**).³⁹ *N*-Acyliminium ions can be formed by protonation of an enamide (**Scheme 26A**) or by condensation of an imine on an acyl chloride or an aldehyde (**Scheme 26B**). Electrochemical oxidation of amides also allows the formation of NAI ions (**Scheme 26C**).



Scheme 26: *N*-acyliminium ion access routes

b. Nucleophilic addition of tertiary enamides to N-acyliminium ions

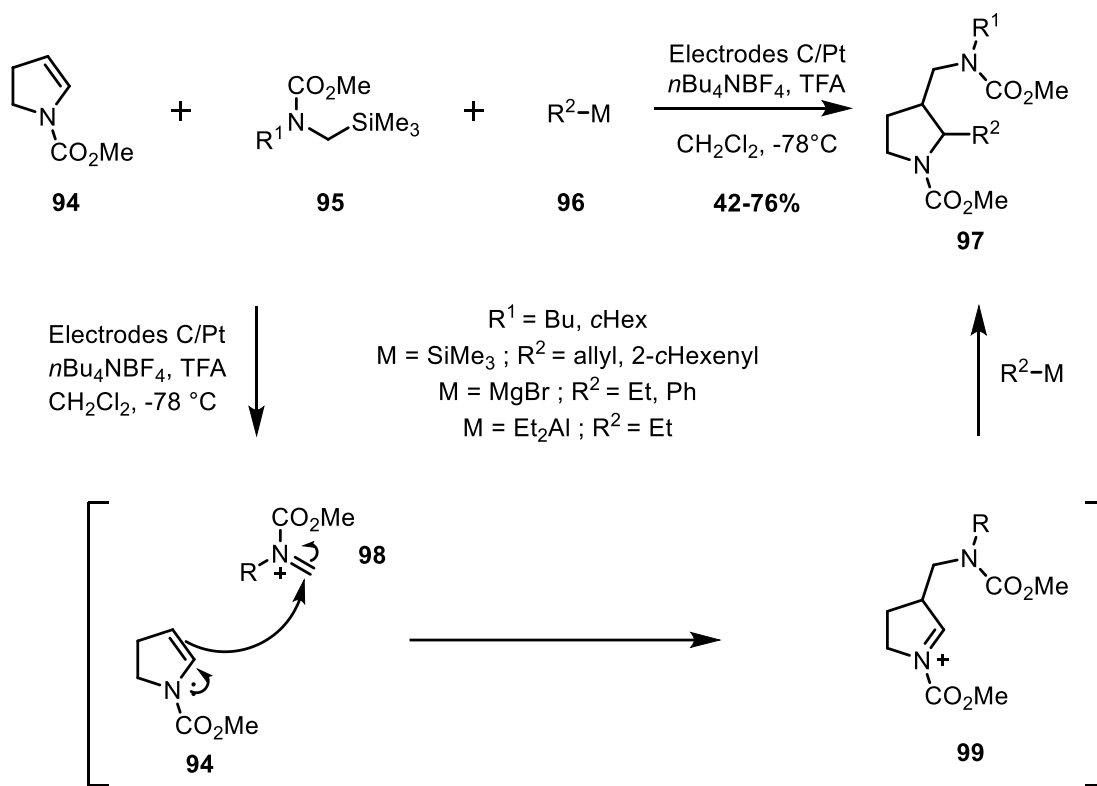
Enamines can also react with iminium ions formed *in situ*.⁴⁰ In 2004, Yoshida *et al.* generated iminium ions by a so-called « cation pool » method.⁴¹ The *N*-acyliminium ions **98** are obtained from the « cation pool », namely from carbamate **95**, at low temperature by

³⁹ B. E. Maryanoff, H.-C. Zhang, J. H. Cohen, I. J. Turchi, and C. A. Maryanoff, *Chem. Rev.* **2004**, *104*, 1431–1628. P. Wu, T. E. Nielsen, *Chem. Rev.* **2017**, *117*, 7811–7856.

⁴⁰ L. Eberson, M. Malmberg, K. Nyberg, *Acta Chem. Scand.* **1984**, *38*, 391–396.

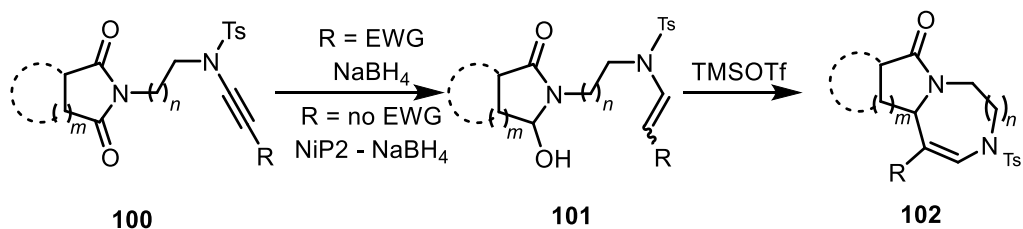
⁴¹ S. Suga, T. Nishida, D. Yamada, A. Nagaki, J. Yoshida, *J. Am. Chem. Soc.* **2004**, *126*, 14338–14339.

elimination of a silyl group (**Scheme 27**).⁴² Tertiary enamide **94** was added to the *N*-acyliminium ion **98** formed *in situ* to obtain iminium ion **99**. Addition of an external nucleophile R²-X, whether it is a Grignard reagent, an allylsilane, or even a silylated enol ether, allows the formation of pyrrolidines **97** with good yields.



Scheme 27: Tetrahydropyridine synthesis

Recently, our group has shown that tertiary enamides react with *N*-acyliminium ions to obtain medium-sized diaza-heterocycles. Enamides equipped with *N*-acyliminium ion precursors were obtained through reduction of ynamides tethered to *N*-imides. Intramolecular TMSOTf-mediated trapping of *N*-acyliminium ions provided diazepines, diazocanes and diazonanes of putative pharmacological interest.

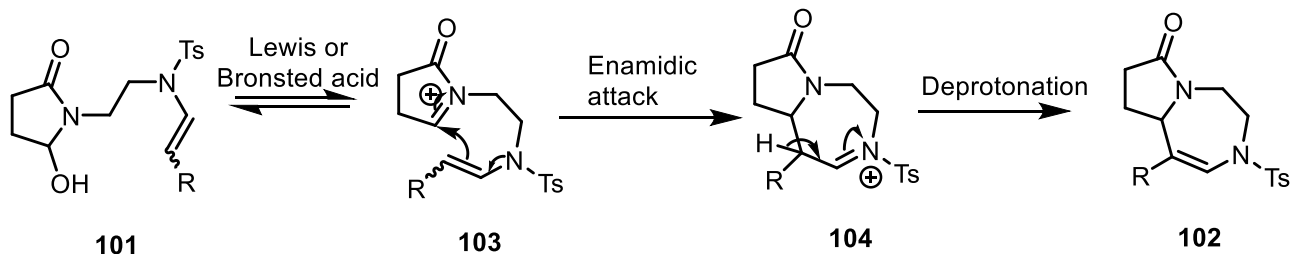


Scheme 28: Synthesis of Diaza Heterocycles

The mechanism to explain the formation of diaza-heterocycles **102** starts with the formation of the *N*-acyliminium ion **103** in the presence of Brønsted or Lewis acids. The latter is trapped by the tertiary enamide moiety, providing intermediate **104**. The bicyclic diazepine evolves

⁴² J. Yoshida, S. Suga, *Chem. - Eur. J.* **2002**, *8*, 2650–2658.

upon deprotonation of the β -disubstituted enamide **104** (**Scheme 29**) to form the corresponding diazepines.



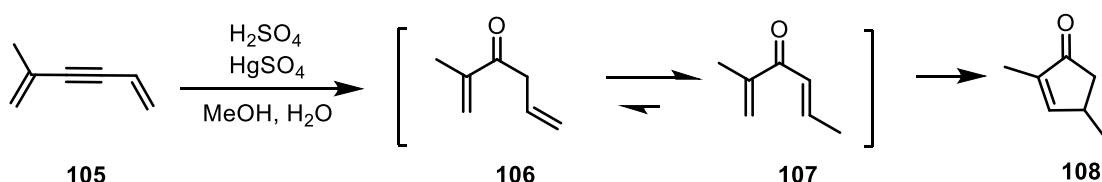
Scheme 29: Plausible mechanism

I.2. The Nazarov cyclization

I.2.1. Introduction

Cyclopentenones are frequently used as key building blocks and are themselves present within a variety of bioactive and complex natural products.⁴³ In this context, the Nazarov reaction has been considered one of the most direct and atom-economical transformations for the synthesis of cyclopentenones.

This reaction was first reported in 1942 by a prominent Russian scientist, Ivan Nikolaevich Nazarov.⁴⁴ During his work on hydration of alkynes, this Russian chemist treated divinyl alkyne **105** with mercury sulfate and concentrated sulfuric acid in a methanol/ water mixture and obtained cyclopentenone **108**. (**Scheme 30**).



Scheme 30: First Nazarov reaction

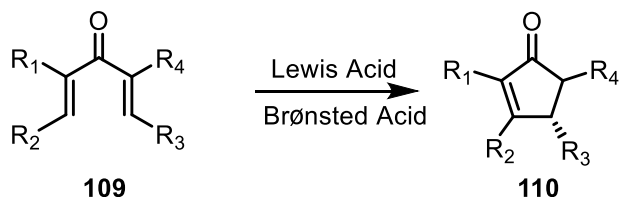
Since this discovery, the Nazarov cyclization has evolved to become a primary tool for the synthesis of cyclopentenones.⁴⁵ The classical version consists of the conversion of divinyl

⁴³ M. G. Vinogradov, O. V. Turova, S. G. Zlotin, *Org. Biomol. Chem.*, **2017**, *15*, 8245–8269.

⁴⁴ I. N. Nazarov, I. I. Zaretskaya, *Izv. Akad. Nauk. USSR, Ser. Khim.* **1941**, 211–224.

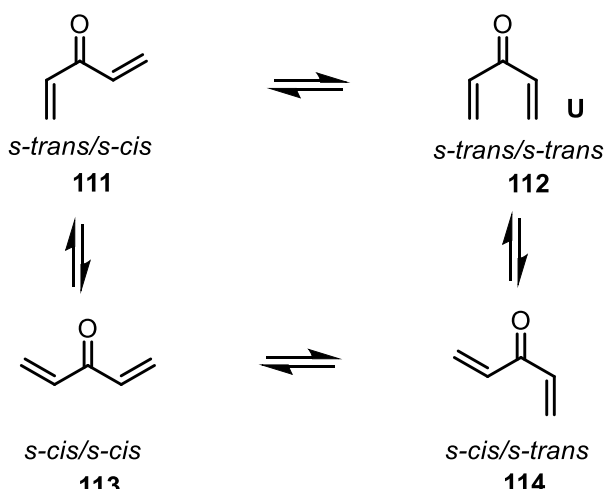
⁴⁵ K. L. Habermas, S. E. Denmark, *Org. React.* **1994**, *45*, 1–158. H. Pellissier, *Tetrahedron* **2005**, *61*, 6479–6517. A. J. Frontier, C. Collison, *Tetrahedron* **2005**, *61*, 7577–7606. T. N. Grant, C. J. Rieder, F. G. West, *Chem. Commun.* **2009**, 5676–5688. T. Vaidya, R. Eisenberg, A. J. Frontier, *ChemCatChem* **2011**, *3*, 1531–1548. W. T. Spencer III, T. Vaidya, A. J. Frontier, *Eur. J. Org. Chem.* **2013**, *18*, 3621–3633. M. C. Martin, R. Shenje, S. France, *Isr. J. Chem.* **2016**, *56*, 499–511. M. G.

ketones to cyclopentenones promoted by a Lewis- or Brønsted acid. The Nazarov cyclization is part of the electrocyclization reaction family and is a 4π electrocyclic ring closure. (**Scheme 31**)



Scheme 31: Classical Nazarov reaction

The mechanism of this transformation was highlighted by Shoppee in 1969.⁴⁶ The Nazarov cyclization requires an *s-trans/s-trans* conformation for the divinyl ketone, also referred to as the **U** conformer (**Scheme 32**)

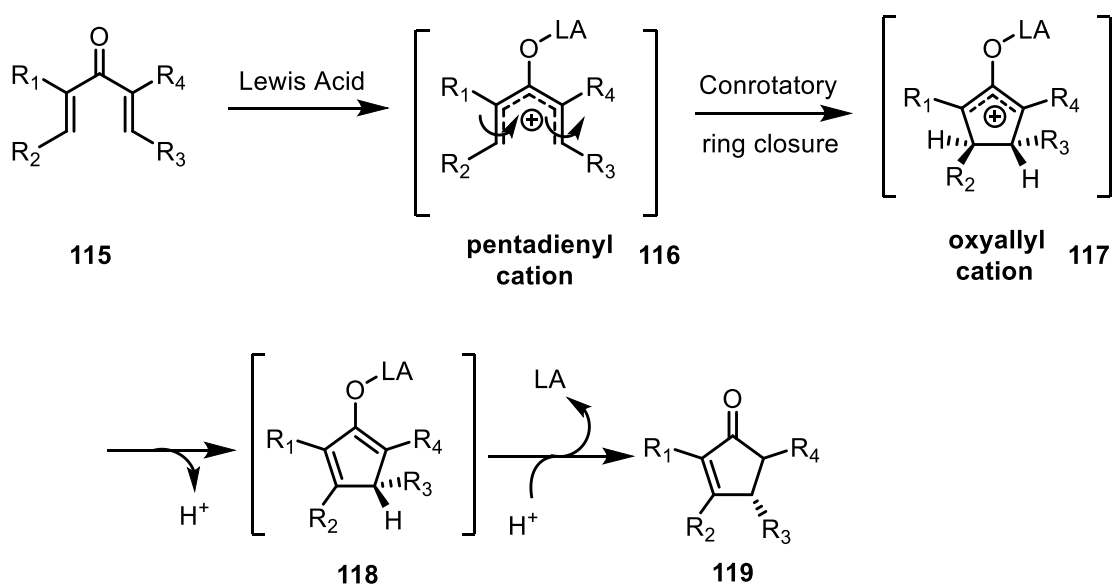


Scheme 32: Possible conformers for the divinyl ketone.

The commonly adopted mechanism is the following: the divinyl ketone **115** complexes to the Lewis acid to give a pentadienyl cation **116**. Conrotatory ring closure gives an oxyallyl cation **117**, and elimination of a proton gives a Lewis-acid bound enolate **118**. Finally, protonation of the enolate **118** leads to the cyclopentenone product **119** (**Scheme 33**)

Vinogradov, O. V. Turova, S. G. Zlotin, *Org. Biomol. Chem.*, **2017**, 15, 8245–8269. A. J. Frontier, J. J. Hernandez, *Acc. Chem. Res.* **2020**, 53, 1822–1832.

⁴⁶ C. W. Shoppee, R. E. Lack, *J. Chem. Soc. C* **1969**, 1346-1349.



Scheme 33: Mechanism of the Nazarov reaction.

To make this reaction interesting from a synthetic point of view, control of reactivity, regioselectivity, and stereochemistry are essential.

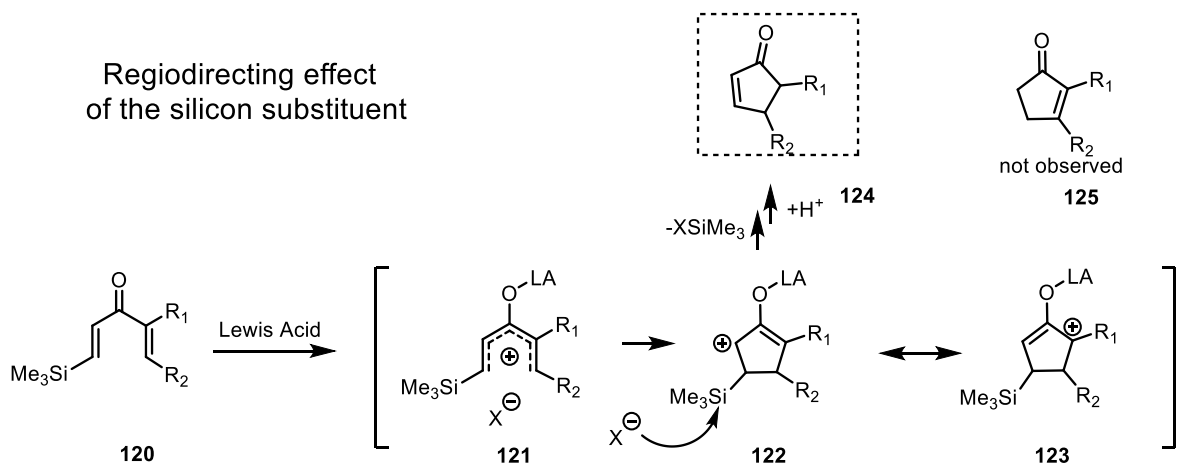
I.2.2. Directed Nazarov reactions

I.2.2.1. Silicon-directed Nazarov reactions

In the 1980s, Denmark *et al.* developed a silicon–directed Nazarov cyclization.⁴⁷ Indeed, the silicon atom makes it possible to control the position of the double bond, but also decreases the activation energy of this reaction by taking advantage of the β effect of silicon.⁴⁸ When a cross-conjugated dienone is substituted by a trimethylsilyl group (TMS) **120**, it is possible to orientate the position of the oxyallyl cation during the 4π electrocyclization process. The most stable carbocation is found β to the silicon **122**. After elimination, the less substituted, thermodynamically least stable regioisomer, **124**, is then obtained (**Scheme 34**).

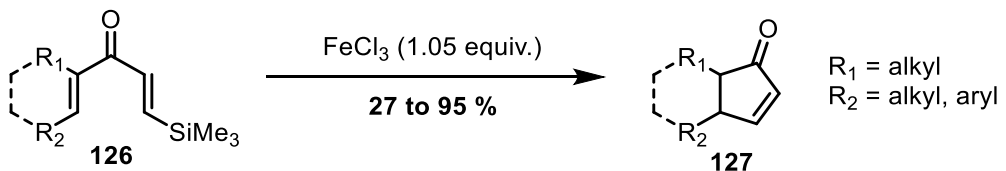
⁴⁷ S. E. Denmark, T. K. Jones, *J. Am. Chem. Soc.* **1982**, *104*, 2642-2645.

⁴⁸ W. P. Weber, In *Silicon reagents for organic synthesis.*; Springer-Verlag: Université du Michigan, **2012**; chapitre 1, 2.



Scheme 34: Mechanism of silicon-directed Nazarov cyclization.

Demark *et al.* determined optimal reaction conditions to obtain Nazarov product **127** by using iron(III) trichloride (FeCl_3) as a promoter. Dienone **126** (80 mM in CH_2Cl_2 or DCE or PhMe) was treated with FeCl_3 to provide cyclopentenones **127** with yields from 27 to 95% (**Scheme 35**).

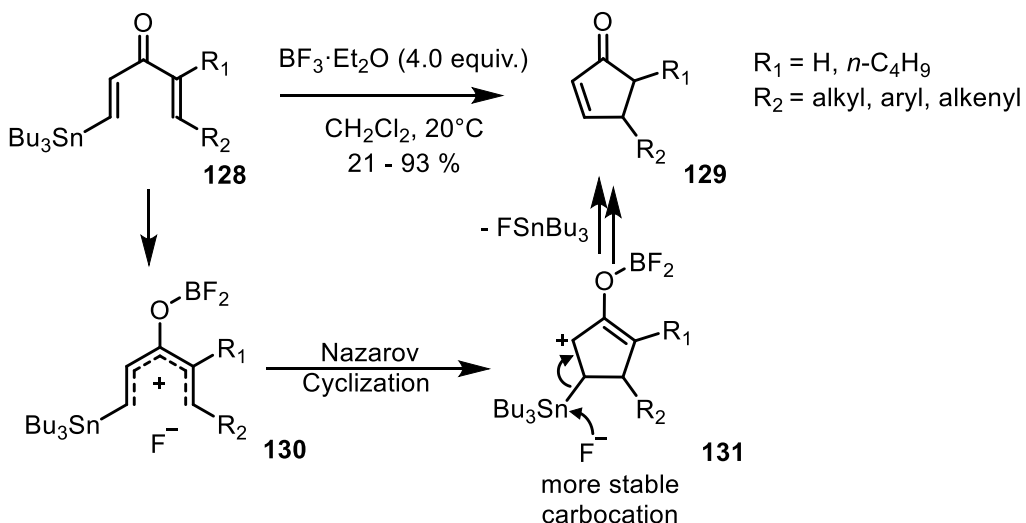


Scheme 35: FeCl_3 -promoted silicon-directed Nazarov cyclization.

1.2.2.2. Tin directed Nazarov reactions

Pee and Johnson developed a Nazarov cyclization using tin-substituted divinyl ketones as precursors.⁴⁹ Starting from cross-conjugated dienones **128** by treatment with boron trifluoride etherate ($\text{BF}_3 \cdot \text{OEt}_2$) in CH_2Cl_2 , 4,5-disubstituted cyclopentenones **129** were obtained with yields ranging from 21 to 93%. The tributyltin group stabilizes the β oxyallyl cation in a similar manner to that of the silyl group and thus directs the position of the double bond. By analogy with the work of Denmark, the elimination of tributyltin fluoride provides the less substituted alkene (**Scheme 36**)

⁴⁹ I. M. R. Pee, C. R. Johnson, *Tetrahedron Letters* **1986**, 27, 5947–5950.

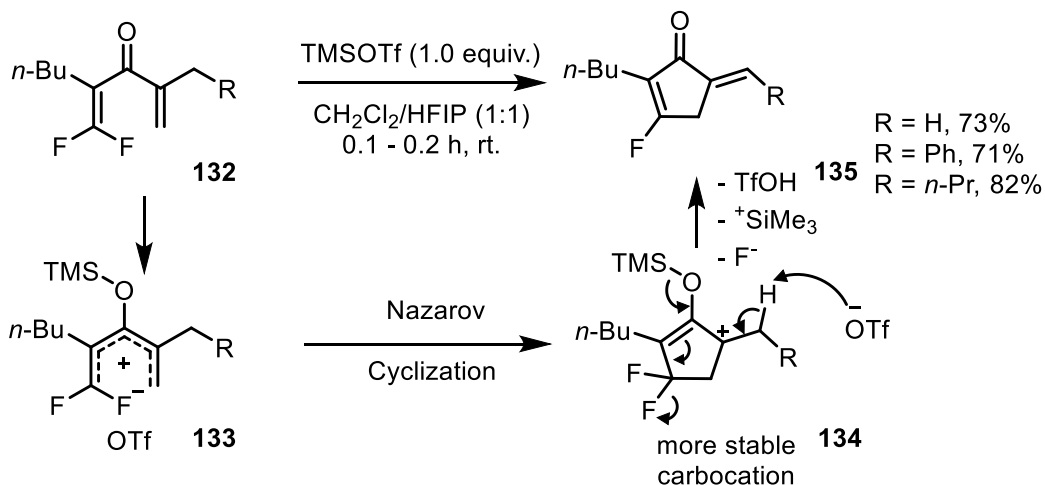


Scheme 36: Tin-directed Nazarov reaction.

I.2.2.3. Fluorine-directed Nazarov reactions

a. β -Fluorine-directed Nazarov reaction

Ichikawa *et al.* reported three new Nazarov reactions based on the electronic properties of fluorine to guide the Nazarov reaction.⁵⁰ Unlike the work of Denmark, Junji Ichikawa's team studied the destabilizing effect of the fluorine atom on a carbocation in a β position and the ability of this atom to be a good leaving group. β,β Difluorinated divinyl ketones **132** were treated with trimethylsilylfluoromethanesulfonate (TMSOTf) in a mixture of CH_2Cl_2 and hexafluoropropan-2-ol (HFIP) at room temperature. Alkenyl cyclopentenones **135** were obtained regioselectively with good yields (**Scheme 37**).^{50a}



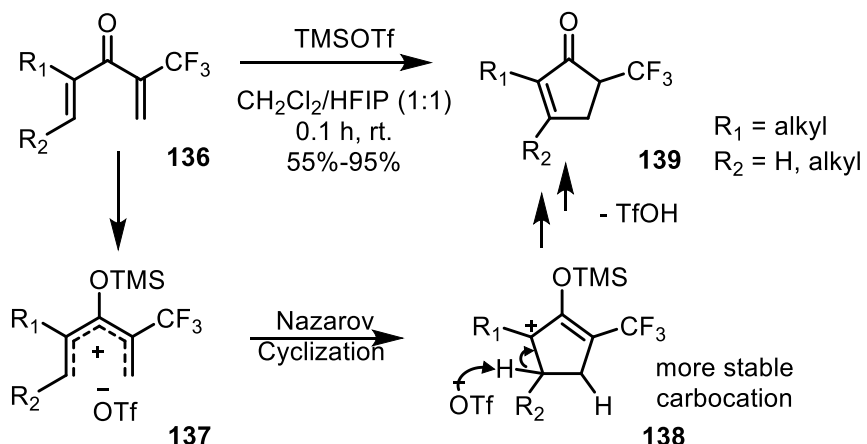
Scheme 37: β -Fluorine directed Nazarov reaction.

⁵⁰ J. Ichikawa, S. Miyazaki, M. Fujiwara, T. Minami, *J. Org. Chem.* **1995**, *60*, 2320–2321. J. Ichikawa, M. Fujiwara, T. Okauchi, T. Minami, *Synlett* **1998**, *8*, 927–929. J. Ichikawa, *Pure Appl. Chem.* **2000**, *72*, 1685–1689.

The influence of the fluorine atom has been demonstrated by using a non-fluorinated compound such as 2-butylcyclopentenone. In this case a mixture of three compounds was obtained (two endocyclic and one exocyclic compound).

b. Trifluoromethyl-directed Nazarov reaction

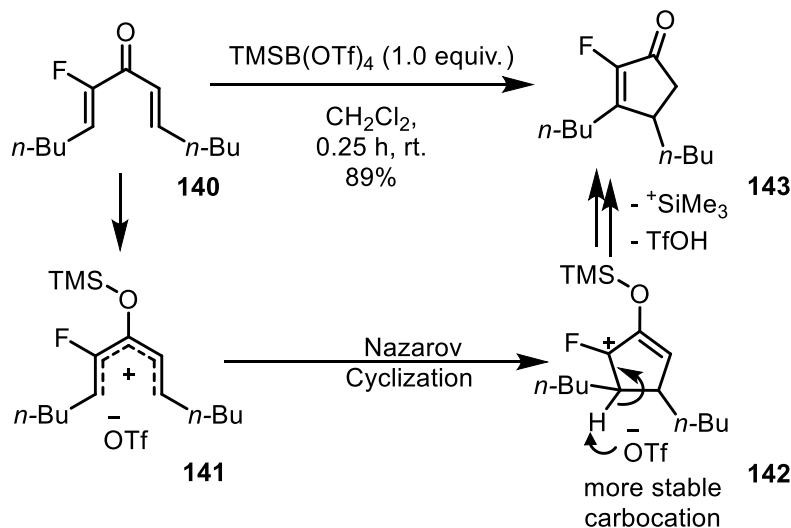
After this first work, Ichikawa *et al.* developed in 1998^{50b} a second Nazarov-type reaction, providing cyclopentenones substituted with a trifluoromethyl group (CF_3) **136**. In this case, the position of the double bond was defined by the electronic properties of the CF_3 group. The carbocation is thus destabilized in the β -position and directs the double bond to the distal position. Cyclopentenones **139** were obtained with yields ranging from 53 to 95% (**Scheme 38**).



Scheme 38: Trifluoromethyl-directed Nazarov reaction.

c. α -Fluorine-directed Nazarov reaction

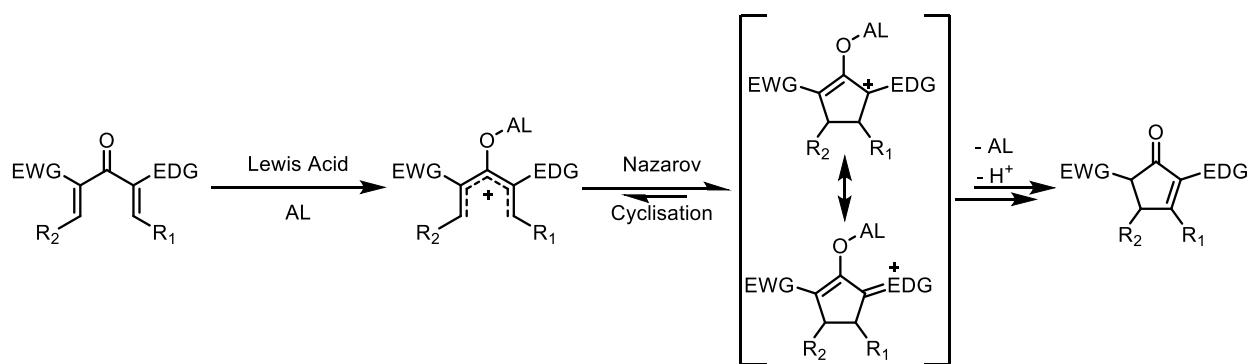
In 2000, Ichikawa *et al.*^{50c} developed a Nazarov reaction based on the stabilization of carbocations α to the fluorine atom through one of its non-bonding lone pairs. By treating the α -fluorinated dienone **140** in CH_2Cl_2 at room temperature with trimethylsilyl boron tetratriflate [$\text{TMSCl}(\text{OTf})_3$], the fluorocyclopent-2-one **141** was obtained with 89% yield with total control of regioselectivity (**Scheme 39**).



Scheme 39: α -Fluorine directed Nazarov reaction.

I.2.3. Polarized Nazarov cyclizations:

Another way to control the regioselectivity of the Nazarov cyclization is to use polarized dienones as starting substrates. Thus, in 2000 Alison J. Frontier *et al.* developed the concept of polarized Nazarov cyclizations by using divinyl ketones substituted in the α position on one side by an electron-donating group (EDG), and on the other side, by an electron-withdrawing group (EWG). This polarization confers a stabilization to one of the two mesomeric forms of the oxyallyl cation, thus directing the regioselectivity of the elimination of the β -proton (**Scheme 40**).⁵¹



Scheme 40: Regioselectivity of the polarized Nazarov reaction.

The influence of the presence of an EDG and an EWG was examined when the divinyl ketones were treated with copper(II) triflate in DCE to obtain cyclopentenones **145a-d**. If the substrate is not substituted by an EDG nor an EWG, the efficiency of the Nazarov cyclization is less than 50% (**Table 1, Entry 4**). Adding only an EDG allows a yield of 60% after 0.5 h (**Table 1, Entry 2**), while with only an EWG, similar yields were obtained but with an extended reaction time of 14 h (**Table 1, Entry 3**). This observation was attributed to the

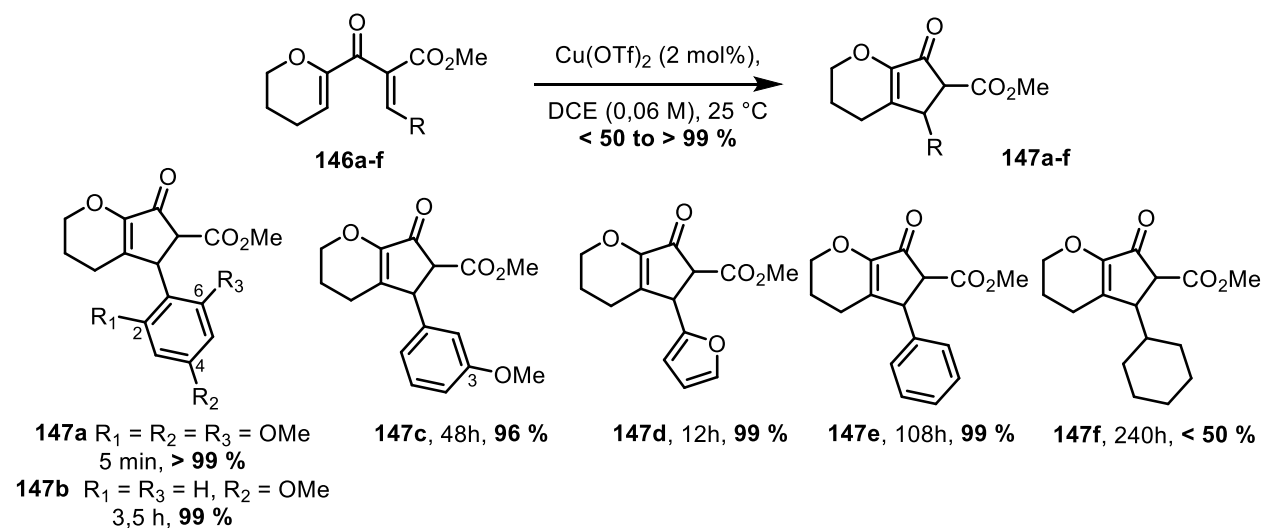
⁵¹ W. He, X. Sun, A. J. Frontier, *J. Am. Chem. Soc.* **2003**, 125, 14278–14279.

stabilization of the carbocation by the EDG. The simultaneous substitution of an EDG and an EWG allows quantitative yields after 2 h (**Table 1, Entry 1**).

 144a-d	145a-d						
Entry n°	Product	X	R ₁	R ₂	T °C	Time (h)	% Yield
1	144a	O	CO ₂ Me	C ₆ H ₁₁	55	2	> 99
2	144b	O	H	C ₆ H ₁₁	55	0.5	60
3	144c	CH ₂	CO ₂ Me	C ₆ H ₁₁	65	14	70
4	144d	CH ₂	H	C ₆ H ₁₁	65	4	37 – 42

Table 1 : Influence of the presence of EDGs and EWGs on the Nazarov cyclization

The use of the polarized Nazarov reaction allows total regioselectivity regarding the position of the double bond. The study of the scope of the reaction has shown that the more the electrophilic double bond is stabilized, the faster the reaction. Indeed, a substitution in the β -position (electrophilic vinyl) by an electron-rich group increases the efficiency of the reaction as shown by the quantitative formation of **147a** in five minutes with similar yield for **147b** in 3.5 hours. Switching from a mesomeric donor group to an inductive donor group decreases the efficiency of the reaction as shown by the synthesis of **147a-e** and **147f** (**Scheme 41**).

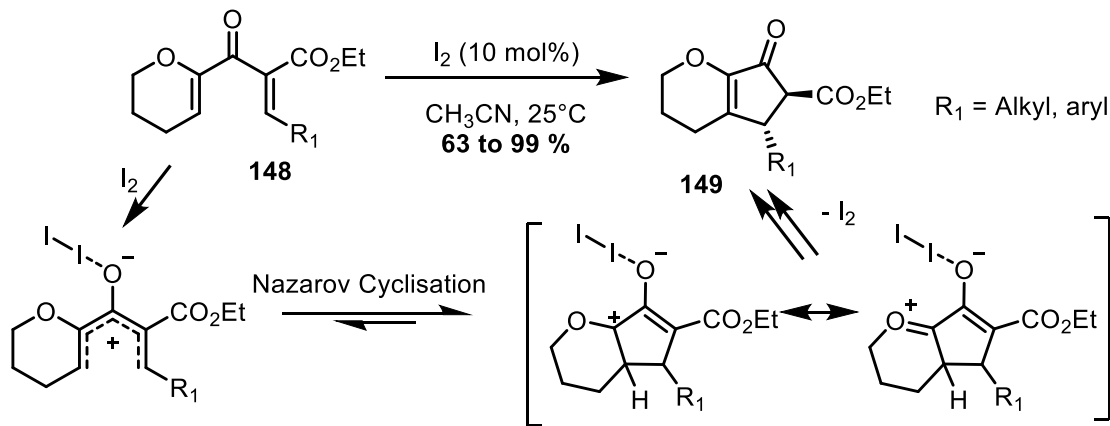


Scheme 41: Influence of stabilization of the electrophilic double bond

Since the pioneering work of Alison J. Frontier, numerous other polarized Nazarov reactions have been developed.⁵²

⁵² C. Bee, E. Leclerc, M. A. Tius, *Org. Lett.* **2003**, 5, 4927–4930. G.-X. Liang, S. N. Gradi, D. Trauner, *Org. Lett.* **2003**, 5, 4931–4934. S. Raja, W. Ieawsuwan, V. Korotkov, M. Rueping, *Chem Asian J.* **2012**, 7, 2361–2366. M. Hoffmann, J.-M. Weibel, P. Frémont, P. Pale, A. Blanc, *Org. Lett.* **2014**, 16, 908–911. V. K. Aggarwal, A. J. Belfield, *Org. Lett.* **2003**, 5, 5075–5078. G. Liang, D. Trauner, *J. Am. Chem.*

Koenig *et al.*⁵³ developed a method involving molecular iodine under mild conditions. By treating polarized divinyl ketones **148** with a catalytic amount of I₂, it is possible to obtain cyclopentenones **149** with total regio- and diastereoccontrol with yields ranging from 63 to 99%. These authors observed the same tendency in terms of reactivity as Frontier's group, i.e., the more the electrophilic double bond is stabilized, the more efficient the reaction (**Scheme 42**).



Scheme 42: Polarized Nazarov reaction catalyzed by molecular iodine

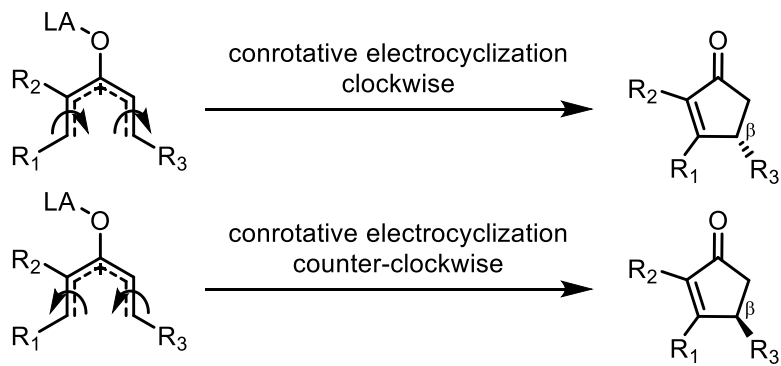
I.2.4. Asymmetric Nazarov reactions

I.2.4.1. Torquoselectivity

According to the Woodward-Hoffmann rules⁵⁴ and regarding the conservation of orbital symmetry during pericyclic reactions, electrocyclizations involving 4n electrons of π orbitals are dictated by a conrotatory mechanism under thermal conditions. For the rotatory mode, two directions of rotation are possible - the rotation can be clockwise or counterclockwise. This is referred to as the torquoselectivity. The control of the direction of rotation depends on the absolute configuration of the β -carbon in the product of the Nazarov reaction, whereas the absolute configuration of the α -carbon depends on the facial selectivity of the enolate protonation (**Scheme 43**).

Soc. **2004**, 126, 9544–9545. M. Rueping, W. Leawsuwan, A. P. Antonchick, B. J. Nachtsheim, *Angew. Chem. Int. Ed.* **2007**, 46, 2097–2100. I. Walz, A. Togni, *Chem. Commun.* **2008**, 4315–4317. A. K. Basak, N. Shimada, W. F. Bow, D. A. Vicic, M. A. Tius, *J. Am. Chem. Soc.* **2010**, 132, 8266–8267. W. F. Bow, A. K. Basak, A. Jolit, D. A. Vicic, M. A. Tius, *Org. Lett.* **2010**, 12, 440–443. G. E. Hutson, Y. E. Turkmen, V. H. Rawal, *J. Am. Chem. Soc.* **2013**, 135, 4988–4991. A. Jolit, P. M. Waller, G. P. A. Yap, M. A. Tius, *Angew. Chem. Int. Ed.* **2014**, 53, 6180–6184. K. Kitamura, N. Shimada, C. Stewart, A. C. Atesin, T. A. Atesin, M. A. Tius, *Angew. Chem., Int. Ed.* **2015**, 54, 6288–6291. G.-P. Wang, M.-Q. Chen, S.-F. Zhu, Q.-L. Zhou, *Chem. Sci.*, **2017**, 8, 7197–7202. J. Jin, Y. Zhao, A. Gouranourimi, A. Ariafrad, P. W. H. Chan, *J. Am. Chem. Soc.* **2018**, 140, 5834–5841. T. Mietke, T. Cruchter, V. A. Larionov, T. Faber, K. Harms, E. Meggers, *Adv. Synth. Catal.* **2018**, 360, 2093–2100. L. Suisse, M. Vogler, M. Mewald, B. Kemper, E. Irran, M. Oestreich, *Angew. Chem. Int. Ed.* **2018**, 57, 11441–11444.
⁵³ Koenig, J. J. Arndt, T. Gildemeister, N., Neudörfl, J.-M. Breugst, M. J. Org. Chem. **2019**, 84, 7587–7605.

⁵⁴ Woodward, R. B., Hoffmann, R. *Angew. Chem. Int. Ed.* **1969**, 8, 781–853.



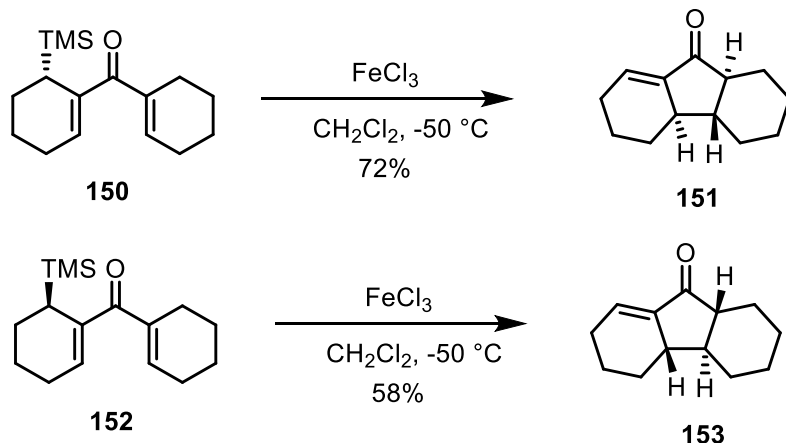
Scheme 43: Torquoselectivity

Many asymmetric Nazarov reactions have been developed in recent decades.⁵⁵ Two strategies can be distinguished: the cyclization in which the source of chirality is present on the substrate or a cyclization where this source is external.

I.2.4.2. Internal source of chirality

a. Traceless chirality

Denmark's group, during their studies on silicon-directed Nazarov cyclizations, revealed the first example of chirality transfer in their reaction. The enantiomerically enriched β -silyldivinyl ketones **150** and **152** each formed an enantiomer of tricyclic product **151** and **153** without loss of enantiomeric excess compared to the starting substrate (**Scheme 44**).⁵⁶



Scheme 44: Traceless chirality

The direction of rotation is dictated by the geometry of the TMS-group, which allows continuous orbital overlap of the C-Si bond with the oxyallyl cation. The TMS group being eliminated by the chloride ion at the end of the process, induces a «traceless» chirality transfer.

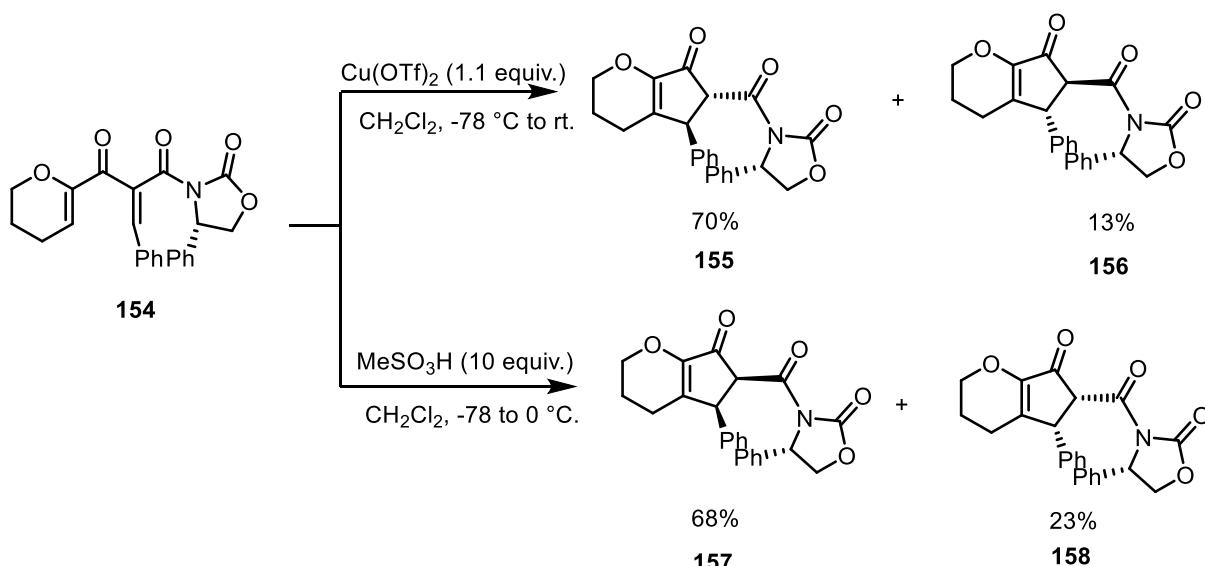
⁵⁵ G. Liang, S. N. Gradl, D. Trauner, *Org. Lett.* **2003**, 5, 4931–4934. K. Yaji, M. Shindo, *Synlett* **2009**, 2524–2528. M. Kawatsura, K. Kajita, S. Hayase, T. Itoh, *Synlett* **2010**, 1243–1246. P. E. Harrington, T. Murai, C. Chu, M. A. Tius, *J. Am. Chem. Soc.* **2002**, 124, 10091–10100.

⁵⁶ Denmark, S. E. Wallace, M. A. Walker, C. B., *J. Org. Chem.* **1990**, 55, 5543–5545.

b. Evans chiral oxazolidinones to induce chirality

In 1999, Lendon Pridgen introduced the potential of Evans's oxazolidinones to induce chirality in Nazarov reactions.⁵⁷

About ten years later, Flynn's group reported further examples of torque-selective Nazarov cyclisations based upon oxazolidinones. They reported an example of *cis/trans* selectivity for the transformation of divinyl ketone **154** by tuning the acid involved. The reaction, carried out from -78 °C to room temperature with a Lewis acid such as copper(II) triflate, led to the thermodynamically more stable *trans* compounds **155** and **156** in 83% overall yields as determined by NMR. In contrast, the use of a Brønsted acid such as methanesulfonic acid from -78 °C to 0 °C resulted in the formation of the kinetic *cis* compounds **157** and **158** with 91% overall yield (**Scheme 45**).



Scheme 45: Evans chiral oxazolidinones to induce chirality

The temperature is a key parameter in this case, because when the reaction is carried out in the presence of methanesulfonic acid and brought to room temperature, the *trans* compounds are obtained. These results must be qualified in terms of the modest effectiveness of the chiral inducer regarding the selectivity of the stereogenic center bearing the phenyl group. In this work, in both cases (for *trans* and *cis* stereoisomers), the yield of the major compound does not exceed 70%, resulting in a modest torque-selectivity.

In the enamide-assisted Nazarov cyclizations section below, the nature of these phenomena will be discussed in terms of how these observations were the source of new investigations by this Australian group. Specifically, they found that by bringing the chiral inducer nearer to the created stereogenic center, very high stereoselectivity were achieved (see Section II.7.1.1)

⁵⁷ L. N. Pridgen, K. Huang, S. Shilcrat, A. Tickner-Eldridge, C. DeBrosse, R. C. Haltiwanger, *Synlett* **1999**, 10, 1612-1614.

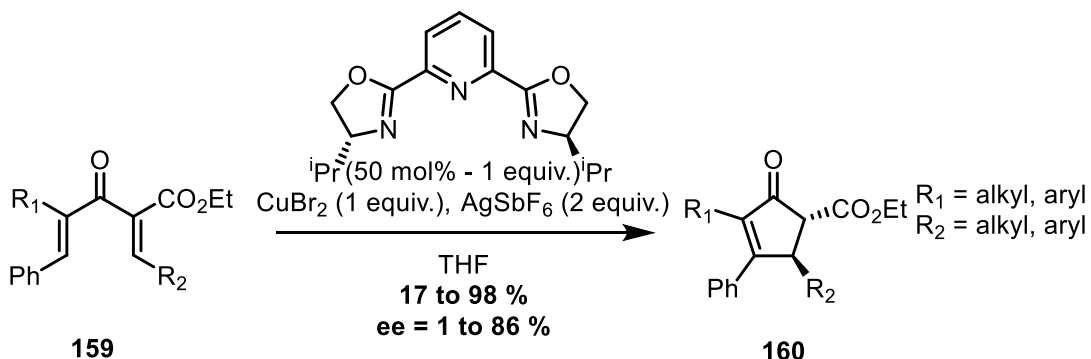
I.2.4.3. External source of chirality

The introduction of a chiral reagent to induce facial selectivity is a good way to control the torquoselectivity of the Nazarov reaction. External sources of chirality can be organometallic catalysts (Lewis acids) or Brønsted acids, for example.

a. With Lewis acids

In 2003, Aggarwal *et al.* and Trauner *et al.* were the first to develop organometallic complexes to control stereochemistry in the Nazarov reaction by using chiral ligands such as pyridyl-bisoxazolines (PyBOX) coordinated to Lewis acids.

Aggarwal *et al.*⁵⁸ used divinyl ketones **159** substituted with an ester group in the α position. Treatment with a copper complex made it possible to obtain the corresponding cyclopentenones **160**. The authors determined that the more bulky the substituents R₁ and R₂, the greater the enantioselectivity. In fact, the steric interactions between these two groups and the isopropyl group present on the ligand during the transition state control the torquoselectivity (**Scheme 46**). However, in some cases it is necessary to introduce stoichiometric amounts of coordination complexes to obtain acceptable yields.

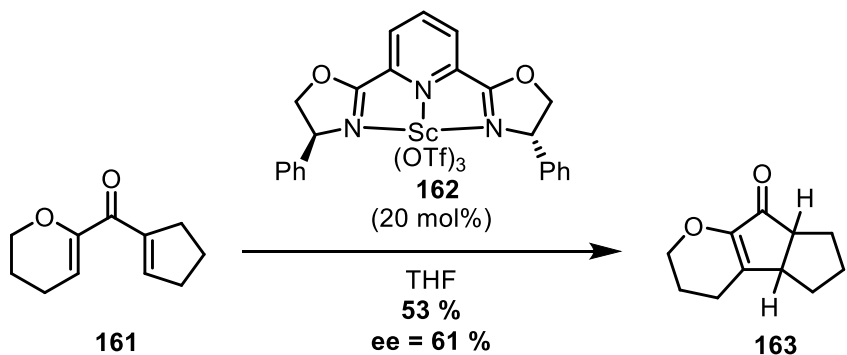


Scheme 46: Chiral induction by a Cu-PyBOX complex

Trauner *et al.*⁵⁹ demonstrated the use of a PyBOX-scandium(III) complex **162** in the synthesis of tricyclic system **163**. The reaction was carried out with 20 mol% of complex **162**. The yield as well as the enantiomeric excess are moderate. The configuration of the major enantiomer obtained was not described (**Scheme 47**).

⁵⁸ V. K. Aggarwal, A. J. Belfield, *Org. Lett.* **2003**, 5, 5075–5078.

⁵⁹ G. Liang, S. N. Gradl, D. Trauner, *Org. Lett.* **2003**, 5, 4931–4934.

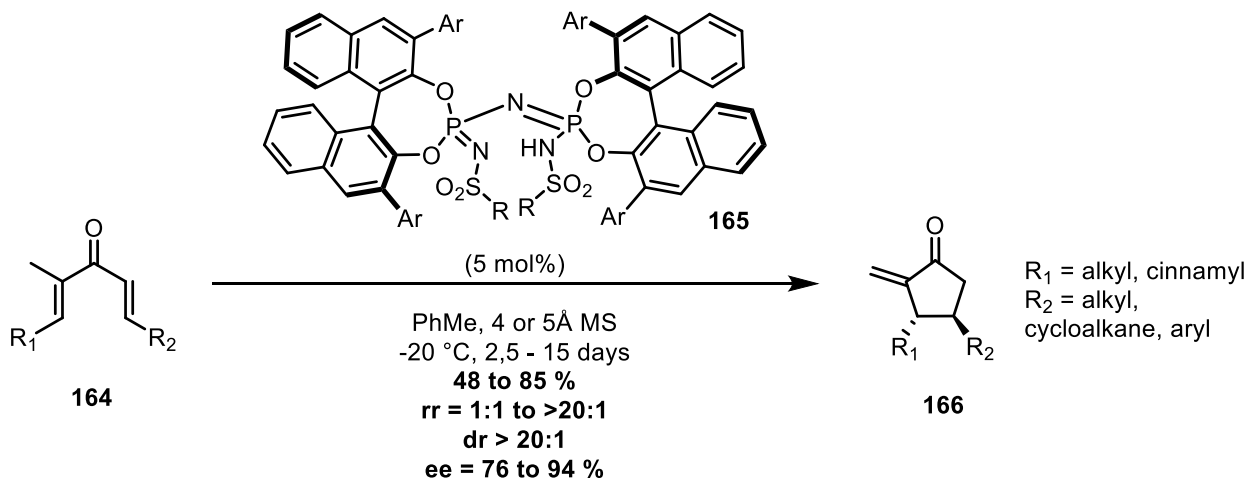


Scheme 47: Enantioselective synthesis of a tricyclic derivative

b. With Brønsted acids

Recently List's group published the use of a strong, sterically rigid acid to promote asymmetric Nazarov cyclizations.⁶⁰ The use of an imidodiphosphorimidate known as a strong, chiral Brønsted acid favors the active conformation of dienone **164** (*s-trans/s-trans*) and increases the reaction kinetics while inducing enantioselectivity.

By treating dienones **164** with a catalytic amount of chiral Brønsted acid **165** in toluene at 20 °C, cyclopentenones **166** were obtained. This method tolerates a large number of groups at both R₁ and R₂ such as aliphatic chains, cycloalkanes, and aromatic derivatives, while allowing almost exclusive access to the trans diastereoisomer (dr > 20 :1). Thanks to the geometry of the catalyst, the least substituted double bond [regiometric ratio (rr) 1 :1 to >20 :1] is obtained. Cyclopentenones **166** were synthesized with very good enantiomeric excesses ranging from 76 to 94 % (**Scheme 48**).

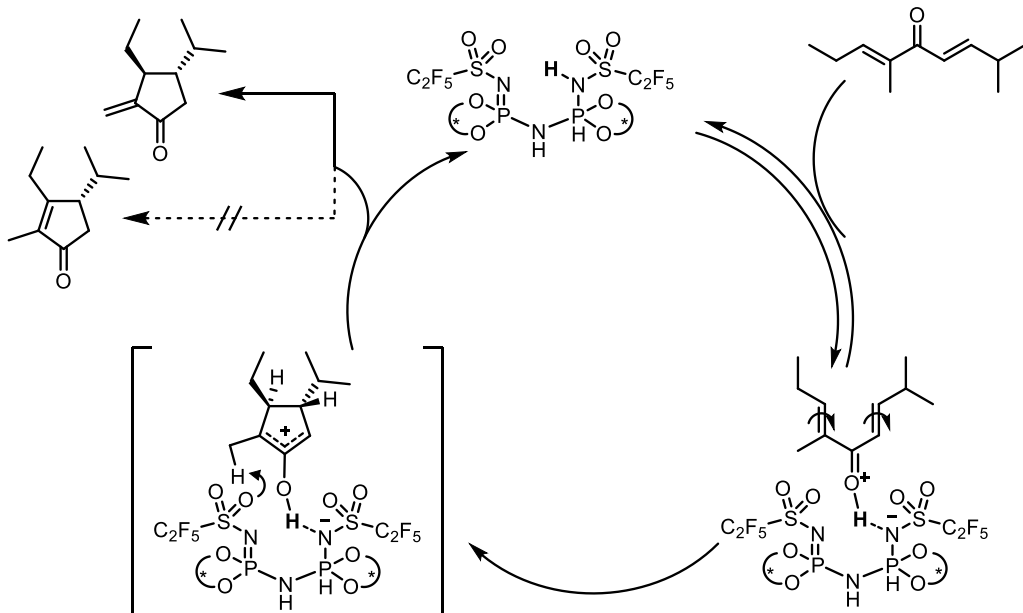


Scheme 48: Using a chiral Brønsted acid for the Nazarov reaction

The following mechanism was proposed by the authors to explain the regio- and enantioselectivities observed.

⁶⁰ J. Ouyang, J. L. Kennemur, C. K. De, C. Farès, B. List, *J. Am. Chem. Soc.* **2019**, *141*, 3414–3418.

First, the divinyl ketone is protonated thanks to the sulfonamide proton, and the chirality of the catalyst induces the active configuration of the divinyl ketone. Then, the 4-electron π electrocyclization takes place clockwise to form the oxyallyl cation. Deprotonation is driven by the oxygen basicity of the sulfonamide and thus directs the reaction toward the formation of the exocyclic cyclopentenone, where two stereogenic centers are created (**Scheme 49**).



Scheme 49: Mechanism of the Brønsted-catalyzed Nazarov reaction

I.2.5. Application of the Nazarov reaction in the total synthesis of natural products

Numerous total syntheses of natural products involving a Nazarov cyclization have been developed.⁶¹

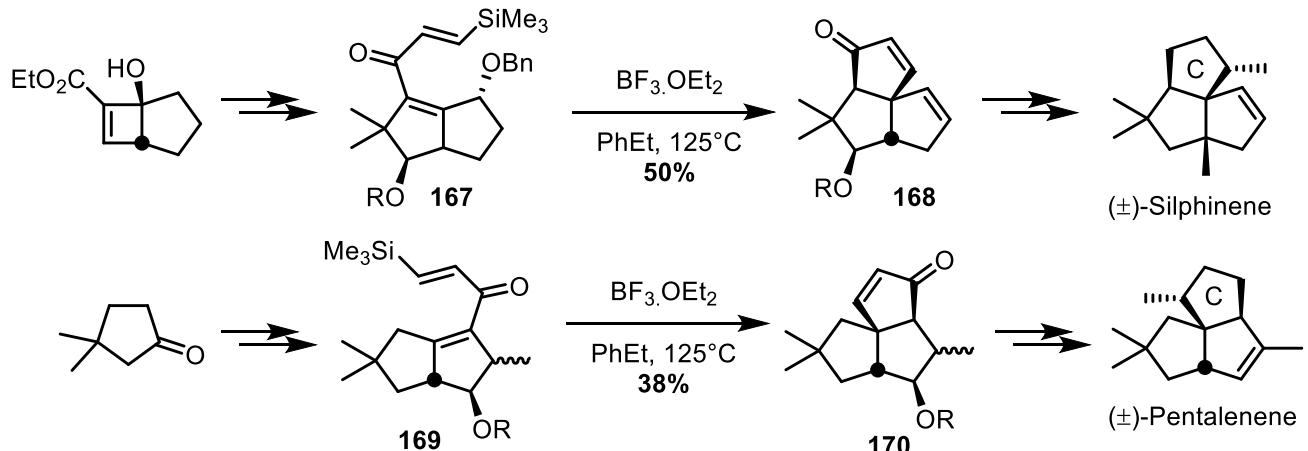
I.2.5.1. Total synthesis of (\pm) -Silphinene and (\pm) -Pentalenene

Our team developed two synthetic pathways for the total synthesis of (\pm) -Silphinene⁶² and (\pm) -Pentalenene⁶³ involving a silicon-directed Nazarov reaction. These two trquinanes were

⁶¹ M. G. Vinogradov, O. V. Turova, S. G. Zlotin, *Org. Biomol. Chem.* **2017**, *15*, 8245–8269. J. Bergman, L. Venemalm, *Tetrahedron* **1992**, *48*, 759–768. J. Motoyoshiya, T. Hara, N. Takahashi, M. Hirai, T. Moriwake, *Synlett.* **1993**, *3*, 237–238. A. F. Mateos, E. Martín de la Nava, G. P. Coca, A. R. Silvo, R. R. González, *Synlett.* **1998**, *8*, 1372–1374. A. F. Mateos, E. M. Martín de la Nava, and R. R. González, *J. Org. Chem.* **2001**, *66*, 7632–7638. D. L. J. Clive, M. Sannigrahi, S. Hisaindee, *J. Org. Chem.* **2001**, *66*, 954–961. P. Kraft, R. Cadalbert, *Synthesis* **2002**, *34*, 2243–2253. W.-D. Z. Li, Y.-Q. Wang, *Org. Lett.* **2003**, *5*, 2931–2934. A. F.-Mateos, L. M. Burón, E. M. Martín de la Nava, R. R. González, *J. Org. Chem.* **2003**, *68*, 3585–3592. L.-F. Wan, M. A. Tius, *Org. Lett.* **2007**, *9*, 647–650. K. Yaji, M. Shindo, *Tetrahedron Letters* **2010**, *51*, 5469–5472. K. Yaji, M. Shindo, *Tetrahedron* **2010**, *66*, 9808–9813. W.-D. Z. Li, W.-G. Duo, C.-H. Zhuang, *Org. Lett.* **2011**, *13*, 3538–3541. B. J. Moritz, D. J. Mack, L. Tong, R. J. Thomson, *Angew. Chem. Int. Ed.* **2014**, *53*, 2988–2991. K. Morisaki, Y. Sasano, T. Koseki, T. Shibuta, N. Kanoh, W.-H. Chiou, Y. Iwabuchi, *Org. Lett.* **2017**, *19*, 5142–5145. Y.-L. Que, H. Shao, H.-B He, S.-H Gao, *Angew. Chem. Int. Ed.* **2020**, *29*, 7444–7449.

⁶² M. Miesch, L. Miesch-Gross, M. Franck-Neumann, *Tetrahedron* **1997**, *53*, 2103–2110.

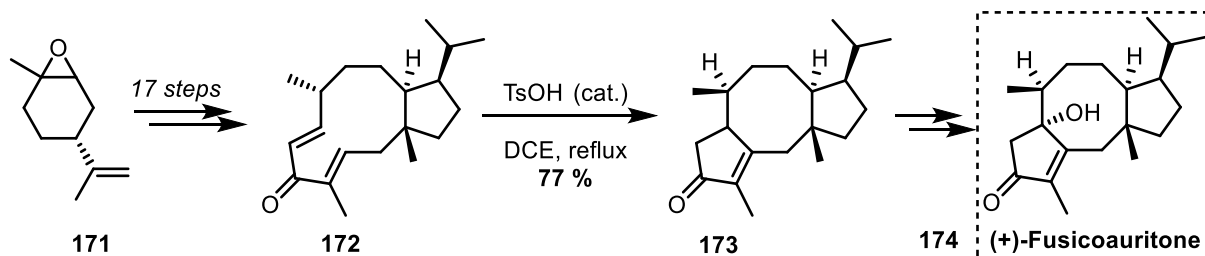
isolated from a perennial plant in North America (*Silphium perfoliatum*) and a bacterium (*streptomyces griseochromogenes*), respectively. The strategy proposed used divinyl ketones **167** and **169** substituted at the β -position by a TMS group, which makes it possible through Nazarov cyclization with $\text{BF}_3 \cdot \text{OEt}_2$ in ethylbenzene at reflux to introduce the C ring present in the natural products (**Scheme 50**).



Scheme 50: Total synthesis of (\pm)-Silphinene and (\pm)-Pentalenene

I.2.5.2. Total synthesis of (+)-Fusicoauritone

In 2007, Williams *et al.* reported the total synthesis of (+)-Fusicoauritone starting from optically pure epoxide **171**. To achieve the ring contraction with control of the enone regiochemistry, divinyl ketone **172** was prepared and treated with triflic acid (TsOH) in DCE at reflux. As such, the complete tricyclic scaffold present in (+)-Fusicoauritone was obtained with 77% yield (**Scheme 51**).⁶⁴



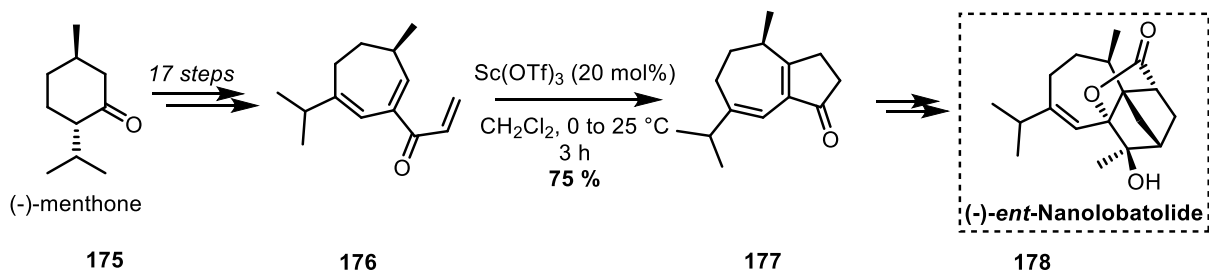
Scheme 51: Total synthesis of (+)-Fusicoauritone

⁶³ M. Miesch, L. Miesch-Gross, M. Franck-Neumann, *Tetrahedron* **1997**, *53*, 2111–2118.

⁶⁴ D. R. Williams, L. A. Robinson, C. R. Nevill, J. P. Reddy, *Angew. Chem. Int. Ed.* **2007**, *46*, 915–918.

I.2.5.3. Total synthesis of ent-Nanolobatolide

In the synthesis of ent-Nanolobatolide reported by Chen *et al.* trienone **175** was the best choice to construct the cyclopentenone ring via scandium triflate $[\text{Sc}(\text{OTf})_3]$ -catalyzed Nazarov cyclization leading to dienone **177** in 75% yield (**Scheme 52**).⁶⁵



Scheme 52: Total synthesis of ent-Nanolobatolide

I.2.5.4. Total synthesis of Englerin A

Englerin A is a biomolecule extracted in 2009 by Beutler *et al.* from the bark of *Phyllanthus Engleri*, a plant found in East Africa. Englerin A is a sesquiterpene, belonging to the guaianas family which has anti-cancer properties that are selective for kidney cancer. This compound is characterized by an 8-oxabicyclo [3.2.1] octane molecular substructure (**Figure 7**).⁶⁶

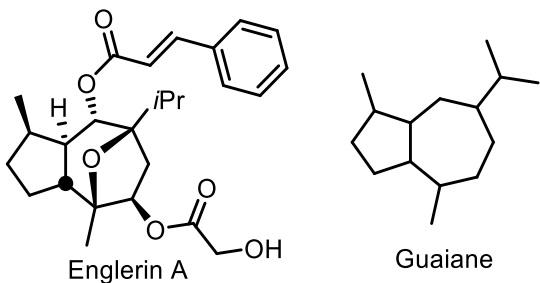


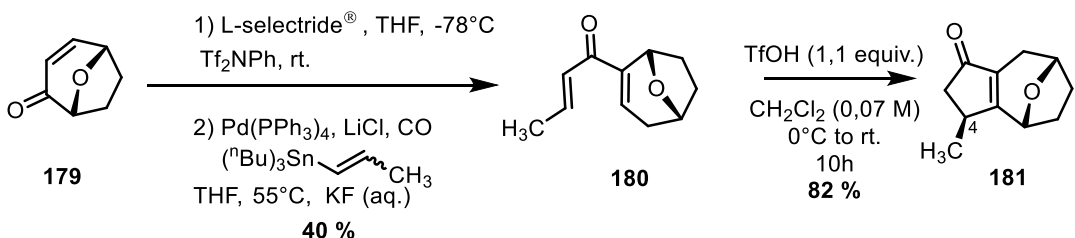
Figure 7: Englerin A and Guaiane

Iwabuchi *et al.* developed a diastereoselective pathway for bicyclo[5.3.0]decanes involving a Nazarov reaction. The precursor of the Nazarov reaction, **180**, was obtained from oxabicyclooctene **179** after 1,4 addition of a hydride using L-Selectride® and subsequent trapping of the enol by a triflate group. Carbonylative Stille cross-coupling led to cross-conjugated dienone **180** in 40% yield after isomerization. The Nazarov cyclization was then carried out using triflic acid to yield cyclopentenone **181** in 82% yield (**Scheme 53**).⁶⁷

⁶⁵ H. M. Cheng, W. Tian, P. A. Peixoto, B. Dhudshia, D. Y.-K. Chen, *Angew. Chem. Int. Ed.* **2011**, *50*, 4165–4168.

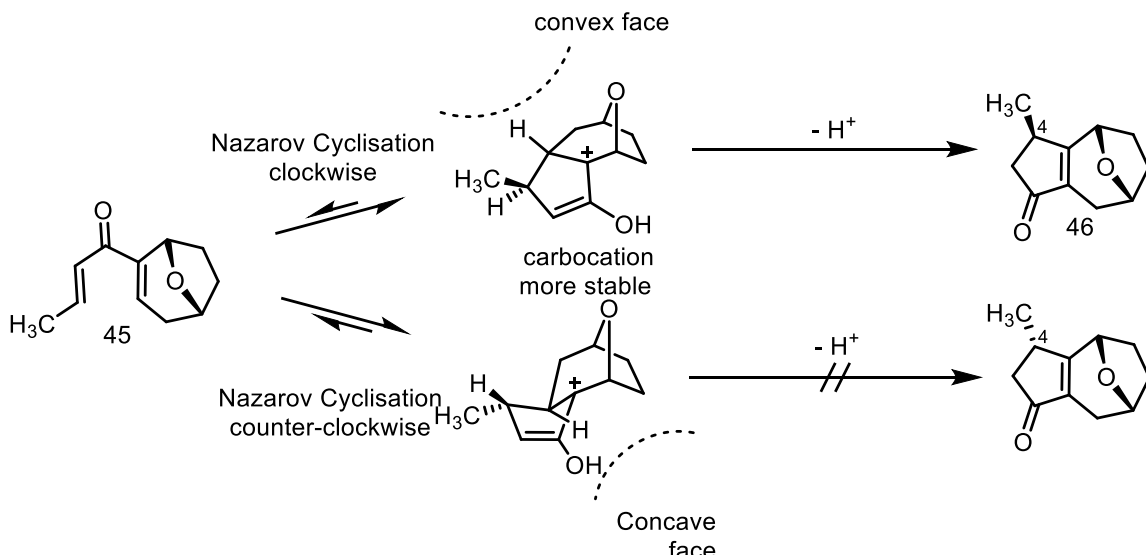
⁶⁶ R. Ratnayake, D. Covell, T. T. Ransom, K. R. Gustafson, J. A. Beutler, *Org. Lett.* **2009**, *11*, 57–60.

⁶⁷ K. Morisaki, Y. Sasano, T. Koseki, T. Shibuta, N. Kanoh, W.-H. Chiou, Y. Iwabuchi, *Org. Lett.* **2017**, *19*, 5142–5145.



Scheme 53: Iwabuchi's strategy to prepare guaiane compound **181**

This reaction allows full control of the stereochemistry of carbon 4 during the Nazarov cyclization. The authors explained this torquoselectivity by the fact that only the proton located on the convex face of the molecule can be eliminated (**Scheme 54**).



Scheme 54: Explanation proposed for the torquoselectivity observed.

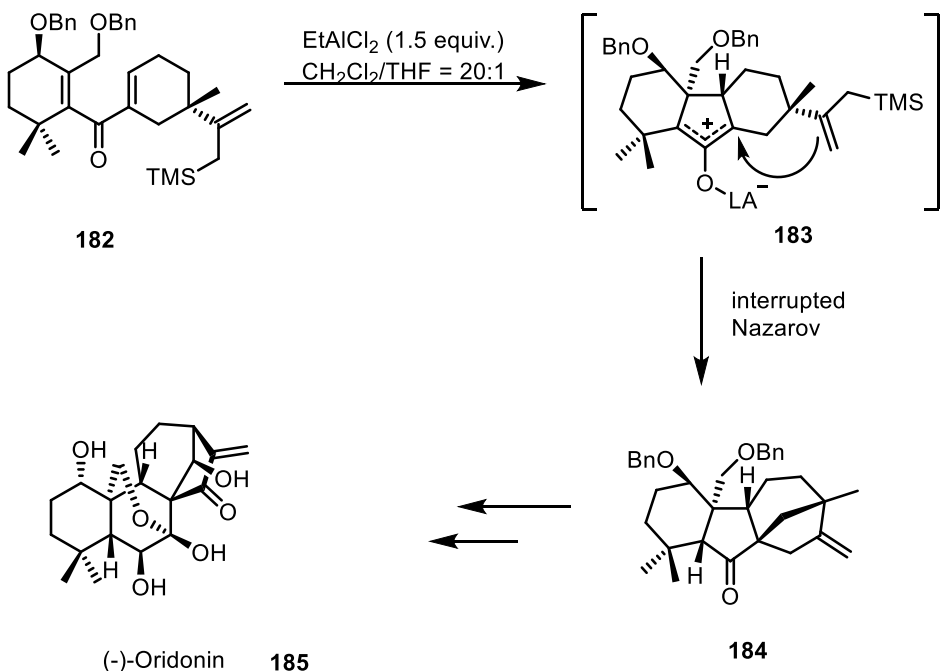
1.2.5.5. Total synthesis of (-)-Oridonin

Luo *et al.* reported in 2019 an interrupted-Nazarov approach for the total synthesis of (-)-Oridonin. The interrupted-Nazarov cyclization stands for a domino reaction involving the electrocyclic ring closure of a dienone to form the cyclopentenyl cation as the first step. In the interrupted Nazarov reaction, a nucleophilic trapping of the cyclopentenyl cation occurs, giving rise to substituted cyclopentanones with the creation of up to four new stereocenters.⁶⁸

The torquoselectivity observed during the conrotatory ring closure in this EtAlCl₂-triggered Nazarov reaction was rationalized by the steric interactions of the OBn groups at position C1 and C20 of the divinyl ketone **182**. During the formation of the interrupted Nazarov compound **183**, the π -nucleophile, allylsilane, smoothly approached C8 *anti* to the adjacent C9 hydrogen in compound **183** (**Scheme 55**).⁶⁹

⁶⁸ T. N. Grant, C. J. Rieder, F. G. West, *Chem. Commun.* **2009**, 5676–5688. A. V. Yadykov, V. Z. Shirinian, *Adv. Synth. Catal.* **2020**, 362, 702–723.

⁶⁹ L.-R. Kong, F. Su, H. Yu, Z. Jiang, Y.-D. Lu, T.-P. Luo, *J. Am. Chem. Soc.* **2019**, 141, 20048–20052.



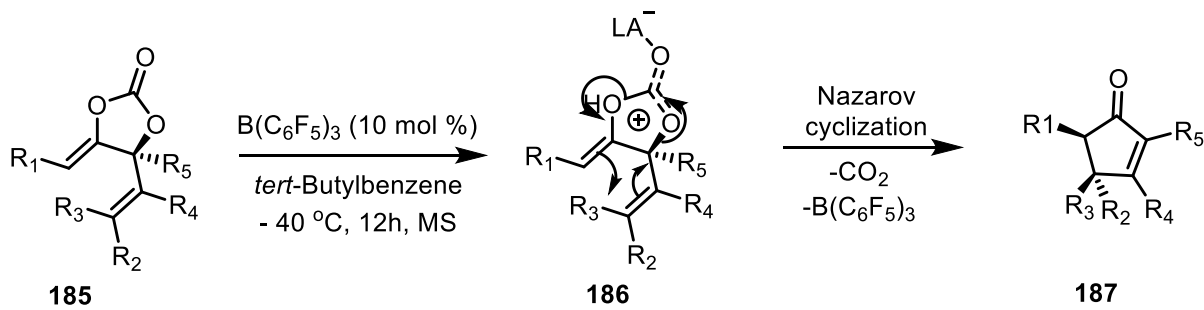
Scheme 55: Total synthesis of (-)-Oridonin

I.2.6. Recent trends for the Nazarov reaction

Recent trends for the Nazarov reaction show that this transformation still occupies a prominent position in the organic chemistry toolbox.

I.2.6.1. Decarboxylative Nazarov cyclization

In 2019, Yamada's team reported a decarboxylative Nazarov cyclization of optically active cyclic enol carbonates. B(C₆F₅)₃-Catalyzed decarboxylative Nazarov cyclization was achieved with yields ranging from 65 to 99%. The stereochemical outcome at the 4,5-position of the cyclopentenones obtained was elucidated by determining the stereochemistry of the starting material and the products.⁷⁰

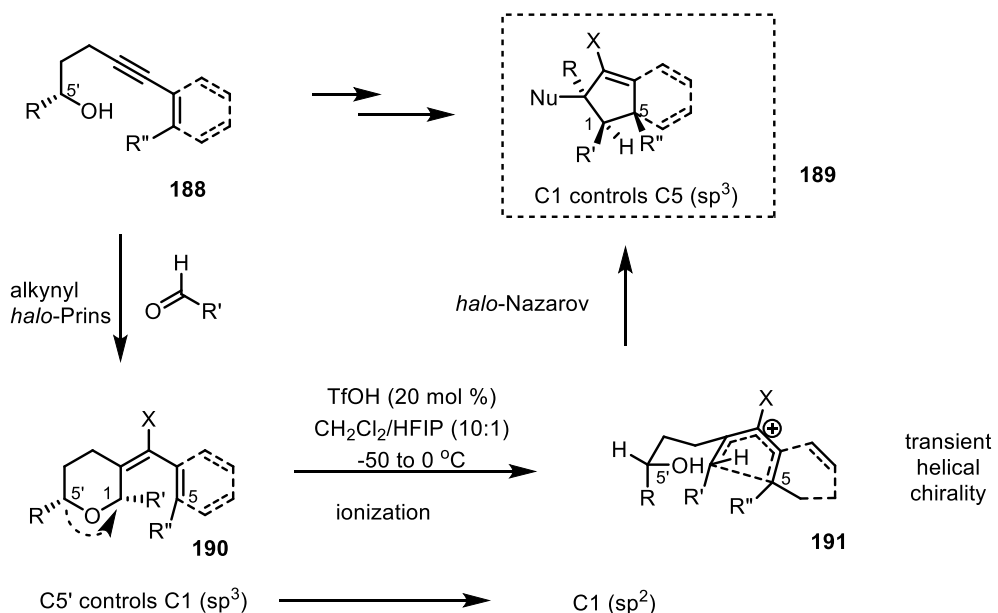


Scheme 56: Decarboxylative Nazarov cyclization

⁷⁰ K. Komatsuki, A. Kozuma, K. Saito, T. Yamada, *Org. Lett.* **2019**, 21, 6628–6632

I.2.6.2. Halo-Prins/halo-Nazarov cyclization

In 2020, Alison Frontier *et al.* reported a halo-Prins/halo-Nazarov cyclization with memory of chirality. The diastereoselective alkynyl Prins cyclization provided a dihydropyran intermediate with a curved backbone. The specific helical alignment of this chiral precursor dictates the direction of the electrocyclization. The authors claim that despite the loss of the sp^3 stereogenic center during ionization, the low halo Nazarov barrier enables efficient capture of the cation with dynamic conformational chirality. In fact, the chiral information from secondary alcohol **188** is relayed throughout the whole process.⁷¹



Scheme 57: Halo-Prins/halo-Nazarov cyclization

I.2.7. Tertiary enamide/enamine promoted Nazarov cyclizations

To overcome the relatively low reactivity of divinyl ketones, these substrates have been activated by adjacent heteroatoms to stabilize the oxyallyl cation. Taking into account our project, we will exclusively focus on nitrogen-substituted divinyl ketones for the Nazarov cyclization.

I.2.7.1. α -Aza-substituted divinyl ketones for the Nazarov cyclization

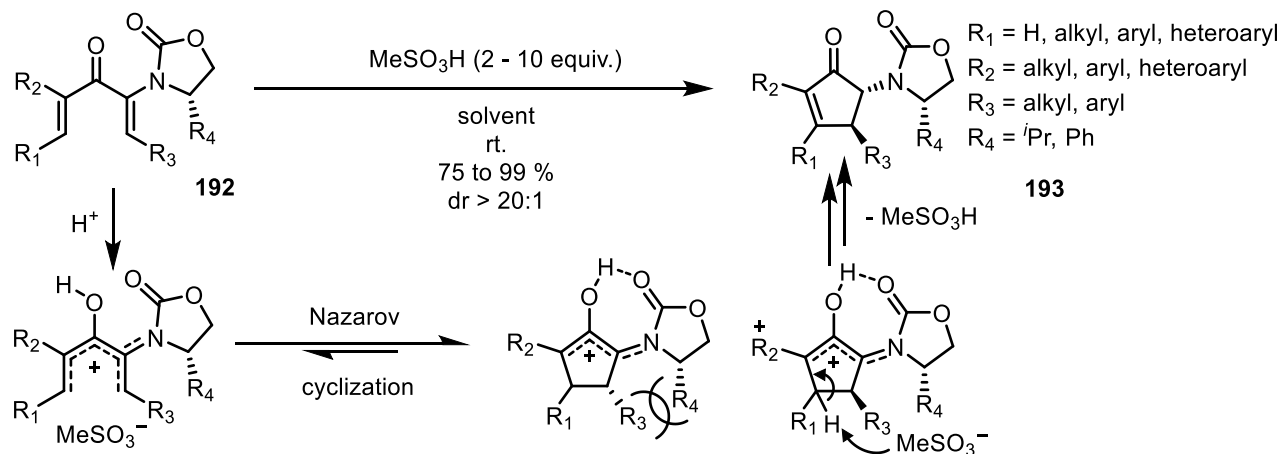
a. Nazarov cyclization using chiral oxazolidinones

Torquoselective Nazarov reaction

In the 2010s, Bernard F. Flynn's team used chiral oxazolidinones to perform torquoselective Nazarov reactions. Indeed, when the cross-conjugated dienone **192** was substituted in the α -position with a chiral oxazolidinone, it was possible to discriminate one of the two diastereoisomers owing to steric hindrance between the R_3 substituent on the

⁷¹ G. Alachouzos, C. Holt, A. J. Frontier, *Org. Lett.* **2020**, 22, 4010–4015.

cyclopentenone and the R₄ group on the oxazolidinone moiety. Cyclopentenone **193**, where the substituents R₃ and R₄ are in a *trans* relationship, were thus obtained almost exclusively with the double bond in the distal position of the oxazolidinone. This method led to very good yields ranging from 75 to 99% and good diastereomeric ratios (dr) (>20 :1), while tolerating a large variety of dienones (**Scheme 58**).⁷²



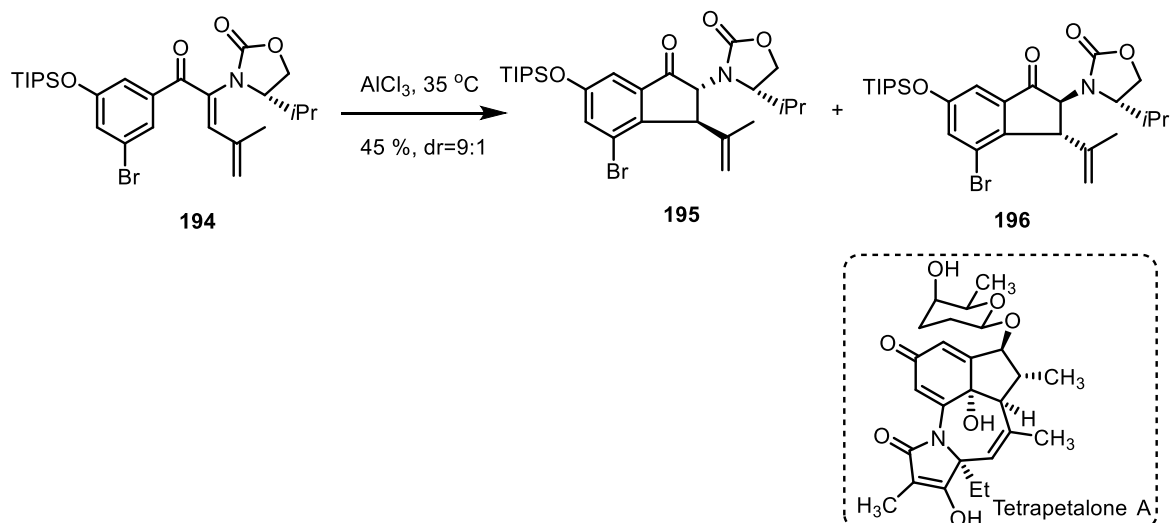
Scheme 58: Asymmetrization of Nazarov cyclization by using oxazolidinones

Application to the synthesis of tetrapetalone A

Alison Frontier used Flynn's Nazarov cyclization studies toward the asymmetric synthesis of tetrapetalone A. Aryl enone **194** containing Evan's auxiliary was treated with AlCl₃ to provide indanones **195** and **196** as a 9/1 mixture in 45% yield. Compound **195** was then converted into a key intermediate of tetrapetalone A-Me aglycon.⁷³

⁷² D. J. Kerr, M. Miletic, J. H. Chaplin, J. M. White, B. L. Flynn, *Org. Lett.* **2012**, *14*, 1732–1735. B. L. Flynn, N. Manchala, E. H. Krenske, *J. Am. Chem. Soc.* **2013**, *135*, 9156–9163. N. Manchala, H. Y. L. Law, D. J. Kerr, R. Volpe, R. J. Lepage, J. M. White, E. H. Krenske, B. L. Flynn, *J. Org. Chem.* **2017**, *82*, 6511–6527.

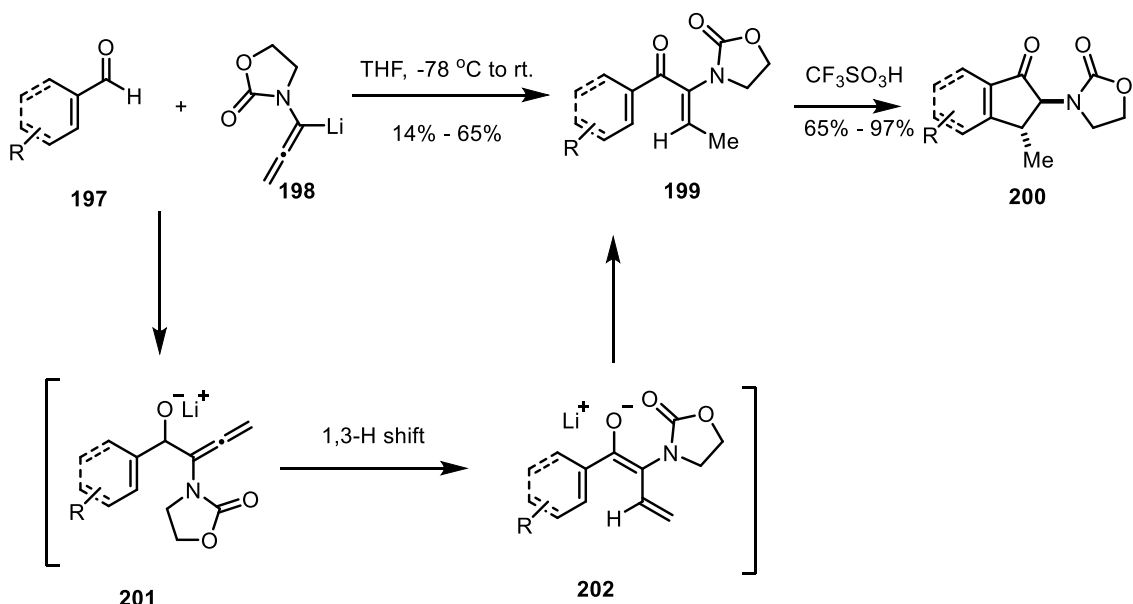
⁷³ P. N. Carlsen, E. G. Stoutenburg, A. J. Frontier, *Synthesis* **2018**, *50*, 1238-1245.



Scheme 59: Application of Flynn's strategy toward Tetrapetalone A

b. Construction of α -amido-indanones via allenamide hydroacylation and Nazarov cyclization

A one-step coupling reaction between aldehydes **197** and lithiated allenamides **198** was investigated by West's group to synthesize amido-substituted Nazarov precursors (**Scheme 60**).⁷⁴



Scheme 60: Hydroacylation of allenamides and Nazarov cyclization.

In this case, a 1,3-hydrogen shift, favored by alkoxide substitution of the allenamide⁷⁵ and by the oxazolidinone group, led to aryl diene intermediate **202**, which after work up led to divinyl

⁷⁴ Y. K. Wu, T. M. Niu, F. G. West, *Chem. Commun.*, **2012**, 48, 9186–9188.

⁷⁵ R. Hayashi, J. B. Feltenberger, A. G. Lohse, M. C. Walton R. P. Hsung, *Beilstein J. Org. Chem.* **2011**, 7, 410–420.

ketone **199**. Highly reactive dicationic intermediate **203** or protosolvated species **204** are proposed for this TfOH-mediated Nazarov cyclization (**Figure 7**).

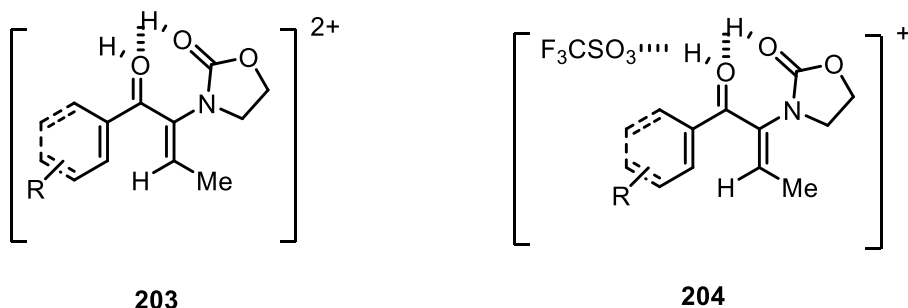
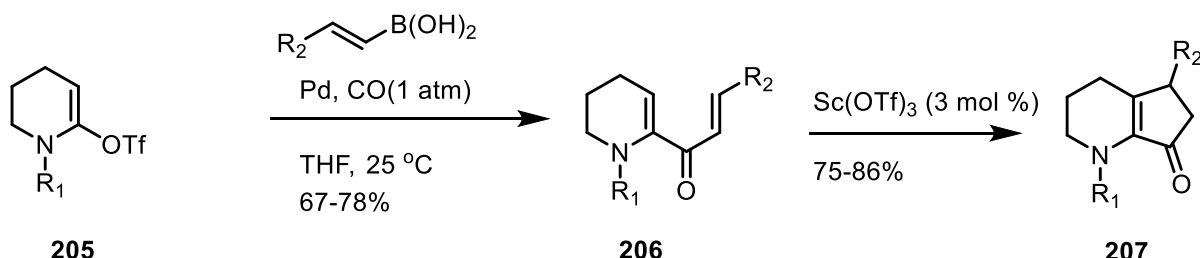


Figure 8: Proposed superelectrophilic intermediates

c. Nazarov cyclization from divinyl ketones being part of N-heterocyclic structures

Synthesis of the pyridine systems

The Prandi and Occhiato groups studied the Nazarov reaction in which one of the double bonds is embedded in a substituted *N*-heterocyclic structure.⁷⁶ They also took this advantageously polarized system to develop a new approach to the core of Roseophilin.⁷⁷ One year later, Occhiato *et al.* developed a highly efficient carbonylative Suzuki-Miyaura coupling reaction of lactam-derived vinyl triflates **205** and alkenylboronic acids to obtain the requisite Nazarov precursors **206**. The Lewis-acid catalyzed Nazarov reaction provided good yields to pyridine systems **207** (**Scheme 61**).⁷⁸



Scheme 61: The Lewis-acid-catalyzed Nazarov reaction performed by Occhiato's group

Tandem gold(I)-catalyzed rearrangement/Nazarov reaction

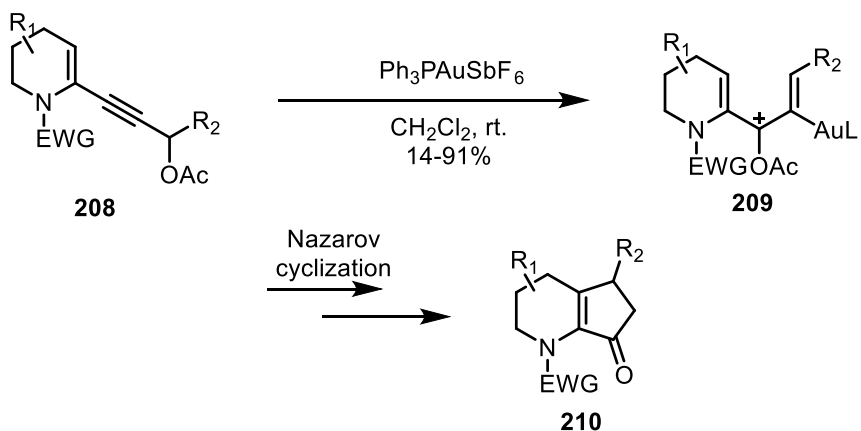
In their ongoing efforts on the Nazarov reaction, Occhito *et al.* explored gold(I)-catalyzed [3, 3]-rearrangement/Nazarov reactions of propargylic ester derivatives for the synthesis of cyclopenta-fused heterocycles. The [3,3]-sigmatropic rearrangement of the propargyl acetate **208** generates the requisite pentadienyl cation **209**, which after Nazarov reaction and

⁷⁶ E. G. Occhiato, C. Prandi, A. Ferrali, A. Guarna, P. Venturello, *J. Org. Chem.* **2003**, 68, 9728–9741.

⁷⁷ E. G. Occhiato, C. Prandi, A. Ferrali, A. Guarna, *J. Org. Chem.* **2005**, 70, 4542–4545.

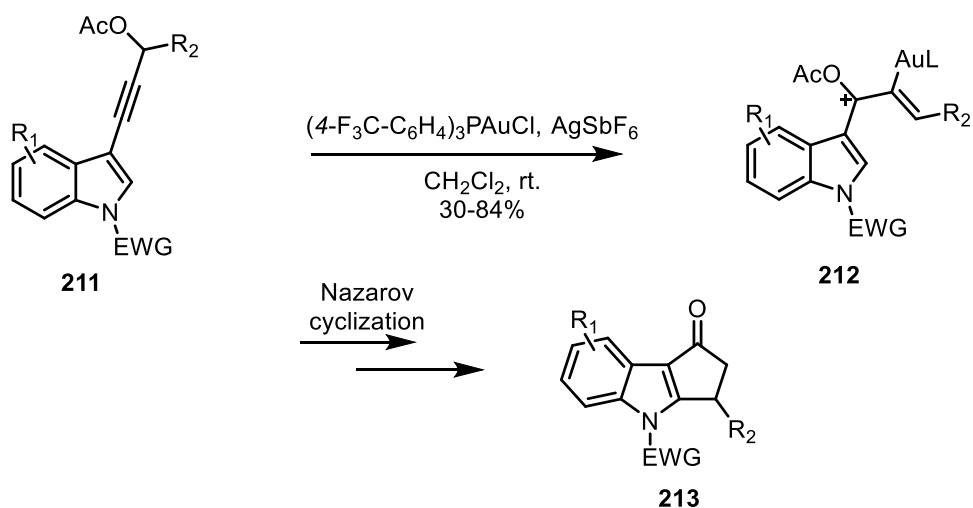
⁷⁸ P. Larini, A. Guarna, E. G. Occhiato, *Org. Lett.* **2006**, 8, 781–784.

protodeauration provided the corresponding cyclopenta-fused *N*-heterocyclic structures **210**. (**Scheme 62**).⁷⁹



Scheme 62: Gold-catalyzed rearrangement/Nazarov cyclization

This strategy was used by Occhiato's group in 2016 to convert enynyl acetates **211** to cyclopenta [b] indol-1-ones **213**. The developed transformation was used for the first total synthesis of bruceoline H (**Scheme 63**)



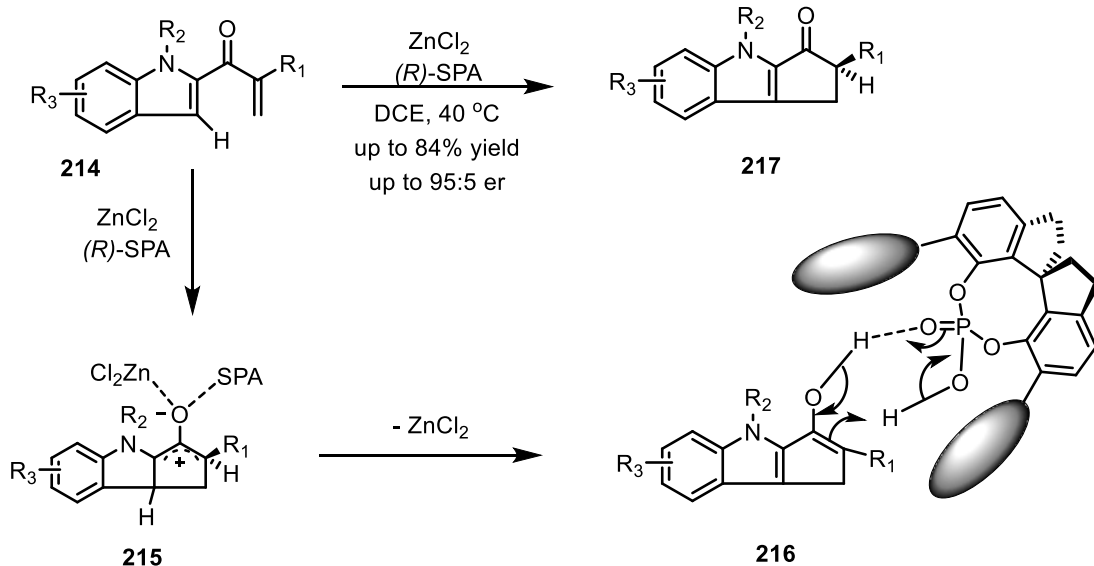
Scheme 63: Construction of cyclopenta[b]indol-1ones by tandem gold-catalyzed rearrangement/Nazarov cyclization

Enantioselective Nazarov cyclization

In 2017 Zhou *et al.* performed a cooperative catalysis using Lewis acids and chiral Bronsted acids to control the stereochemistry of the tertiary α -carbon of the cyclopentanone ring. With $ZnCl_2$ and a chiral spiro phosphoric acid (SPA) as catalysts, the enantioselective construction of cyclopenta[b]indoles with a chiral α -carbon via Nazarov cyclization was achieved. The

⁷⁹ M. Petrović, D. Scarpi, B. Fiser, E. Gómez-Bengoa, E. G. Occhiato, *Eur. J. Org. Chem.* **2015**, 3943–3956.

Lewis acid and the SPA promote the cyclization cooperatively. The SPA promotes the proton transfer reaction of the enol intermediate and exerts enantioselective control over the tertiary α -carbon chiral center created during the Nazarov cyclization (**Scheme 64**).⁸⁰

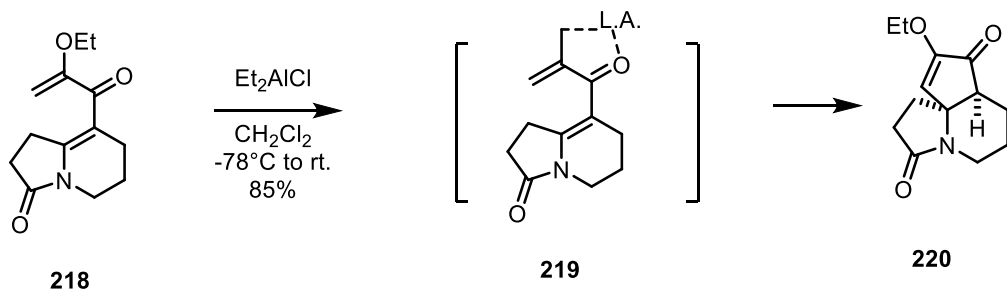


Scheme 64: Catalytic asymmetric Nazarov cyclization of indole enones

I.2.7.2. β -Aza-substituted divinyl ketones for the Nazarov cyclization

a. Synthesis of the tricyclic core of cephalotaxine

Nazarov cyclizations involving dienones substituted with a nitrogen at the β -position are scarce. Cha and Kim reported a Nazarov cyclization of a β -aza-substituted divinyl ketone to achieve the synthesis of the tricyclic core present in cephalotaxine, a promising antileukemic agent (**Scheme 64**).⁸¹ The desired ring closure was accomplished in 85% yield by using diethylaluminium chloride to afford cyclopentenone **220**. Other Lewis acids [e.g., FeCl_3 , $\text{BF}_3\text{-OEt}_2$, TiCl_4 , $\text{TiCl}(\text{O}i\text{Pr})_3$, $\text{Cu}(\text{OTf})_2$ and $\text{Mg}(\text{OTf})_2$] proved to be less efficient to induce the Nazarov cyclization. Crucial to the successful cyclization is the formation of a bidentate chelate **219** to trigger the subsequent conrotatory ring closure (**Scheme 65**).



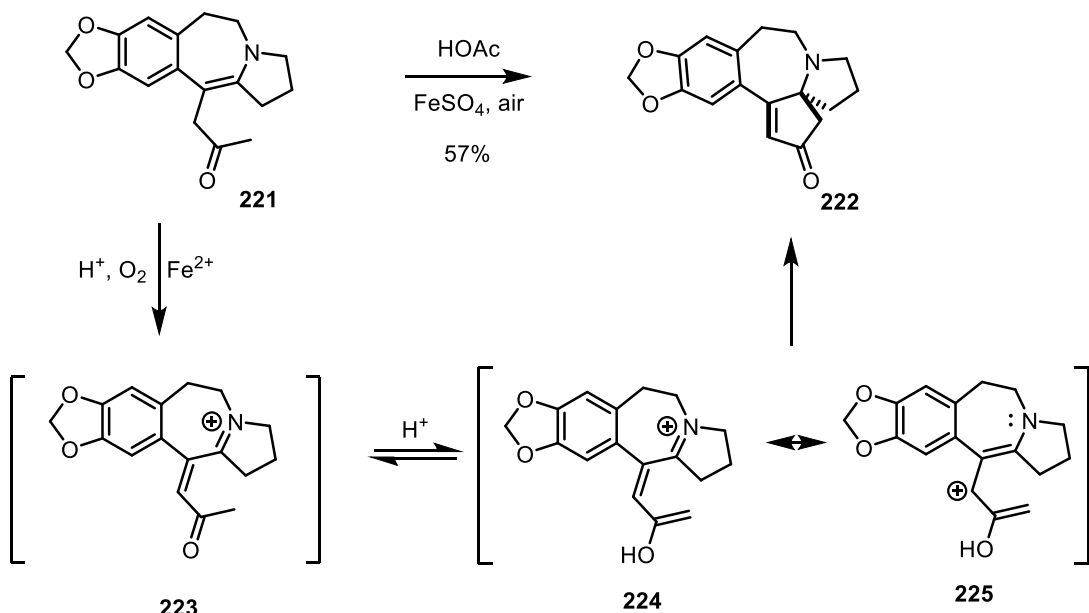
⁸⁰ G.-P. Wang, M.-Q. Chen, S.-F. Zhu, Q.-L. Zhou, *Chem. Sci.*, **2017**, *8*, 7197–7202.

⁸¹ S.-H. Kim, J. K. Cha, *Synthesis* **2000**, *14*, 2113–2116.

Scheme 65: Synthesis of the tricyclic core of cephalotaxine

b. Total synthesis of cephalotaxine

In 2013, Li and Wang reported an efficient total synthesis of cephalotaxine.⁸² An unusual endocyclic enamine cyclopentenone annulation was discovered and rationalized as an aza-Nazarov-type cyclization. Keto enamine **221** in glacial acetic acid as solvent in an open flask was treated with a stoichiometric amount of FeSO₄ to provide spiro-cyclopentenone **222**. In this O₂-dependent process, the unusual aza-Nazarov-type cyclization is initiated by an acid-catalyzed autoxidation. Endocyclic enamine **221** is a direct enamine alkylation product. Therefore, this Nazarov type cyclization can be regarded as an enamine cyclopentenone annulation (**Scheme 66**).⁸³



Scheme 66: Key step for the total synthesis of cephalotaxine

I.3. Tertiary Enamide-Promoted Diastereoselective Domino: N-Acyliminium Ion Trapping and Nazarov Cyclization

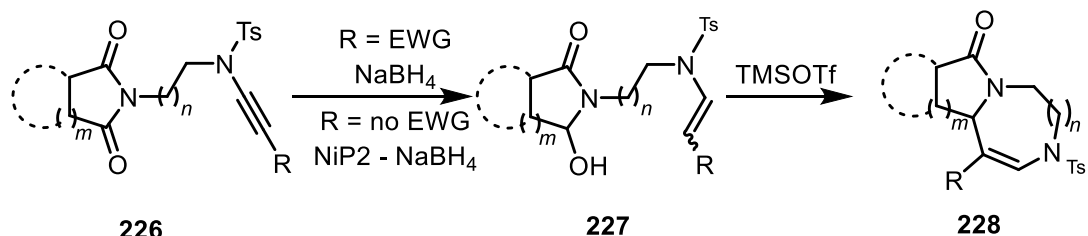
I.3.1. The aim of our project

In paragraph 1.2.8.2, we showed that tertiary enamides were able to add to *N*-acyliminium ions (NAI) to form various heterocyclic compounds. In particular, enamides equipped with *N*-acyliminium ion precursors were valuable substrates to construct nitrogen-containing molecules. Thus, we have shown that ynamides incorporating an *N*-imide can be

⁸² W.-D. Z. Li, Y.-Q. Wang, *Org. Lett.* **2003**, 5, 2931–2934.

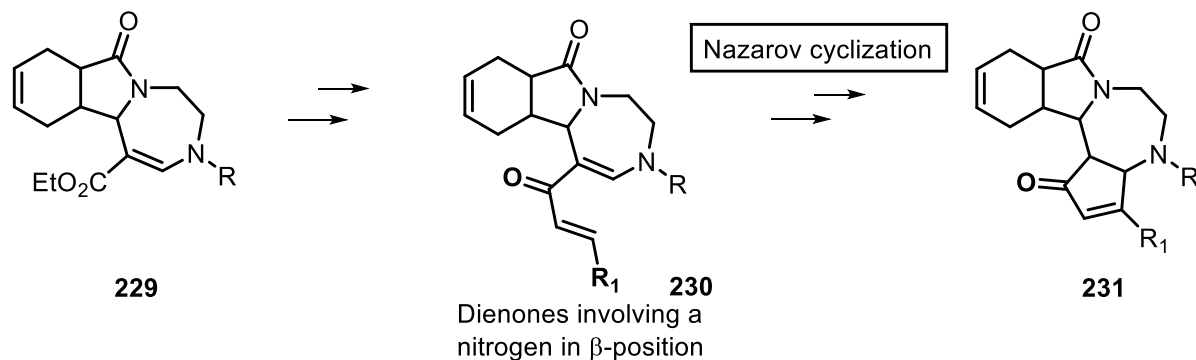
⁸³ R. V. Stevens, *Acc. Chem. Res.* **1977**, 10, 193–198.

transformed into tertiary enamides equipped with a precursor of an *N*-acyliminium ion (NAI). In acidic medium, the tertiary enamide adds to the *N*-acyliminium species to form diazepine drug substructures (**Scheme 67**). Various imides, different spacer lengths, as well as different substituents on the ynamide were tolerated.⁸⁴



Scheme 67. Synthesis of Diaza Heterocycles

The aim of the PhD project was to take advantage of the tertiary enamide present in diazepines **229** to trigger Nazarov reactions via dienone **230** to access more complex cyclopenta-diazepine motifs **231** (**Scheme 68**).



Scheme 68. First strategy to access cyclopenta-diazepine motifs

Among those polarized Nazarov cyclizations, nitrogen-substituted cross-conjugated divinyl ketones at the α -position have been frequently investigated. In contrast, Nazarov cyclization involving dienones substituted with a nitrogen atom at the β -position are scarce (see paragraph II 7.2.1).

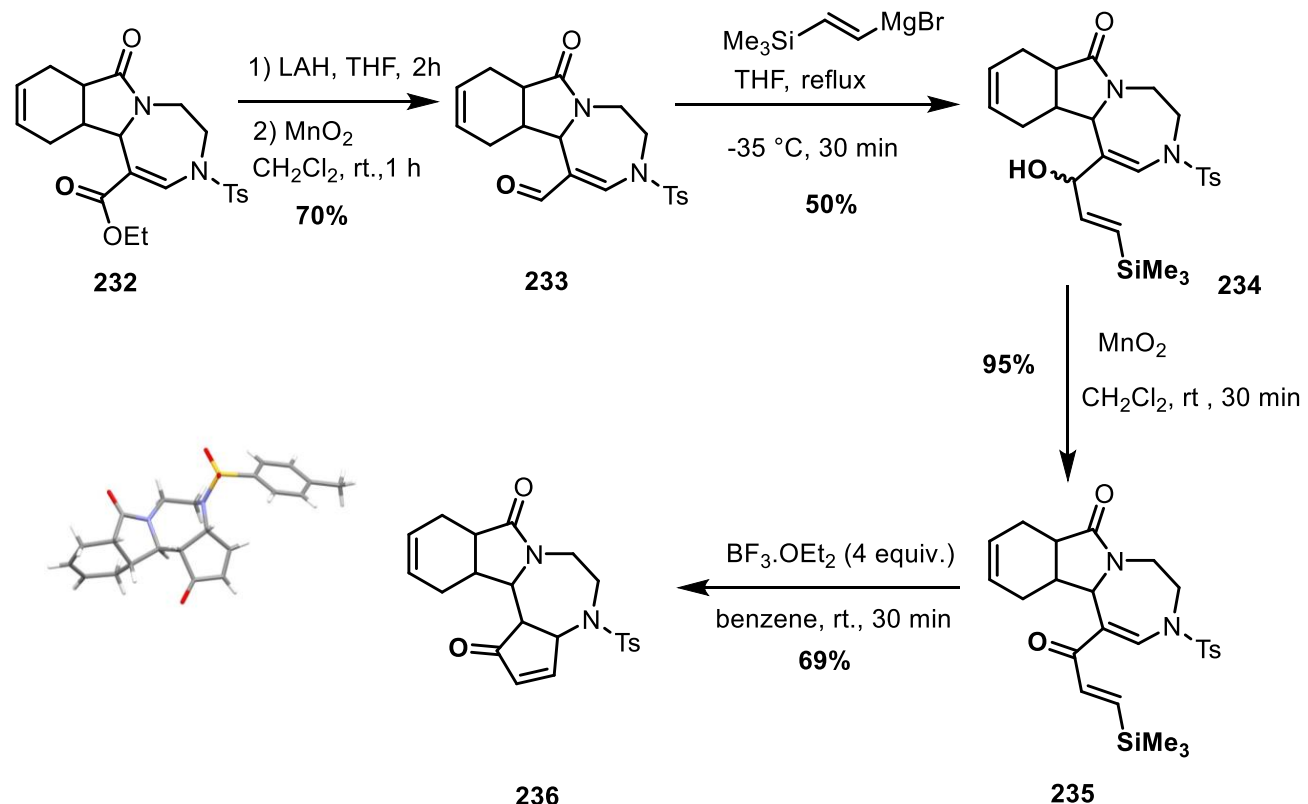
I.3.2. Previous work

The first trials were performed by Lucile Andna on our team. The goal was to transform the α , β -unsaturated ester present in diazepine **232** into a divinyl ketone **235** to promote the Nazarov reaction. For this purpose, the ester function was reduced to the primary alcohol, and the latter was then oxidized to the corresponding aldehyde **233**. Addition of the alkenyl silylated Grignard reagent to the aldehyde led to the corresponding dienol. Our idea was to use Denmark's silicon-directed Nazarov cyclization protocol⁴⁷ to add a cyclopentenone ring on the molecule. Oxidation of alcohol **234** provided the required cross-conjugated dienone

⁸⁴ L. Andna, L. Miesch, *Org. Lett.* **2018**, *20*, 3430.

235, precursor for the Nazarov cyclization. Finally, treatment with $\text{Et}_2\text{O}\bullet\text{BF}_3$ afforded the desired diazepine fused with a cyclopentenone ring **236** (**Scheme 69**).

Thus, these preliminary results validated the concept, and an X-ray structure confirmed the presence of the desired tetracycle **236** (**Scheme 69**.)



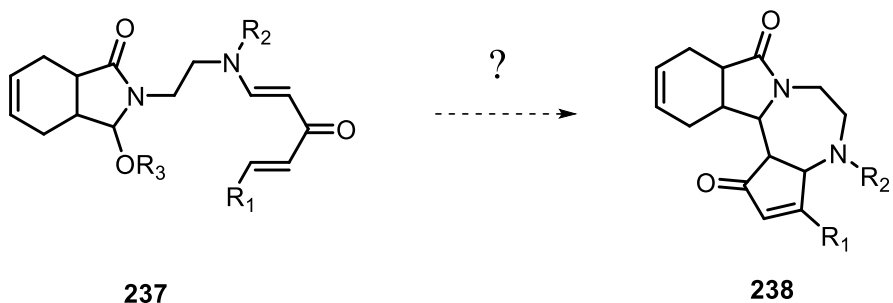
Scheme 69. First attempt for the synthesis of cyclopenta-diazepine motifs

However, although effective, the synthesis of this cyclopenta-diazepine motif is long and cannot be generalized. Indeed, several substrates did not allow the indicated yields to be obtained.

I.3.3. New route to the synthesis cyclopenta-diazepine motifs

I.3.3.1. Objective

Following the concept of atom economy for the construction of complex organic architectures, we then anticipated that in acidic media, well-designed tertiary enamides may provide an efficient starting point for the synthesis of polyheterocyclic scaffolds involving an *N*-bridgehead backbone. Thus, we envisioned that NAI precursors tethered with tertiary enamidyl vinyl ketones would offer the possibility of promoting two reactions simultaneously: nucleophilic addition of the enamide to the NAI and subsequent Nazarov reaction.



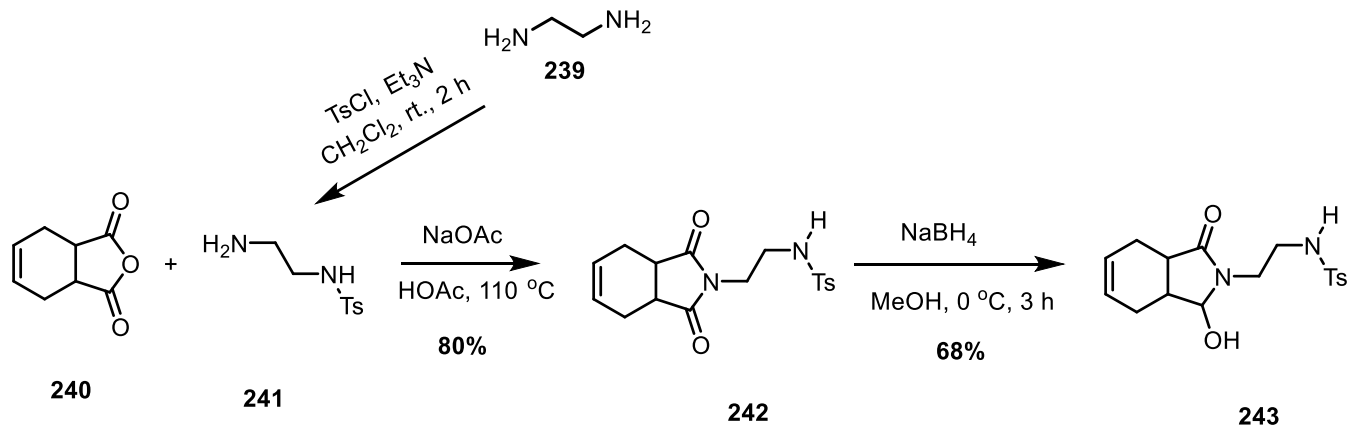
Scheme 70: *N*-Acyliminium ion trapping followed by Nazarov reaction.

To assess our domino reaction, we had to synthesize the requisite cross-conjugated dienones **237**.

I.3.3.2. The case of tertiary enamidyl vinyl ketones substituted with a phenyl group

a. Synthesis of *N*-imide sulfonamides

To synthesize the *N*-imide sulfonamides we used the protocol described by Roy et al.⁸⁵ Monoprotected ethylenediamine **241** was obtained from ethylenediamine **239** and tosyl chloride under basic conditions. Condensation of anhydride **240** with monoprotected ethylenediamine **241** in the presence of sodium acetate in refluxing acetic acid provided *N*-imide sulfonamide **242** in 80% yield. Reduction of the latter took place with sodium borohydride to afford succinamidal **243** (**Scheme 71**).



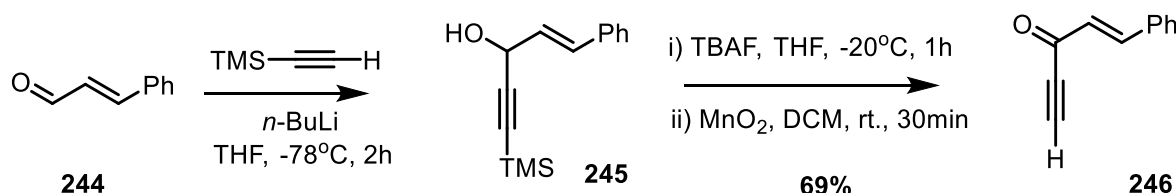
Scheme 71: Synthesis of α -hydroxylated amide

⁸⁵ A. K. Maity, S. Roy, *Adv. Synth. Catal.* **2014**, 356, 2627. M. S. Abdel-Maksoud, M. R. Kim, M. I. El-Gamal, M. M. Gamal El-Din, J. H. Tae, S. Choi, K. T. Lee, K. H. Yoo, C. H. Oh, *Eur. J. Med. Chem.* **2015**, 95, 453.

b. Synthesis of tertiary enamidyl vinyl ketones substituted with a phenyl group

c. Synthesis of the ene-yne-one **246**

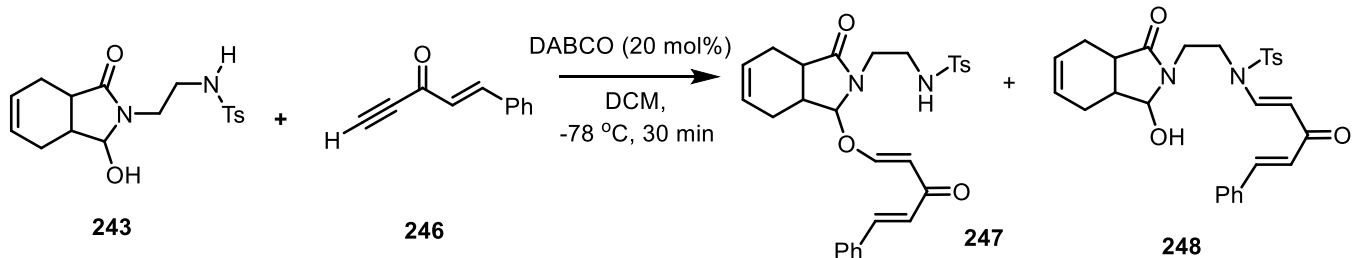
Activated enesulfonamides can be obtained by reaction of terminal alkynes with sulfonamides by using Triton B⁸⁶ or DABCO.⁸⁷ We assumed that the more expedient way to obtain the required cross-conjugated dienone would be to prepare enyne-one **246**. The latter was obtained through a three-step sequence: addition of lithiated trimethylsilylacetylene to cinnamaldehyde provided ene-yne-ol **245** with 90 % yield, deprotection of the triple bond with TBAF and finally oxidation of the propargylic alcohol **245** afforded the desired ene-yne-one **246**.



Scheme 72: Synthesis of the ene-yne-one **246**

d. Synthesis of cross-conjugated dienones

Enesulfonamides **248** were prepared using Gharpure's method⁸⁶ by using a catalytic amount of DABCO in dichloromethane. In this case we obtained an inseparable mixture of the desired tertiary enamide **248**, but also the O-alkylated compound **247** obtained by 1, 4-addition of the hydroxyl group of **243** on the ene-yne one **246** (**Scheme 73**).



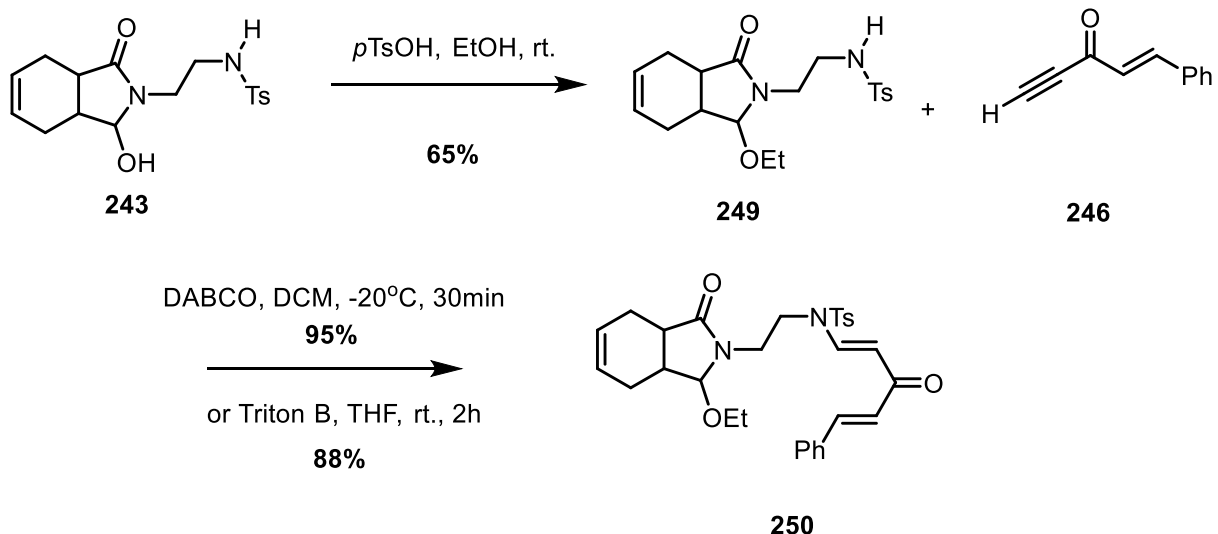
Scheme 73: Synthesis of cross-conjugated dienones

To avoid the O-alkylated compound **247**, we decided to transform the hydroxylated *N*-acyliminium precursor **243** into the corresponding ethyl ether **249**. In this way, the required

⁸⁶ L. Andna, L. Miesch, *Org. Biomol. Chem.* **2019**, *17*, 5688

⁸⁷ S. J. Gharpure, V. Prasath, V. Kumar, *Chem. Commun.* **2015**, *51*, 13623.

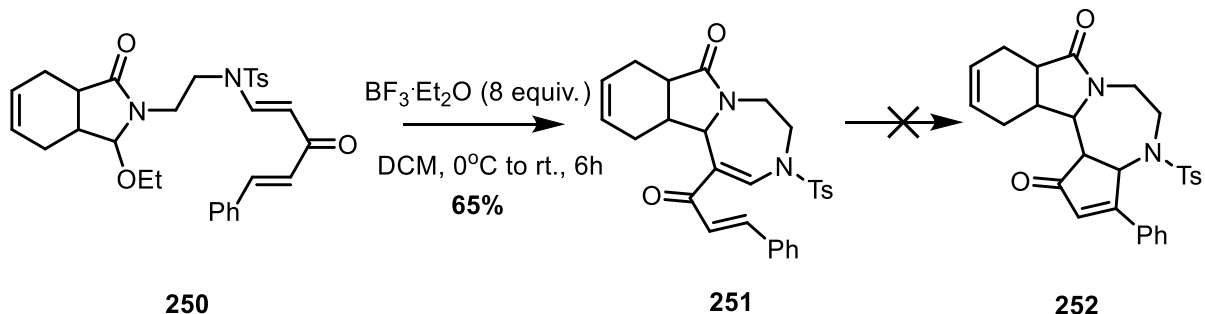
dienone **250** was obtained by addition of the tosylsulfonamide **249** onto the triple bond of ene-yne-one **246** in the presence of DABCO or Triton B in good yields (**Scheme 74**).



Scheme 74: Synthesis of cross-conjugated dienones

e. Cyclization

Having the NAI precursor equipped with the cross-conjugated enamidyl vinyl ketone **250**, we attempted to initiate the domino reaction by using $\text{Et}_2\text{O}\cdot\text{BF}_3$ to generate the NAI precursor. With the phenyl substituent, although the trapping of the *N*-acyliminium ion was efficient, the Nazarov reaction did not take place (**Scheme 75**).



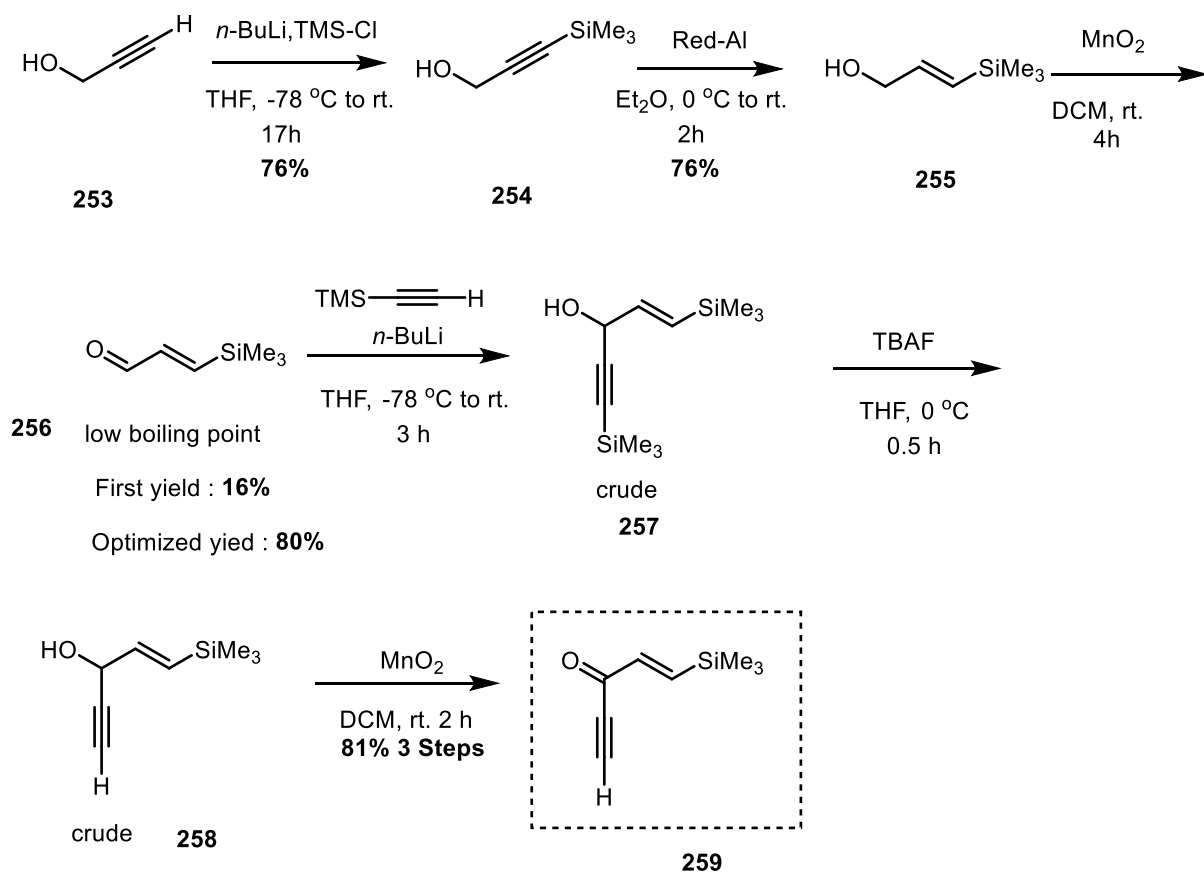
Scheme 75: Nazarov cyclizations involving β -aza-substituted cross-conjugated divinyl ketones.

I.3.3.3. The case of tertiary enamidyl vinyl ketones substituted with a silicon group

a. Synthesis of cross-conjugated dienones

b. Synthesis of the ene-yne-one

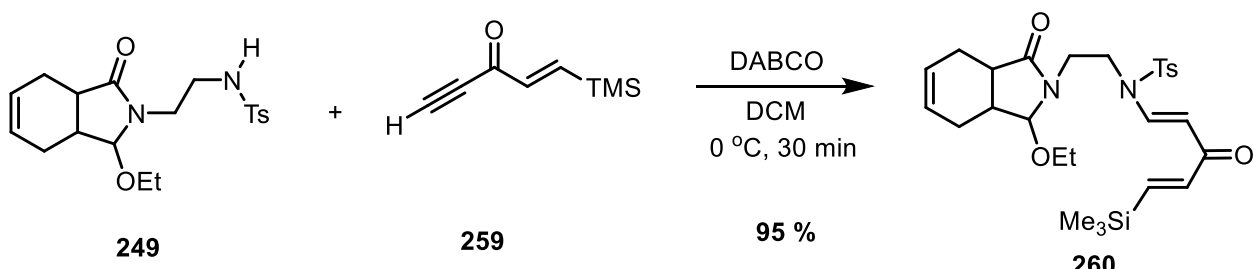
Taking in account our previous results (see paragraph III 1.1), we rationalized that a divinyl ketone substituted with a silicon atom would provide an efficient solution to this issue by taking advantage of the β -silicon effect to facilitate the Nazarov reaction. Thus, we established an efficient route to ene-yne-one **259** starting from propargylic alcohol **253**. To do so, propynol **253** was silylated with *n*-BuLi in the presence of trimethylsilyl chloride (TMSCl). Hydrogenation of the triple bond was achieved with Red-Al, and the oxidation of allylic alcohol **255** with manganese dioxide provided α,β -unsaturated aldehyde **256**. The latter was very volatile, and thus the first yield we obtained was very low. By taking adequate precautions we could improve the yield to 80%. Addition of lithiated TMS-acetylene provided the propargylic alcohol **257**. Deprotection of the triple bond and subsequent oxidation of ene-yne-ol **258** finally provided the desired ene-yne-one **259** in 6 steps with 37% overall yield (**Scheme 76**).



Scheme 76: Synthesis of ene-yne-one **259** substituted with a silicon.

c. Synthesis of the enamidyl vinyl ketone

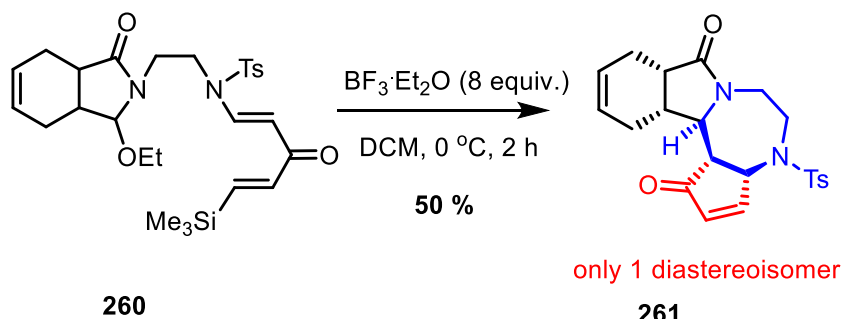
By reacting the corresponding tosyl sulfonamide **249** with *E* configured ene-yne-one **259** in the presence a catalytic amount of DABCO, the desired dienone **260** was obtained in a very good yield. Further, NMR studies showed that the desired (*E, E*) cross-conjugated enamidyl vinyl ketone was obtained exclusively (**Scheme 77**).



Scheme 77: Synthesis of enamidyl vinyl ketone **260**.

d. Domino reaction

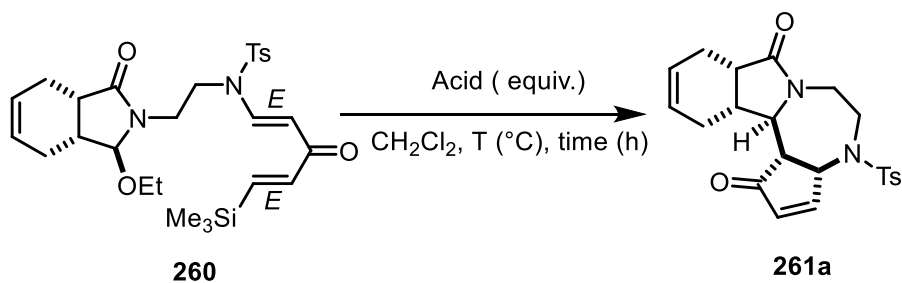
Gratifyingly, using Et₂O•BF₃, we obtained the desired tetracycle **261** as a single diastereomer in one pot from *N*-functionalized alkoxyamide **260**. The trapping of the *N*-acyliminium ion and the subsequent Nazarov reaction were achieved in 50% yield, and the torquoselectivity was controlled via factors that are challenging to pinpoint owing to the peculiar structure of the cross-conjugated dienone, thus leading stereoselectively to a single aza-polycyclic framework bearing three more stereogenic centers.



Scheme 78: Domino: NAI trapping and Nazarov cyclization

1.3.3.4. Screening of the acid

Screening of Lewis and Brønsted acids revealed that only a few Lewis acids were able to promote this domino reaction (**Table 2**, entries 6 to 9). Brønsted acids such as *p*-TsOH, TfOH, MeSO₃H (**Table 2**, entries 1-2, 3 and 4, respectively) led either to the starting material or degradation. We had more success with Et₂O•BF₃, although a minimum temperature of 0 °C is required (**Table 2**, entry 6), and a greater amount of the Lewis acid as well as a longer reaction time has a positive influence on the yield of the reaction (**Table 2**, entries 7 and 8, respectively). TMSOTf was as effective as Et₂O•BF₃ and provided the aza-fused polycyclic derivative in similar yields (**Table 2**, entry 9). Using Lewis acids such as AlCl₃, FeCl₃ and Y(OTf)₃, the outcome for the domino reaction remained the same - degradation or no transformation (**Table 2**, entries 10, 11 and 12, respectively).

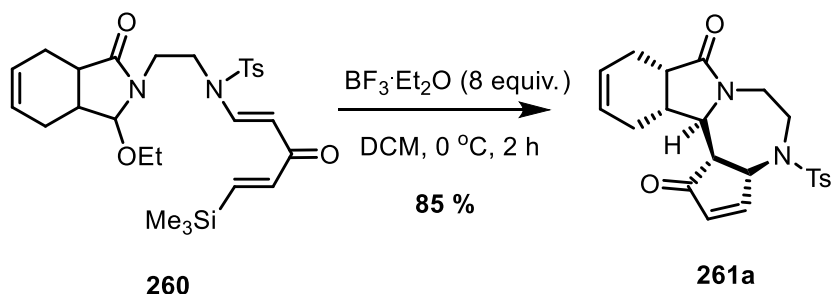


Entry	Acid (equiv)	Temp (°C)	Time (h)	Yield (%)
1	p-TsOH (8)	0 to rt	3	- ^b
2	p-TsOH (8)	0 to rt	6	traces
3	TfOH (8)	0	4	- ^c
4	MeSO ₃ H (8)	0	1	- ^c
5	Et ₂ O•BF ₃ (8)	-30	2	- ^b
6	Et ₂ O•BF ₃ (8)	0	2	50
7	Et ₂ O•BF ₃ (8)	0	6	77
8	Et ₂ O•BF ₃ (10)	0	6	85
9	TMSOTf (8)	0	4	85
10	AlCl ₃ (8)	0	6	- ^c
11	FeCl ₃ (8)	0	2	- ^c
12	Y(OTf) ₃ (8)	0	6	- ^b

Table 2 : Screening the acid

1.3.3.5. Optimal reaction conditions

After an extensive screen of Lewis acids and various reaction conditions, the optimal conditions for the domino reaction are the use of 8 equivalents of Et₂O•BF₃ or TMSOTf in dichloromethane at 0 °C, thereby providing cyclopenta-diazepine **261a** in 85% yield (**Scheme 79**).



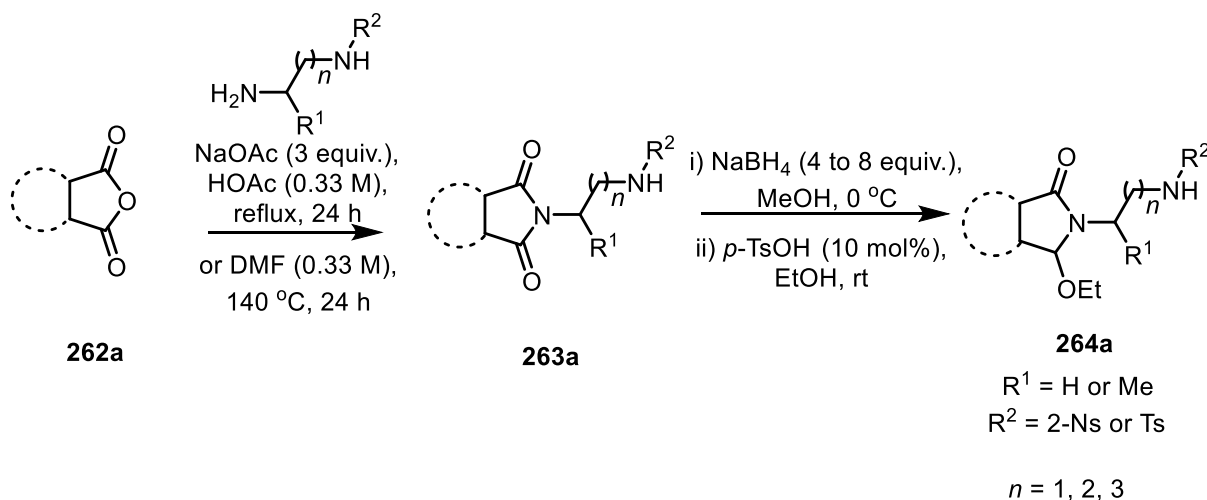
Scheme 79: Optimal reactions conditions

Once the optimal reaction conditions were determined, we evaluated the scope of the domino reaction.

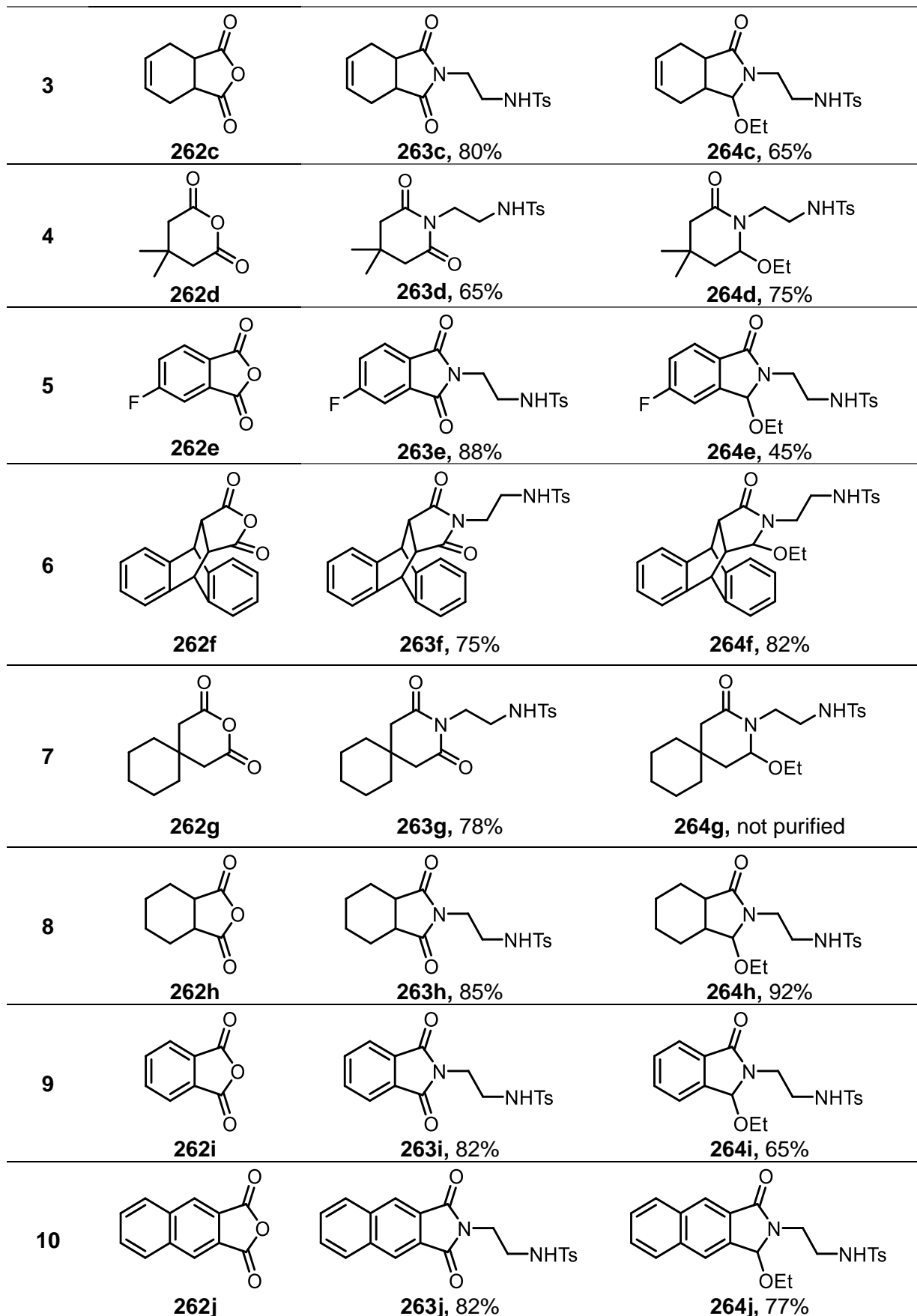
I.3.3.6. Scope of the domino reaction

a. Synthesis of α -alkoxy amides

The *N*-imidyl sulfonamides **264a-r** were synthesized by reacting the corresponding anhydrides **262a-r** with the monoprotected diamine according to the method previously described (Scheme 71, p 50). The Ts/Ns/Ms-sulfonamidyl imides were obtained with good yields ranging from 50 to 95% (**Table 3**). To obtain the *N*-acyliminium precursors, imides **263a-r** were reduced with sodium borohydride, providing α -alkoxy amides **264a-r** with yields ranging from 0 to 93%. Because of its instability, compound **264g** was not purified, but was used directly in the next step. We were able to obtain α -alkoxy amides with three carbon and four carbon linker chains with good yields (compounds **264n**, **264o**, **264p**). Nosyl and mesyl groups easier to deprotect were tolerated as well (compounds **264q** and **264r**). Tetrafluorinated compound **264l** did not undergo reduction of the imide, probably because of the electron-withdrawing effect of the fluorine atoms of the phenyl ring or due to steric hindrance. In the case of methylated compound **264m**, we only isolated the major compound out of four diastereoisomers formed (**Table 3**, entry 13).



Entry	Anhydrides	Sulfonamides	α -Alkoxy Amides
1			
2			

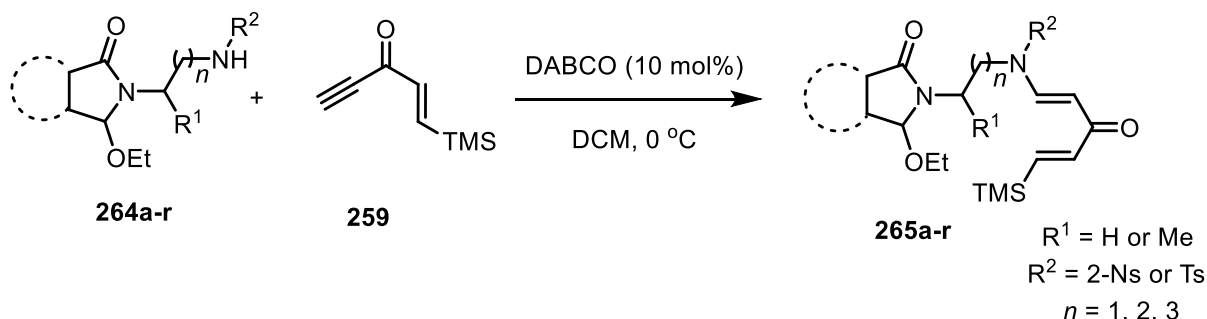


11			
12			
13			
14			
15			
16			
17			
18			

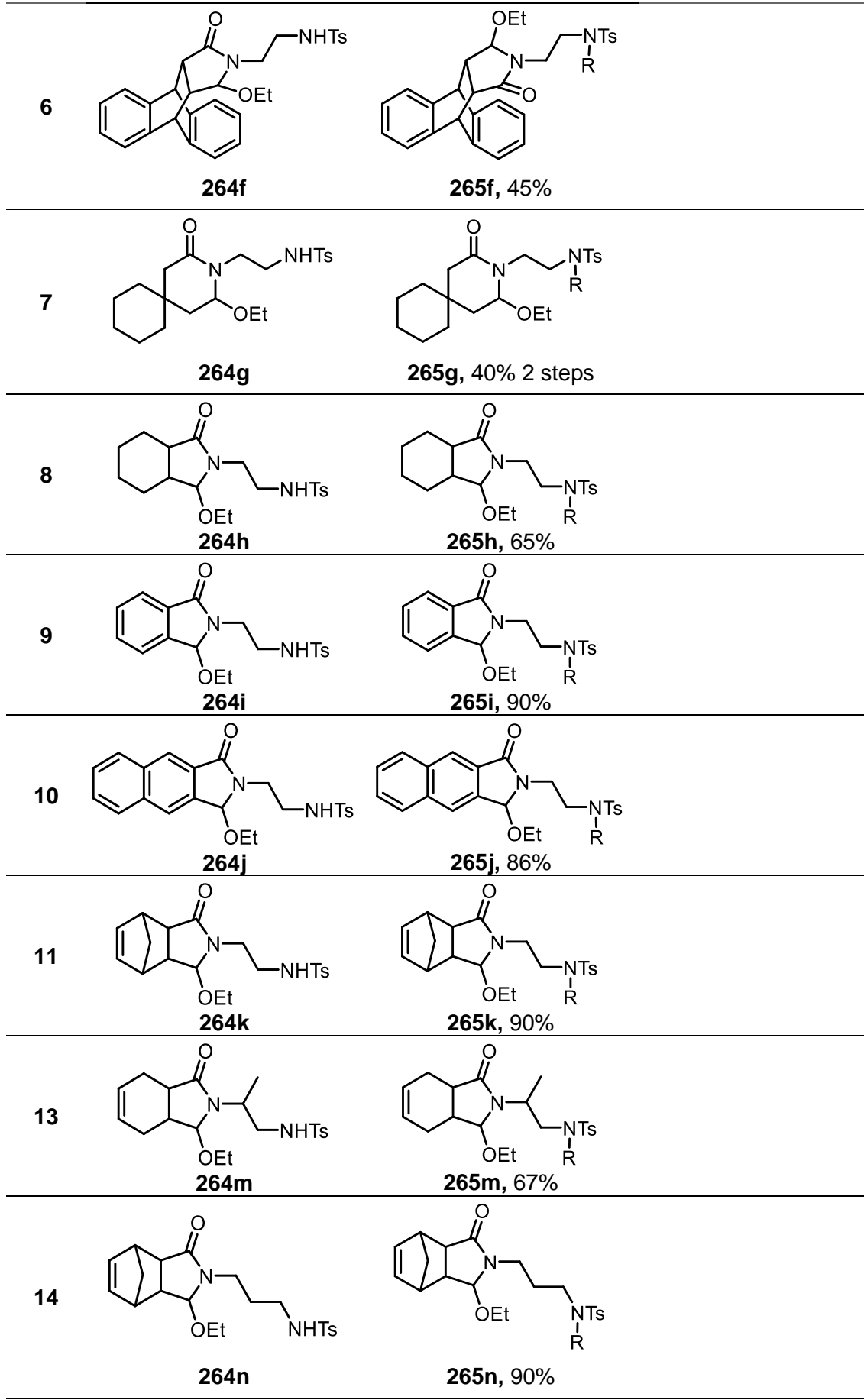
Table 3: Synthesis of α -alkoxy amides

b. Synthesis of cross-conjugated enamidyl vinyl ketones

Enamidyl vinyl ketones **265a** to **265r** were prepared according Gharpure's method⁸⁶ by reacting the corresponding tosyl sulfonamides **264a** to **264r** with *E*-configured ene-ynone **259** in the presence of a catalytic amount of DABCO with yields ranging from 40 to 95%. Notably, according to the NMR spectra in all cases, we obtained exclusively (*E,E*) configured cross-conjugated enamidyl vinyl ketone substrates **265a-r** (**Table 4**).



Entry	α -Alkoxy Amides	Dienones
1		
2		
3		
4		
5		



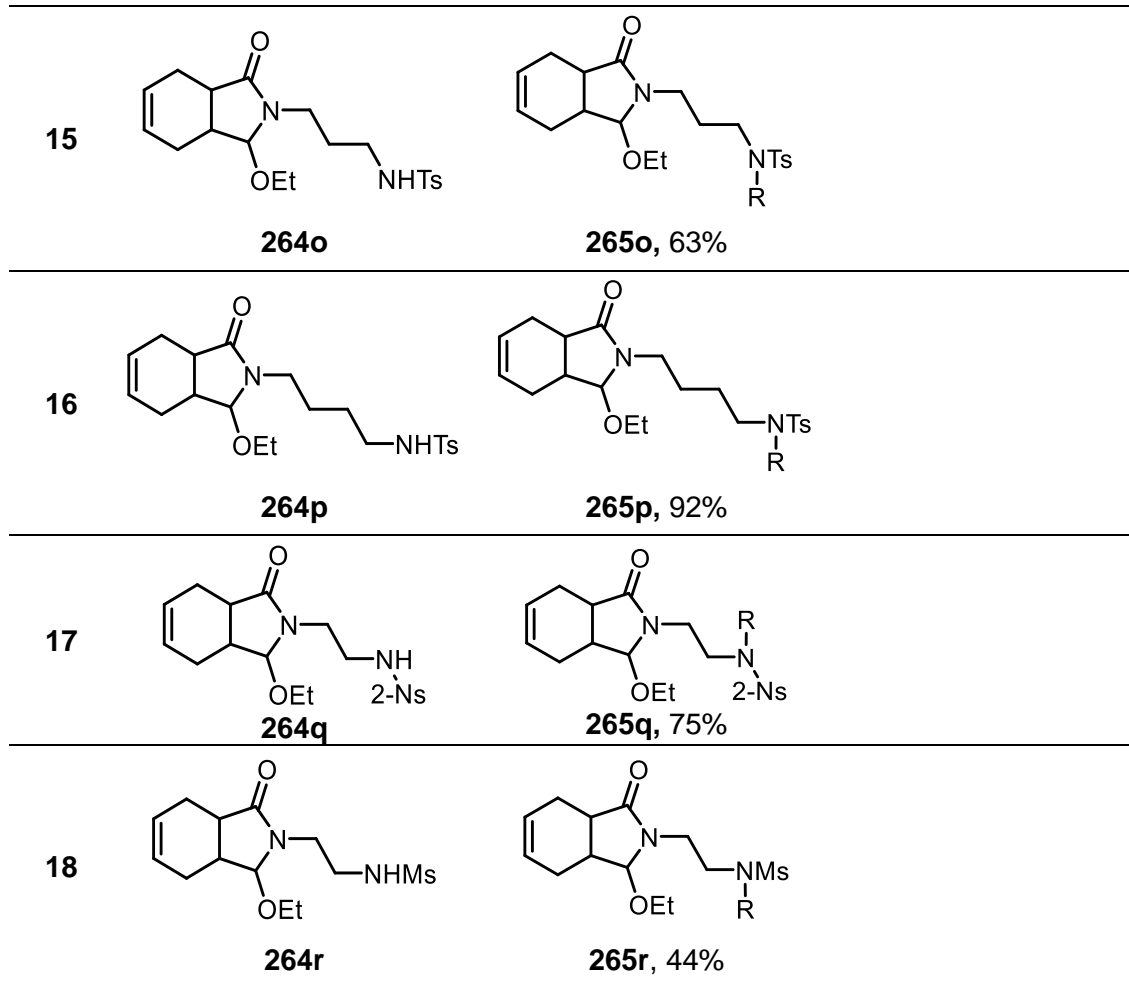
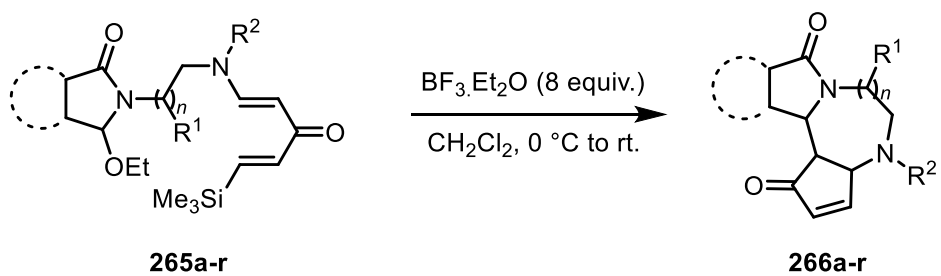


Table 4 : Synthesis of Dienones

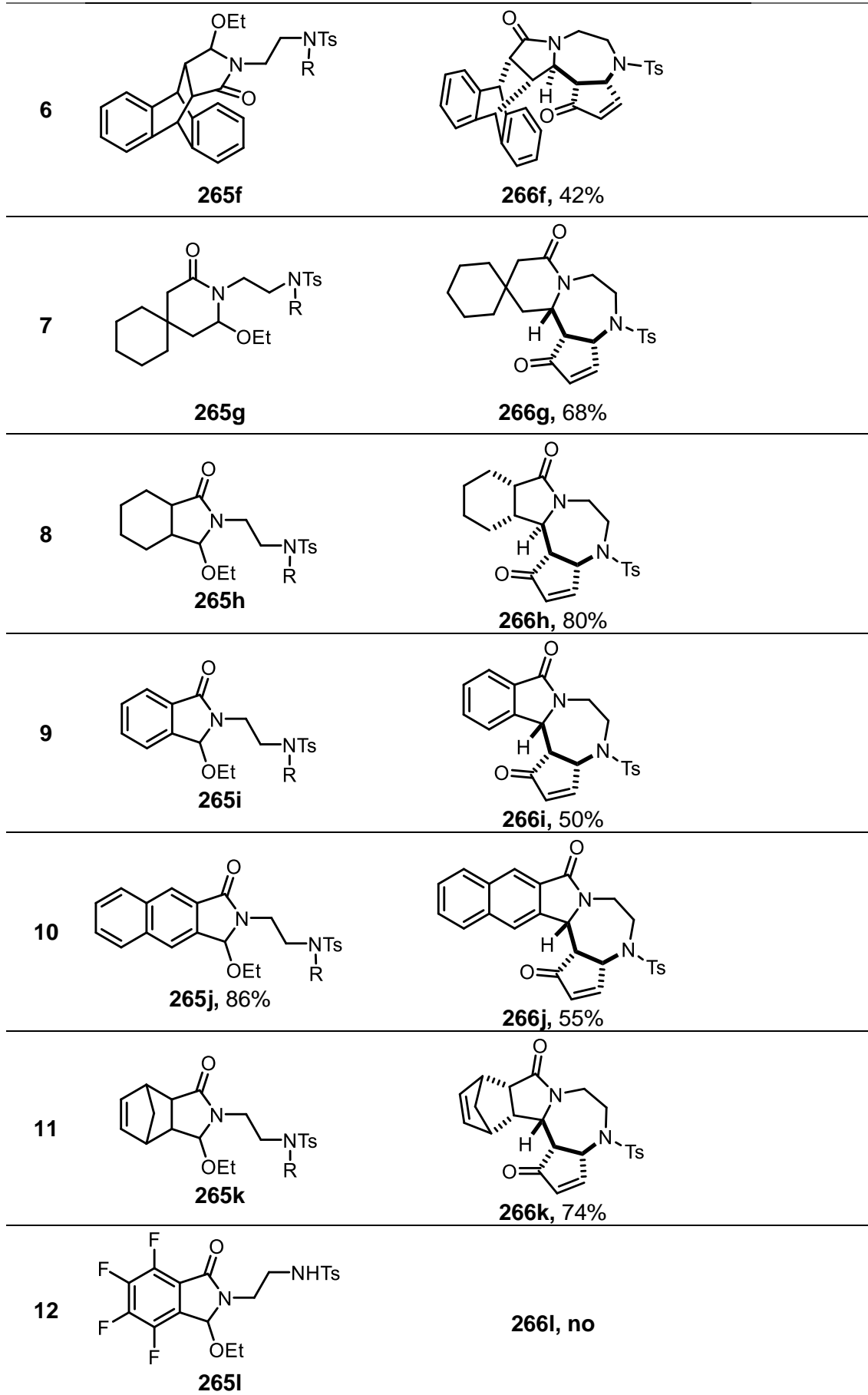
c. Synthesis of *N*-bridgehead diazepines bearing a cyclopentenone ring

The *N*-bridgehead diazepines bearing a cyclopentenone ring **266a-q** were obtained by reacting cross-conjugated enamidyl vinyl ketones **265a-q** in the presence of $\text{Et}_2\text{O}\cdot\text{BF}_3$ using the established optimal reaction conditions. Through trapping of the *N*-acyliminium ion and subsequent Nazarov reaction we obtained various cyclopenta-diazepine motifs **266a-q** with yields ranging from 41 to 89%. We noticed that this domino reaction was completely diastereoselective, as only one polycyclic diazepine was obtained in each case.

The methylated compound **265m** led to a unique aza-fused polycyclic system **266m** bearing four stereogenic centers. The protecting group on the nitrogen moiety of the tertiary enamide was also investigated to facilitate post-annulation deprotection - modification of the protecting group showed no influence on the outcome of the reaction. Diazepine **266q** was obtained with a poorer yield than for compound **266a**. Three methylene units for the spacer length were also allowed, providing an eight-membered fused polycyclic system **266n**.



Entry	Dienones	<i>N</i> -Bridgehead Diazepines
1	 265a	 266a, 44%
2	 265b	 266b, 65%
3	 265c	 266c, 85%
4	 265d	 266d, 67%
5	 265e	 266e, 41%



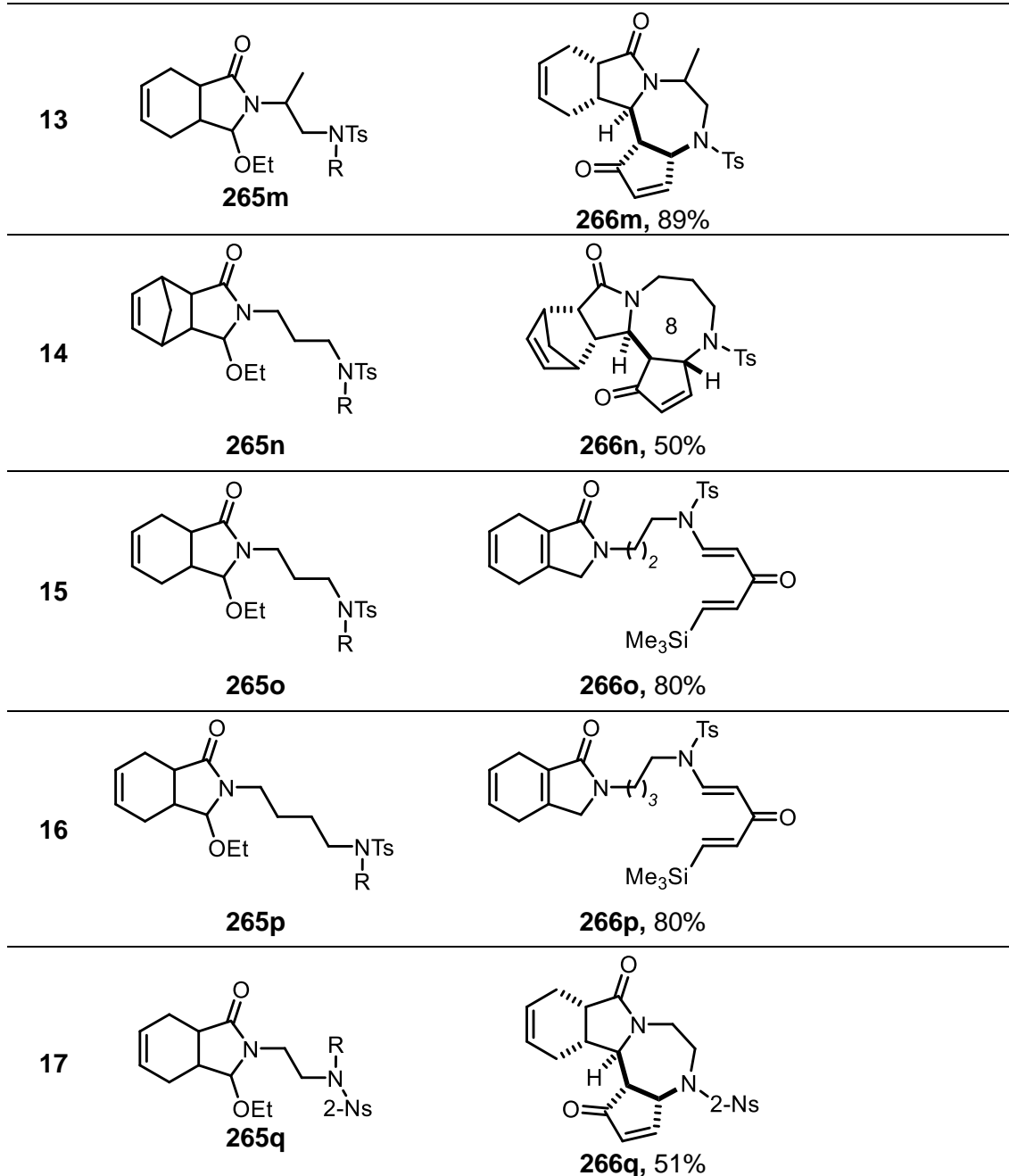


Table 5 : Synthesis of N-bridgehead diazepines

The homolog **265p** with four methylene units did not undergo this domino reaction. In this case, elimination of EtOH took place, leading to the more stable conjugated alkene **266p**.⁸⁸

⁸⁸ J. B. P. A. Wunberg, H. E. Schoemaker, W. N. Speckamp, *Tetrahedron* **1978**, *34*, 179–187.

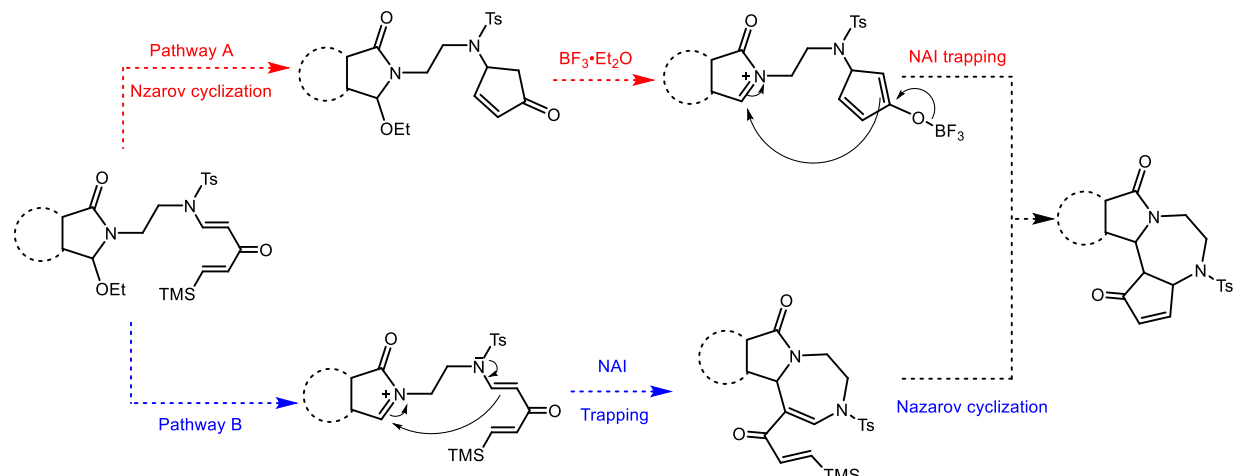
I.3.4. Mechanistic studies of the domino: *N*-acyliminium ion trapping and Nazarov cyclization

I.3.4.1. Plausible reaction pathways for the domino reaction

Considering the mechanism involved, the sequence of the reactions was uncertain.

-Pathway A: First Nazarov cyclization with the formation of the cyclopentenone ring and subsequent *N*-acyliminium ion trapping by the boron enolate (**Scheme 80**, A)

-Pathway B: First *N*-acyliminium ion trapping by tertiary enamidyl vinyl ketone followed by Nazarov cyclization. (**Scheme 80**, B)



Scheme 80 : Plausible reaction pathways

To gain more insight into the preferred reaction sequence, cyclic voltammetry (CV) was employed.

I.3.4.2. Cyclic voltammetry

a. Introduction

Electrochemistry is a powerful tool to investigate reactions involving electron transfers.⁸⁹ Electrochemistry relates the flow of electrons in chemical transformations. In this context, cyclic voltammetry (CV) is a popular chemical technique commonly employed to investigate the reduction and oxidation processes of molecular species. Thus, CV is essential to study electron transfer-initiated processes, including catalysis.

Typically, a cyclic voltammetry profile is provided in a figure called a voltammogram. The x-axis represents the applied potential (E) in volts, while the y-axis is the response, i.e., the resulting current (i) in amperes (**Figure 9**).

⁸⁹ N. Elgrishi, K. J. Rountree, B. D. MacCarthy, E. S. Rountree, T. T. Eisenhart, J. L. Dempsey, *J. Chem. Educ.* **2018**, 95, 197-206.

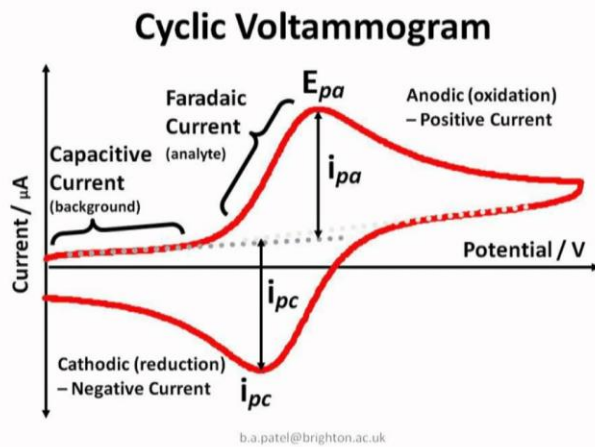


Figure 9: Cyclic voltammetry profile

The scan rate in V/s is an important parameter, indicating the speed variation of the potential during the experiment.

To collect the data for a CV experiment, an electrochemical cell is required (**Figure 10**). Different components are needed to assemble an electrochemical cell, such as an electrolyte solution, a working electrode, and a reference electrode

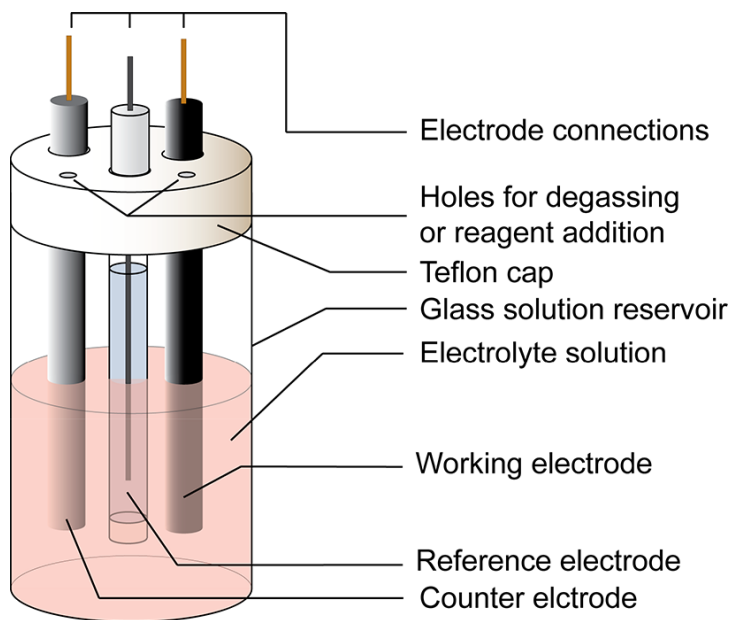


Figure 10 : Schematic representation of an electrochemical cell for CV experiments

Electrical neutrality is maintained via migration of ions in solution during electron transfer. Therefore, an **electrolyte solution** is necessary. Ammonium salts have become the electrolytes of choice for electrochemistry experiments. For dichloromethane or acetonitrile solutions, tetrabutylammonium (+NBu₄) salts are commonly used.

The working electrode carries out the electrochemical event of interest. Glassy electrodes can be used as their surface is very reactive once they are activated by polishing.

A reference electrode has a well defined and stable equilibrium potential and is used as a reference. The applied potential is thus typically reported as « vs » a specific reference. Some commonly used reference electrodes are the saturated calomel electrode (SCE), standard hydrogen electrode (SHE), and the AgCl/Ag electrode.

b. Results of cyclic voltammetry related to the domino reaction.

The aim of the cyclic voltammetry studies was not to mimic the mechanism, because in our domino reaction *i.e.*, *N*-acyliminium ion trapping and Nazarov cyclization, no electron transfer is involved.

The objective was to assess the affinity of the Lewis acid for the two functional groups in the starting material, namely the ethoxy-lactam and the dienone. For this purpose, we decided to synthesize two mimics of these functional groups; *N*-methyl dienone **267** as well as *N*-methyl-ethoxy lactam **268** (**Figure 11**).

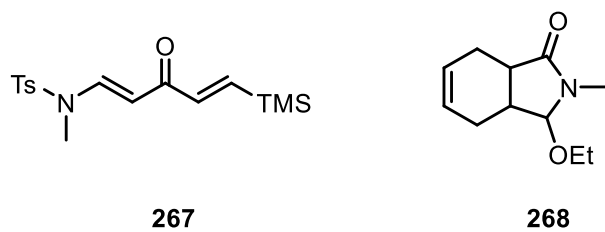


Figure 11: Compounds prepared for cyclic voltammetry experiments

Two comparative cyclic voltammetry experiments were performed. The first one with enamidyl vinyl ketone **267** alone and by adding Et₂O•BF₃ and the second one by mixing enamidyl vinyl ketone **267** and lactam **268** with or without Et₂O•BF₃ (**Figure 11**).

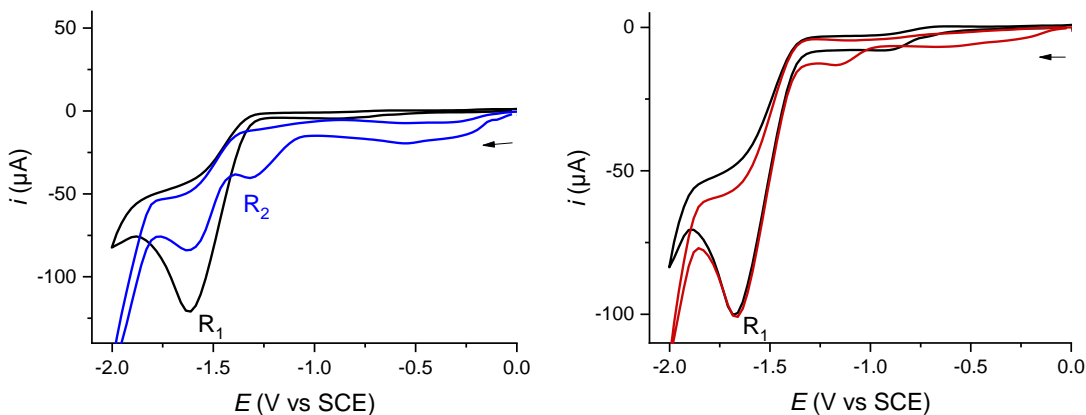


Figure 11: Cyclic voltammetry (CV) performed toward reduction potential of a 4 mM solution in CH₂Cl₂ containing 0.1 M of *n*-Bu₄NBF₄ using a glassy carbon working electrode (d = 3 mm) with a Pt wire as counter-electrode and saturated calomel electrode (SCE) as reference electrode, at a scan rate of 0.1 V s⁻¹ at 20 °C. Left: Black curve: **267** alone, Blue curve: **267**

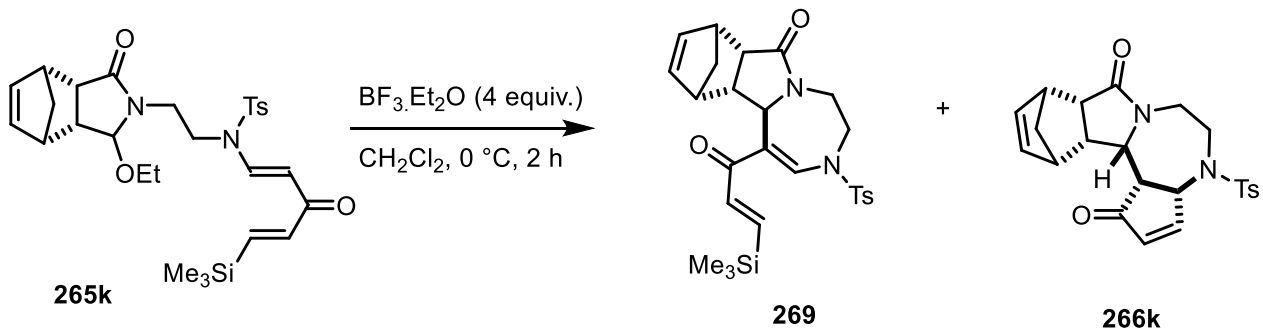
with 1 equivalent of $\text{Et}_2\text{O}\bullet\text{BF}_3$ at rt. Right: Black curve: **267** with 1 equivalent of **268**, Red curve: **267** with 1 equivalent of **268** and 1 equivalent of $\text{Et}_2\text{O}\bullet\text{BF}_3$ at rt.

Enamidyl vinyl ketone **267** was characterized by its reduction peak potential at -1,6V vs SCE (saturated calomel electrode) in CH_2Cl_2 . The CV pattern instantaneously evolved after addition of 1 equivalent of $\text{Et}_2\text{O}\bullet\text{BF}_3$ with a less cathodic reduction peak at -1,3V vs SCE (**Figure 11 left**). Cyclic voltammetry studies were also performed with 8 equivalents of $\text{Et}_2\text{O}\bullet\text{BF}_3$. In this case, the CV are difficult to interpret, perhaps because of secondary reactions taking place under these conditions.

When adding the Lewis acid in the presence of the aminal precursor **268**, no modification of the CV was observed just after addition of $\text{Et}_2\text{O}\bullet\text{BF}_3$ (**Figure 11, right**). This experiment shows that in the presence of the lactam part **268**, the enamidyl vinyl ketone does not interact with the Lewis acid, consistent with an enhanced affinity of $\text{Et}_2\text{O}\bullet\text{BF}_3$ for the ethoxy lactam **268** rather than for the dienone **267**.

c. Additionnal chemical experiments.

When we performed the reaction starting from enamidyl vinyl ketone **265k** in the presence of $\text{Et}_2\text{O}\bullet\text{BF}_3$, by shortening the reaction time we observed the formation of a small amount of diazepine **269** (**Scheme 81**).



Scheme 81: synthesis of intermediate 269

The production of non-cyclized dienone **269** together with the CV experiments provide evidence that route B is the more likely mechanistic pathway.

d. Proposed mechanism

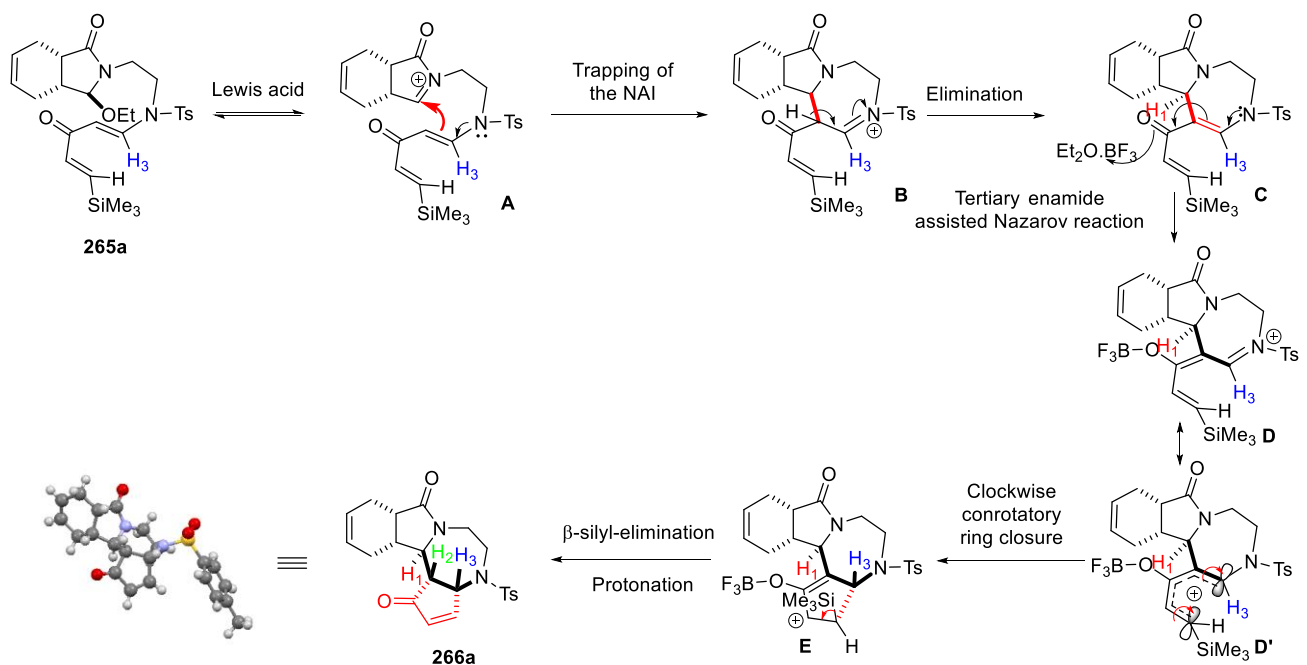
Taking into account the previous experiments and to explain the one-pot formation of fused polycyclic ring system **266**, the mechanism outlined in **Scheme 82** is thus proposed.

According to the NMR studies and the X-ray structures, two trends were observed. With lactam rings fused to conformationally more flexible rings (compounds **266a**, **266b**, **266c**, **266f**, **266h** and **266m**), a trans relationship between lactam proton H₁ and the two ring

junction protons (H_2 and H_3) was observed. Whereas with lactam rings fused to conformationally more rigid cycles, *i.e.*, more conformationally constrained environment (compounds **266d**, **266e**, **266i**, **266j**, **266j**, and **266k**), a *cis* relationship between the lactam proton (H_1) and the two ring junction protons (H_2 and H_3) was observed.

Treatment of dienone **265a** with the Lewis acid provides the *N*-acyliminium ion **A**. In this case, the prochiral iminium ion **A** will be attacked from the less hindered side by the tertiary enamide (convex face), leading to iminium ion **B**. After deprotonation, the cross-conjugated dienone **C** undergoes tertiary enamide-assisted Nazarov cyclization.

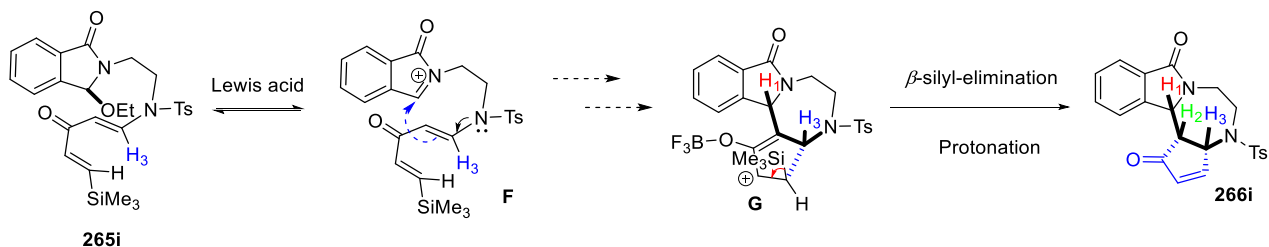
Indeed, the presence of the nitrogen moiety at the divinyl ketone lowers the energy barrier for the formation of the oxyallyl cation, allowing the Nazarov reaction to take place at 0 °C or room temperature.⁹⁰ Once the stereochemistry of the aminal proton (H_1) is set, clockwise, conrotatory ring closure of **D'** pushes down the newly formed five-membered boron enolate **E**. The latter evolves upon β -silyl-elimination, and protonation will occur from the less hindered convex face, thus generating the thermodynamically more stable *cis* fused 5-7 membered polycyclic system **266a** (**Scheme 82**).



Scheme 82 : Mechanism with lactam rings fused to conformationally more flexible rings

In the case of divinyl ketone **265i**, the conformationally constrained environment of the lactam will induce an attack from the enamide under the plane of the lactam as drawn, thus pushing the lactam proton H_1 above the plane of the lactam moiety, also pushing down the newly formed five-membered boron enolate **G**, through a clockwise conrotatory ring closure. Protonation of **G** will occur to generate the thermodynamically more stable *cis*-fused 5-7 membered polycyclic system **266i** (**Scheme 83**).

⁹⁰ D. J. Kerr, M. Miletic, J. H. Chaplin, J. M. White, B. L. Flynn, *Org. Lett.* **2012**, *14*, 1732-1735. N. Manchala, H. Y. L. Law, D. J. Kerr, R. Volpe, R. J. Lepage, J. M. White, E. H. Krenske, B. L. Flynn, *J. Org. Chem.* **2017**, *82*, 6511-6527;



Scheme 83: Mechanism with more constrained divinyl ketones

Compound **266n** involving an 8-membered ring shows an unusual *cis-trans* behavior and would be structurally related to the lactams fused to a flexible ring, but protonation of the enol-boronate occurs from the less hindered side and thus provides a *trans* ring junction because of the presence of the diazocane (**Figure 12**).

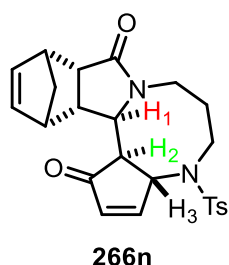
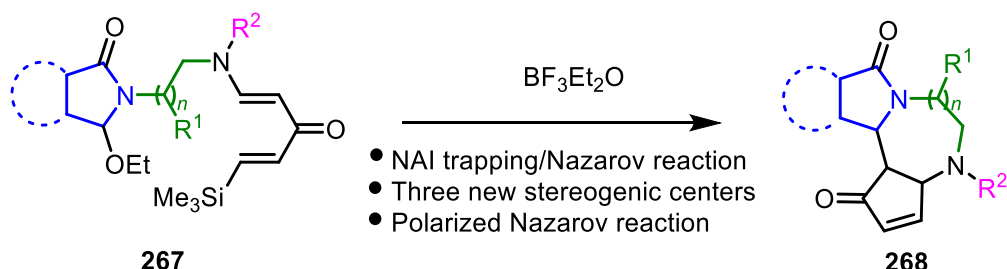


Figure 12: Relative stereochemistry of compound **266n**

I.4. Conclusion

In conclusion, we have shown that NAI generated from tertiary enamidyl vinyl ketones undergo cyclization followed by tertiary enamide-assisted Nazarov cyclization to afford in each case a single diastereomeric polycyclic diazepine bearing a cyclopentenone ring. Torquoselectivity of the domino reaction can be attributed to the particular design of the divinyl ketones involved. Various NAI precursors as well as different chain lengths were accommodated. Electrochemical experiments revealed a higher affinity of the Lewis acid for the aminal part of the substrate than for the divinyl part, thus corroborating the order of the reaction sequence within the domino reaction (**Scheme 84**).



Scheme 84: Domino-reaction

II. CHAPTER 2 SYNTHESIS OF CF₂H-SUBSTITUTED 2-AMIDOFURANS VIA COPPER-CATALYZED ADDITION OF α -DIFLUORINATED-DIAZOACETONE TO YNAMIDES.

II.1. Introduction.

Organofluorine compounds are widely used in the fields of pharmaceuticals, agrochemicals, and materials science.⁹¹ As a consequence, much effort has been devoted to the selective incorporation of fluorine-containing moieties into organic molecules to modulate their biological properties. In this view, a difluoromethyl group is a critical fluorinated functional group as it can act as a hydrogen bond donor and consequently be considered as a bioisostere of a hydroxyl or a thiol group that brings out its potential value in drug design.⁹²

Heterocycles containing difluoromethyl groups are emerging, but are still a scarcely investigated class of organofluoro molecules.⁹³

Furans have gained intensive attention from the synthetic community because of their abundance in a wide variety of biological, pharmaceutical and agrochemical molecules.⁹⁴ Among this family, 2-amido-furans have been identified as valuable building blocks for the total synthesis of natural compounds.⁹⁵ Furans substituted with a CF₂H moiety are scarce.

In this chapter, we will first focus on the synthesis of 2-amino-/amidofurans, describe the few syntheses reported of CF₂H substituted furans, and finally present our contribution in this field. Notably, the state of the art will not be exhaustive and only highlights a limited number of papers to provide an overview in this field.

II.2. Synthesis of amino-/amidofurans

Myriad syntheses have been devoted to the preparation of furans, but only limited protocols exist for the construction of 2-amino-/amidofurans.

⁹¹ P. Kirsch, Applications 2nd edn (Wiley-VCH, Weinheim, **2013**). W. K. Hagmann, *J. Med. Chem.* **2008**, *51*, 4359–4369. M. Shimizu, T. Hiyama, *Angew. Chem. Int. Ed.* **2005**, *44*, 214–231.

⁹² C. D. Sessler, M. Rahm, S. Becker, J. M. Goldberg, F. Wang, S. J. Lippard, *J. Am. Chem. Soc.* **2017**, *139*, 9325–9332. Y. Zafrani, G. Sod-Moriah, D. Yeffet, A. Berliner, D. Amir, D. Marciano, S. Elias, S. Katalan, N. Ashkenazi, M. Madmon, E. Gershonov, S. Saphier, *J. Med. Chem.* **2019**, *62*, 5628–5638.

⁹³ J. Hu, W. Zhang, F. Wang, *Chem. Commun.* **2009**, 7465–7478. B. Gao, C. Ni, J. Hu, *Chimia* **2014**, *68*, 414. C. Ni, L. Zhu, J. Hu, *Acta Chim. Sin.* **2015**, *73*, 90; P. Xu, S. Guo, L. Wang, P. Tang, *Synlett* **2015**, *26*, 36–39. B. Chen, D. A. Vicic, *Top. Organomet. Chem.* **2015**, *52*, 113. Y. Lu, C. Liu, Q.-Y. Chen, *Curr. Org. Chem.* **2015**, *19*, 1638. M.-C. Belhomme, T. Basset, T. Poisson, X. Pannecoucke, *Chem. Eur. J.* **2015**, *21*, 12836–12865.

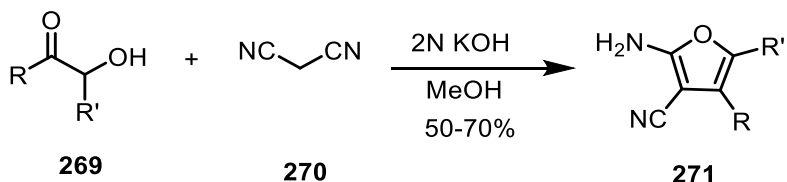
⁹⁴ B. A. Keay, J. M. Hopkins, P. W. Dibble, *In Comprehensive Heterocyclic Chemistry III*. A. R. Katritzky, C. A. Ramsden, E. F. V. Scriven, R. J. K. Taylor, Eds.; Elsevier: Amsterdam, **2008**; Vol. 3, p 571. K.-S. Yeung, X.-S. Peng, J. Wu, R. Fan, X.-L. Hou, *Prog. Heterocycl. Chem.* **2013**, *25*, 183. Y. Ji, Z.-Y. Xin, Y.-B. Shi, H.-B. He, S. H. Gao, *Org. Chem. Front.* **2020**, *7*, 109–112. Y. Ji, Z.-Y. Xin, H.-B. He, S.-H. Gao, *J. Am. Chem. Soc.* **2019**, *141*, 16208–16212.

⁹⁵ K.-S. Yeung, X.-S. Peng, J. Wu, R. Fan, X.-L. Hou, *Prog. Heterocycl. Chem.* **2013**, *25*, 183–215. B. M. Trost, P. J. McDougall, *Org. Lett.* **2009**, *11*, 3782–3785. P. Wipf, F. R. Petronijevic, *J. Am. Chem. Soc.* **2011**, *133*, 7704–7707.

II.2.1. By using nitriles

II.2.1.1. Base-promoted reaction of α -hydroxy ketones with malononitrile

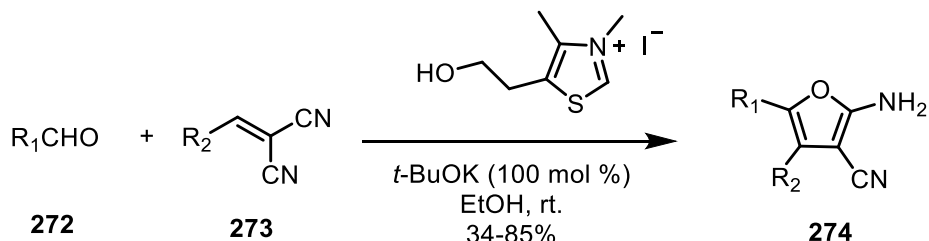
The first synthesis of aminofurans was achieved by Karl Gewald through a Knoevenagel-type condensation involving α -hydroxy ketones and malononitrile. The corresponding furans **271** were obtained by treatment of α -hydroxy ketones with malononitrile in the presence of trimethylamine or diethylamine with yields ranging from 50 to 70% (**Scheme 85**).⁹⁶



Scheme 85: First synthesis of aminofurans

Using similar reactivity, Tanji *et al.* used halo-ketones with malononitriles to obtain aminofurans.⁹⁷

An efficient method for the synthesis of 4,5-disubstituted 2-aminofuran-3-carbonitriles *via* Stetter- δ -ketonitrile cyclization has been developed by Hu *et al.* Aromatic aldehydes **272** were treated with acylidenemalononitriles **273** in the presence of an N-heterocyclic carbene (NHC) and *t*-BuOK at room temperature to provide tetrasubstituted furans **274** with yields ranging from 34 to 85%. Aromatic and heteroaromatic aldehydes reacted successfully by using an inexpensive catalyst under mild conditions (**Scheme 86**).⁹⁸



Scheme 86: Synthesis of aminofurans using Stetter's δ -ketonitrile cyclization

II.2.1.2. Palladium-catalyzed cycloisomerization of 2-(cyanomethyl)phenyl esters

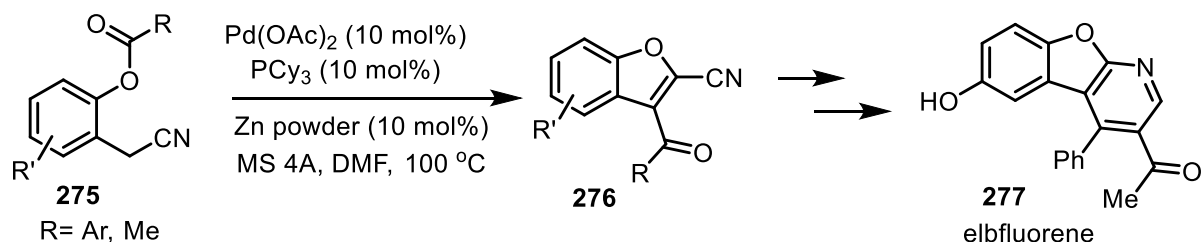
Ohe *et al.* reported a palladium-catalyzed cycloisomerization of 2-(cyanomethyl)phenyl esters with a catalytic amount of Pd(OAc)₂, PCy₃, and zinc powder. In this way, benzofurans **276** were obtained with yields ranging from 50 to 91%. This process allowed these authors to achieve the total synthesis of elbfluorene **277**, a CDK (cyclin-dependent kinase) (**Scheme 87**).⁹⁹

⁹⁶ K. Gewald, *Chem. Ber.* **1966**, *99*, 1002–1007.

⁹⁷ T. Kato, H. Kimura, K. Tanjil, *Chem. Pharm. Bull.* **1978**, *26*, 3880–3883.

⁹⁸ P. Liu, M. Lei, L. Ma, L.-H. Hu, *Synlett* **2011**, *8*, 1133–1136.

⁹⁹ M. Murai, K. Mikia, K. Ohe, *Chem. Commun.*, **2009**, 3466–3468.

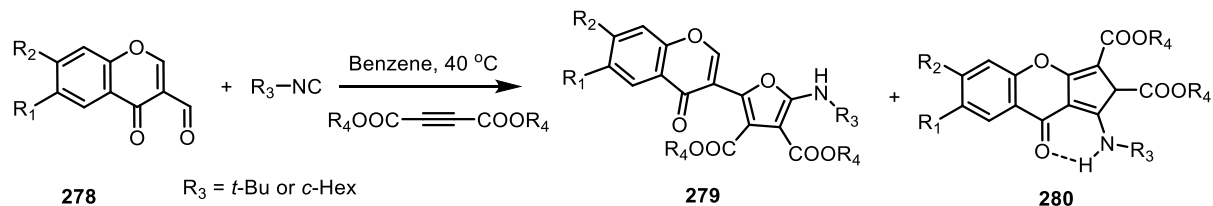


Scheme 87: Ohe's synthesis of aminofurans

II.2.2. Three-component coupling of isocyanides, alkynes, and carbonyl compounds

II.2.2.1. With aldehydes

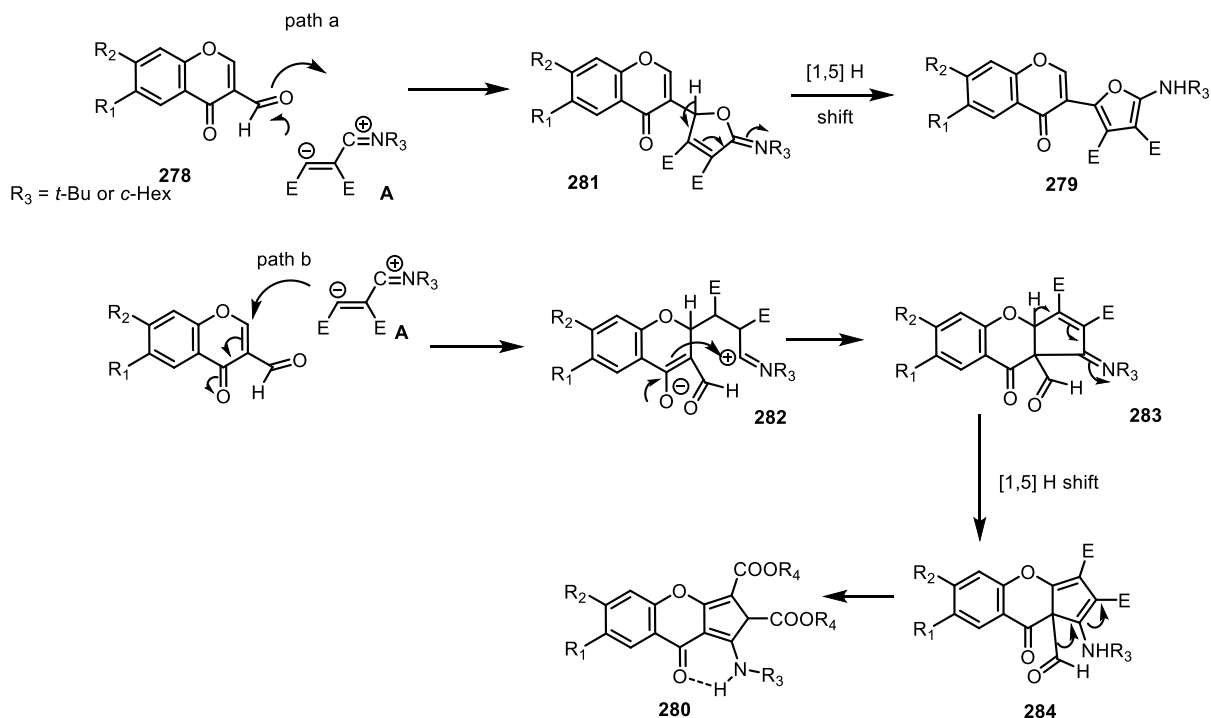
A three-component coupling reaction involving 3-formylchromones **278**, isocyanides, and acetylenedicarboxylates has been reported by Tsoleridis *et al.* Thus, dimethyl acetylenedicarboxylate with an electron-donating substituent in the chromone moiety favors formation of chromenylfurandicarboxylates **279**, whereas electron-withdrawing substituents favor a reaction involving a C2-C3 double bond, leading to cyclopentachromenedicarboxylates **280**. By changing the dimethyl acetylenedicarboxylate to diethyl acetylenedicarboxylate, the cyclopentachromenedicarboxylates **280** were preferentially formed in all cases (**Scheme 88**).¹⁰⁰



Scheme 88: Tsoleridis' synthesis of aminofurans

A plausible reaction mechanism supported by DFT calculations is proposed. Reaction between isocyanide and acetylenedicarboxylate forms the zwitterionic intermediate **A**. The latter adds to the aldehyde to form **281**. Subsequent cyclization and [1,5] hydride shift ends with the formation of the chromenyldicarboxylates **279** (**Scheme 88, path a**). However, electron-withdrawing substituents in the 6-position of the chromone moiety render the C-2 carbon more electron-deficient than the carbonyl aldehyde, thus favoring the 1,4 addition, which upon ring closure and [1,5] hydride shift forms intermediate **284**. Deformylation then takes place, providing cyclopentachromenedicarboxylates **280** (**Scheme 89, path b**).

¹⁰⁰ M. A. Terzidis, J. Stephanidou-Stephanatou, C. A. Tsoleridis, *J. Org. Chem.* **2010**, *75*, 1948–1955.



Scheme 89: Plausible reaction mechanism for the formation of **279** and **280**

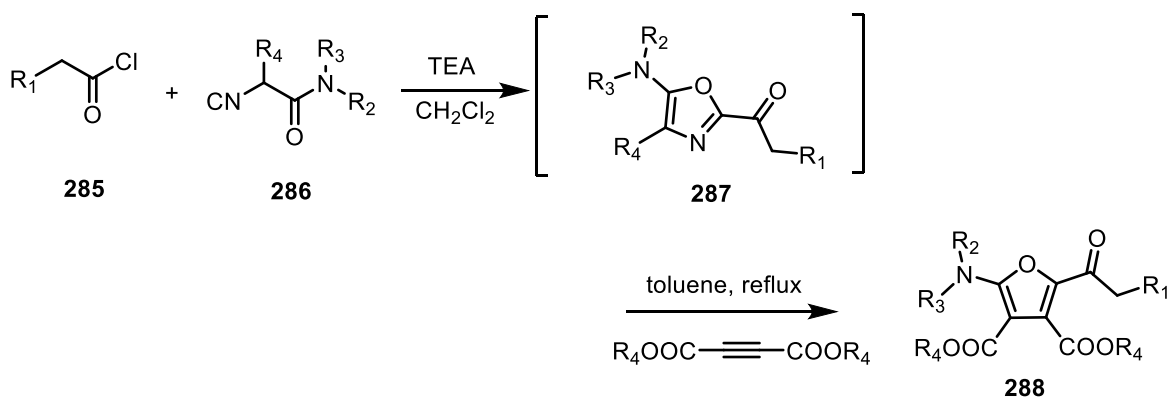
The three-component reaction was also investigated by Reddy *et al.* In this case, the condensation of isocyanides, α,β -unsaturated aldehydes, and dialkyl acetylenedicarboxylates took place in polyethylene glycol (PEG 400) at room temperature to afford the corresponding styrylfuran derivatives.¹⁰¹

II.2.2.2. With acyl chlorides

The production of aminofurans was also proposed by Pirali *et al.* via condensation of isocyano acetamides, acyl chlorides, and dialkyl acetylenedicarboxylates. Treatment of acyl chloride **285** with isocyanide **286** in the presence of triethylamine via amino oxazole **287** provided the correspondind furans **288** with yields ranging from 55 to 79% (**Scheme 90**).¹⁰²

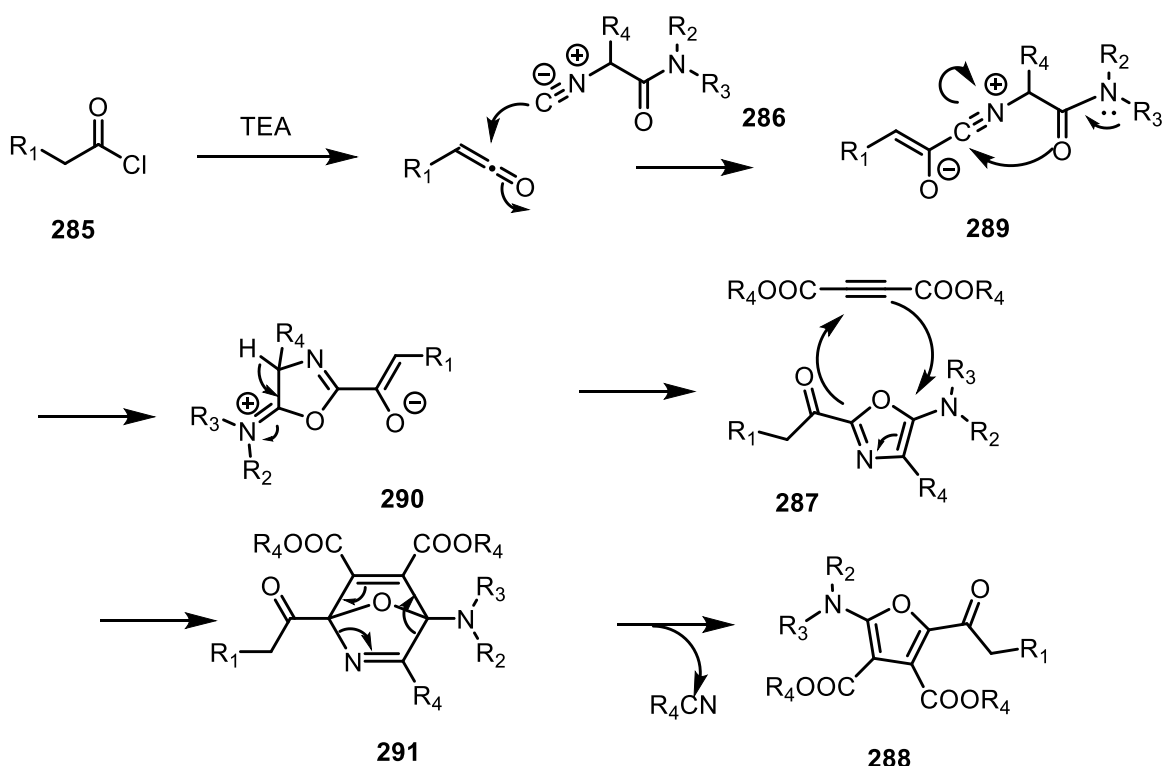
¹⁰¹ B. V. Subba Reddy, D. Somashekara, A. Mallikarjun Reddy, J. S. Yadava, Balasubramanian Sridhar, *Synthesis* **2010**, 2069-2074

¹⁰² R. Mossetti, D. Caprioglio, G. Colombano, G. C. Tron, T. Pirali, *Org. Biomol. Chem.*, **2011**, 9, 1627-1631



Scheme 90: Synthesis of aminofurans via condensation of isocyano acetamides

The postulated mechanism involves a ketene intermediate obtained by reaction of acyl chlorides and triethylamine. The latter is trapped by isocyanide, providing nitrilium ion **289**. Subsequent cyclization and proton transfer afforded amino-oxazole **287**. [4+2] Cycloaddition followed by [4+2] cycloreversion and elimination of acetonitrile ends with the formation of aminofurans **288** (**Scheme 91**).

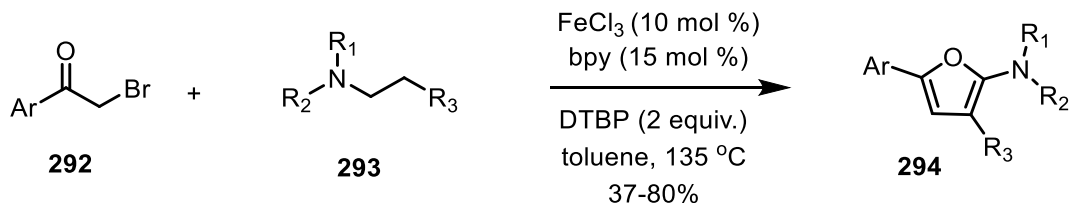


Scheme 91: Proposed mechanism for the formation of **288**

II.2.3. Synthesis of 2-aminofurans from 2-haloketones

Recently Wu *et al.* reported an iron-catalyzed synthesis of 2-aminofurans from 2-haloketones and tertiary amines or enamines. By using 2,2'-bipyridyl as the ligand, DTBP as an oxidant in

toluene, and FeCl_3 as catalyst, the aminofurans **294** were obtained by reacting 2-haloketones with various tertiary amines at $135\text{ }^\circ\text{C}$ (**Scheme 92**).¹⁰³

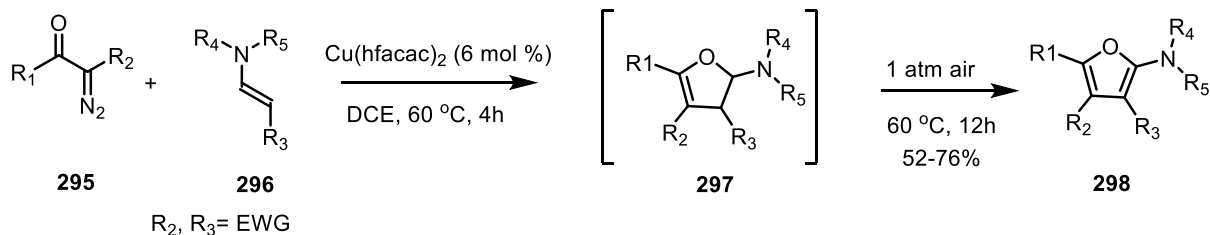


Scheme 92: Iron-catalyzed synthesis of 2-aminofurans

This reaction was extended to aryl-substituted enamines with better yields for the aminofurans.

II.2.4. Amino/amidofuran synthesis using enamines

Park *et al.* reported copper-catalyzed [3+2] cycloaddition of carbenoids with enamines. Treatment of activated enamine **296** with $\text{Cu}(\text{hfacac})_2$ in DCE at $60\text{ }^\circ\text{C}$ provided 2-aminofurans with yields ranging from 52 to 76% (**Scheme 93**).¹⁰⁴

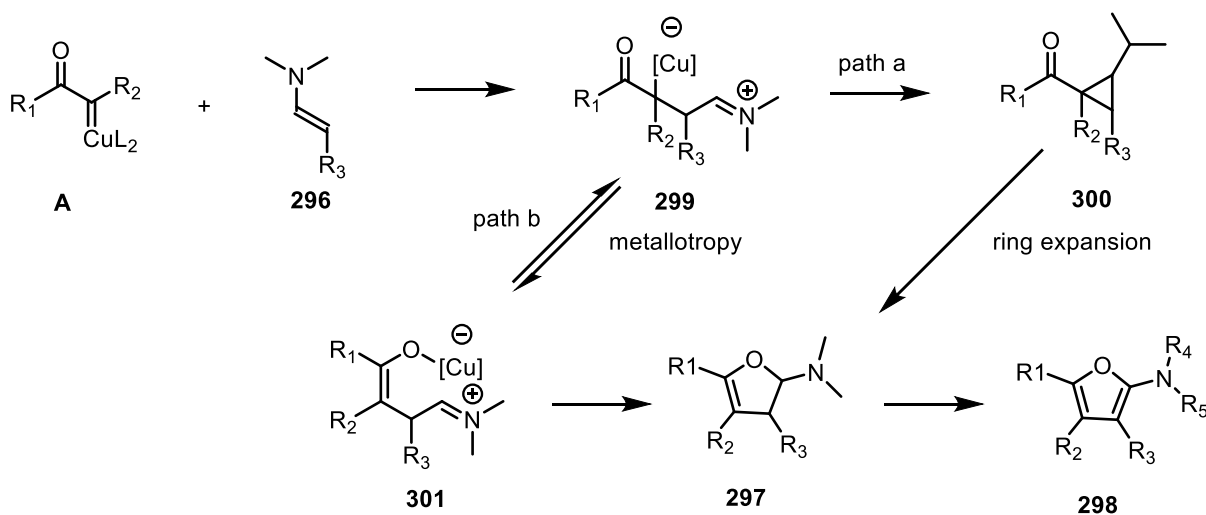


Scheme 93: Copper-catalyzed [3+2] cycloaddition of carbenoids with enamines

The proposed mechanism involves a nucleophilic attack of the enamine **296** on copper-carbenoid **A**, providing iminium **299**. Two pathways are then possible: a cyclopropanation to give **300**, and subsequent ring expansion (pathway A). Another possibility would be a direct cyclization of **301** via metallotropy to form dihydrofuran **297** followed by aromatization.

¹⁰³ L.-C. Wang, H.-Q. Geng, J.-B. Peng, X.-F. Wu, *Eur. J. Org. Chem.* **2020**, 2605-2616.

¹⁰⁴ Y. Jiang, V. Z. Y. Khong, E. Lourdusamy, C.-M. Park, *Chem Commun.* **2012**, 48, 3133-3135.

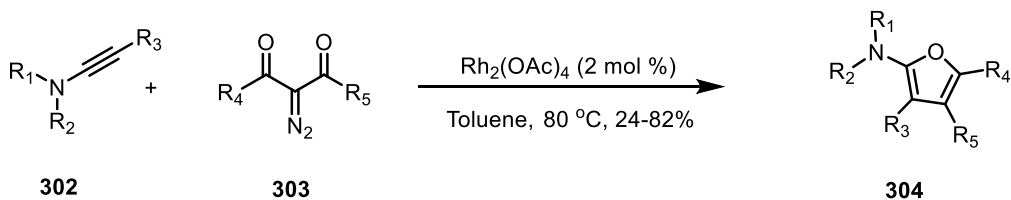


Scheme 94: Proposed mechanism for the copper-catalyzed synthesis of **298**

II.2.5. Synthesis of amidofurans using ynamides

II.2.5.1. Rh(II)-catalyzed cyclopropanations of ynamides

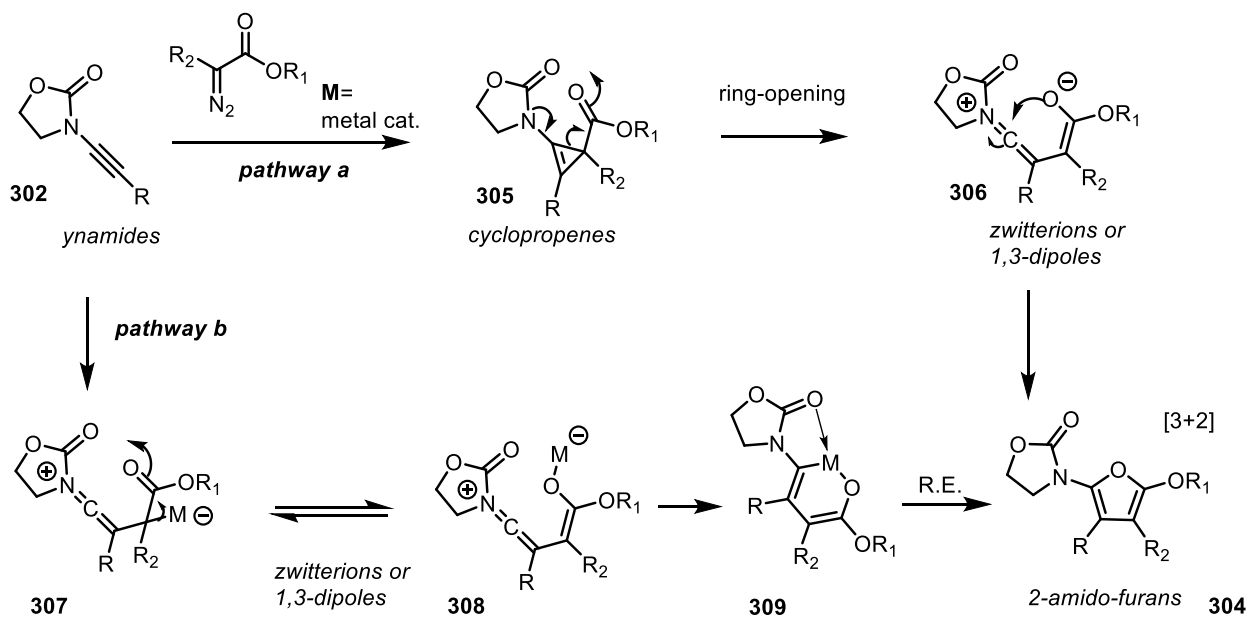
Hsung *et al.* reported a Rh(II)-catalyzed cyclopropanation of ynamides **302**, providing a facile entry to substituted 2-amidofurans **304**. Ynamides **302** were treated with diazo malonates **303** in the presence of $\text{Rh}_2(\text{OAc})_4$ to afford the corresponding amidofurans **304** with yields ranging from 24 to 82% (**Scheme 95**).¹⁰⁵



Scheme 95: Rh(II)-catalyzed cyclopropanations of ynamides

Cyclopropanation of ynamide **302** is proposed via metal decomposition of α -diazoacetates. Ring-opening of the cyclopropane **305** will lead to iminium **306**. Finally, addition of the enolate onto the iminium **306** will provide 2-amidofurans (**Scheme 96, pathway a**). A second mechanism is proposed through formal [3+2] cycloaddition via metal-bound zwitterionic species **307** and **308**, providing metallo-oxocyclohexadiene **309**. Reductive elimination of the latter would provide **304** (**Scheme 96, pathway b**).

¹⁰⁵ H-Y Li, Richard. P. Hsung, *Org. Lett.* **2009**, *11*, 4462–4465.



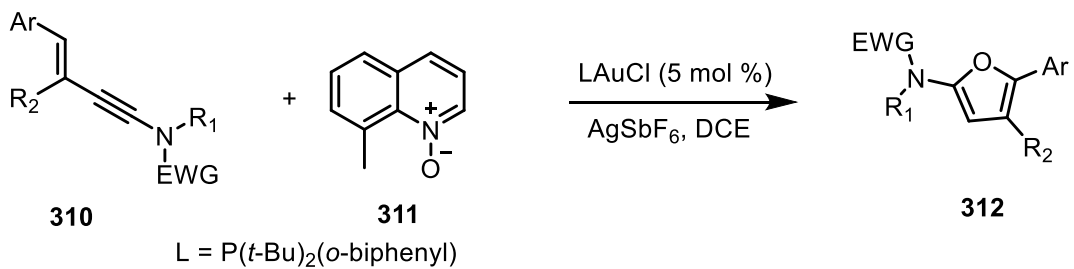
Scheme 96: Proposed reaction mechanism

Initial attempts with ethyl- α -diazoacetate led to 2-amidofurans with very poor yields. The success of the reaction is restricted to the use of diazomalonates and iodonium ylides. As diazomalonates are better cyclopropanating agents than iodonium ylides, the former led to much better yields than the latter.

II.2.5.2. Cyclizations from enynamides

a. Gold-catalyzed formal [4+1]-cycloadditions of enynamides

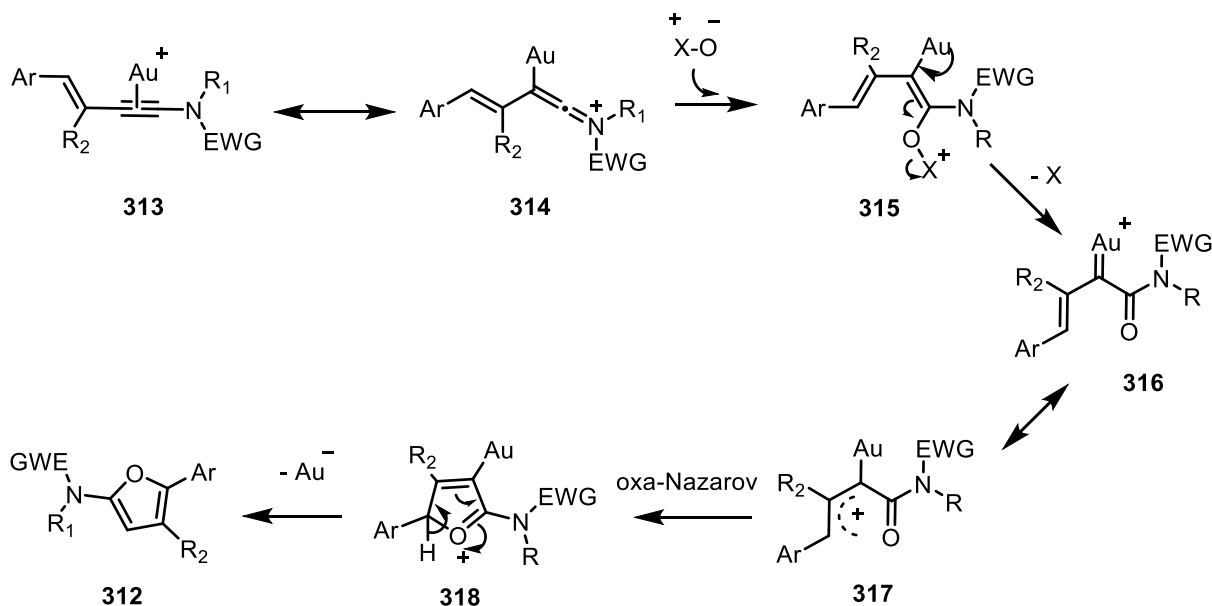
Liu *et al.* explored a gold-catalyzed [4+1] cycloaddition reaction between 3-en-1-ynamides **310** and 8-methylquinoline oxide. Highly substituted furans were obtained, depending on the efficiency of the substituents on the nitrogen atom and the aryl substituents of the enynamides (**Scheme 97**).



Scheme 97: Gold-catalyzed [4+1] cycloaddition

Gold-catalysis will provide alkenylgold carbenoid **315** after addition of 8-methylquinoline oxide onto the ketene-iminium **314**. The authors hypothesized an oxa-Nazarov cyclization of

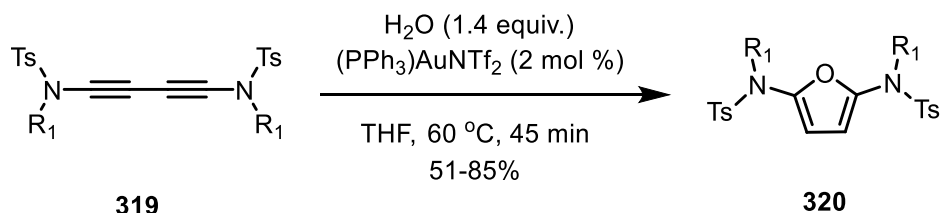
the Au(I)-stabilized allyl cation **316** to generate, after deprotonation and protodemettalation, the desired amidofurans **312** (**Scheme 98**).¹⁰⁶



Scheme 98: Proposed mechanism for the gold-catalyzed [4+1] cycloaddition

b. Gold catalyzed-hydroamination

Skrydstrup *et al.* proposed a double hydroamination of dimerized ynamides with $(Ph_3P)AuNTf_2$ as catalyst, providing 2,5-diamidofurans **320**. Dimerized ynamides **319** were treated with 2 mol % $(Ph_3P)AuNTf_2$, and 1.4 equivalents of water in THF. After 45 minutes, the diamidofurans **320** were isolated in good yields (**Scheme 99**).¹⁰⁷



Scheme 99: Hydroamination of dimerized ynamides

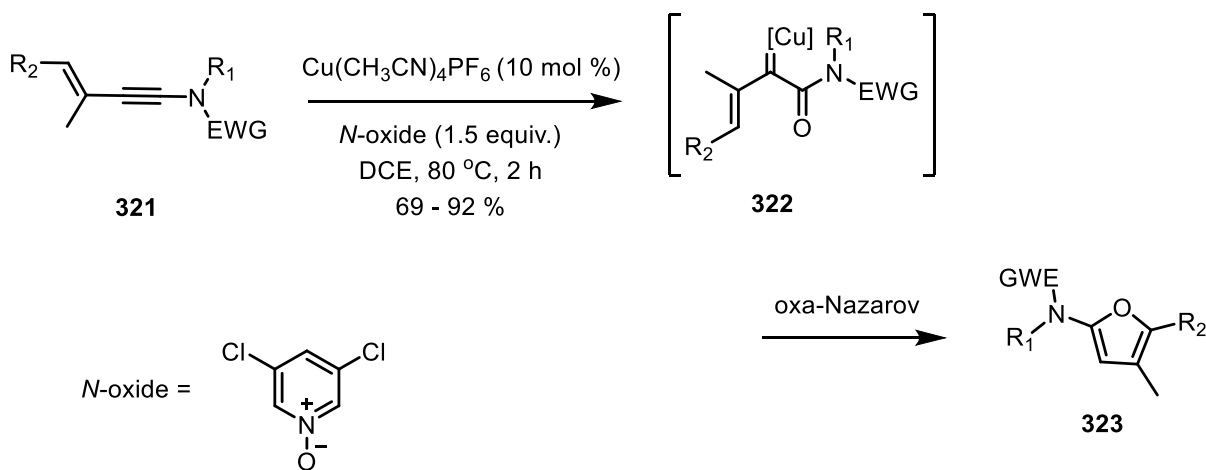
c. Copper-catalyzed oxidative cyclization of enynamides

Employing aryl-tethered enynamides **321** as starting material, Shen *et al.* described an α -oxo-copper carbene intermediate **322** followed by an oxa-Nazarov reaction by treatment of enynamides **321** with $Cu(CH_3CN)_4PF_6$ in dichloroethane (DCE) at 80 °C (**Scheme 100**).¹⁰⁸

¹⁰⁶ R. B. Dateer, K. Pati, R.-S. Liu, *Chem. Commun.* **2012**, 48, 7200-7202.

¹⁰⁷ S. Kramer, J. L. H. Madsen, M. Rottländer, T. Skrydstrup, *Org. Lett.* **2010**, 12, 2758-2761

¹⁰⁸ W.-B. Shen, X.-T. Tang, T.-T. Zhang, S.-Y. Liu, J.-M. He, T.-F. Su, *Org. Lett.* **2020**, 22, 6799-6804

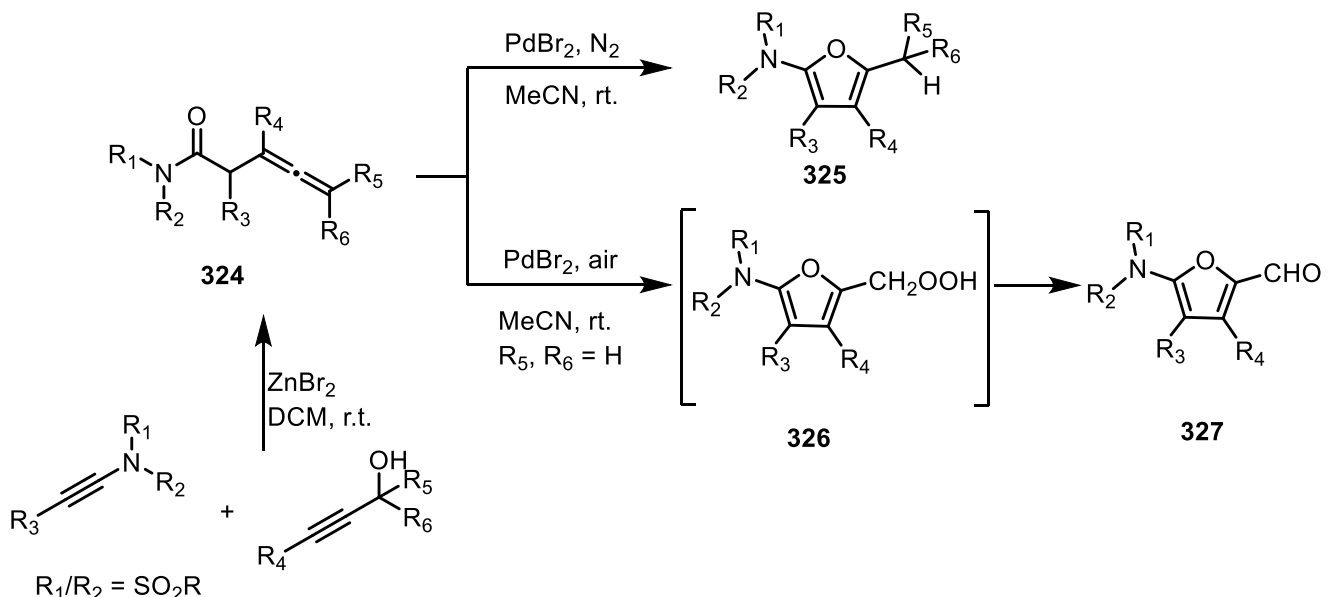


Scheme 100: Copper-catalyzed cyclization of enynamides

II.2.6. Synthesis of furans *via* homoallenyl amides

II.2.6.1. Palladium-catalyzed cycloisomerization of homoallenyl amides

Zhu *et al.* developed a palladium-catalyzed cycloisomerization of homoallenyl amides **324** to form 2-aminofurans **325** and **327**. The homoallenyl amides were prepared from *N*-sulfonyl ynamides, propargyl alcohols, and ZnBr₂ in dry CH₂Cl₂ at room temperature. The 2-amino-5-alkyfurans **325** were obtained by treatment of allenyl amides **324** with PdBr₂ under an N₂ atmosphere, whereas under aerobic oxidative conditions the homoallenyl amides led to 2-amino-5-formylfurans **327** with good yields. The authors postulate that peroxide **326** may be a key intermediate for the Pd-catalyzed radical aerobic process (**Scheme 101**).¹⁰⁹



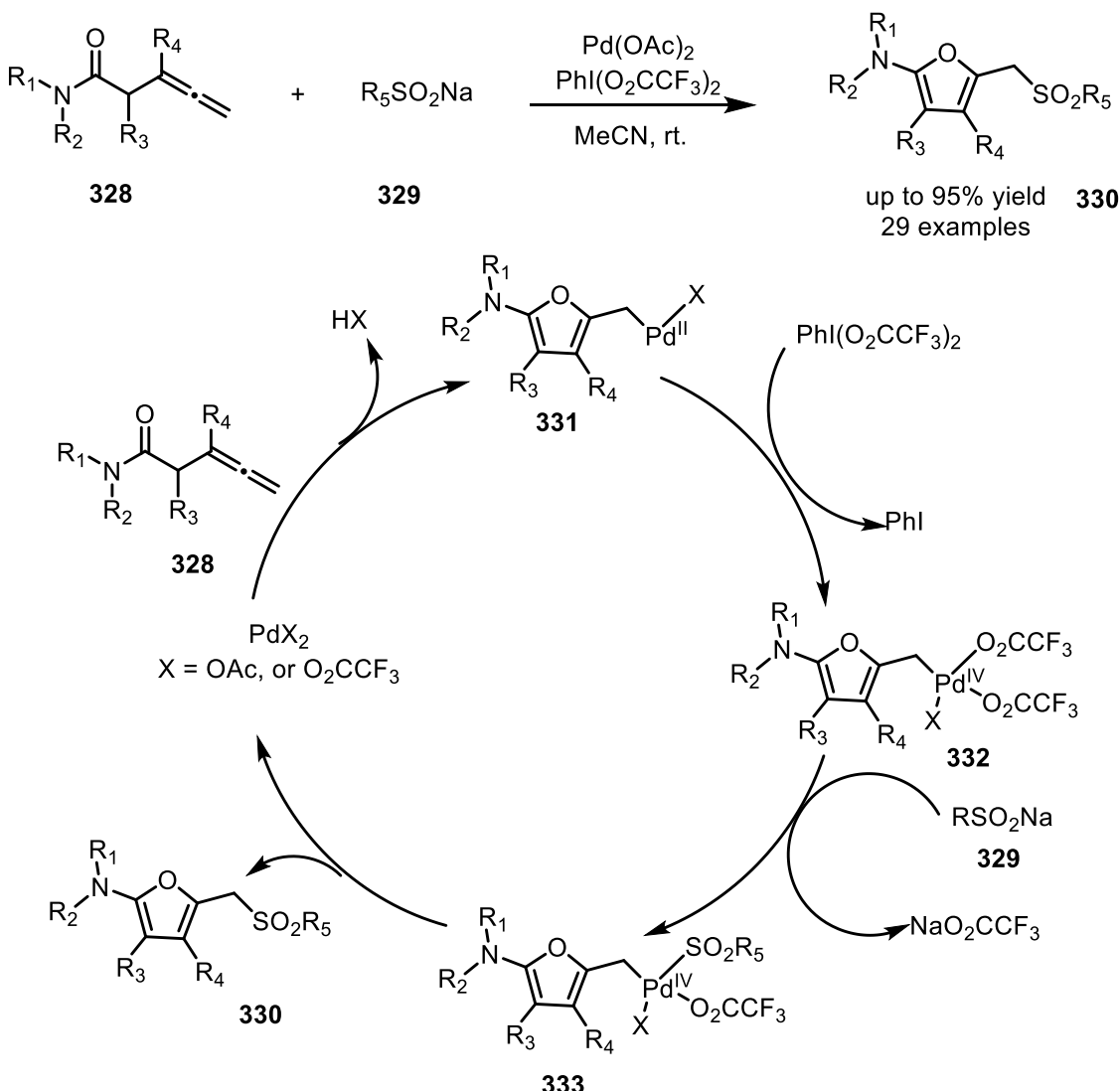
Scheme 101: Palladium-catalyzed cycloisomerization of homoallenyl amides.

¹⁰⁹ C.-G. Cheng, S.-Y. Liu, G. Zhu, *Org. Lett.* **2015**, *17*, 1581–1584

In 2016, these authors extended this process to the synthesis of azido derivatives¹¹⁰

II.2.6.2. Palladium-catalyzed tandem cyclization/sulfonylation of homoallenyl amides

A palladium-catalyzed cyclative sulfonylation of homoallenyl amides **328** using bench-stable sodium sulfonates and a hypervalent iodine reagent $\text{PhI}(\text{O}_2\text{CCF}_3)_2$ is described by Zhu *et al.* The reaction takes place at room temperature, producing 2-amino-5-sulfonylmethylfurans **330** in good to excellent yields. A plausible reaction mechanism is proposed, which involves an oxypalladation of the terminal C-C bond of the allene of **328** followed by deprotonation to provide intermediate **331**. Oxidation of **331** by $\text{PhI}(\text{O}_2\text{CCF}_3)_2$ provides **332**. A ligand exchange with sodium sulfonates **329** and subsequent reductive elimination provides **330** along with the Pd(II) catalyst, which is used in the next catalytic cycle (**Scheme 102**).¹¹¹



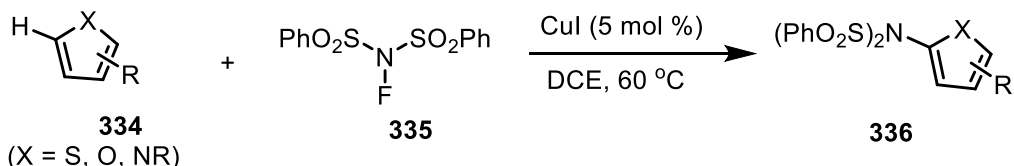
¹¹⁰ Q. Huang, H. Zheng, S. Liu, L. Kong, F. Luo, G. Zhu, *Org. Biomol. Chem.* **2016**, *14*, 8557-8563.

¹¹¹ Y.-M. Wan, J. Zhang, Y.-T. Chen, L.-C. Kong, F. Luo, G.-G. Zhu, *Org. Biomol. Chem.*, **2017**, *15*, 7204-7211

Scheme 102: Palladium-catalyzed tandem cyclization/ sulfonylation of homoallenyl amides

II.2.7. Copper-catalyzed direct amidation of furans

Another possibility was explored by Pan, *et al.* They suggest to simply functionalize the existing furan skeletons **334**. In this way, a highly efficient amidation reaction has been developed with *N*-fluorobenzenesulfonimide **335** (NFSI). This reaction is also applicable to other heterocycles, the amidation is selective, high yields are obtained, and excellent functional group tolerance is observed (**Scheme 103**).¹¹²



Scheme 103: Copper-catalyzed direct amidation of furans

II.3. Synthesis of CF₂H-substituted furans

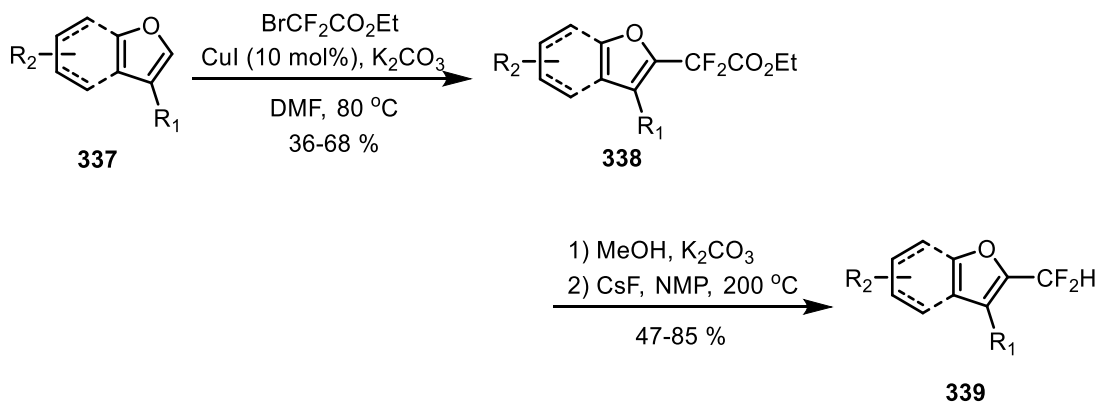
In this section, we will focus on the state of the art concerning the synthesis of CF₂H -substituted furans. CF₂H-substituted furans are exclusively obtained through functionalization of furans. Although different methods exist to functionalize heterocycles, only a very few reports mention the synthesis of CF₂H -substituted furans.

II.3.1. Difluorination of furans via CF₂CO₂Et functionalization

Pannecoucke *et al.* reported a selective introduction of the CF₂CO₂Et moiety at C-2 using CuI as a catalyst. A catalytic amount of CuI, BrCF₂CO₂Et as fluorinating agent, 1,10-phenanthroline, and K₂CO₃ as a base were used to obtain the fluorinated compounds **338** from furans **337** as starting materials, with yields ranging from 36 to 68%. After saponification and treatment with CsF at 200 °C, decarboxylation took place, and the CF₂H-derivatives were isolated with yields from 47 to 85% (**Scheme 104**).¹¹³

¹¹² S.-C. Wang, Z.-Q. Ni, X. Huang, J.-C. Wang, Y.-J. Pan, *Org. Lett.* **2014**, *16*, 5648–5651.

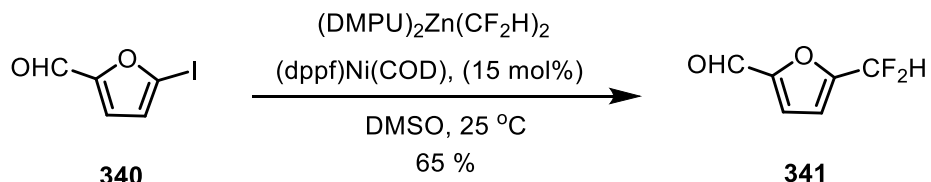
¹¹³ M.-C. Belhomme, T. Poisson, X. Pannecoucke, *J. Org. Chem.* **2014**, *79*, 7205-7211.



Scheme 104: Difluorination of furans via $\text{CF}_2\text{CO}_2\text{Et}$ functionalization

II.3.2. Difluoromethylation of aryl iodides

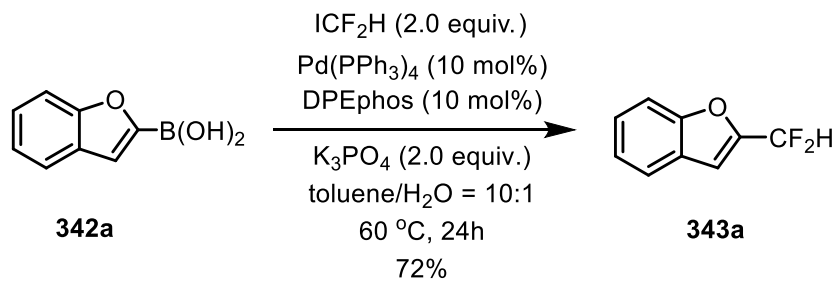
A direct difluoromethylation of aryl halides *via* base metal catalysis was described by Vicic and Xu. A stable difluoromethylzinc reagent has been prepared from ICF_2H , diethylzinc, 1, 3-dimethyl-3,4,5,6-tetrahydro-2-pyrimidinone (DMPU) in combination with a nickel catalyst (*dppf*) $\text{Ni}(\text{COD})$ in DMSO at room temperature and allowed the difluoromethylation of furan **340** with 65% yield (**Scheme 105**).¹¹⁴



Scheme 105: Direct difluoromethylation via base metal catalysis

II.3.3. Palladium-catalyzed difluoromethylation of aryl boronic acids

The protocol proposed by Mikami *et al.* involves a palladium-catalyzed Suzuki-Miyaura cross-coupling reaction of aryl boronic acids with difluoroiodomethane (ICF_2H). Benzofuran **343a** was obtained by reacting the corresponding boronic acid in the presence of $\text{Pd}(\text{PPh}_3)_4$, DPEphos, and K_3PO_4 in a mixture of toluene and water at 60 °C. In this way the authors isolated benzofuran **343a** in 72% yield (**Scheme 106**).¹¹⁵

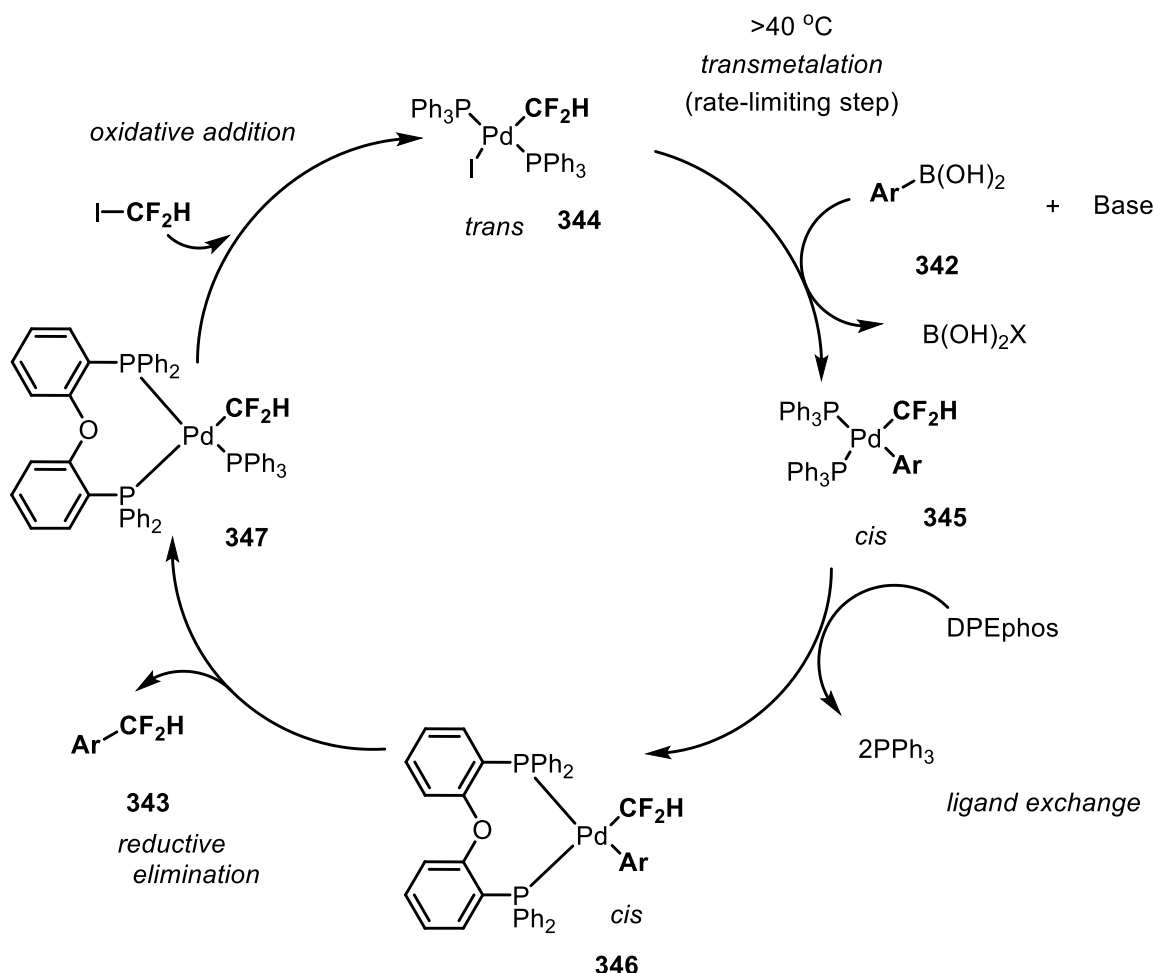


¹¹⁴ L. Xu, D. A. Vicic, *J. Am. Chem. Soc.* **2016**, *138*, 2536-2539.

¹¹⁵ K. Hori, H. Motohashi, D. Saito, K. Mikami, *ACS Catal.* **2019**, *9*, 417-421.

Scheme 106: Difluoromethylation *via* Suzuki-Miyaura cross-coupling

A plausible mechanism is proposed: the authors suggest an oxidative addition of $\text{Pd}(\text{PPh}_3)_4\text{DPEphos}$ catalyst to difluoriodomethane, providing a square-planar *trans*- $\text{Pd}(\text{II})(\text{PPh}_3)(\text{CF}_2\text{H})\text{I}$ complex **344** defined by X-ray crystallographic analysis. The *trans*- $\text{Pd}(\text{PPh}_3)(\text{CF}_2\text{H})\text{I}$ complex is transformed into *cis*- $\text{Pd}(\text{PPh}_3)(\text{CF}_2\text{H})\text{I}$ **345** *via* transmetalation with arylboronic acids. The reductive elimination of **346** takes place *via* ligand exchange to $\text{DPEphosPd}(\text{CF}_2\text{H})\text{Ph}$ to give $\text{Ph-CF}_2\text{H}$ after reductive elimination with the formation of $\text{Pd}(\text{PPh}_3)_2/\text{DPEphos}$ catalyst **345** (**Scheme 107**).

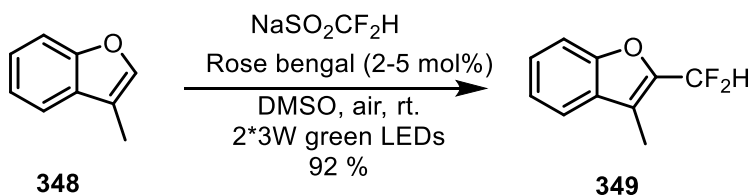


Scheme 107: Proposed mechanism for the palladium-catalyzed difluoromethylation

II.3.4. Direct C-H difluoromethylation *via* organic photoredox catalysis

A visible light-promoted direct C-H difluoromethylation using sodium difluoromethane sulfonate ($\text{CF}_2\text{HSO}_2\text{Na}$) as difluoromethyl radical precursor and Rose bengal as photocatalyst under aerobic conditions was reported by Li, Meng *et al.* When benzofuran **348** was treated with $\text{CF}_2\text{HSO}_2\text{Na}$, Rose bengal (2 mol%) with 3 W LEDs in DMSO, difluorinated benzofuran **349** was obtained in 92% yield (**Scheme 108**).¹¹⁶

¹¹⁶ W. Zhang, X.-X. Xiang, J. Chen, C. Yang, Y.-L. Pan, J.-P. Cheng, Q. Meng, X. Li, *Nature Communications*, **2020**, *11*, 638.

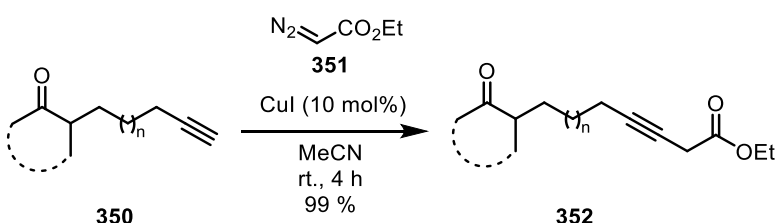


Scheme 108: Difluoromethylation *via* organic photoredox catalysis

II.4. Synthesis of CF₂H-Substituted 2-Amidofurans via Copper-Catalyzed Addition of α -Difluorinated Diazoacetone to Ynamides.

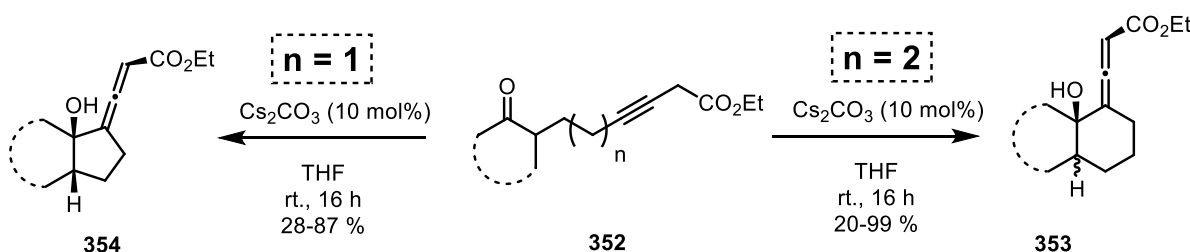
II.4.1. Previous results

One of the key subjects in our team concerned the reactivity of acetylenic ω -ketoesters.¹¹⁷ In this context, we were also interested in the reactivity of keto-3-alkynoates. Among the strategies allowing access to keto-3-alkynoates, we opted for the method developed by G. Fu *et al.* because of its easy processing.¹¹⁸ By treating the alkynyl ketone **350** with ethyl diazoacetate **351** in the presence of a catalytic amount of copper iodide in acetonitrile, we obtained the keto-3-alkynoates **352** exclusively with an excellent yield (**Scheme 109**).¹¹⁹



Scheme 109: Synthesis of keto-3-alkenoates using Fu's procedure

During this work, we noticed that keto-3-alkynoates **352** reacted in the presence of a catalytic amount of cesium carbonate, providing bicyclic allenates **353** and **354** with a total selectivity regarding the allenate stereochemistry. The stereochemistry of the allenate is maintained with modification of the cycloalkanone ring as well as with the carbon linker chain. With a spacer of two methylene units, the diastereoselectivity is total with respect to the ring junction and the allenate **354** (**Scheme 110**).



Scheme 110: Reactivity of keto-3-alkynoates with Cs₂CO₃

¹¹⁷ C. Schfer, M. Miesch, L. Miesch, *Chem. Eur. J.* **2012**, *18*, 8028-8031.

¹¹⁸ A. Suarez, G. C. Fu, *Angew. Chem. Int. Ed.* **2004**, *43*, 3580-3582.

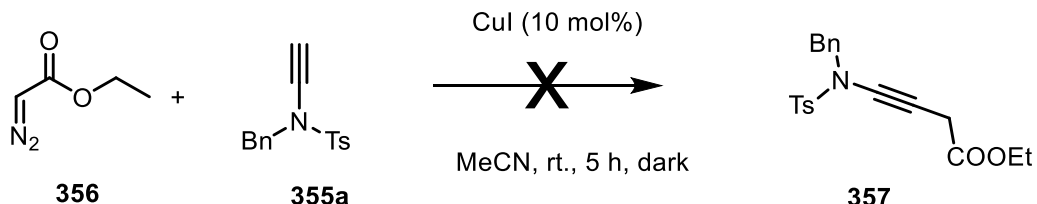
¹¹⁹ C. F. Heinrich, M. Miesch, L. Miesch, *Org. Biomol. Chem.* **2015**, *13*, 2153-2156.

Based on these results, we became interested in the reactivity of ynamides toward ethyl diazoacetate.

II.4.2. Addition of diazo-carbonyl compounds to ynamides

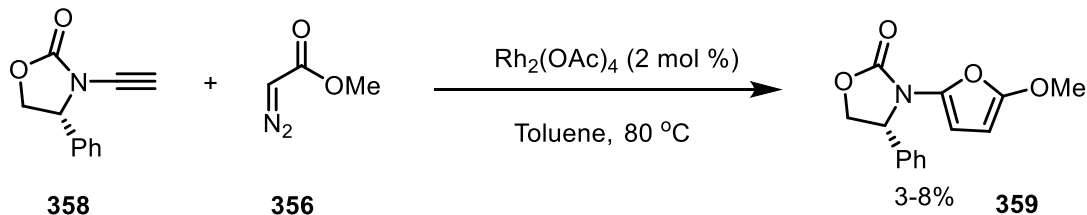
II.4.2.1. First attempts

When ynamide **355a** was treated with ethyl diazoacetate **356** under copper catalysis, we did not obtain the expected functionalized ynamide **357**, but only degradation (**Scheme 111**).



Scheme 111: First attempts of Fu's reaction on ynamides

In this context, Hsung *et al.* reported a Rh(II)-catalyzed cyclopropenation of ynamides **358**. When these authors treated ynamide **358** with ethyl diazoacetate in the presence of $\text{Rh}_2(\text{OAc})_4$, they obtained the corresponding amidofuran **359** with yields ranging from 3 to 8% (**Scheme 112**).¹²⁰



Scheme 112: Hsung's trials with ethyl diazoacetate

II.4.2.2. Objective : Addition of diazo-ketones to ynamides

Taking into account these experiments, we envisioned that the less reactive diazoacetone compared to ethyl diazoacetate would react with the corresponding ynamide under copper catalysis. To do so, we had first to synthesize diazoacetone.

a. Synthesis of diazoacetone **360**

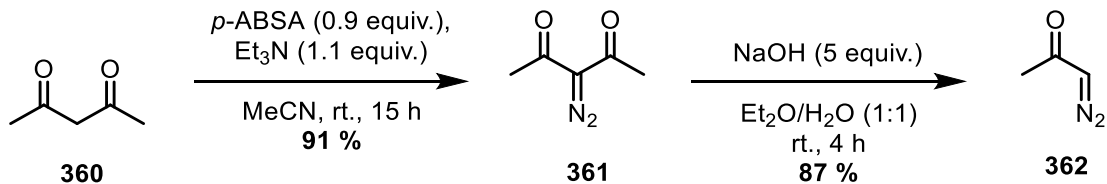
Diazoacetone **362** was synthesized in two steps. The first step consists of a diazo transfer to acetyl acetone **360**. To do so, we relied on the work of Baum *et al.*¹²¹ and Gaulon *et al.*,¹²²

¹²⁰ H.-Y. Li, Richard P. Hsung, *Org. Lett.* **2009**, *11*, 4462–4465.

¹²¹ J. S. Baum, D. A. Shook, Huw M. L. Davies, H. D. Smith, *Synth Commun* **1987**, *17*, 1709-1716.

¹²² A. Lancou, H. Haroun, U. K. Kundu, F. Legros, N. Zimmermann, M. Mathe-Allainmat, J. Lebreton, G. Dujardin, C. Gaulon-Nourry, P. Gosselin, *Tetrahedron*, **2012**, *68*, 9652-9657.

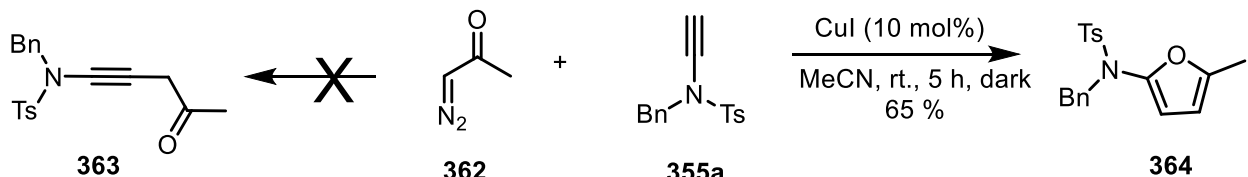
who used *p*-acetamidobenzenesulfonyl azide (*p*-ABSA) as diazo-transfer reagent to synthesize diazoketones and diazoesters. The diazo transfer was thus carried out starting from acetyl acetone **360** in the presence of *p*-ABSA and trimethylamine in acetonitrile overnight at room temperature. The diazopentanedione **361** thus obtained was then deacetylated in the presence of sodium hydroxide in a 1/1 water/ether mixture, providing the corresponding diazoacetone **362** in 87% yield (**Scheme 113**).



Scheme 113: Synthesis of diazoacetone **362**

b. Copper catalyzed addition of diazoacetone to ynamide

Regarding our previous results, we wondered whether diazoacetone would react with ynamide **355a** under copper catalysis to afford the corresponding functionalized ynamide. Surprisingly, instead of the desired keto-substituted ynamide **363**, we obtained the corresponding amidofuran **364** in 65% yield (**Scheme 114**).

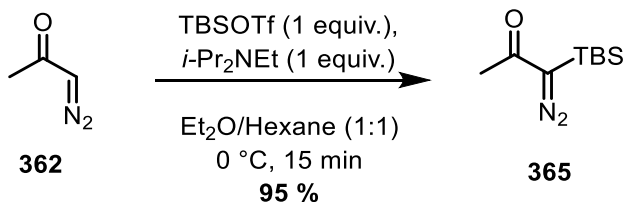


Scheme 114: Synthesis of amidofuran **364**

This result prompted us to have a closer look into this reaction.

c. With disubstituted diazo-compounds

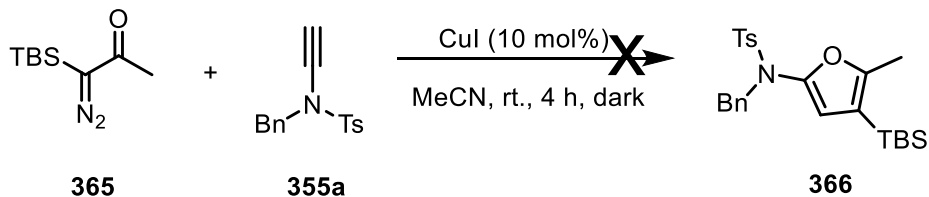
To evaluate the scope of this reaction, we wondered whether disubstituted diazo compounds would react under these conditions. In this way, we prepared *tert*-butyldimethylsilyl-diazoacetone from diazoacetone in the presence of TBSOTf and Hunig's base (**Scheme 115**).¹²³



Scheme 115: Synthesis of TBS-diazoacetone **365**

¹²³ R. Bruckmann, G. Maas, *Chern. Ber.* **1987**, *120*, 635-643.

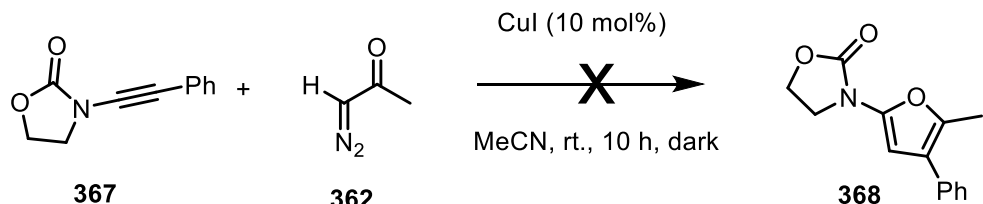
When we treated ynamide **355a** with TBS-diazoacetone **365** in the presence of a catalytic amount of copper iodide, the starting ynamide **355a** was totally recovered (**Scheme 116**).



Scheme 116: First trial with a disubstituted diazo compound **365**

d. With substituted ynamides

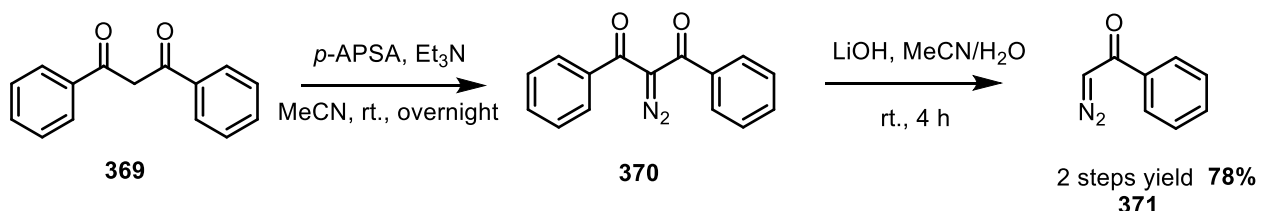
Likewise, substituted ynamides do not react under these conditions. When the reaction was carried out with substituted ynamide **367** and diazoacetone **362** in the presence of 10 mol % Cul, the starting material **367** was completely recovered (**Scheme 117**).



Scheme 117: First trial with substituted ynamide **367**

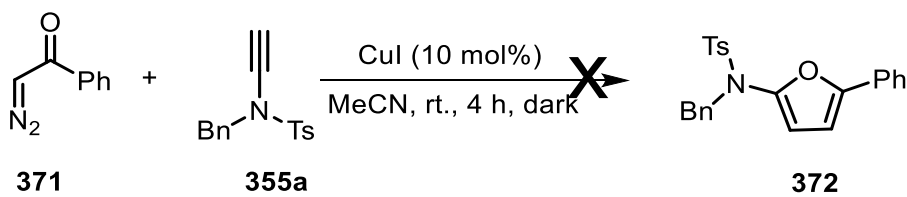
e. With non-enolisable diazo-carbonyl compounds

We also tested non-enolisable diazo-carbonyl compounds. First, we prepared diazo-acetophenone **373** using our previously described protocol from 1,3-diphenylpropane-1,3-dione **371** in two steps, through diazo-transfer followed by treatment with base. Diazoacetophenone **373** was obtained in 78% yield (**Scheme 118**).



Scheme 118: Synthesis of diazoacetophenone **371**

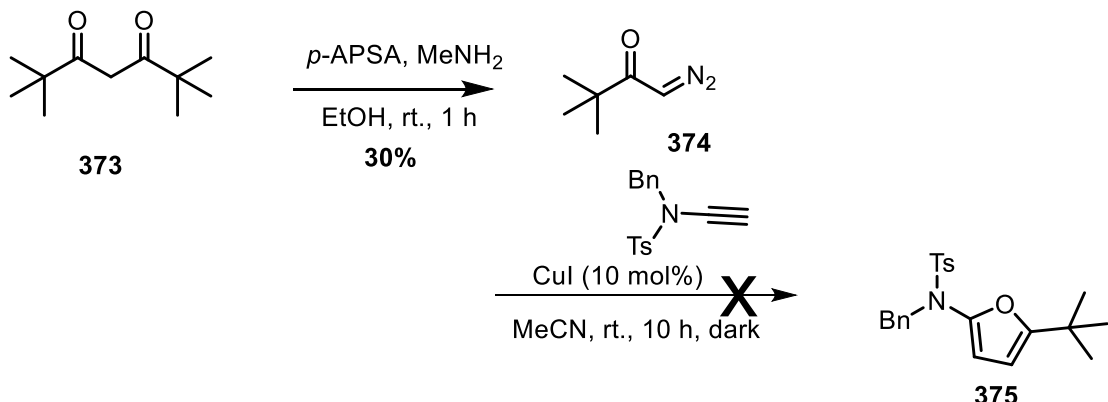
The synthesis of the corresponding furan again failed when ynamide **365** was treated with diazo-acetophenone **371**, and the starting ynamide was recovered (**Scheme 119**).



Scheme 119: Trial with diazoacetophenone

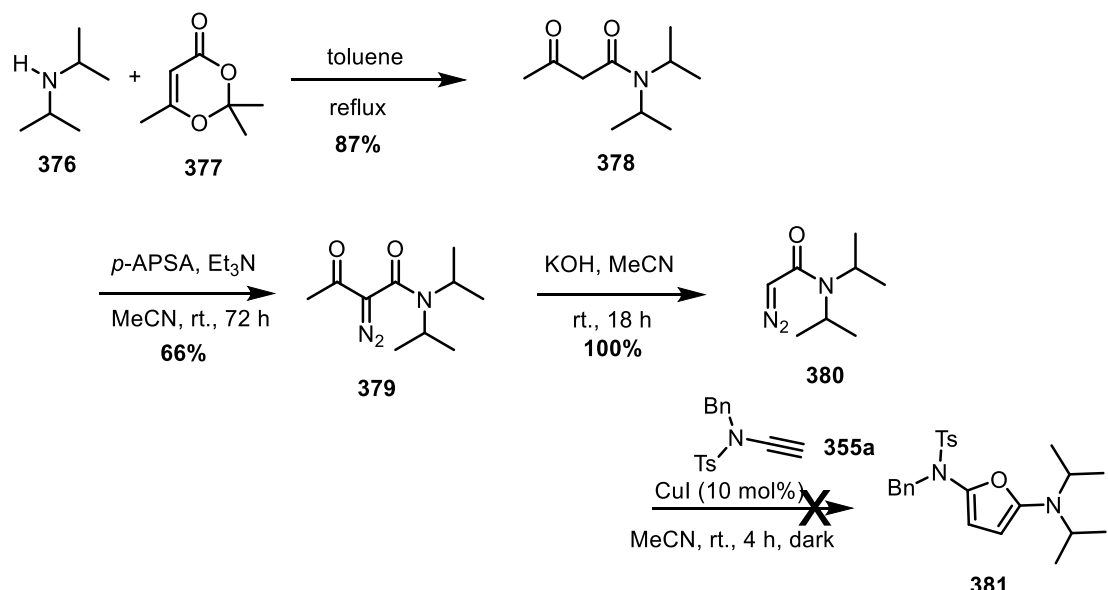
f. With alpha trisubstituted diazo ketones

Using alpha trisubstituted diazo ketone **374**, the outcome was similar, and the corresponding furan **375** could not be obtained (**Scheme 120**).¹²⁴



Scheme 120: Trial with trisubstituted diazo ketone **374**

To confirm that non-enolizable ketones would not provide the corresponding furan using copper catalysis, we prepared 2-diazo *N,N*-diisopropylacetamide **380**. For this purpose, Diisopropylamine was treated with 2,2,6-trimethyl-4H-1,3-dioxin-4-one in refluxing toluene to obtain *N,N*-diisopropyl-3-oxobutanamide **378** in 87% yield.¹²⁵ Diazotization and basic treatment afforded 2-diazo *N,N*-diisopropylacetamide **379** in 66% yield in two steps. Finally, ynamide **355a** did not react with 2-diazo *N,N*-diisopropylacetamide **380**, corroborating the previous experiments (**Scheme 121**).



¹²⁴ J.-L. Zhang, W.-W. Chen, D.-Y. Huang, X.-B. Zeng, X.-Y. Wang, Y.-F. Hu, *J. Org. Chem.* **2017**, *82*, 9171–9174.

¹²⁵ N. Döben, H. Yan, M. Kischkewitz, J.-C. Mao, A. Studer, *Org. Lett.* **2018**, *20*, 7933–7936.

Scheme 121: Trial with 2-diazo *N*, *N*-diisopropylacetamide **380**

Considering these preliminary experiments, we concluded that a proton alpha to the carbonyl function is required to obtain the furan skeleton. Given these preliminary results, the scope of this new reaction seemed strongly compromised.

II.4.3. Synthesis of CF₂H-substituted 2-amidofurans

To highlight the potential of this new synthesis of 2-amidofurans from ynamides and diazo compounds, we decided to introduce a difluorinated moiety into the molecule to enhance the versatility of the protocol.

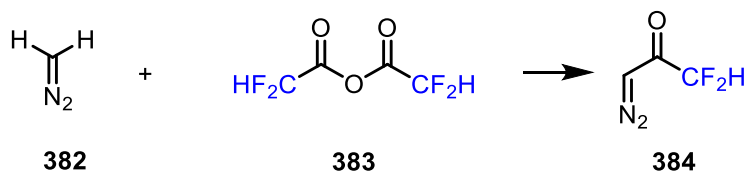
As mentioned in the introduction, heterocycles containing difluoromethyl groups are emerging, but still are a scarcely investigated class of organofluorine molecules. Given their biological properties they cannot be overlooked in the conception of new drugs.

To do so we decided to prepare difluorinated diazoacetone **384**. This reagent was previously non-existent among the toolbox of the difluorinating reagents.

II.4.3.1. Synthesis of difluorodiazooacetone.

a. First synthesis

Even if chemical synthesis using diazomethane requires strict safety regulations,¹²⁶ the use of the latter has proven to be beneficial for the synthesis of diazocarbonyl compounds.¹²⁷ Taking into account Strazzolini's work,¹²⁸ we prepared 3-diazo-1,1-difluoropropan-2-one by reacting diazomethane **382** with 2,2-difluoroacetic anhydride **383** (**Scheme 122**).



Scheme 122: Synthesis of difluorodiazooacetone using diazomethane

The ethereal solution of difluorodiazomethane can be kept a few weeks at 4 °C without any alteration.

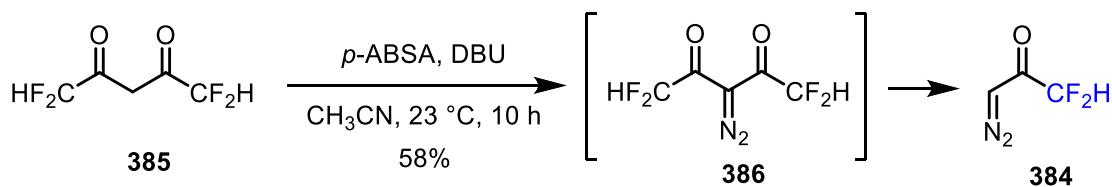
b. Second synthesis

¹²⁶ S. P. Green, K. M. Wheelhouse, A. D. Payne, J. P. Hallett, P. W. Miller, J. A. Bull, *Org. Process Res. Dev.* **2020**, 24, 67–84.

¹²⁷ P. Besse, T. Sokoltchik, Veschiede, *Tetrahedron: Asymmetry*, **1998**, 9, 4441–4457. V. Pace, G. Verniest, J.-V. Sinisterra, A. R. Alcantara, N. D. Kimpe, *J. Org. Chem.* **2010**, 75, 5760–5763.

¹²⁸ P. Strazzolini, A. G. Giumanini, A. Gambi, G. Verardo, G. Cerioni, *Can. J. Chem.* **1996**, 74, 1348–1359.

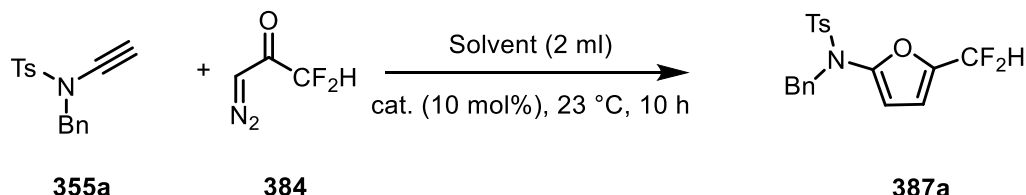
As the first synthesis of difluorodiazomethane requires the use of diazomethane, which is potentially toxic and explosive, we decided to develop a more convenient synthesis for this new difluorinating agent. Taking into account Nikolaev's work,¹²⁹ we prepared 3-diazo-1,1-difluoro-propan-2-one **384** in a one-step procedure by reacting commercially available 1,1,5,5-tetrafluoropentane-2,4-dione **385** in the presence of a diazo-transfer reagent [*p*-acetamidobenzenesulfonyl azide (*p*-ABSA)] and DBU. Spontaneous deacylation of the difluorinated diazodiketone **386** intermediately took place in the presence of the base, providing the desired difluoro-diazoacetone **384** in 58% yield (**Scheme 123**).



Scheme 123: Synthesis of 3-diazo-1,1-difluoro-propan-2-one *via* diazotization and deacylation

II.4.3.2. Synthesis of difluorinated furans.

When ynamide **355a** was treated with difluorinated diazoacetone at room temperature, we obtained the corresponding difluorinated amidofuran **387a** in good yield (**Scheme 124**).

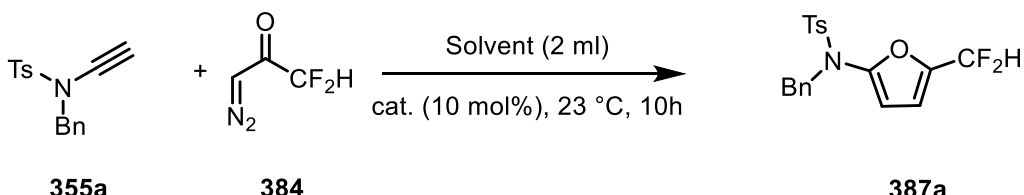


Scheme 124: Synthesis of difluorinated amidofuran **387a**

II.4.3.3. Optimization of the reaction conditions

We began our investigations, adapting the reaction conditions developed by varying the solvent, the copper catalyst, and by adding a base. We subjected ynamide **355a** to difluorodiazooacetone **384** in the presence of diverse copper catalysts (**Table 6**). As illustrated in Table 6, only copper(I) iodide and copper(I) bromide proved to be effective (**Table 6**, entries 1-4), although copper(I) bromide led to a huge erosion of the yield (37%). When the metal is in oxidation state II, the starting ynamide **355a** underwent degradation in almost all cases (**Table 6**, entries 5-7), albeit traces of amido-difluorinated furan **389a** were observed (**Table 6**, entry 5). The choice of the solvent is critical: use of tetrahydrofuran (THF), dichloroethane (DCE), dioxane, toluene, or ether did not lead to the target molecule (**Table 6**, entries 8-12), and the starting ynamide was recovered. Dimethylformamide allowed this transformation, but led to significantly lower yield (**Table 6**, entry 13, 27%). A control experiment using difluorodiazooacetone without any catalyst did not promote this transformation (**Table 6**, entry 14).

¹²⁹ V. M. Zakharova, L. Hennig, V. A. Nikolaev, *Synthesis* **2005**, 2871-2874.



Entry	Solvent	Catalyst	Yields (%) ^[a] ^[b]
1	MeCN	CuI	71
2	MeCN	CuBr	37
3	MeCN	CuCl	- ^[d]
4	MeCN	Cu(MeCN) ₄ PF ₆	- ^[d]
5	MeCN	CuCl ₂	traces
6	MeCN	CuSO ₄	- ^[d]
7	MeCN	Cu(OTf) ₂	- ^[d]
8	THF	CuI	- ^[c]
9	DCE	CuI	- ^[c]
10	dioxane	CuI	- ^[c]
11	toluene	CuI	- ^[c]
12	Et ₂ O	CuI	- ^[c]
13	DMF	CuI	27
14	MeCN	-	- ^[c]

[a] Reaction conditions: to a solution of **4a** (0.2 mmol), catalyst (10 mol%), solvent (2 mL), **3** (1.5 equiv, 0.5 mol/L in Et₂O) was added dropwise at 23 °C. [b] Isolated yields. [c] Starting material **4a** was fully recovered. [d] Degradation was observed.

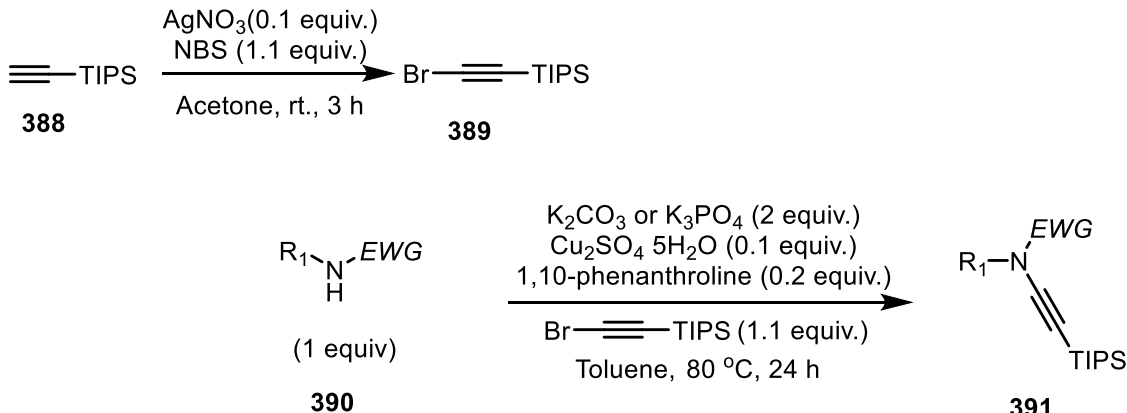
Table 6: Optimization of the reaction conditions

II.4.3.4. Scope of the reaction

a. Synthesis of the Ynamides

Copper-catalyzed coupling reaction

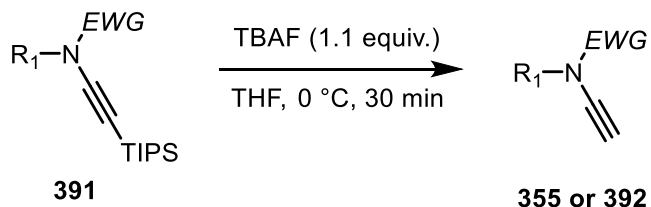
The ynamides **391** were obtained according to Hsung's procedure¹³⁰ through a copper-catalyzed coupling reaction between various amides **390** and bromoalkynes **389**. The latter were prepared from commercially available triisopropylmethyne (TIPS-ethyne) by using *N*-bromosuccinimide (NBS) and silver nitrate (AgNO_3) according to Wulff's procedure¹³¹ (**Scheme 125**).



Scheme 125: Synthesis of the TIPS-protected ynamide **391**

Synthesis of the terminal ynamides

The synthesized ynamides **391** were deprotected with tetrabutylammonium fluoride (TBAF) to provide the requisite terminal ynamides **355** for the synthesis of amido-difluorinated furans (**Scheme 126**).



Scheme 126: Synthesis of terminal ynamides

¹³⁰ Y.-S. Zhang, Richard P. Hsung, M. R. Tracey, K. C. M. Kurtz, E. L. Vera, *Org. Lett.* **2004**, *6*, 1151–1154.

¹³¹ M. X. Jiang, M. Rawat, W. D. Wulff, *J. Am. Chem. Soc.* **2004**, *126*, 5970–5971.

Scope of ynamides

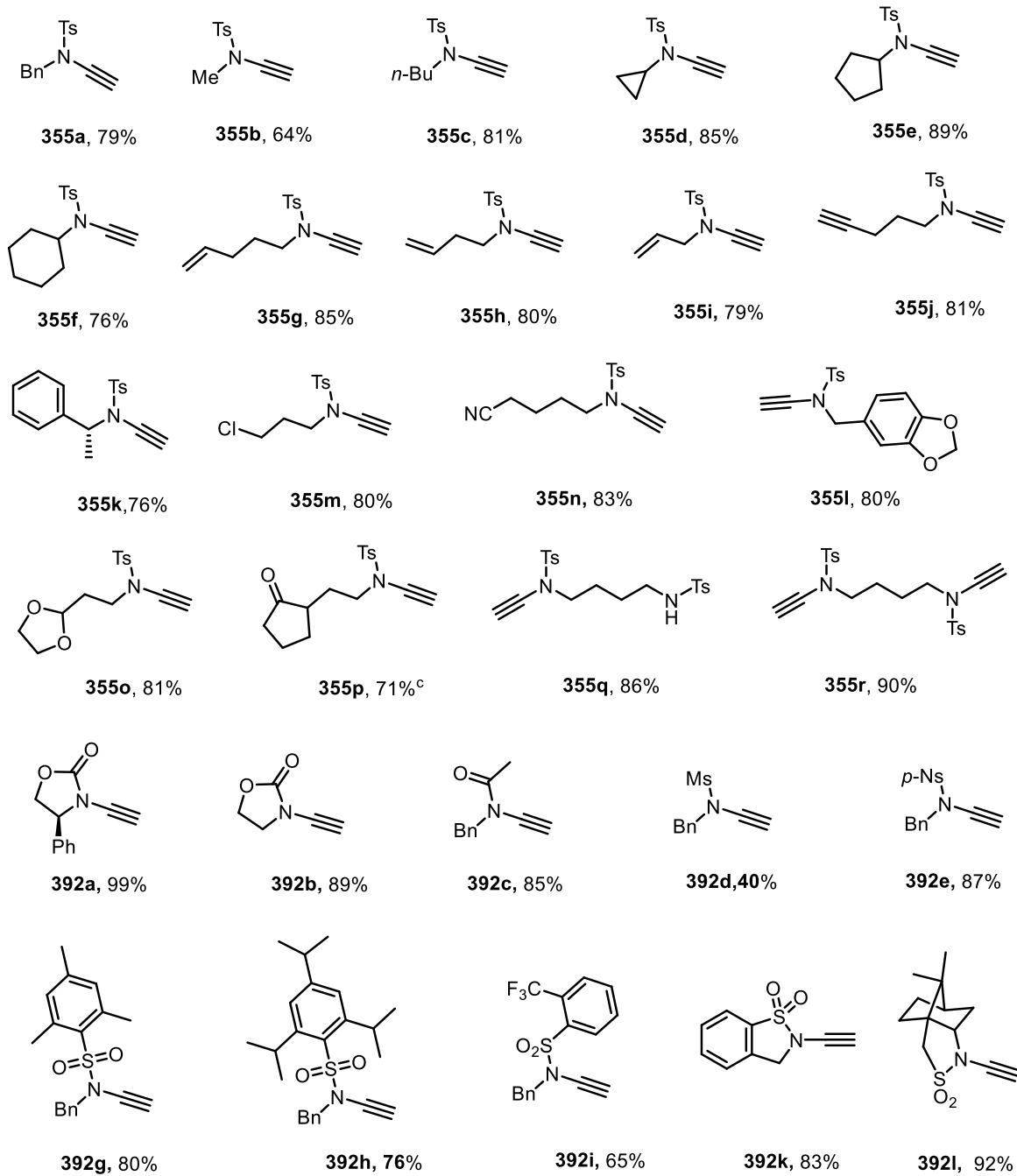


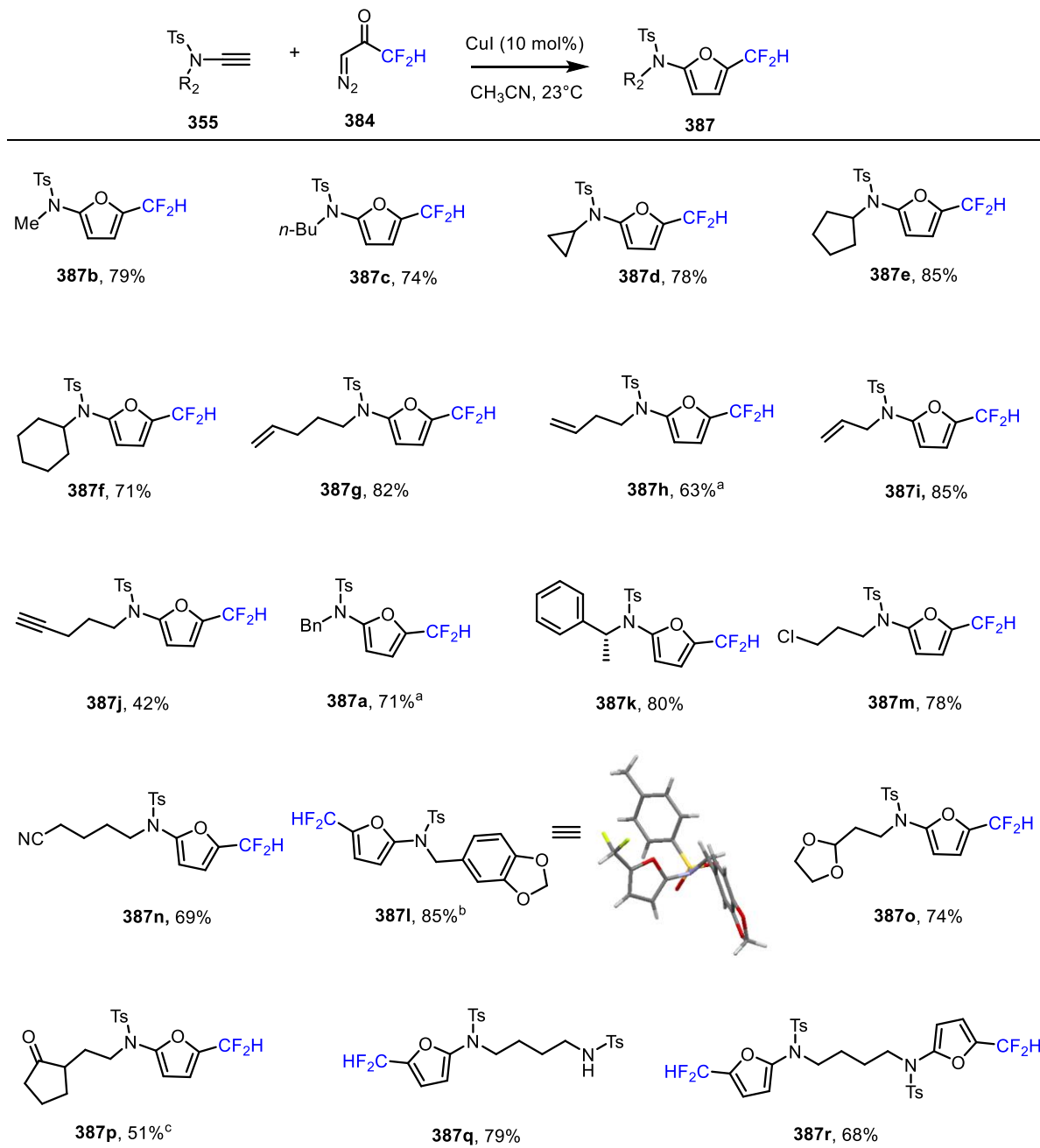
Table 7: Scope of ynamides

In this way, we obtained a large panel of diverse ynamides to establish a broad scope for the synthesis difluorinated amidofurans.

II.4.3.5. Synthesis of the Furans

a. Scope of the reaction regarding the ynamide moiety

With the optimized reaction conditions in hand (**Table 6**, entry 1), we investigated the generality of this transformation. A diverse array of ynamides bearing diverse functional groups were tested. Linear alkanes, *i.e.*, methyl (**387b**), butyl (**387c**) or cyclic alkanes: cyclopropyl (**387d**), cyclopentyl (**387e**) or cyclohexyl (**387f**) substituents were perfectly accommodated. The reaction is not restricted to saturated substituents; unsaturated side chains with diverse carbon linker chains (**387g-j**) as well as aryl groups (**387a**, **387k**, **387l**) were tolerated as well, albeit the yield of the furan **389j** bearing a terminal alkyne tether is moderate. X-Ray analyses of **387l** confirmed the structure of amido-difluorinated furan **387l** obtained (CCDC 2071668). Notably, even halogens (**387m**), nitriles (**387n**), protected aldehydes (**387o**), ketones (**387p**), and amides (**387q**, **3897r**) could be used, broadening even more the substrate scope and providing the corresponding difluorinated furans in good yields. (**Table 8**).



Scope of the synthesis of amido-difluorinated furans regarding the ynamide. [a] Performed on 0.4 mmole scale; [b] See [17] for CCDC deposition numbers; [c] yield of the two-step process: deprotection of the ynamide and cyclization.

Table 8: Scope of the synthesis of amido-difluorinated furans

b. Modification of the electronwithdrawing group

The influence of the electron-withdrawing group on the nitrogen atom was also explored. Furans bearing an oxazolidinone (**393a**, **393b**) and amides (**393c**) were obtained. Sulfonyl groups such as mesyl (**393d**), nosyl (**393e**), and trimethyl/triisopropyl/trifluoromethyl-benzenesulfonamides (**393g**, **393h**, **393i**) were revealed to be suitable for this transformation. More hindered cyclic sulfonamides were notably effective, providing the corresponding furans

(393j, 393k, 393l) with good yields. Sulfamoyl derivatives that are easily deprotected could also be adapted providing furan 393f in 70% yield (**Table 9**).

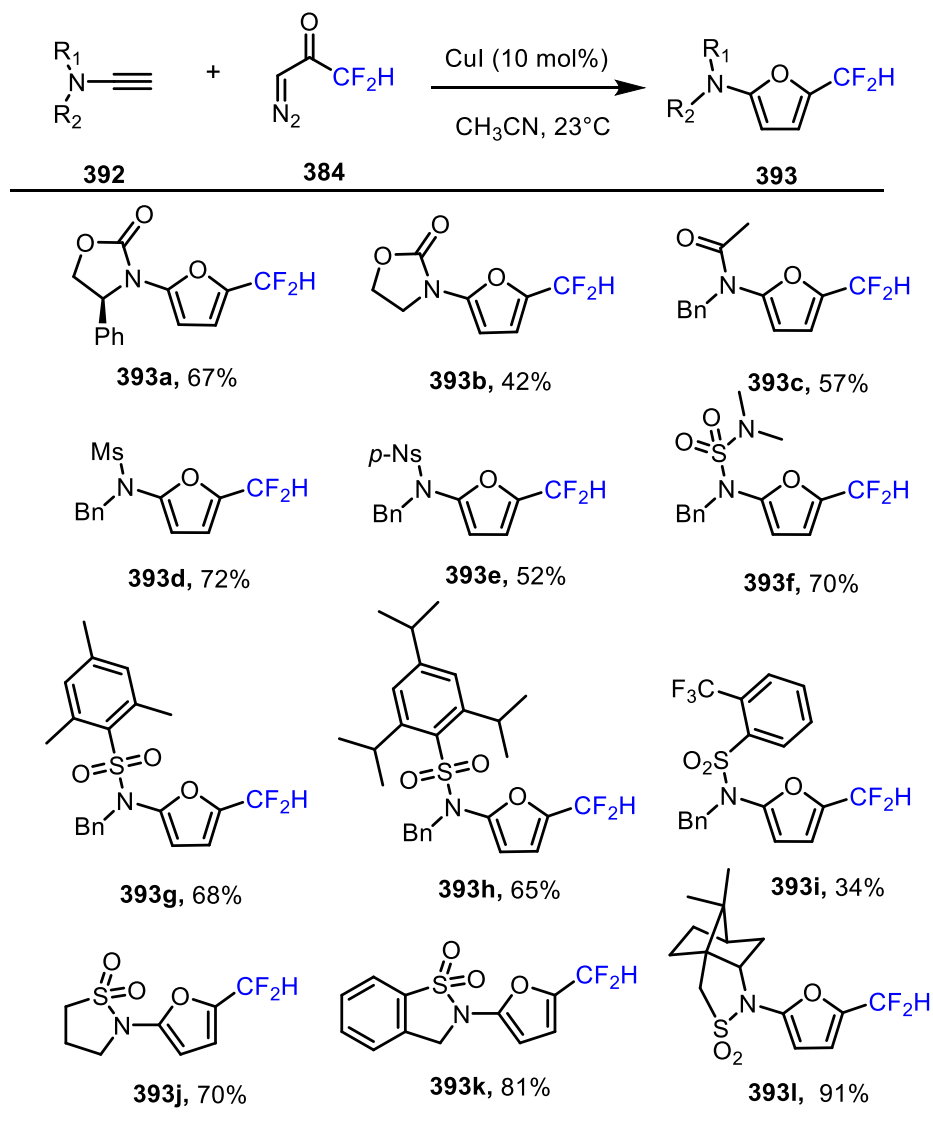


Table 9: Modification of the electron-withdrawing group on the nitrogen

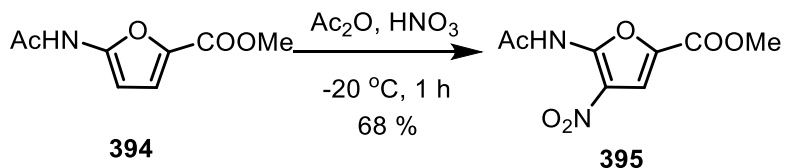
II.4.4. Difluorinated amido-furans as platforms to synthesize more complex heterocycles

To further highlight the diversification potential of these difluorinated amido-furans, we used them as building blocks to prepare various relevant heterocycles. In this way, we involved those amido-furans as platforms in nitration reactions, intramolecular oxidative coupling reactions, and in intramolecular Diels-Alder cycloadditions.

II.4.4.1. Nitration of furans

a. Dri's work

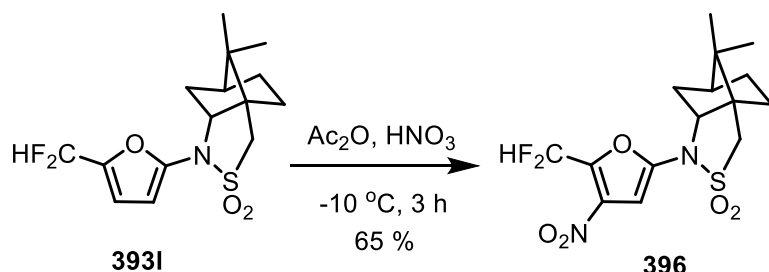
Dri *et al.* performed nitration of amido-furan **395** under strictly controlled temperature conditions. These authors obtained exclusively the nitro group alpha to the amido-group (**Scheme 127**).¹³²



Scheme 127: Nitration of furan performed by Dri

b. With amido-difluorinated furan **393I**

Amido-difluorinated compound **393I** underwent nitration under the same conditions; the nitro group being located alpha to the CF_2H -group exclusively (**Scheme 128**).

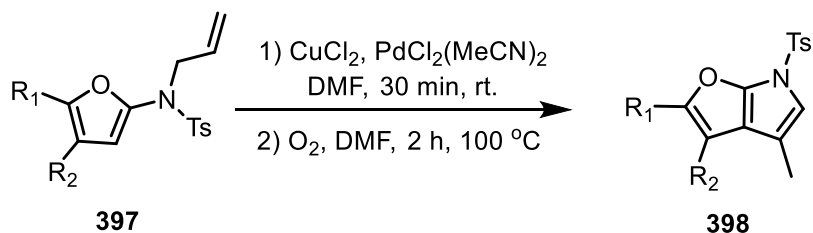


Scheme 128: Nitration of compound **393I**.

II.4.4.2. Intramolecular oxidative coupling reaction.

a. Broggini's work

In 2008 Broggini *et al.* performed an intramolecular Pd(II)-catalyzed oxidative coupling of furans to produce furo-pyrrole derivatives of potential interest in pharmacology. The best conditions are $\text{PdCl}_2(\text{MeCN})_2$ as catalyst, CuCl_2 as co-catalyst, and an environmentally friendly reoxidant such as O_2 to promote the catalytic cycle (**Scheme 129**).¹³³



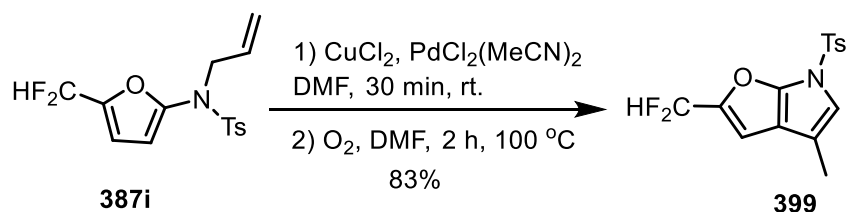
¹³² A. Bianco, M. Brufani, D. A. Dri, C. Melchioni, L. Filocamo, *Letters in Organic Chemistry*, **2005**, 2, 83-88.

¹³³ E. M. Beccalli, E. Borsini, G. Broggini, M. Rigamonti, S. Sottocornola, *Synlett* **2008**, 1053-1057.

Scheme 129: Oxidative coupling of furans performed by Broggini

b. With difluorinated amidofurans

When we treated compound **387i** with Broggini's reaction conditions, we obtained the corresponding difluorinated furopyrrole **399** in good yield (**Scheme 130**).



Scheme 130: Oxidative coupling reaction on furan **387i**

II.4.4.3. Intramolecular Diels-Alder reaction of furans (IMDAF)

The Diels-Alder reaction remains one of the most frequently used method for the construction of six-membered ring systems. Among these [4+2]-cycloaddition processes, the ones using furans as the 4 π diene component were among the first studied by Diels and Alder.¹³⁴ Indeed, the addition of maleic anhydride to furan is a classic textbook example of this prominent organic reaction. The intramolecular Diels-Alder reactions of furans, often designated as IMDAF, has been proven to be extremely valuable for the construction of complex heterocycles, especially for the synthesis of complex natural products.¹³⁵

a. Trost's work

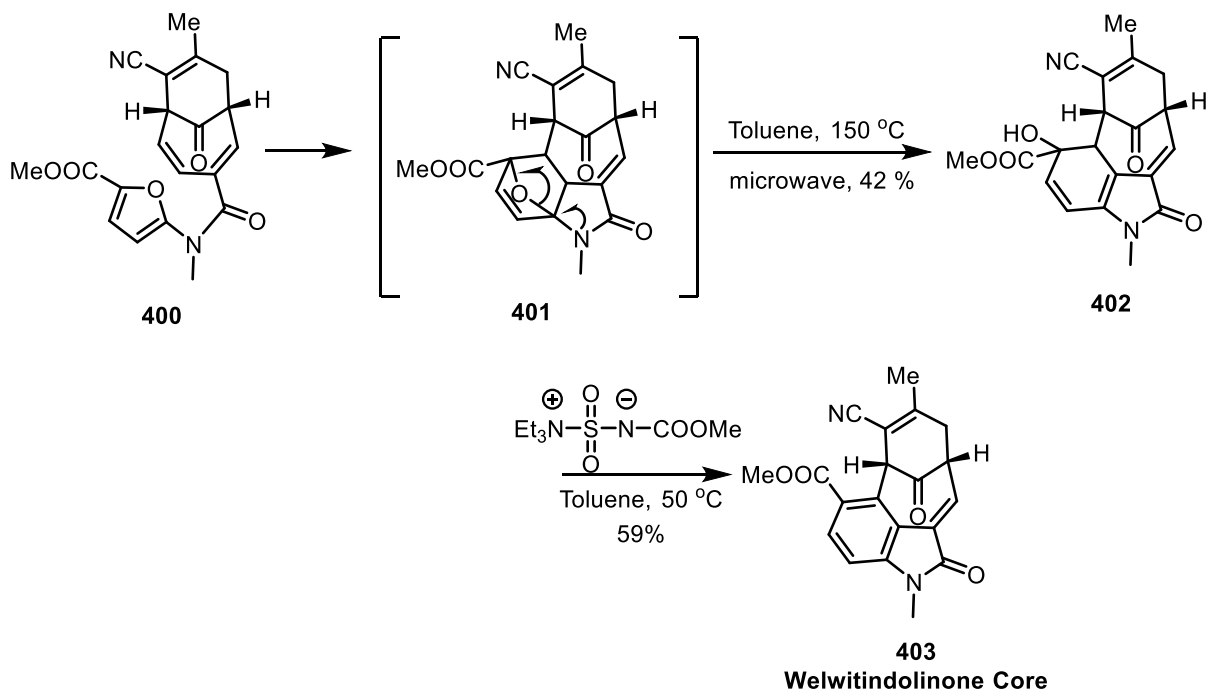
In this context, Trost and MacDougall in 2009¹³⁶ used an IMDAF reaction on amidofurans to achieve the synthesis of the core skeleton of welwitindoline alkaloids. By heating under microwaves at 150 °C, compound **400** underwent a [4+2] cycloaddition, providing tertiary alcohol **402**. Dehydration to the oxindole to generate the oxindole core was not spontaneous; the dehydrating agent developed by Burgess¹³⁷ was required to obtain the desired oxindole **403** (**Scheme 131**).

¹³⁴ O. Diels, K. Alder, *Liebig Ann. Chem.*, **1928**, 460, 98-122.

¹³⁵ Y. Ji, Z.-Y. Xin, H.-B. He, S.-H. Gao, *J. Am. Chem. Soc.* **2019**, 141, 16208–16212. Y. Ji, Z.-Y. Xin, Y.-B. Shi, H.-B. He, S.-H. Gao, *Org. Chem. Front.*, **2020**, 7, 109-112

¹³⁶ B. M. Trost, P. J. McDougall, *Org. Lett.* **2009**, 11, 3782–3785

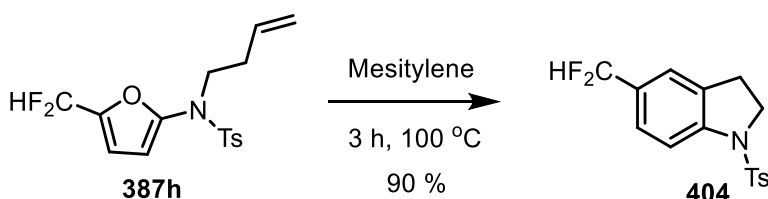
¹³⁷ E. M. Burgess, H. R. Penton, E. A. Taylor, W. M. Williams, *Organic Syntheses*; Wiley: New York, 1988; Collect. Vol. 6, p 788.



Scheme 131: Trost's IMDAF reaction prepare Welwitindolinone Core

b. With difluorinated amidofurans

Difluorinated amidofuran **387h** underwent intramolecular [4+2] cycloaddition in mesitylene at 100 °C, providing the 5-substituted difluorinated indoline **404** directly in 90% yield. Of note, the 5-substituted difluorinated indolines would be very challenging to obtain otherwise (**Scheme 132**).

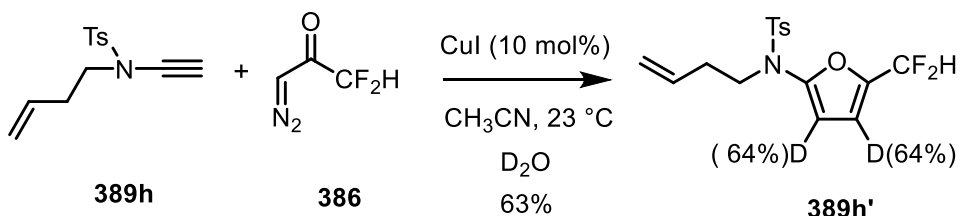


Scheme 132: IMDAF with difluorinated amidofuran **387h**

II.4.5. Mechanistic studies

II.4.5.1. Additional experiment

To gain more insights into the mechanism, we performed the synthesis of amido-difluorinated furans by adding D₂O. We observed the incorporation of 64% of deuterium at position 3 and position 4 (**Scheme 133**).



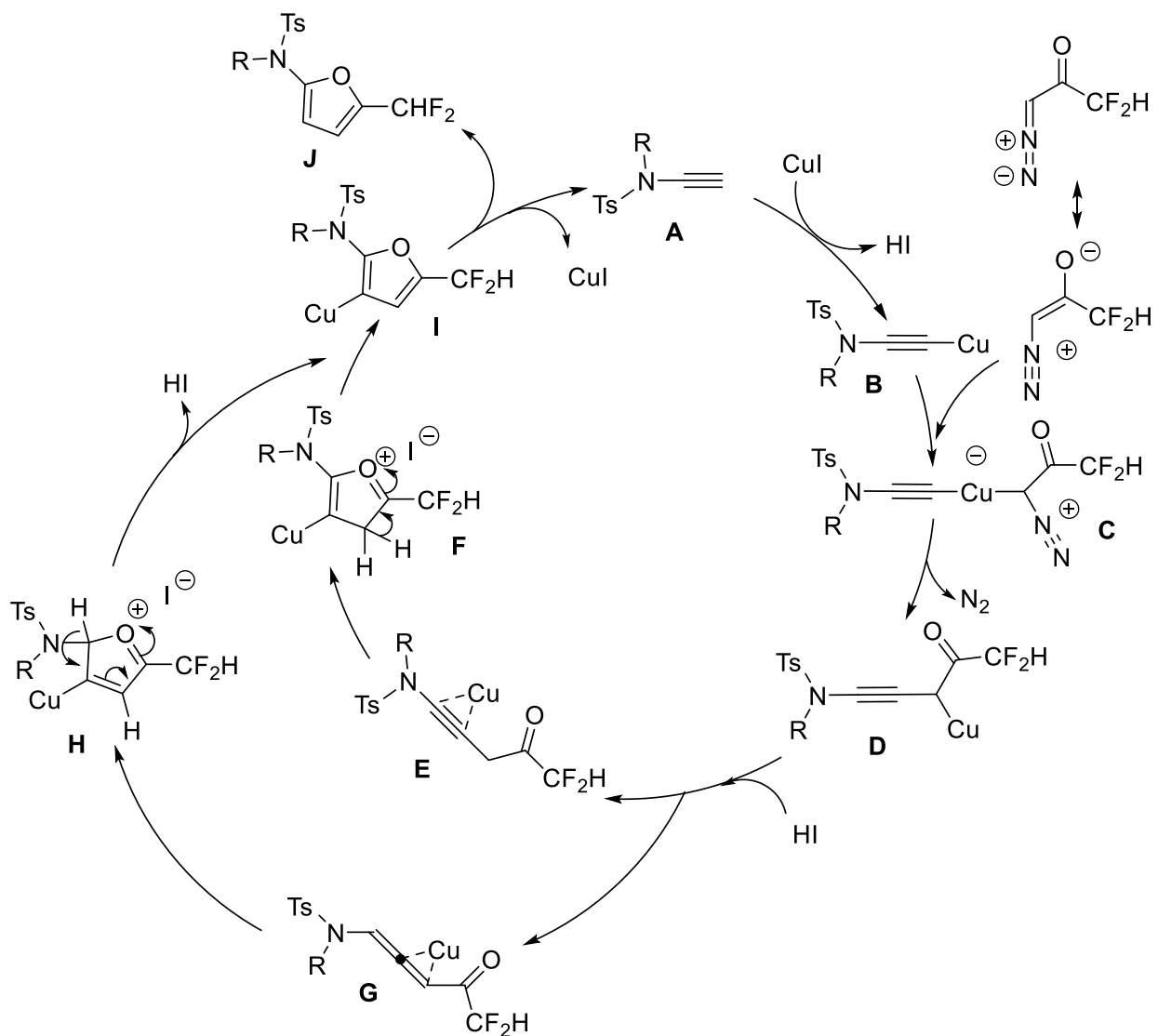
Scheme 133: D_2O experiment

II.4.5.2. Proposed mechanism

Based both on literature data and on DFT calculations, we propose the following mechanism. In the presence of copper(I) salt, ynamide **A** leads to copper-ynamidyl **B**. The reaction of the latter with difluorodiazooacetone forms copper specie **C**. Rearrangement and loss of N_2 leads to copper intermediate **D**¹³⁸ At this point, two reactions pathways were envisioned: Protonation α to the carbonyl moiety leading to a Fu type compound **E**¹³⁹ or protonation γ to the carbonyl moiety providing intermediate **G**. Both pathways were examined by DFT based calculations and have been found to be kinetically and thermodynamically possible (see Supporting Information for detailed description). O-alkylation on ynamide **E** or *N*-allenamide **G** followed by rearomatization of **F** and **H** and decupration of **I** regenerates the copper iodide and forms the amido-difluorinated furan **J**. The proposed reaction mechanism are in agreement with the fact that addition of D_2O in the reaction mixture leads to equal incorporation of deuterium at position 3 and 4 (**Scheme 134**).

¹³⁸ Q. Xiao, Y. Xia, H. Li, Y. Zhang, J. Wang, *Angew. Chem. Int. Ed.* **2011**, *50*, 1114-1117.

¹³⁹ A. Suarez, G. C. Fu, *Angew. Chem. Int. Ed.* **2004**, *43*, 3580-3582.

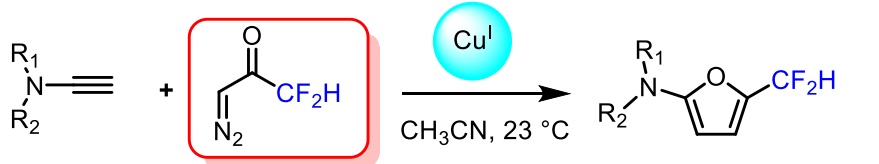


Scheme 134: Plausible Mechanism

II.5. Conclusion

In conclusion, we have developed a copper-catalyzed synthesis of difluorinated amidofurans through addition of difluorodiazoacetone to ynamides. Difluorodiazoacetone was prepared for the first time and proved to be the ideal reagent to perform this transformation. The method exhibits broad functional tolerance and led to a great diversity of high-value scaffolds. Different ynamides accommodate this transformation as well as different electron-withdrawing groups on the nitrogen, some of which can be easily deprotected for further transformations.

Finally, these newly designed difluorinated amidofurans could serve as platforms to construct a diverse set of more complex difluorinated heterocyclic molecules valuable for drug design.

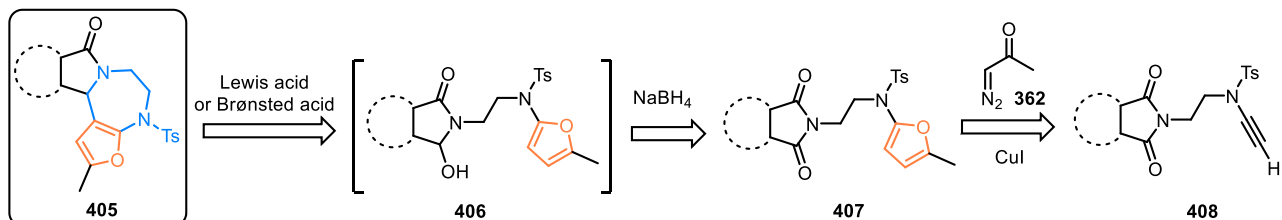


- New difluorinating reagent
- Broad substrate scope
- Easy to handle
- CF₂H-containing building blocks

II.6. Perspectives

Regarding the perspectives of chapter 1 and chapter 2 of this manuscript, the idea would like to be to combine both strategies to further enhance the chemical space of diazepine compounds. The goal would be to synthesize diazepines fused with furans starting from ynamides.

The strategy we propose would be the following: diazepines fused with furans **405** could be obtained through acidic treatment of α -hydroxylated amides equipped with furans **406**. The latter would be obtained from terminal ynamides **407** by reaction with diazo-ketone **362** to form the corresponding imides **408** followed by reduction of the imide function. A final treatment with a Lewis acid should allow the simultaneous formation of the *N*-acyliminium ion followed by intramolecular tertiary enamide assisted SE_{Ar} of the furan to form diazepines fused with furans **405** (**Scheme 135**).



Scheme 135: Perspectives

III. CHAPTER 3 COPPER-CATALYZED SYNTHESIS OF TERMINAL VS. FLUORINE SUBSTITUTED N-ALLENAMIDES VIA ADDITION OF DIAZO-COMPOUNDS TO TERMINAL YNAMIDES.

III.1. Introduction : *N*-allenamines vs *N*-Allenamides

The third chapter of this manuscript will deal with the synthesis of *N*-allenamides. Therefore, a brief introduction on *N*-allenamides will be given. Due to the immense number of contributions in this field, this introduction will mainly focus on the preparation of *N*-allenamides.

Allenes have always been a structural curiosity and became one of the most powerful building blocks in organic synthesis.¹⁴⁰

An allene can be considered as a diene with two consecutive double bonds. The central carbon atom is *sp* hybridized while its two neighbors are *sp*² hybridized. The terminal methylenes of the allene define two planes perpendicular to each other because the two *p* orbitals of the central carbon are perpendicular (**Figure 13**).

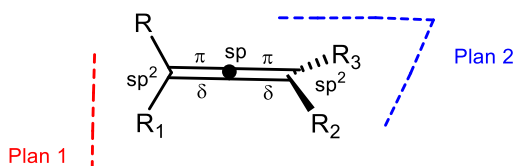


Figure 13: Geometry of an allene

Among heteroatom-substituted allenes, we can distinguish systems such as allenol ethers¹⁴¹, allenyl sulfides¹⁴² and allenamines¹⁴³ (**Figure 14**).

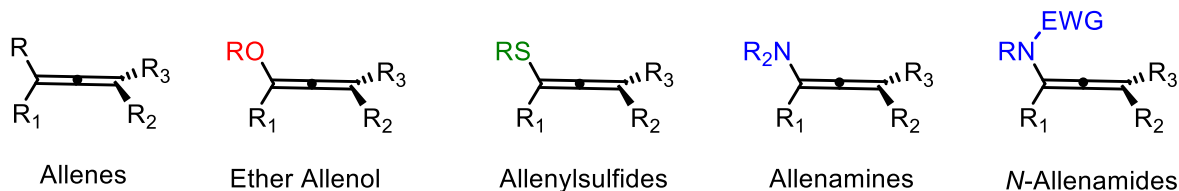


Figure 14: Hetero-substituted allenes

Allenamines *i.e* nitrogen-substituted allenes have been known for more than 40 years since their first preparation and characterizations in 1968 by Viehe.¹⁴⁴ The π -donating ability of the nitrogen atom enriches and polarizes the allenic moiety thereby predisposing them to electrophilic activations. Through delocalization of the nitrogen lone pair toward the allenic moiety, regioselective transformations can be achieved with consecutive addition of electrophiles and nucleophiles (**Figure 15**).

¹⁴⁰ D. R. Taylor, *Chem. Rev.* **1967**, *67*, 317–359.

¹⁴¹ R. Zimmer, *Synthesis* **1993**, *02*, 165–178.

¹⁴² E. Moreno-Clavijo, A. T. Carmona, H.-U. Reissig, A. J. Moreno-Vargas, E. Alvarez, I. Robina, *Org. Lett.* **2009**, *11*, 4778–4781.

¹⁴³ L. Wei, H. Xiong, R. P. Hsung, *Acc. Chem. Res.* **2003**, *36*, 773–782.

¹⁴⁴ A. J. Hubert, H. G. Viehe, *J. Chem. Soc. C*, **1968**, 228–230.

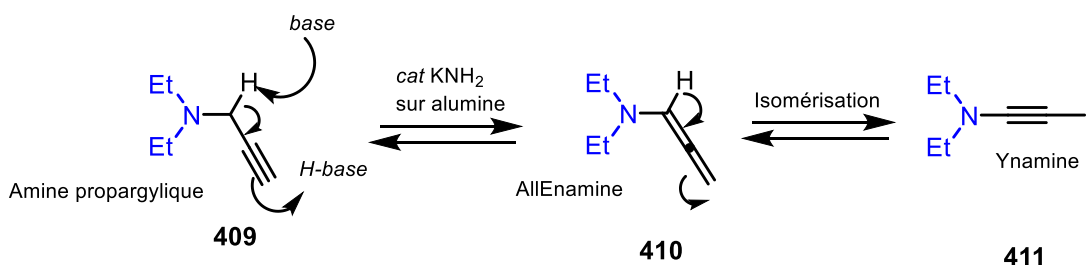


Figure 15: Viehe's synthesis of allenamines and ynamines

However, the development involving those substrates has been hampered by severe drawbacks: allenamides are highly sensitive toward hydrolysis with a tendency to polymerize, creating serious difficulties in their preparation and handling.

Therefore, *N*-Allenamides bearing an electron-withdrawing group on the nitrogen became ideal candidates to enhance the stability of allenamines. Delocalization of the nitrogen lone-pair into the electron-withdrawing amido group diminish the donating effect toward the allenic moiety thereby increasing the stability (**Figure 16**).

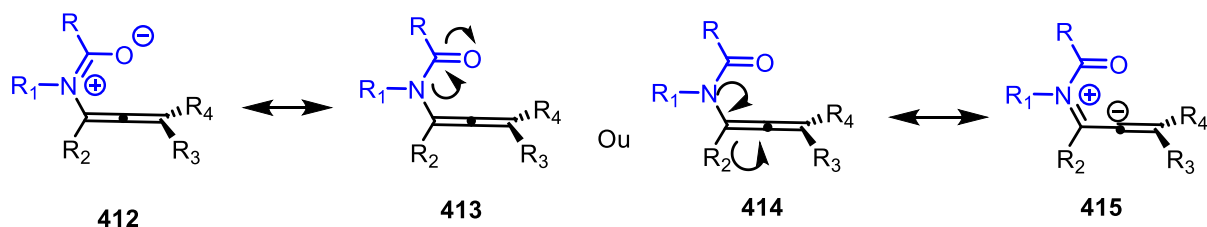


Figure 16: Resonance forms of *N*-allenamides

As a consequence, *N*-Allenamides can be considered as allenamine-equivalents exhibiting the right balance in terms of stability and reactivity.¹⁴⁵ Consequently, this new class of compounds received considerable attention from the synthetic organic community during the past decade, notably, in addition¹⁴⁶, cycloaddition¹⁴⁷ reactions as well as metal-induced cyclizations.¹⁴⁸

III.2. Synthesis of *N*-allenamides

Different pathways for *N*-allenamide synthesis have been developed. In this part, we will identify the most used methods for their preparation.

Method N°1: Base-induced isomerizations¹⁴⁹

¹⁴⁵ T. Lu, Z. Lu, Z.-X. Ma, Y. Zhang, R. P. Hsung, *Chem. Rev.* **2013**, *113*, 4862–4904.

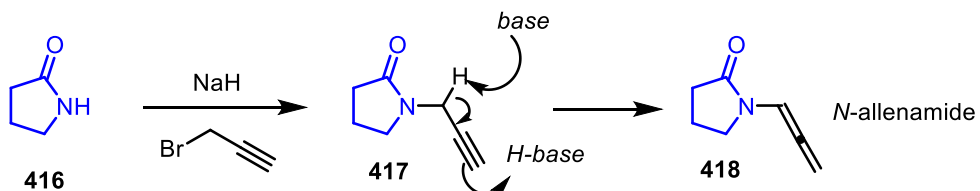
¹⁴⁶ X. Yang, F. D. Toste, *Chem. Sci.* **2016**, *7*, 2653–2656.

¹⁴⁷ H. Faustino, I. Varela, J. L. Mascareñas, F. López, *Chem. Sci.* **2015**, *6*, 2903–2908

¹⁴⁸ Y. Wang, P. Zhang, D. Qian, J. Zhang, *Angew. Chem. Int. Ed.* **2015**, *54*, 14849–14852.

¹⁴⁹ B. Corbel, J.-P. Paugam, M. Dreux, P. Savignac, *Tetrahedron Lett.* **1976**, *17*, 835–838. A. Padwa, T. Caruso, S. Nahm, A. Rodriguez, *J. Am. Chem. Soc.* **1982**, *104*, 2865–2871. C. Bogentoft, Ö. Ericsson, P. Stenberg, B. Danielsson, *Tetrahedron Lett.* **1969**, *10*, 4745–4748. L.-L. Wei, J. A. Mulder, H. Xiong, C. A. Zifcsak, C. J. Douglas, R. P. Hsung, *Tetrahedron* **2001**, *57*, 459–466. L. J. V. Boxtel, S. Körbe, M. Noltemeyer, A. D. Meijere, *Eur. J. Org. Chem.* **2001**, 2283–2292. J. Huang, H. Xiong, R. P.

The first synthesis of *N*-allenamides took place in 1967. Dickinson *et al.* treated a propargylic amide with sodium hydride (NaH). Instead of obtaining amide **417**, they directly observed the formation of the corresponding allenamide **418** (**Scheme 136**).¹⁵⁰

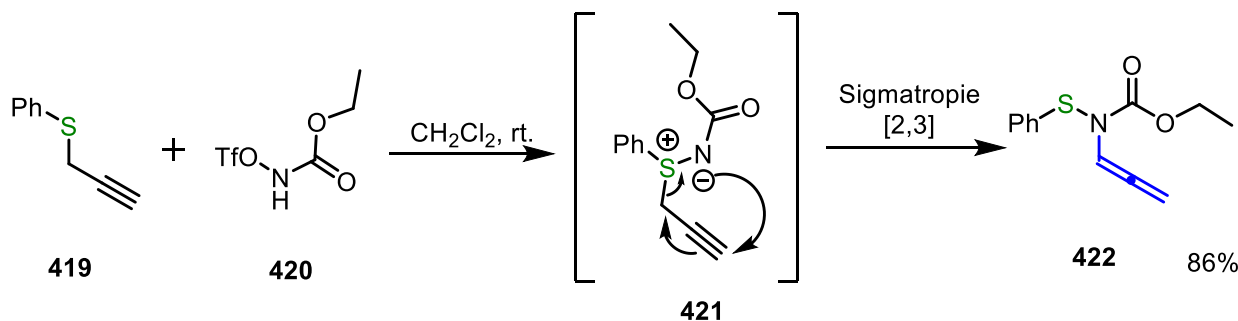


Scheme 136: Base-induced isomerization of propargylic amide

Although this method represents the simplest way to access *N*-allenamides, the harsh conditions used are not always compatible with functionalities present in the starting molecules.

Method N°2: Sigmatropic rearrangements¹⁵¹

In 1981, Tamura *et al.*¹⁵² reported a [2,3] sigmatropic rearrangement of phenyl propargyl sulfide through S-amination to obtain sulfilimine **422** in 86% yield (**Scheme 137**).



Scheme 137: Sigmatropic rearrangement

Method N°3: Palladium-induced synthesis of *N*-allenamides¹⁵³

Mori *et al.* developed a synthesis of different ring-size heterocycles from propargyl alcohol derivatives via allenylpalladium complexes. Oxidative addition of **423** to Pd(0) produced palladium complex **426** and then palladium complex **427** could be formed. From **427**, carbacepham **424** was obtained. Carbacepham **425** was formed via amidation of allenylpalladium **426** by addition on the central carbon of the allenic moiety (**Scheme 138**).¹⁵⁴

Hsung, C. Rameshkumar, J. A. Mulder, T. P. Grebe, *Org. Lett.* **2002**, 4, 2417–2420. X.-Z. Yu, X.-Y. Xin, B.-S. Wan, X.-W. Li, *J. Org. Chem.* **2013**, 78, 4895–4904.

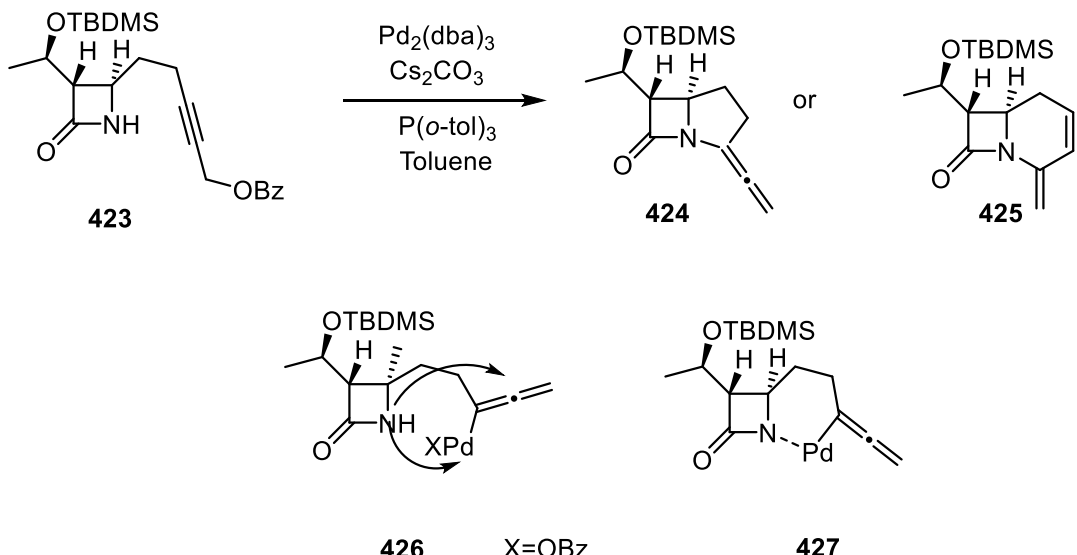
¹⁵⁰ W. B. Dickinson, P. C. Lang, *Tetrahedron Lett.* **1967**, 8, 3035–3040.

¹⁵¹ L. E. Overman, L. A. Clizbe, R. L. Freerks, C. K. Marlowe, *J. Am. Chem. Soc.* **1981**, 103, 2807–2815. A. Padwa, L. A. Cohen, *J. Org. Chem.* **1984**, 49, 399–406. J. P. Bacci, K. L. Greenman, D. L. Van Vranken, *J. Org. Chem.* **2003**, 68, 4955–4958. A. Armstrong, D. P. G. Emmerson, *Org. Lett.* **2009**, 11, 1547–1550. A. M. Danowitz, C. E. Taylor, T. M. Shrikian, A. K. Mapp, *Org. Lett.* **2010**, 12, 2574–2577.

¹⁵² Y. Tamura, H. Ikeda, C. Mukai, I. Morita, M. Ikeda, *J. Org. Chem.* **1981**, 46, 1732–1734.

¹⁵³ M. Kimura, Y. Wakamiya, Y. Horino, Y. Tamaru, *Tetrahedron Letters*, **1997**, 38, 3963–396.

¹⁵⁴ Y. Kozawa, M. Mori, *Tetrahedron Letters*, **2002**, 43, 1499–1502.



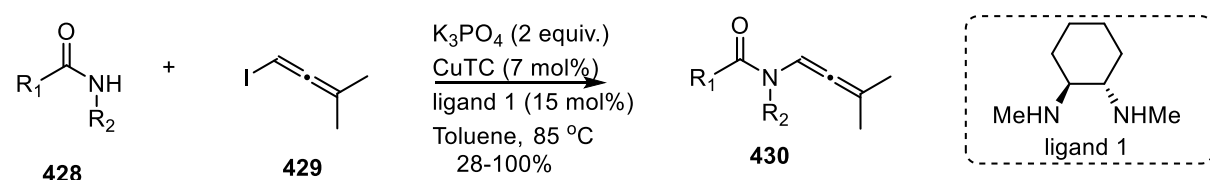
Scheme 138: Palladium-induced synthesis of *N*-allenamides

Although method N°2 and N°3 are elegant, they require specific substrates and lack general application.

Method N°4: Copper-induced synthesis of *N*-allenamides

*Trost's method*¹⁵⁵

N-substituted allenes **430** have been synthesized by copper-catalyzed coupling reaction between allenyl halides and amides, carbamates and ureas. Inspired by Buchwald's amidation, this reaction offers a nice alternative for the synthesis of *N*-allenamides although, the synthesis of allenyl halides is required and heating is mandatory for the reaction to take place (**Scheme 139**).



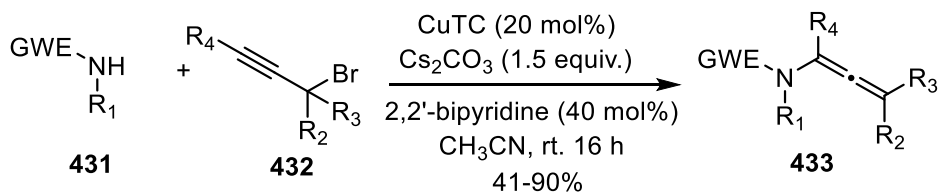
Scheme 139: Copper-induced synthesis of *N*-allenamides

*Evano's method*¹⁵⁶

Propargylic bromides were found to be suitable partners for the allenylation of oxazolidinones and hydantoins upon activation with a combination of copper catalyst a 2, 2'-bipyridine derivatives in the presence of an inorganic base. This method although restricted to oxazolidinones and hydantoins allows the preparation of mono-, di-, as well as trisubstituted allenamides (**Scheme 140**).

¹⁵⁵ B. M. Trost, D. T. Stiles, *Org. Lett.* **2005**, *7*, 2117–2120.

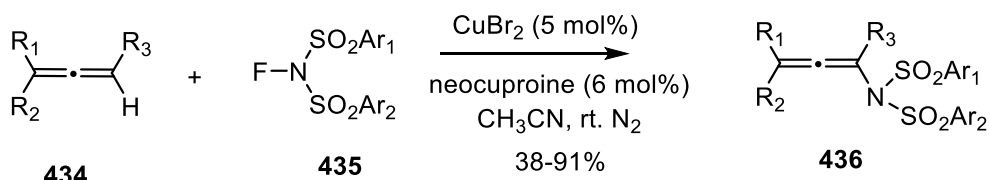
¹⁵⁶ C. S. Demmer, E. Benoit, G. Evano, *Org. Lett.* **2016**, *18*, 1438–1441.



Scheme 140: Evano's method synthesis of *N*-allenamides

Zhang's method¹⁵⁷

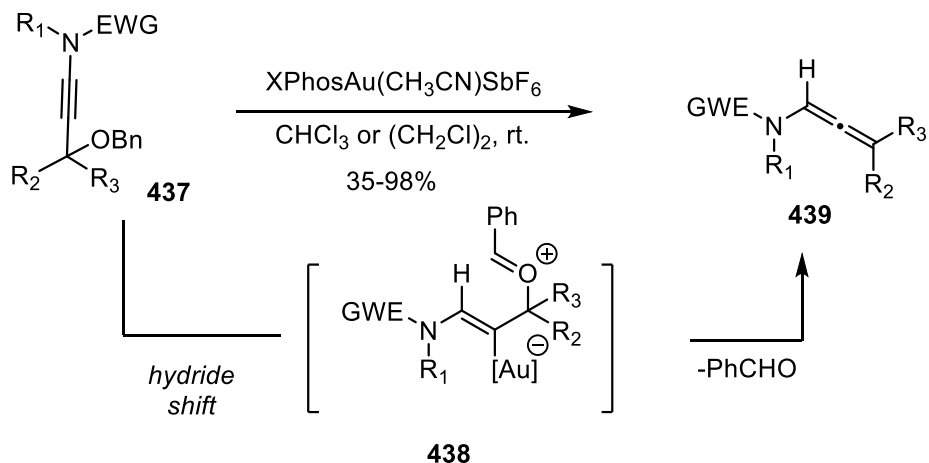
A regioselective radical amination of allenes with *N*-fluoroarylsulfonimide **435** proceeded under mild reaction conditions and allowed the synthesis of *N*-allenamides **436** with good yields. Although this method is direct and efficient, functional group compatibility other than aryle and alkyl groups seems to be compromised (**Scheme 141**).



Scheme 141: Radical amination

Method N°5: Gold-catalyzed synthesis of *N*-allenamides¹⁵⁸

Under gold-catalysis, ynamides equipped with a benzyloxy group **437** were efficiently converted into the corresponding *N*-allenamides **439** via 1, 5-hydride shift. Although the method is original, the benzyloxy group is a requisite on the ynamide moiety (**Scheme 142**).



Scheme 142: Gold-catalyzed synthesis of *N*-allenamides

Despite their popularity as building blocks in organic synthesis, the limited number of methods known for the preparation of *N*-allenamides are often hampered by a poor substrate scope and restrained structural diversity.

¹⁵⁷ G. Zhang, T. Xiong, Z.-N. Wang, G.-X. Xu, X.-D. Wang, and Q. Zhang, *Angew. Chem.* **2015**, *127*, 12840–12844.

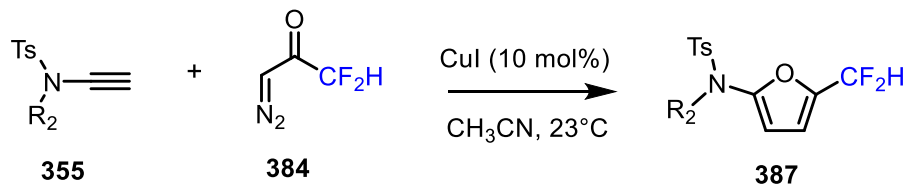
¹⁵⁸ Q. Zhao, F. Gagosz, *Adv. Synth. Catal.* **2017**, *359*, 3108–3113.

In this context, we propose a new approach for the synthesis of *N*-allenamides *via* copper catalysis starting from ynamides.

III.3. Copper-catalyzed synthesis of terminal vs. fluorine substituted *N*-allenamides *via* addition of diazo-compounds to terminal ynamides.

III.3.1. Previous work

In chapter 2 we studied the reactivity of ynamides towards difluorinated diazoacetone and we obtained difluorinated amidofurans (**Scheme 143**).

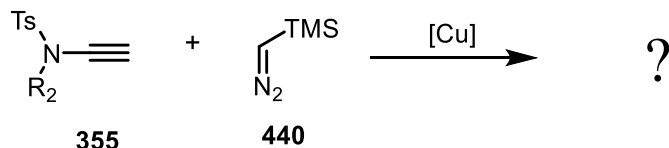


Scheme 143: Synthesis of amidodifluorinated furans from ynamides

Note: With ethyl diazoacetate under copper-catalysis, we failed to obtain any furan compound

III.3.2. Objective

Taking in account those results, we wondered whether TMS-diazomethane **440** would react with terminal ynamides **355** under copper-catalysis (**Scheme 144**).



Scheme 144: New objective

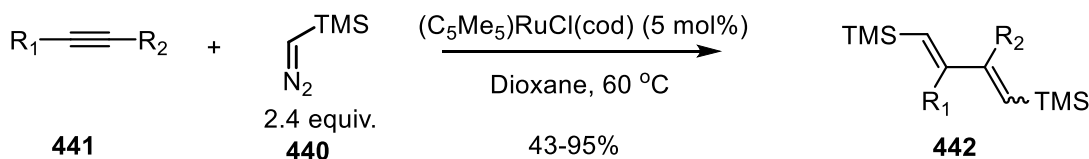
III.3.3. State of the art : Addition of TMS-diazomethane to alkynes

In this context, the literature mentions a few examples where TMS-diazomethane has been added to alkynes.

III.3.3.1. Addition of TMS-diazomethane to alkynes

Dixneuf *et al.* reported in 2010 a ruthenium-catalyzed synthesis of functional conjugated dienes *via* addition of two carbene units to alkynes.¹⁵⁹ Conjugated dienes have been obtained through reaction of a variety of alkynes with TMS-diazomethane in the presence of CpRuCl(cod) (**Scheme 145**).

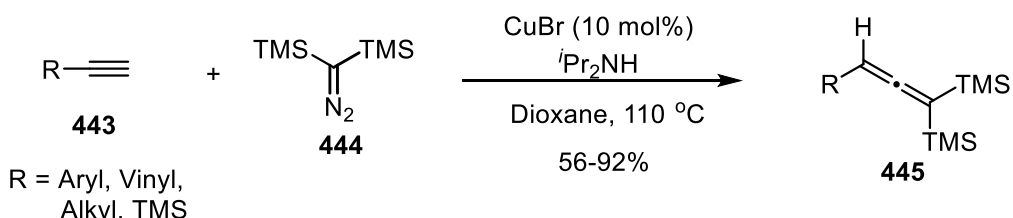
¹⁵⁹ J. L. Pailh, C. V.-L. Bray, S. Dérien, P. H. Dixneuf, *J. Am. Chem. Soc.* **2010**, 132, 7391–7397.



Scheme 145: Addition of TMS-diazomethane to alkynes

III.3.3.2. Addition of bis(trimethylsilyl)diazomethane to alkynes

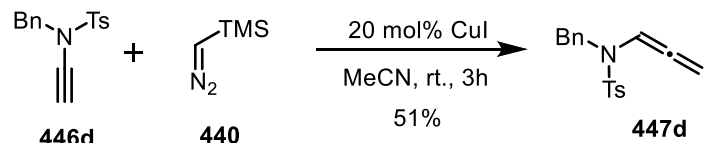
Wang *et al.* demonstrated that Cu(I)-catalyzed cross-coupling reaction between bis(trimethylsilyl)diazomethane and terminal alkynes provided 1,1-disilyl allenes with yields ranging from 56 to 92 %. Heating in refluxing dioxane is essential, copper bromide provided best yields and the reaction is restricted to the formation of 1,1-disilyl allenes substituted with an aryl, alkyl or an additional silyl group (**Scheme 146**).¹⁶⁰



Scheme 146: Addition of bis(trimethylsilyl)diazomethane to alkynes

III.3.4. Copper-catalyzed addition of TMS-diazomethane to terminal ynamides.

When terminal ynamides **446d** was treated with TMS-diazomethane **440** at room temperature after 3 hours, we obtained *N*-allenamides **447d** in 51% yield (**Scheme 147**).



Scheme 147: My first synthesis of *N*-allenamides from ynamides

III.3.5. Batiste Moegle's contribution

In order to better understand the progress of this work, I will introduce Batiste Moegle's contribution of this production.

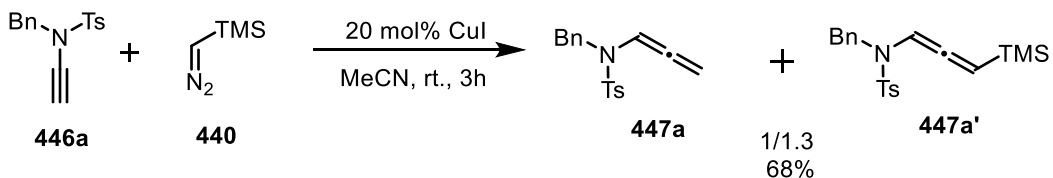
Batiste Moegle's work

III.3.5.1. Optimization

Batiste Moegle a PhD student in our group had a closer look into this cross-coupling reaction and found out that a second *N*-allenamide was formed **447a'** in this reaction. In fact,

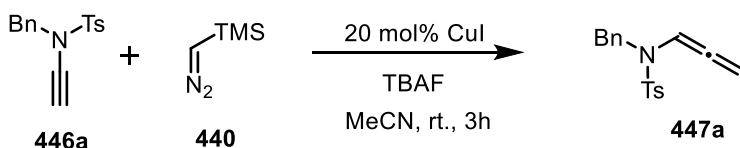
¹⁶⁰ S. Xu, R. Chen, Z.-H. Fu, Y.-P. Gao, J.-B. Wang, *J. Org. Chem.* **2018**, *83*, 6186–6192.

a mixture of two *N*-allenamides **447a** and **447a'** (ratio 1/1.3) in 68 % yield was observed (**Scheme 148**).



Scheme 148: Baptiste Moegle's result

After optimization of the reaction conditions, Baptiste found out that it is possible to orientate the reaction toward the formation of a unique *N*-allenamide by adding TBAF after total conversion of the terminal ynamide. In this way, he obtained exclusively *N*-allenamide **447a** in 66% yield (**Scheme 149**).



Scheme 149: Optimized reaction condition

III.3.5.2. Substrate scope

Under the optimized reaction conditions the scope of the reaction was explored by varying the ynamide. Addition of TMS-diazo **440** to oxazolidinone derivatives **446b** and **446c** resulted in good yields of *N*-allenamides **447b** and **447c**. Reaction with terminal pyrrolidinone **446d** provided the corresponding *N*-allenamide **447d** with a slight erosion of the yield. Linear alkyls groups [e.g methyl (**447e**) and butyl (**447f**)] as well as cyclic alkyls groups [(cyclopentyl (**447g**) and cyclopropyl (**447h**))] were also suitable compounds for this transformation. X-ray analyses of **447h** confirmed the structure of amido-cyclopropyl allene **447h**. Notably, even alkenes (**447i**), halogens (**447j**), protected aldehydes (**447k**), imides (**447l**) were also convincing, amplifying substantially the substrate scope. The influence of either more labile electron-withdrawing groups on the nitrogen atom such as mesyl (**447m**), nosyl (**447n**) or more hindered cyclic sulfonamides (**447o**, **447p**) revealed to be fully accommodated in this transformation.

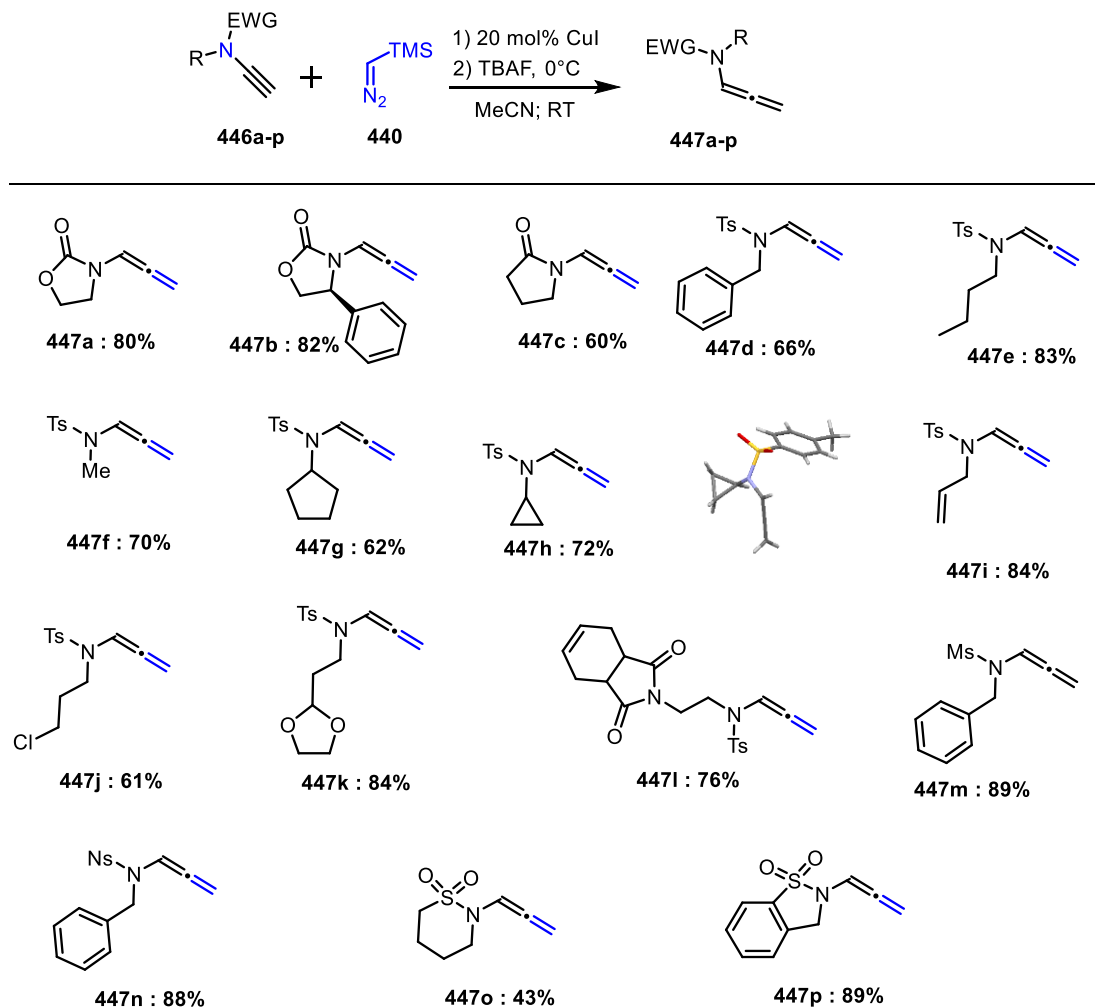


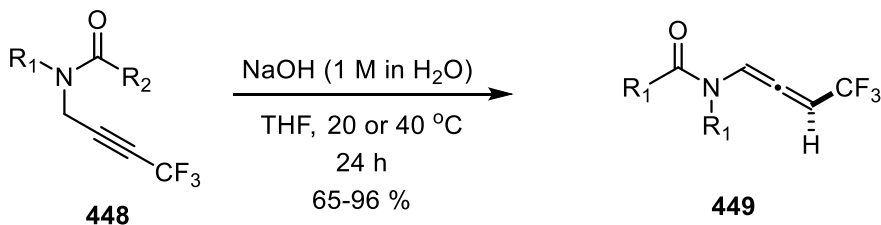
Table 10: Scope for the synthesis of *N*-allenamides.

III.4. Synthesis of fluorinated *N*-allenamides

Taking in account our previous work on fluorinated diazo-compounds (chapter 2) our next idea was to investigate the synthesis of fluorinated allenamides.

III.4.1. Blanchard's work

In this context, Nicolas Blanchard *et al.* developed a synthesis of α -trifluoromethylated *N*-allenamides from trifluorimethylated propargylic amides through basic treatment (**Scheme 150**).¹⁶¹



Scheme 150: Synthesis of γ -CF₃-substituted *N*-allenamides

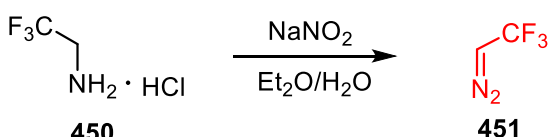
¹⁶¹ C. Guissart, A. Dolbois, C. Tresse, S. Saint-Auret, G. Evano, N. Blanchard, *Synlett* **2016**, 27, 2575–2580.

III.4.2. Our results

III.4.2.1. With trifluorodiazethane

a. Synthesis of trifluorodiazethane

First, we examined the more studied trifluorodiazethane.¹⁶² An ethereal solution of trifluorodiazethane was prepared according to Gilman and Jones.¹⁶³ 2,2,2-trifluoroethylamine hydrochloride **450** was treated with sodium nitrite in ether. After addition of water, the mixture was stirred for two hours at 0°C. After removal of the the water phase, the ethereal solution was stored in the freezer (-20°C) and was used directly in the next step (**Scheme 150**).



Scheme 150: Synthesis of CF₃-diazomethane

b. Addition of trifluorodiazethane to terminal ynamides

Addition of the trifluorodiazethane **451** to the terminal ynamide **452a** under copper-catalysis in acetonitrile provided the corresponding ynamides with a very good yield of 95% provided triethylamine was added to the reaction mixture.

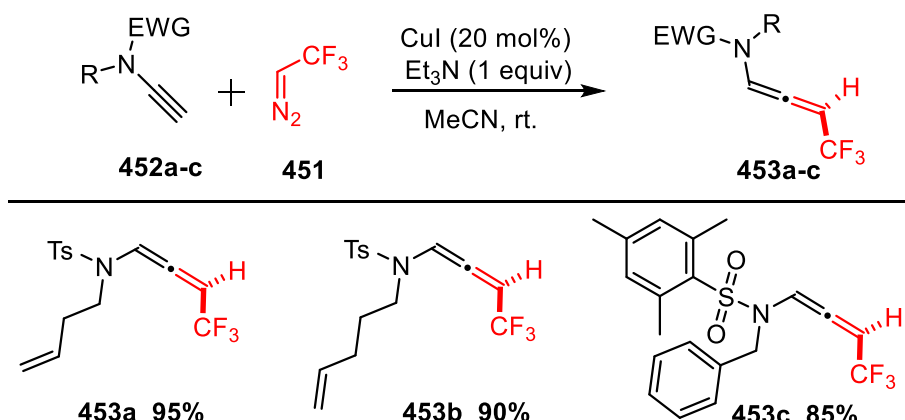


Table 11: Scope for the synthesis of CF₃-substituted N-allenamides.

The scope was also explored on two more terminal ynamides, the expected CF₃-substituted N-allenamides **453b** and **453c** were obtained with respectively 90 and 85% yields (**Table 11**).

III.4.2.2. With CF₂H-diazomethane

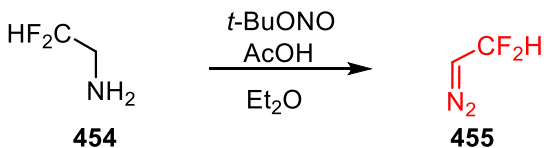
a. Synthesis of CF₂H-diazomethane

Judging by the results obtained, the strategy seems to be viable. As a consequence, we investigated a more challenging fluorine substituent namely the CF₂H-group. Mykhailiuk reported an elegant *in situ* generation of difluoromethyldiazomethane from

¹⁶² L. Mertens, R. M. Koenigs, *Org. Biomol. Chem.* **2016**, 14, 10547–10556.

¹⁶³ H. Gilman, R. G. Jones, *J. Am. Chem. Soc.* **1943**, 65, 1458–1460.

difluoroethylamine¹⁶⁴ for the synthesis of difluorinated pyrazoles *via* [3+2] cycloadditions. A mixture of difluoroethylamine, *tert*-butyl nitrite in the presence of a catalytic amount of acetic acid was heated at reflux for ten minutes. The yellow solution of the reaction mixture indicated the presence of CF₂H-diazomethane **455** (**Scheme 152**).



Scheme 152: Synthesis of CF₂H-diazomethane

b. Addition of CF₂H-diazomethane to ynamides

We directly trapped the putative diazo-compound with the terminal ynamide in the presence of trimethylamine and a catalytic amount of copper iodide in acetonitrile. Whereas Mykhailiuk observed a [3+2] cycloadditions when CF₂HCHN₂ was added on electron deficient alkynes, we obtained CF₂H-substituted *N*-allenamides from terminal ynamides. Oxazolidinone (**457a**), cyclic alkyls groups [cyclopropyl (**457d**)], aryl groups (**457b**, **457c**) as well as protected aldehydes (**457f**) and amides (**457g**) could be accommodated.

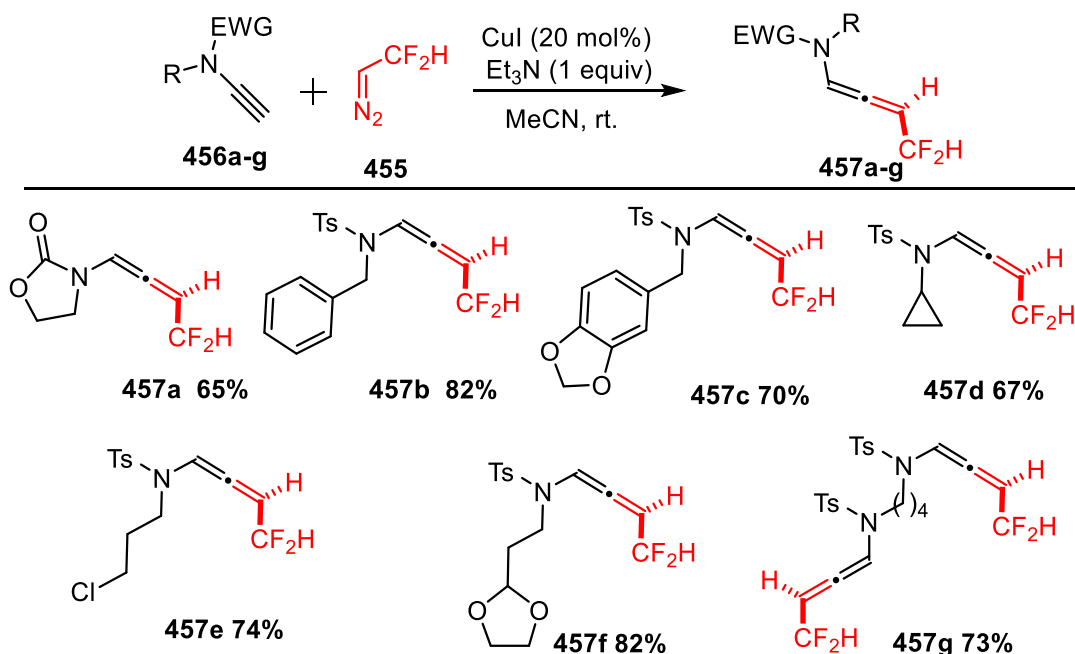


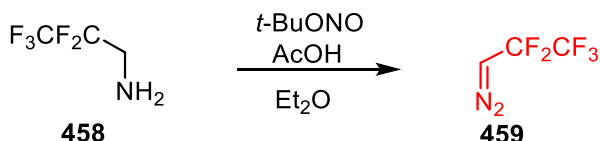
Table 12: Scope for the synthesis of CF₂H-substituted *N*-allenamides.

III.4.2.3. With CF₂CF₃-diazomethane

a. Synthesis of CF₂CF₃-diazomethane

To obtain the perfluorinated diazo-compound, we used the previous procedure. 2,2,3,3,3-perfluoropropylamine was treated with *tert*-butyl nitrite in the presence of a catalytic amount of acetic acid and was heated at reflux for ten minutes. The yellow solution of the reaction mixture indicated the presence of CF₂CF₃-diazomethane (**Scheme 153**).

¹⁶⁴ P. K. Mykhailiuk, *Angew. Chem. Int. Ed.* **2015**, *54*, 6558–6561



Scheme 153: Synthesis of CF_2CF_3 -diazomethane

b. Addition of CF_2CF_3 -diazomethane to terminal ynamides

The highly fluorinated compound **459** bearing a perfluorinated group adapted also perfectly to the formation of *N*-allenamides, in this way, we obtained compound **461a** and compound **461b** with respectively 60 and 64 % yield (**Table 15**).

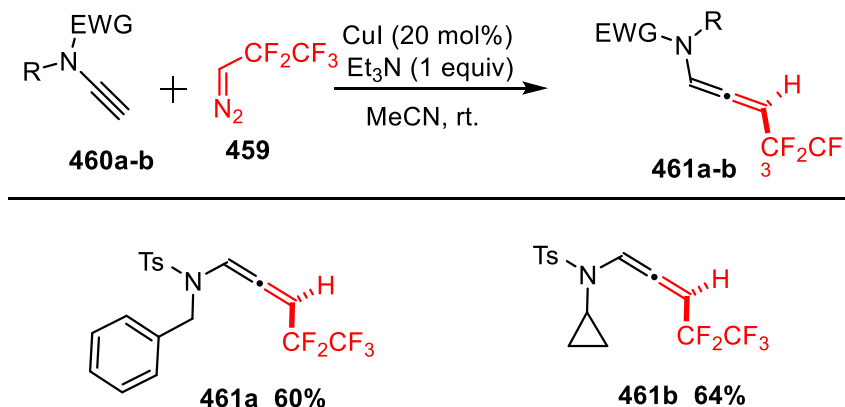


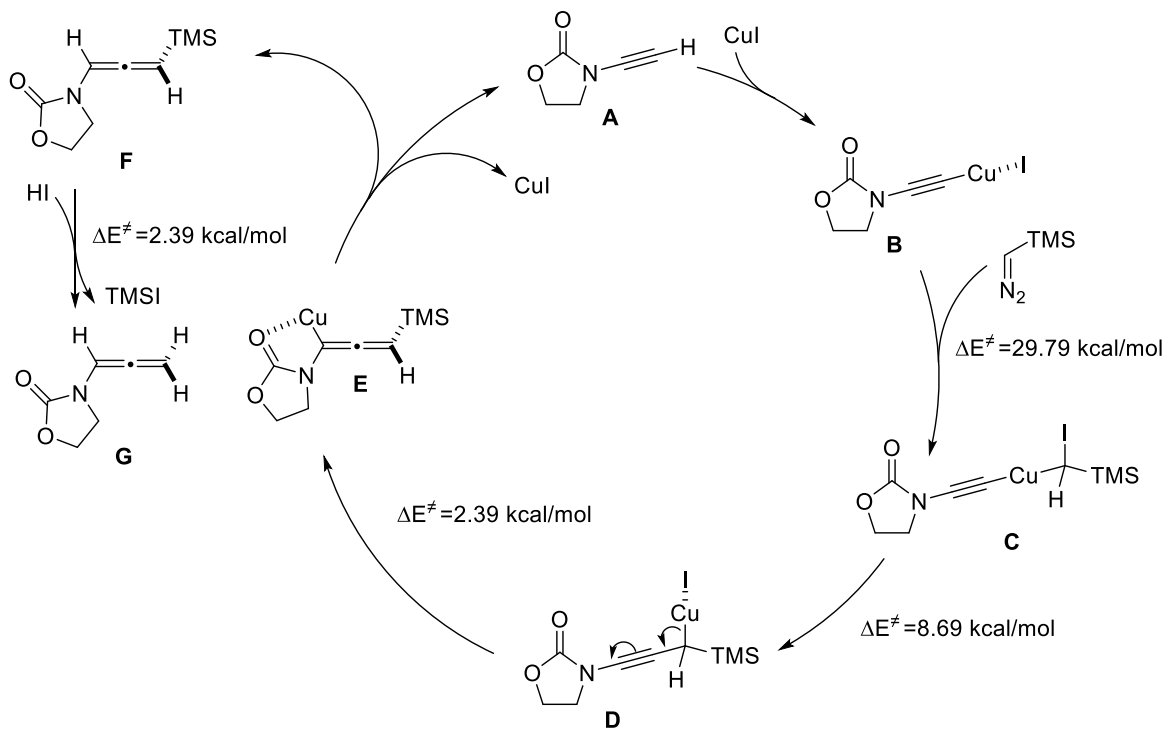
Table 15: Scope for the synthesis of CF_2CF_3 -substituted *N*-allenamides.

III.5. Plausible reaction mechanism

Regarding the mechanism for this transformation, we considered the pathway that has been proposed for cross-coupling reactions of diazo compounds with alkynes.¹⁶⁵ In the presence of copper(I) salt, ynamide **A** leads to copper-ynamidyl **B**. The reaction of the latter with TMS-diazomethane provides copper intermediate **C**. Copper migration-insertion forms **D**. Rearrangement of **D** leads to allene **E**. The low energy barrier between compound **D** and **E** supports not only that the electron-withdrawing group on the ynamide provides enhanced stability but can also serve as coordination site for copper thus allowing a reversal transposition regardless the polarization of the ynamide.¹⁶⁶ Decupration of **E** regenerates the copper iodide and forms TMS-allenamide. The small energy barrier between compound **F** and **G** is fully consistent with the fact that during the reaction both compounds were formed. (**Scheme 154**).

¹⁶⁵ Q. Xiao, Y. Xia, H. Li, Y. Zhang, J. Wang, *Angew. Chem. Int. Ed.* **2011**, *50*, 1114–1117 b) F. Ye, X. Ma, Q. Xiao, H. Li, Y. Zhang, J. Wang, *J. Am. Chem. Soc.* **2012**, *134*, 5742–5745. c) T. Wang, M. Wang, S. Fang, J. Liu, *Organometallics* **2014**, *33*, 3941–3949.

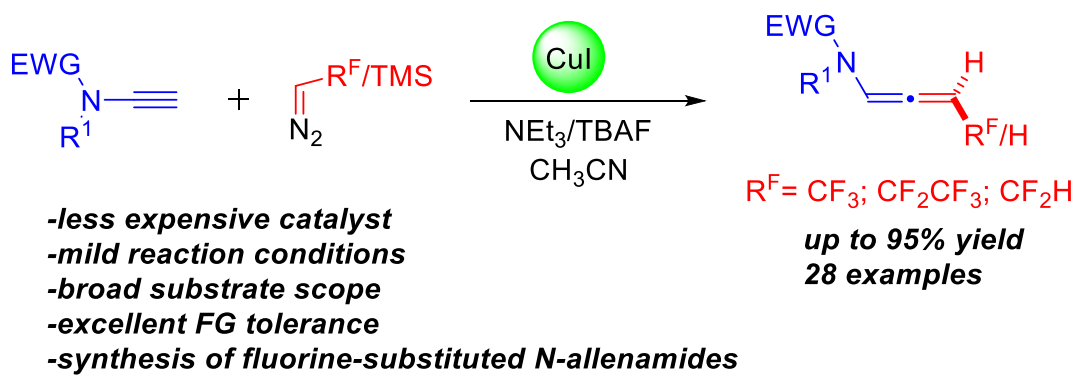
¹⁶⁶ B. Zhou, T.-D. Tan, X.-Q. Zhu, M.-Z. Shang, L.-W. Ye, *ACS Catal.* **2019**, *9*, 6393–6406



Scheme 154: Plausible reaction mechanism.

III.6. Conclusion.

To conclude, we present a straightforward method to obtain *N*-allenamides through copper-catalyzed addition of diazo-compounds to terminal ynamides. DFT-calculations showed provided an accurate mechanism for this transformation. We showed that the classical mechanism postulated for alkynes is energetically too high. Our transformation relies rather on an oncommon reversal mechanism that, regardless of the polarization of the triple bond of the ynamide, favors the addition of the diazo compound at the β -position of the ynamide. The protocol tolerates a wide range of functional groups on the ynamide moiety but also fluorinated diazo-compounds could be accommodated, thus giving access to fluorine substituted *N*-allenamides. This copper-catalyzed process represents the first synthesis of tri-di or per-fluorinated *N*-allenamides (**Scheme 155**).



Scheme 155: Synthesis of *N*-allenamides *via* Ynamides

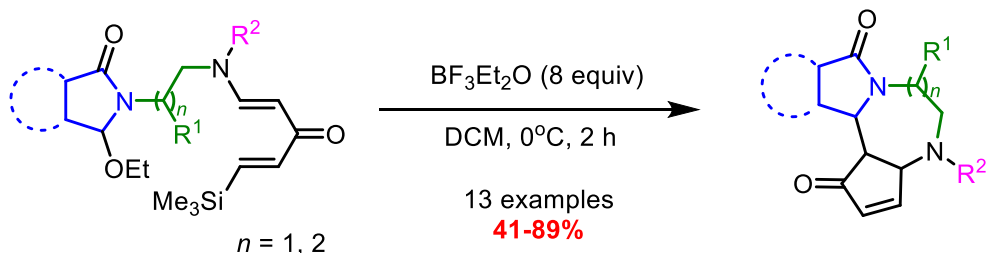
IV. GENERAL CONCLUSION

This thesis work covers three chapters during which we have shown that the reactivity of tertiary enamides allows access to polycyclic diazepines via domino reaction on one hand. On the other hand, we have studied the reactivity of ynamides with respect to diazo compounds to synthesize first amido-difluorofurans and second *N*-allenamides that are terminal or substituted by fluorinated groups.

Tertiary enamide-promoted diastereoselective domino/ *N*-acyliminium ion trapping and Nazarov cyclization.

In this first chapter, we have continued the work initiated by Dr. Lucile Andna on the reactivity of imide-enamides.

After having prepared the *N*-sulfonamides starting from the corresponding anhydrides and the ene-yne-ones necessary for the formation of the tertiary enamides, the enamidyl vinyl ketones were synthesized. Numerous *N*-functionnalized α -ethoxylamides bearing a dienone comprising a tertiary enamide have been obtained by varying, the starting imide, the substituents on the nitrogen, as well as the spacer between α -ethoxylamide and the dienone moiety (**Scheme 156**). The reaction turned out to be totally diastereoselective and in this way, diazepines fused to cyclopentenones were obtained, thereby creating 3 new stereogenic centers. In one case, we were able to isolate a diazepine intermediate , which proves that the trapping of the NAI ion takes place before the Nazarov reaction. These experimental facts could also be corroborated by cyclic voltammetry studies.

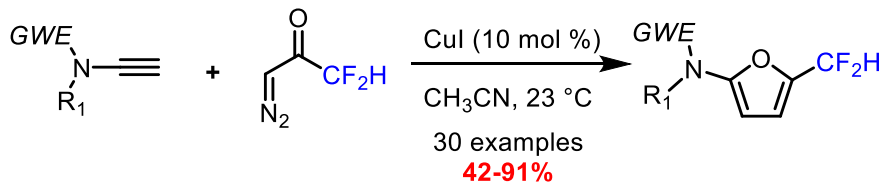


Scheme 156: Domino/ *N*-acyliminium ion trapping and Nazarov cyclization

Synthesis of CF₂H-substituted 2-amidofurans via copper-catalyzed addition of α -difluorinated-diazoacetone to ynamides.

In the second chapter of this work, we reacted terminal ynamides with diazo-compounds. While ethyldiazoacetate only led to degradation products, the addition of diazoacetone to terminal ynamides exclusively led to amido-furans substituted with a methyl group. To broaden the field of applications of these compounds, and given the growing interest in fluorinated compounds, we have developed the first synthesis of difluorinated diazoacetone. This practical reagent is stable at room temperature , easy to handle and proved to be the ideal candidate for introducing a difluorinated group into amido-furans. The addition of

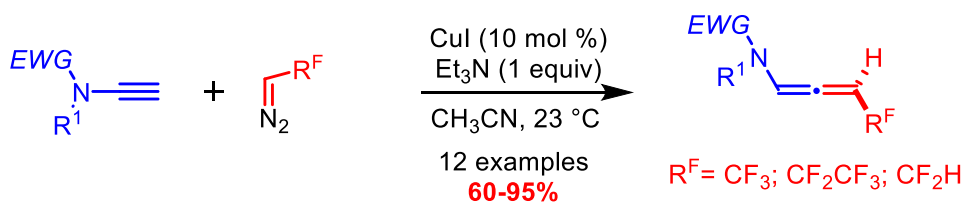
diazoacetone to terminal ynamides at room temperature constitutes the first way to synthesize 2-amido-furans difluorinated at position 5 (**Scheme 157**) The method exhibits a broad functionnal group tolerance. DFT calculations by Dr. Ilaria Ciofini, Dr. Anna Perfetto and Davide Luise at Chimie Paris Tech proved that protonation α or γ to the carbonyl moiety after O-alkylation on an ynamide or an allenamide performs amido-fluorinated furans.



Scheme157: Synthesis of CF₂H-substituted 2-amidofurans

Copper-catalyzed synthesis of terminal vs. fluorine substituted *N*-allenamides via addition of diazo-compounds to terminal ynamides

In the third chapter, we continued our investigations on the reactivity of ynamides towards diazo-compounds. We have shown that terminal ynamides react with TMS-diazomethane to form terminal *N*-allenamides. In this way, it is also possible to functionalize the *N*-allenamides with fluorinated groups. In particular, using CF₃-diazomethane, CF₂H-diazomethane, CF₃CF₂-diazomethane, we obtained the corresponding functionalized *N*-allenamides (**Scheme 158**). The mechanism has been investigated and two possible pathways have been explored in collaboration with Dr. Ilaria Ciofini, Dr. Anna Perfetto and Davide Luise at Chimie Paris Tech. The first one is a classical mechanism involving a copper acetylid and after rearrangement a Fu type compound is obtained. Elimination of copper followed by protonation provides the TMS-allenamide. A « reversal type » mechanism with respect to the ynamide reactivity was also investigated using metal-carbonyl-chelation controlled β -addition on the ynamide. This pathway involves addition of TMS-diazo on β -position of the ynamide. The latter route is preferred due to the minimum energy demand for this pathway.



Scheme158: Synthesis of terminal and fluorinated *N*-allenamides

V. RESUME DE THESE EN FRANÇAIS

V.1. Introduction

Dans ce travail de thèse trois classes de composés incontournables en chimie hétérocycliques ont été étudiées. Les énamides tertiaires qui sont à l'heure actuelle encore peu étudié malgré une réactivité « énaminique » intéressante, les ynamides, des synthons précieux de par leur réactivité particulière et enfin les *N*-allénamides attrayant par leur géométrie particulière. Ces briques moléculaires uniques pour leur utilisation en chimie hétérocyclique possèdent un point commun qui est un atome d'azote substitué par un groupement électroattracteur qui permet de conférer davantage de stabilité à la molécule notamment vis-à-vis de l'hydrolyse.

V.1.1. Les énamides tertiaires

Depuis leur description en 1953 par Stork, les énamines, caractérisées par une double liaison substituée par une amine, ont été largement utilisées notamment pour la formation de liaison C-C.¹ En effet, la délocalisation du doublet de l'azote sur la double liaison permet de rendre ces énamines plus riches en électrons que de simples énols ou éthers d'énols silylés, leur conférant leur réactivité énaminique, nucléophile.² Cependant, les énamines sont peu stables, car elles sont très sensibles à l'hydrolyse et peuvent par conséquent être difficiles à manipuler, à isoler et à conserver (**Schéma 1**).

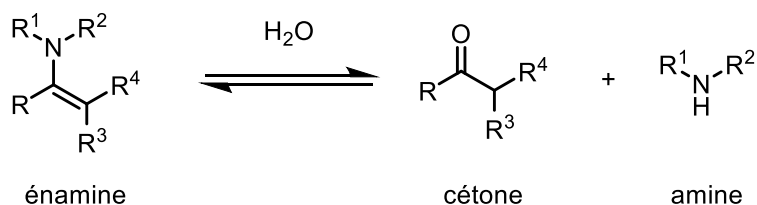


Schéma 1: Hydrolyse des énamines

Afin d'augmenter la stabilité de ces énamines, l'atome d'azote peut être substitué par un groupement électroattracteur, formant ainsi les énamides. Le doublet de l'azote peut dans ce cas se délocaliser sur le groupement électroattracteur en plus de la double liaison. Les énamides sont par conséquent plus stables que les énamines, mais posséderaient une réactivité énamidique réduite comparée aux énamines (**Schéma 2**).

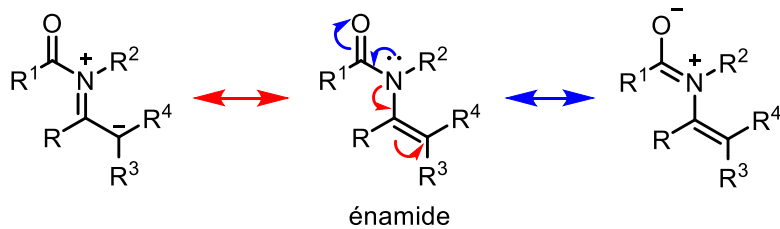


Schéma 2: Représentation schématique des formes mésomères des énamides

Selon la nature du groupement électroattracteur, 3 grandes classes d'énamides peuvent être distinguées (**Figure 1**). Les énecarbamates, où la double liaison est substituée par un groupement amide, les ènecarbamates où le groupement électroattracteur est un ester et enfin les ènesulfonamides, portant un groupement sulfonyle au niveau de l'atome d'azote. Dans ce chapitre, le terme d'énamide tertiaire sera également utilisé de manière générale, pouvant désigner ces trois classes.

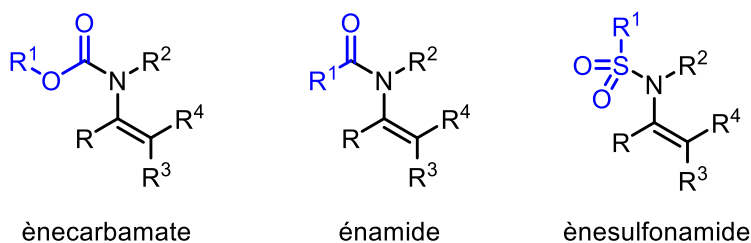


Figure 1. Représentation schématique des différentes classes d'énamides

La réactivité des énamides secondaires, où l'atome d'azote porte un atome d'hydrogène, n'est plus à démontrer, et a fait l'objet de plusieurs publications.³ Les énamides tertiaires, quant à eux, ont longtemps été considérés comme inertes, cependant, ils ont connu un regain d'intérêt, notamment grâce aux travaux de l'équipe de Wang.⁴

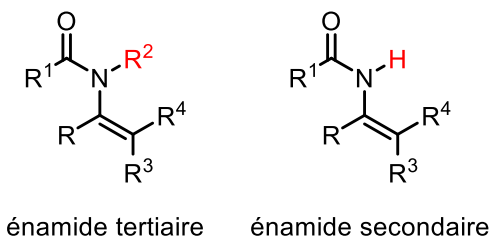


Figure 2. Représentation schématique d'énamides secondaires et tertiaires

Les diazépines sont des composés hétérocycliques insaturés à 7 chaînons comportant deux atomes d'azote. Cette structure est notamment présente dans une famille de molécules appelée benzo-diazépines. Connus surtout pour leur activité psychotrope,⁵ ces anxiolytiques sont très utilisés pour les troubles du sommeil. Ces actions pharmacologiques peuvent être attribuées au fait que les benzodiazépines facilitent l'action d'un neurotransmetteur, le GABA (acide gamma amino butyrique) sur son récepteur dans le cerveau. Le GABA diminue l'excitabilité du système nerveux central. Outre leur activité psychotrope, les diazépines ont

également montré des activités antimicrobiennes⁶ et antibiotiques.⁷ Compte-tenu de ces propriétés extrêmement intéressantes, l'objectif du premier chapitre de cette thèse a été d'utiliser la chimie des énamides tertiaires afin d'apporter davantage de variétés structurelles à cette famille de molécules pour créer de potentielles cibles thérapeutiques. Dans un souci d'économie d'atomes, nous avons ainsi envisagé une réaction domino qui implique un piégeage d'un ion *N*-acyliminium (NAI) suivie directement d'une cyclisation de Nazarov pour obtenir des diazépines condensées à des cyclopenténones.

V.1.2. Les ynamides

Les ynamines sont caractérisées par une liaison entre un atome d'azote et un atome de carbone hybridé *sp*, ce sont ainsi des alcynes substitués par des amines. Les ynamines représentent une classe de composé présentant une haute réactivité du fait de la polarisation de la triple liaison due à la délocalisation du doublet non liant de l'atome d'azote. Malgré les travaux pionniers de Viehe⁸ et Ficini⁹ dans ce domaine, la forte propension des ynamines à s'hydrolyser, et la difficulté à isoler ces composés rendent l'utilisation des ynamines très difficiles en synthèse organique malgré le fort potentiel qu'offrent ces molécules.

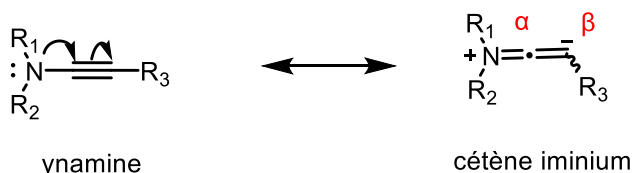


Schéma 3: Forme mésomère ynamine – cétène iminium

La solution apportée pour améliorer la stabilité des ynamines fut de diminuer la densité électronique de la triple liaison en substituant l'atome d'azote par un groupement électroattracteur. Des ynamines électro-déficientes sont alors appelés ynamides. Ainsi, la paire non liante de l'atome d'azote se trouve délocalisée non seulement dans la triple liaison mais aussi dans le groupement électroattracteur ; conférant davantage de stabilité à l'espèce tout en maintenant sa réactivité.

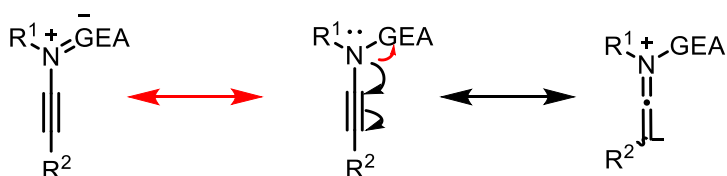


Schéma 3: Délocalisation du doublet non liant de l'azote

Les ynamides possèdent une réactivité unique et particulière. Grâce à une large gamme de méthodes de synthèse développées pour accéder à ces motifs structuraux, les ynamides sont devenus un outil très utile en synthèse organique permettant l'accès à des structures moléculaires de plus en plus complexes.

L'objet du deuxième chapitre a été de synthétiser des amido-furanes difluorés par addition de composés diazo sur des ynamides. Les furanes représentent un motif structurel privilégié dans un bon nombre de produits naturels particulièrement en pharmacochimie ainsi qu'en

agrochimie.¹¹ L'incorporation de groupement fluorés dans des molécules organiques est devenue une stratégie puissante dans la conception de médicaments. Une attention particulière a été accordée au groupement difluorométhyle (CF_2H) en raison de ses propriétés physico-chimiques uniques. Le groupement CF_2H peut agir comme un donneur de liaison hydrogène lipophile et peut être considéré comme un bioisostère métaboliquement stable d'un groupement hydroxyle ou d'un groupement thiol. Comme les interactions de type liaison hydrogène jouent un rôle crucial dans divers processus biochimiques, ce substitut jouit d'une place privilégié dans la recherche de nouveaux médicaments. Nous avons ainsi envisagé l'addition d'un composé diazo-difluoré sur des ynamides terminaux par catalyse au cuivre pour accéder aux amido-furanes difluorés.

Dans le troisième chapitre de ce travail, nous avons poursuivi nos investigations sur la réactivité des ynamides vis-à-vis de composés diazo de nature variés. Fort des résultats obtenus lors du deuxième chapitre, nous avons également utilisés des composés diazo comportant des groupements fluorés afin d'introduire davantage de fonctionnalité dans les produits finaux.

V.2. Résultats et discussions

V.2.1. Réaction DOMINO au départ d'énamides tertiaires substitués par un ion *N*-acyliminium

Les énamines et leurs homologues silylés *i.e* des enoxysilanes, ont été largement utilisés comme nucléophiles dans des réactions d'aldolisations *via* un mécanisme de type aza-ène pour former des liaisons carbone-carbone. Plus tard, les énamides secondaires portant un groupement électroattracteur sur l'azote sont apparus comme de puissants nucléophiles dans une grande variété de réactions catalysées par des acides de Lewis alors que les énamides tertiaires étaient initialement déclarés non réactifs envers les électrophiles. Cependant, des travaux récents sur les énamides tertiaires ont prouvé que ces substrats présentaient une réactivité "énaminique" envers plusieurs classes d'électrophiles, y compris les époxydes, les carbonyles, les imines, les ions nitriles et les alcynes activés. Notre intérêt récent pour la chimie des ynamides nous a incités à étudier la réactivité des énamides tertiaires équipés de précurseurs d'ions *N*-acyliminium pour la synthèse d'hétérocycles d'intérêt pharmacologique comme par exemple les diazépines représentées dans la figure ci-dessous (Figure 3).^{6, 7}

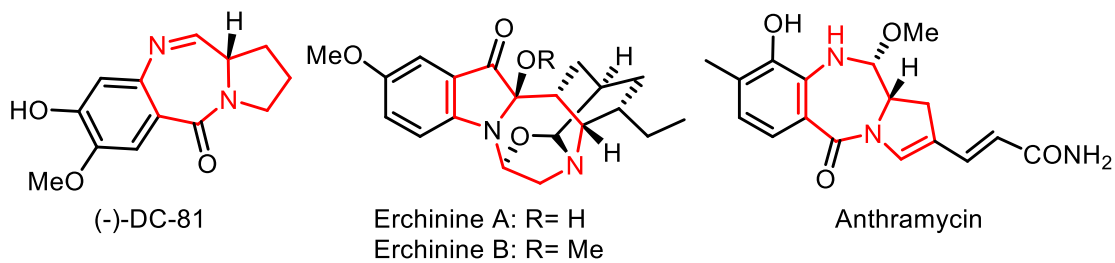


Figure 3 : Des benzodiazépines biologiquement actives

Parmi les méthodes décrites dans la littérature, les énamides tertiaires peuvent être obtenus par réduction des ynamides. Ainsi, dans notre équipe, il a été montré que des ynamides incorporant un *N*-imide peuvent être transformés en énamides tertiaires équipés d'un précurseur d'ion *N*-acyliminium (NAI). En milieu acide, l'énamide tertiaire s'additionne sur l'espèce *N*-acyliminium pour former des diazépines, des sous-structures très utilisées en chimie thérapeutique. Divers imides, différentes longueurs de bras espaceurs ainsi que différents substituants sur l'ynamide se sont avérés efficaces pour réaliser cette transformation (**Schéma 5**).¹²

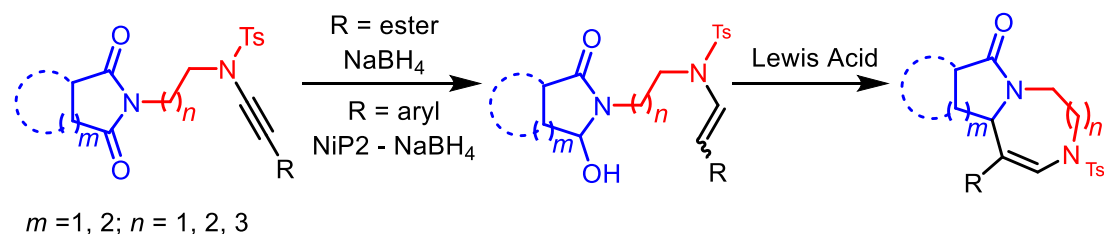


Schéma 5: Piégeage de l'ion NAI par un énamide tertiaire

Le premier objectif de ma thèse était de tirer parti de la présence de l'énamide tertiaire présent sur la diazépine pour réaliser une cyclisation de Nazarov afin d'accéder à des motifs cyclopenta-diazépines plus complexes. Pour confirmer le concept envisagé, l'ester **1** a été transformé en diénone croisée **2**. La réaction de Nazarov a bien donné lieu à la formation du dérivé cyclopenténone tétracyclique **3** souhaité (**Schéma 6**).

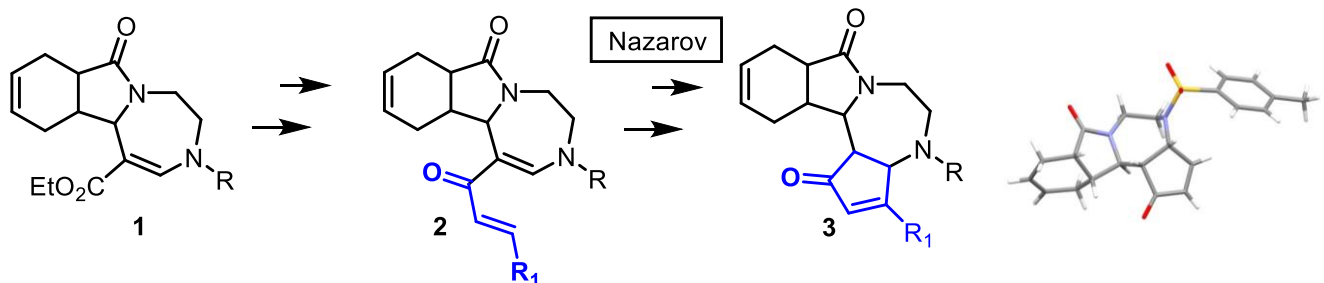


Schéma 6: Synthèse de la cyclopenténone **3** via une cyclisation de Nazarov

Bien que nous ayons obtenu le composé souhaité, cette réaction n'est pas généralisable et les rendements obtenus ne sont pas reproductibles dans tous les cas. En suivant le concept d'économie d'atomes pour la construction de molécules complexes, nous avons anticipé que des précurseurs d'ions *N*-acyliminium équipés de diénones croisées incorporant des énamides tertiaires offriraient la possibilité de favoriser deux réactions de façon simultanée: addition de l'énamide tertiaire sur l'ion *N*-acyliminium suivie d'une réaction de Nazarov (**Schéma 7**).

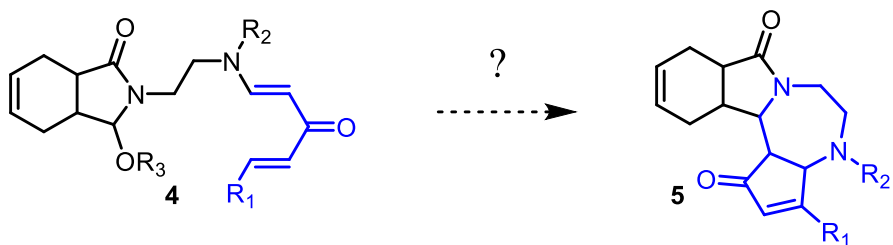


Schéma 7: Piégeage de l'ion NAI suivi d'une réaction de Nazarov.

Les ènesulfonamides actifs peuvent être obtenus par réaction d'alcynes terminaux avec des sulfonamides en utilisant du Triton B¹³ ou du DABCO.¹⁴ Sur la base des résultats précédents, nous avons émis l'hypothèse qu'une divinylcétone substituée par un groupement silyle fournirait une solution efficace pour faciliter la réaction de Nazarov. Ainsi, nous avons établi une voie de synthèse efficace vers l'ène-yne-one **7** à partir de l'alcool propargylique **6** en 6 étapes avec un rendement global de 37% (**Schéma 8**).

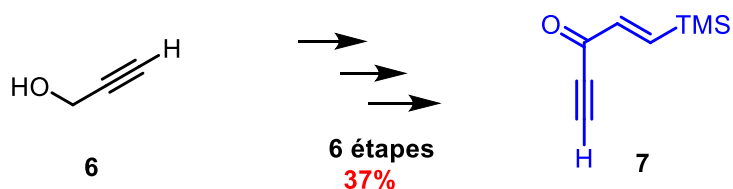


Schéma 8: Synthèse de l'ène-yne-one **7**

L'addition de la tosylsulfonamide **8** sur l'ène-yne-one **7** fournit bien la diénone croisée correspondante **9a**. Le traitement avec un acide de Lewis permet à la fois de réaliser l'addition de l'énamide tertiaire sur le *N*-acyliminium généré intermédiairement suivi de la réaction de Nazarov. La réaction est totalement diastéréosélective. Un seul dérivé tétacyclique comportant une cyclopenténone **10a** est obtenu (**Schéma 9**).

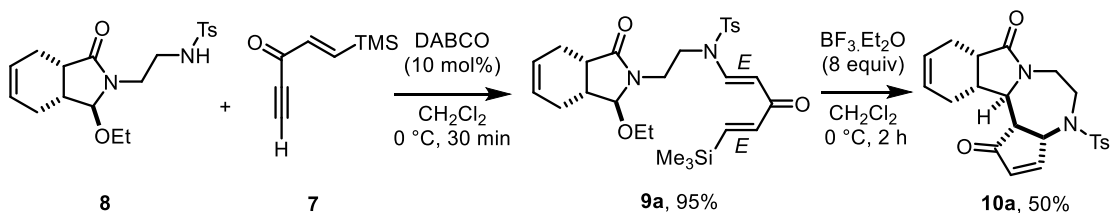


Schéma 9: Synthèse de la diénone croisée **9a** et réaction domino

La réaction domino s'applique à des imides variés, à une chaîne à 3 atomes de carbones entre les deux atomes d'azote ainsi qu'à des groupements protecteurs différents sur l'atome d'azote (**Schéma 10**).

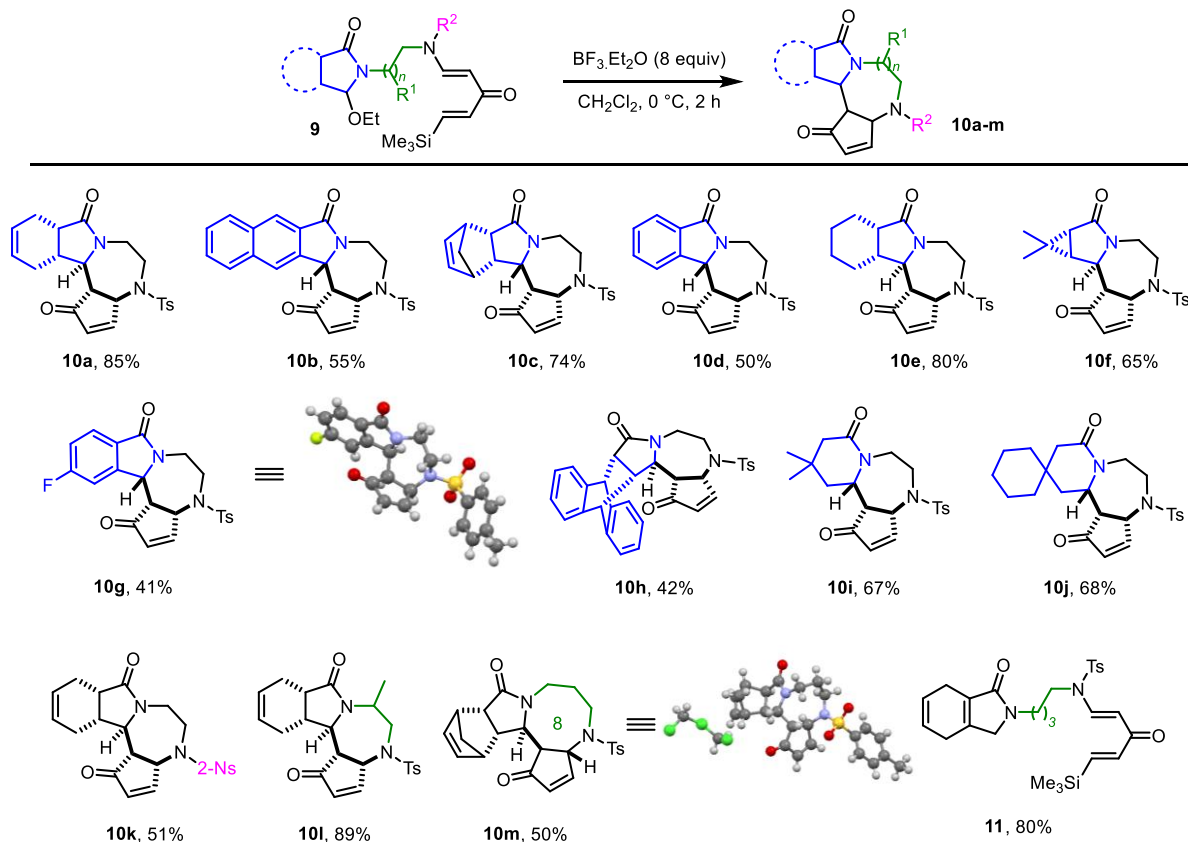


Schéma 10: Exemplification de la réaction domino

La chaîne à quatre unités méthyléniques constitue la limite de la réaction, car dans ce cas, le composé éliminé **11** est obtenu.

V.2.2. Synthèse d'amido-furanes difluorés par addition de difluorodiazoacétone sur des ynamides vrais

Au laboratoire, l'addition de diazoacétate d'éthyle sur des alcynyls-cétones avait conduit à des céto-3-alcynoates.¹⁵ Compte-tenu des résultats obtenus dans la littérature concernant l'addition de diazoacétate d'éthyle sur des ynamides,¹⁶ nous avons envisagé l'addition de la diazoacétone¹⁷ sur un ynamide. En utilisant une catalyse au cuivre, au départ de l'ynamide terminal **12a** en présence de diazoacétone **13**, nous avons obtenu, non pas l'alcyne fonctionnalisé **14** mais l'amido-furan correspondant **15** (**Schéma 11**).

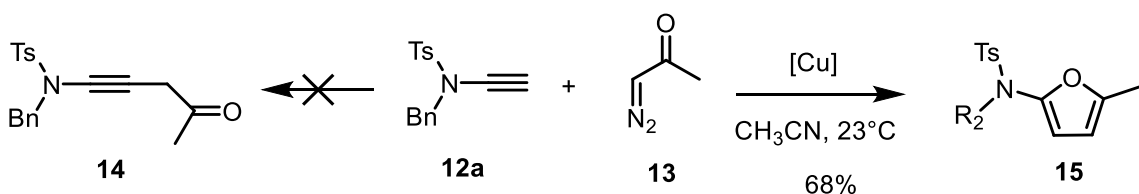


Schéma 11: Synthèse de l'amido-furan **15**.

Des expériences réalisées sur des diazoacétones non énolisables ont montré que ces dernières ne réagissaient pas dans ces conditions et que la présence d'un atome d'hydrogène en alpha du groupement carbonyle était indispensable à la réalisation de cette

transformation. Compte-tenu de l'importance des dérivés difluorés en pharmacochimie et en phytochimie, nous avons décidé de préparer la diazoacétone difluorée afin d'obtenir des furanes difluorés. Le diazoacétone difluorée **18** n'existe pas dans la panoplie des réactifs de difluoration. Nous avons mis au point une nouvelle voie de synthèse de ce composé par transfert de diazo suivi de déacylation à partir de la diénone **16** (**Schéma 12**).

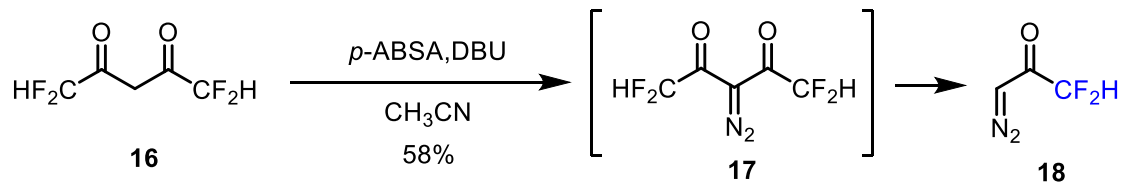


Schéma 12: Synthèse de la diazoacétone difluorée **18**

Stable pendant plusieurs semaines ce réactif est simple d'utilisation et permet d'obtenir une très large gamme d'amido-furanes difluorés **19**. Des fonctionnalités « délicates » comme des triples liaisons, des groupements nitriles, des aldéhydes protégés sont tolérées et les furanes correspondants **19** ont été obtenus avec de bons rendements (**Schéma 13**).

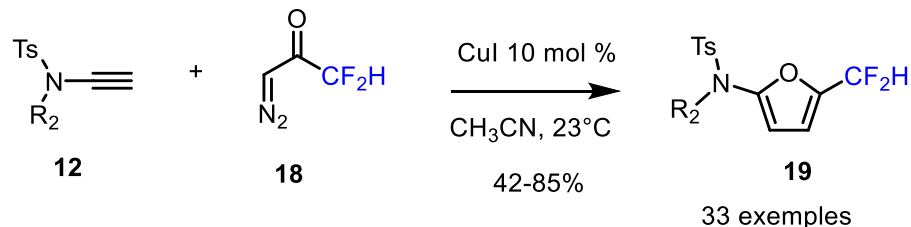


Schéma 13: Synthèse des amido-furanes difluorés **19**

Ces composés ont été utilisés pour réaliser des transformations ultérieures comme des nitrations, des couplages oxydants intramoléculaires ou encore des réactions de Diels-Alder intramoléculaires qui ont abouti à la formation d'autres hétérocycles fluorés plus complexes (**Schéma 14**).

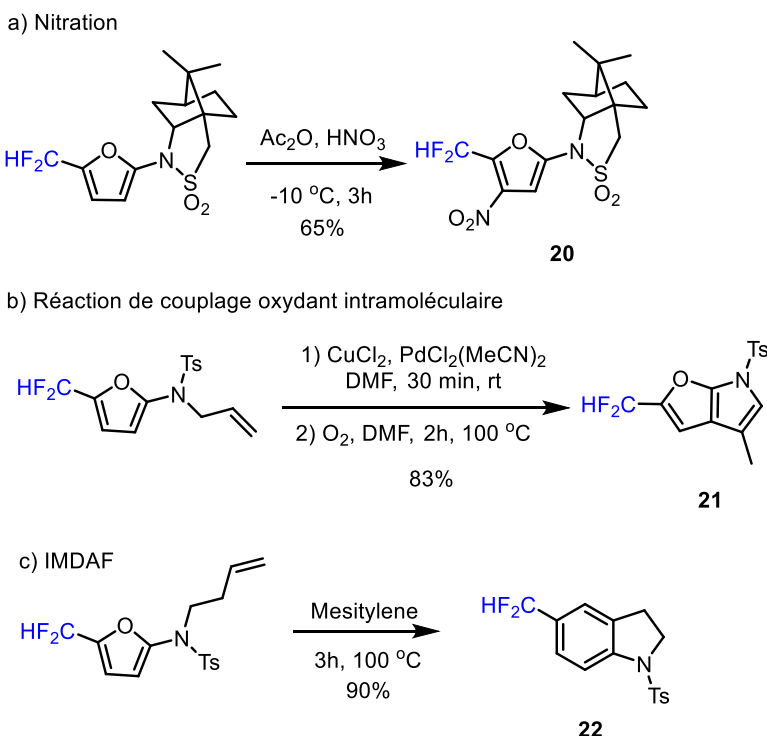


Schéma 14: Applications synthétiques des amido-furanes fluorés

V.2.3. Synthèse cupro-catalysées de *N*-allèniamides terminaux ou fluorés par addition de composés diazo sur des ynamides terminaux.

Les *N*-allèniamides une sous-classe d'allènes, sont devenus des motifs essentiels dans bon nombre de transformations. Malgré leur popularité en tant que briques essentielles pour la construction de composés hétérocycliques, le nombre limité de méthodes connues pour leur préparation est souvent entravé par une faible portée de substrats et surtout par une diversité structurelle restreinte. Inspirés par les travaux de l'équipe portant sur l'ajout de composés diazo sur des triples liaisons , nous avons envisagé que les ynamides réagiraient avec les composés diazo pour former des *N*-allèniamides. Pour tester notre hypothèse , nos premières tentatives ont consisté en une réaction de couplage entre l'ynamide terminal **23d** et un substitut du diazométhane disponible commercialement à savoir le triméthylsilylediazométhane. Après trois heures à température ambiante , nous avons bien obtenu les *N*-allèniamides souhaités sous forme d'un mélange de deux composés **25d** et **25d'** (ratio 1/1.3) avec un rendement de 68%.

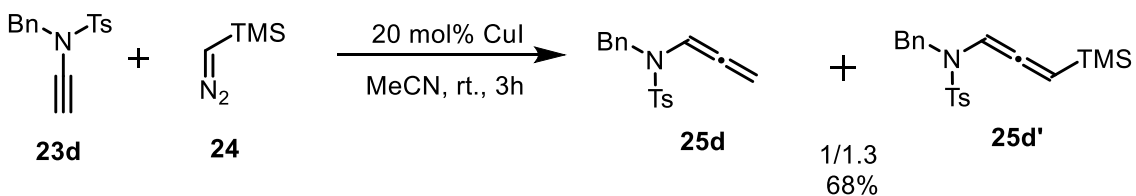


Schéma 15: Synthèse de *N*-allèniamides au départ d'ynamides

L'ajout d'une solution de TBAF, a permis d'orienter cette réaction vers la formation exclusive de l'allène non substitué **25d**.

En utilisant les conditions optimales, toutes une série de *N*-allèniamides terminaux ont pu être préparé avec des rendements allant de 43% à 89%.

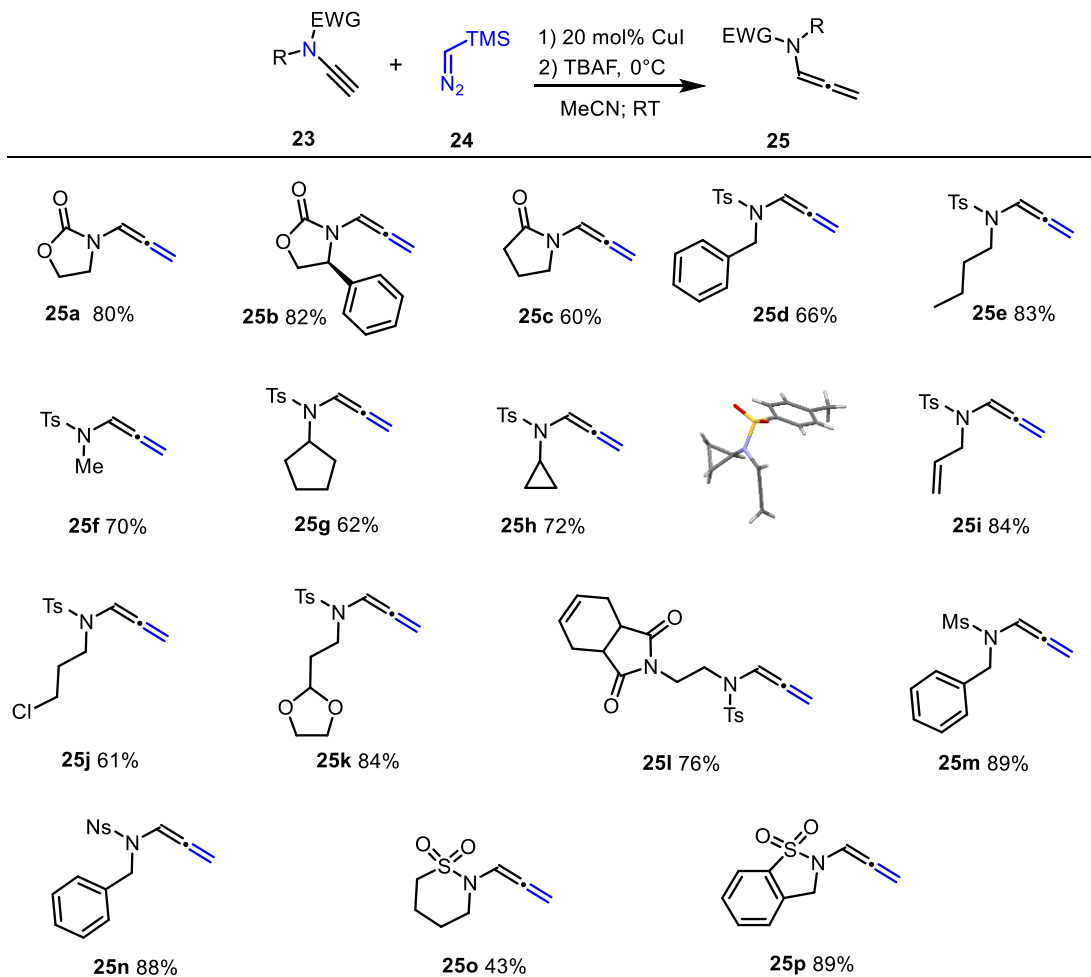


Schéma 16: Portée de la réaction.

Cette transformation a ensuite été appliquée de manière très efficace à la synthèse de *N*-allèniamides fluorés en position γ avec d'excellents rendements.

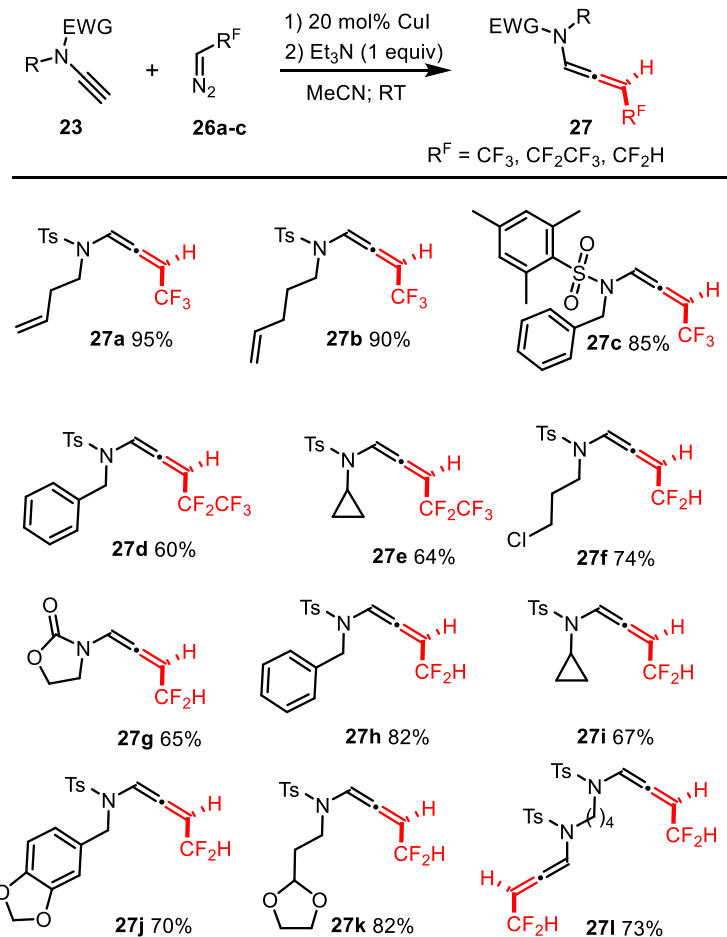


Schéma 16: Synthèse de *N*-allèniamides fluorés

La portée importante de cette transformation a montré non seulement son efficacité mais également sa versatilité. Ce procédé cupro-catalysé représente la première synthèse de *N*-allèniamides fluorés à partir d'ynamides. Ces *N*-allèniamides push-pull constituent des plateformes incontournables pour réaliser d'autres transformations.

V.3. Conclusion Générale

Au cours de ma thèse, nous avons accédé à des sous-structures de composés hétérocycliques azotés d'intérêts pharmacologiques au moyen d'énamides tertiaires. Nous avons également développé une nouvelle méthodologie de synthèse pour obtenir des 2-amido-furanes fluorés au départ d'ynamides. En modifiant la nature du composé diazo, nous avons développé une nouvelle synthèse de *N*-allèniamides non substitués ou fonctionnalisés par des groupements fluorés.

Dans un premier temps, des énamides tertiaires intégrés dans des diénones croisées ont permis d'effectuer une réaction domino impliquant une cyclisation intramoléculaire sur un ion *N*-acyliminium suivie d'une réaction de Nazarov. La réaction est totalement diastéréosélective et fournit dans chaque cas une seule diazépine comportant une cyclopentène. La torquosélectivité observée s'explique par le design particulier de l'énamide tertiaire. Cette réaction s'adapte à des substrats très variés. La voltamétrie cyclique a permis de corroborer le mécanisme proposé.

Une toute autre méthodologie, faisant intervenir une addition cupro-catalysée de diazoacétone difluoré sur des ynamides a permis de mettre au point une nouvelle synthèse d'amido-furanes difluorés très prisés en chimie médicinale et en phytochimie. Ces composés ont ensuite été utilisés comme plateforme pour réaliser la synthèse d'hétérocycles plus complexes.

Finalement, la réactivité particulière des ynamides vis-à-vis de composés diazo, nous a permis de mettre au point une nouvelle synthèse de *N*-allénamides terminaux. En utilisant des composés diazo judicieusement fonctionnalisés, nous avons obtenus des *N*-allénamides push-pull substitués en position γ par un groupement CF_3 , CF_2H ou CF_3CF_2 .

V.4. Références

- ¹ Stork, G.; Dowd, S. R. *J. Am. Chem. Soc.* **1963**, *85*, 2178–2180.
- ² Kempf, B.; Hampel, N.; Ofial, A. R.; Mayr, H. *Chem. - Eur. J.* **2003**, *9*, 2209–2218.
- ³ Matsubara, R.; Kobayashi, S. *Acc. Chem. Res.* **2008**, *41*, 292–301. Carbery, D. R. *Org. Biomol. Chem.* **2008**, *6*, 3455–3460.
- ⁴ Wang, M.-X. *Chem. Commun.* **2015**, *51*, 6039–6049.
- ⁵ Pardo, M.; Tellitu, I.; Domínguez, E. *Tetrahedron* **2010**, *66*, 5811–5818.
- ⁶ Yu, H.-F.; Qin, X.-J.; Ding, C.-F.; Wei, X.; Yang, J.; Luo, J.-R.; Liu, L.; Khan, A.; Zhang, L.-C.; Xia, C.-F.; Luo, X.-D. *Org. Lett.* **2018**, *20*, 4116–4120.
- ⁷ Kaneko, T.; Wong, H.; Doyle, T. W.; Rose, W. C.; Bradner, W. T. *J. Med. Chem.* **1985**, *28*, 388–392.
- ⁸ Viehe, G. H. *Angew. Chem. Int. Ed.* **1967**, *6*, 767–778.
- ⁹ Ficini, J. *Tetrahedron* **1976**, *32*, 1449–1486.
- ¹⁰ Lu, T.; Lu, Z.-J.; Ma, Z.-X.; Zhang, Y.; Hsung, R. P. *Chem. Rev.* **2013**, *113*, 4862–4904.
- ¹¹ Katritzky, A. R. *Comprehensive Heterocyclic Chemistry III*, Elsevier, Amsterdam, New York, 1st Ed., **2008**.
- ¹² Andna, L.; Miesch, L. *Org. Lett.* **2018**, *20*, 3430–3433.
- ¹³ Andna, L.; Miesch, L. *Org. Biomol. Chem.* **2019**, *17*, 5688–5692.
- ¹⁴ Gharpure, S. J.; Prasath, V.; Kumar, V. *Chem. Commun.* **2015**, *51*, 13623–13626.
- ¹⁵ a). Suarez, A.; Fu, G. C. *Angew. Chem. Int. Ed.* **2004**, *43*, 3580–3582. b). Heinrich, C. F.; Miesch, M.; Miesch, L. *Org. Biomol. Chem.*, **2015**, *13*, 2153–2156.
- ¹⁶ Hsung, R. P.; Li, H. *Org. Lett.* **2009**, *11*, 4462–4465.
- ¹⁷ Lancou, A.; Haroun, H.; Kundu, U. K.; Legros, F.; Zimmermann, N.; Mathé-Allainmat, M.; Lebreton, J.; Dujardin, G.; Galon-Nourry, C.; Gosselin, P. *Tetrahedron*, **2012**, *68*, 9652–9657.

VI. EXPERIMENTAL PART

GENERAL REMARKS

Reagents and solvents

When dry reaction conditions were needed the reactions were performed in flamed glassware under an Argon atmosphere. Commercial reagents and solvents were distilled, wherever possible, prior to use:

- dichloromethane, tetrahydrofuran and diethyl ether were purified using a Dry Solvent Station GT S100.
- toluene was distilled at atmospheric pressure and stored on molecular sieve (4 Å).
- *N,N*-dimethylformamide was dried with Na₂SO₄ overnight and then distilled under reduced pressure (63 °C, 40 mbar) and stored on molecular sieves (4 Å) away from light.
- acetonitrile, acetone, ethanol and methanol were used on its own (solvents available from Sigma Aldrich, purity ≥ 99.9%).
- triethylamine was distilled and stored on KOH pellets.

Commercially available *n*-butyllithium was indicated to be 1.6 M solution in hexanes and dosed with before use with diphenylacetic acid in dried tetrahydrofuran. Commercially available TBAF (1 M in THF) and Triton B (40 wt. % in H₂O) were purchased from Sigma-Aldrich and used as received.

Chromatography

Thin layer chromatography (TLC) was performed using TLC Silica gel 60 F₂₅₄ aluminum plates. These ones were read under UV light and revealed either by sulfuric vanillin, by ninhydrin, by a KMnO₄ solution, or by a mixture of phosphomolybdic acid-cerium sulfate; followed by a heating using a heat gun. Merck Geduran® 40-63 µm silica gel was used for column chromatography. The deactivation of silica by triethylamine was performed as follows: silica was first conditioned with 1% of triethylamine in petroleum ether and the column was conditioned as usually. Five drops of triethylamine were added for 100 mL of eluent.

Nuclear Magnetic Resonance (NMR)

NMR spectra were recorded by the "Service Commun de RMN" of the "Institut de Chimie de Strasbourg" using a Bruker AV-300 or AV-400 or AV-500 spectrometer with the solvent residual peak as internal standard. Splitting patterns were reported as s, singlet; d, doublet; t, triplet; q, quartet; qu, quintet; sex, sextet; m, multiplet and br, broad singlet.

Infrared spectroscopy

Infrared spectra were recorded on a Bruker Alpha spectrophotometer and reported in frequency of absorption.

Melting Point

Melting points were recorded with a SMP3 Stuart Scientific microscope in open capillary tubes and are uncorrected.

High resolution mass spectrometry (HRMS)

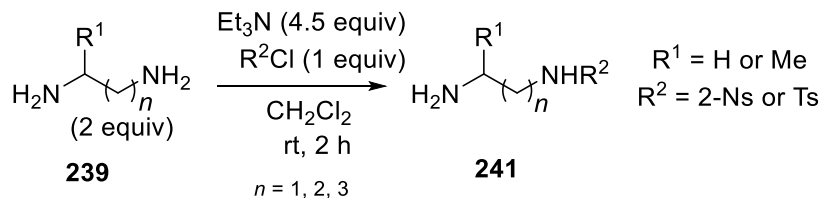
High resolution mass spectrometry (HRMS) data were recorded by the "Service Commun de Spectrométrie de Masse" of the "Institut de Chimie de Strasbourg" on a microTOF spectrometer equipped with an orthogonal electrospray (ESI) interface.

X-Ray Diffraction measurement

X-ray structures were recorded by the "Service Commun de rayons X" of the "Institut de Chimie de Strasbourg" using a KappaCCD diffractometer. The structure was solved and refined using the Bruker SHELXTL Software Package.

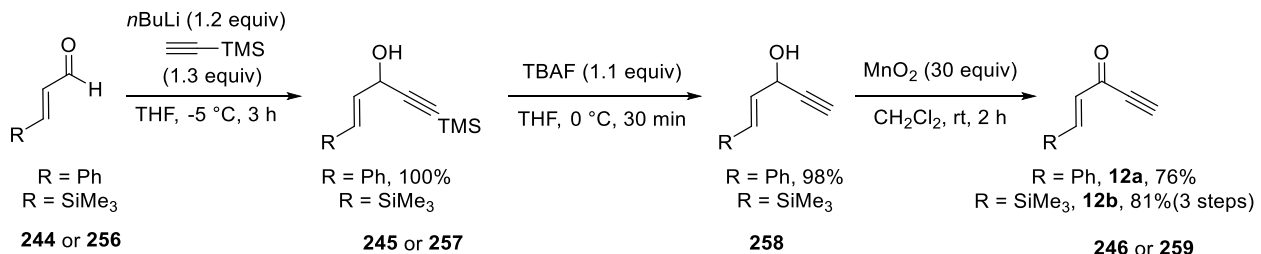
Chapter 1

1. Experimental procedure for **241**

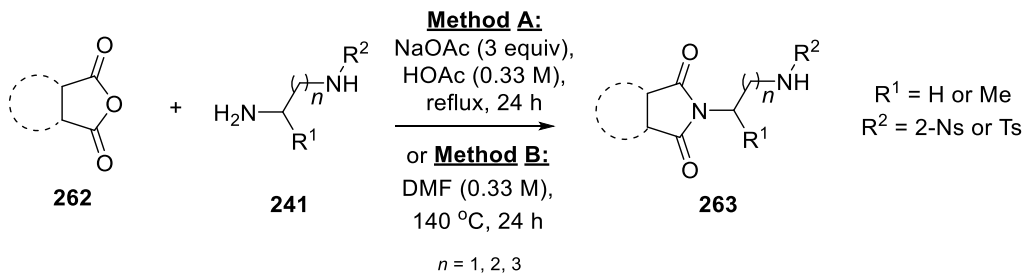


The diamine (30 mmol, 2 equiv) was dissolved in DCM (1.33 M). NEt₃ (67.5 mmol, 4.5 equiv) was added, then R₂Cl (15 mmol, 1 equiv) in DCM (0.66 M) was added dropwise over 2 h. Reaction was monitored by TLC and once judge completed by the full consumption of R₂Cl, the mixture was diluted with aqueous HCl (10 wt%, 20 mL). The organic layer was washed twice with aqueous HCl (10 wt%, 50 mL). The aqueous layers were combined then basified with NaOH 2 M (final pH = 11) and extracted with DCM (3 x 30 mL). The organic layers were combined, dried (Na₂SO₄), filtered and concentrated under reduce pressure (15 mbar, 25 °C). Isolated products were in most cases analytically pure and therefore used without further purification.

2. Experimental procedure for the synthesis of *E*-enye-one:¹⁶⁷



3. Experimental procedure for **263**:



263 were prepared according to the literature without modifications.¹⁶⁸

¹⁶⁷ a) Beltran, F.; Fabre, I.; Ciofini, I.; Miesch, L. *Org. Lett.*, **2017**, *19*, 5042. (and references in the supporting information therein), b) Shen, Y.; Cai, S.; He, C.; Lin, X.; Lu, P.; Wang, Y. *Tetrahedron*, **2011**, *67*, 8338.

¹⁶⁸ Maity, A. K.; Roy, S. *Adv. Synth. Catal.* **2014**, *356*, 2627.

Method A:

A mixture of **241** (5 mmol, 1 equiv), sodium acetate (15 mmol, 3 equiv) and appropriate anhydride (5 mmol, 1 equiv) were taken in glacial acetic acid (0.33 M) and refluxed with an oil bath for 24 h. The mixture was cooled to rt and evaporated to dryness under vacuum. The corresponding residue was diluted with sat. NaHCO_3 (20 mL) and extracted with EtOAc (3 x 25 mL). The combined organic extracts were dried (Na_2SO_4), concentrated under reduce pressure (15 mbar, 25 °C) and purified by column chromatography on silica gel using a mixture of petroleum ether/ EtOAc , $\text{CH}_2\text{Cl}_2/\text{MeOH}$ or $\text{CH}_2\text{Cl}_2/\text{acetone}$ as eluent to afford the desired product **263**.

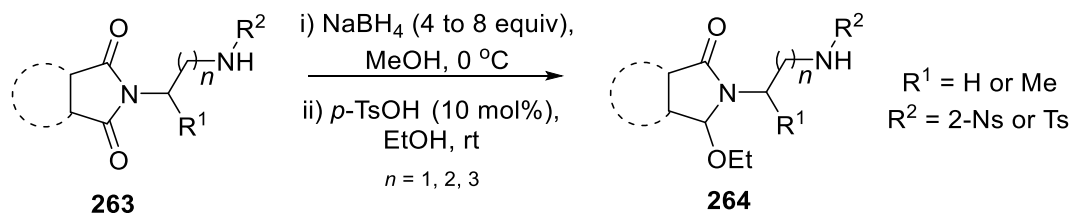
Method B:

A mixture of **241** (5 mmol, 1 equiv), sodium acetate (15 mmol, 3 equiv) and appropriate anhydride (5 mmol, 1 equiv) were taken in DMF (0.33 M) and refluxed with an oil bath for 24 h. The mixture was cooled to rt and evaporated to dryness under vacuum. The corresponding residue was diluted with water (20 mL) and extracted with EtOAc (3 x 25 mL). The combined organic extracts were dried (Na_2SO_4), concentrated under reduce pressure (15 mbar, 25 °C) and purified by column chromatography on silica gel using a mixture of petroleum ether/ EtOAc , $\text{CH}_2\text{Cl}_2/\text{MeOH}$ or $\text{CH}_2\text{Cl}_2/\text{acetone}$ as eluent to afford the desired product **263**.

Compound 263a : *N*-(2-(1,3-dioxo-1,3,3a,4,7,7a-hexahydro-2*H*-isoindol-2-yl)ethyl)-4-methylbenzene sulfonamide

Detailed procedure for 263a: A mixture of **241a** (5 mmol, 3.21 g, 1 equiv), sodium acetate (15 mmol, 1.23 g, 3 equiv) and 3a,4,7,7a-tetrahydroisobenzofuran-1,3-dione (5 mmol, 760.7 mg, 1 equiv) were taken in DMF (0.33 M, 15 mL) and refluxed for 24 h. The mixture was cooled to rt and evaporated to dryness under vacuum. The corresponding residue was diluted with water (20 mL) and extracted with EtOAc (3 x 25 mL). The combined organic extracts were dried (Na_2SO_4), concentrated under reduce pressure (15 mbar, 25 °C) and purified by column chromatography on silica gel using a mixture of $\text{CH}_2\text{Cl}_2/\text{acetone}$ as eluent to afford the desired product **263a** as a white solid (80%, 3.99 mmol, 1.39 g).

4. Experimental procedure for **264a -264o**:



4a-o were prepared according to the literature without modifications.

General procedure:¹⁶⁹ To a solution of **263** (1 mmol, 1 equiv) in $\text{MeOH}/\text{CH}_2\text{Cl}_2$ (1:1, v/v, 0.1 M) at 0 °C was added NaBH_4 (4 mmol, 4 equiv). Reaction was monitored by TLC and every 2 hours 4 equivalents of NaBH_4 were added until reaction completion (up to 8 equiv). After completion, the mixture was concentrated under reduce pressure (15 mbar, 25 °C) and retaken with sat. NaHCO_3 (10 mL). The aqueous layer was extracted with EtOAc (3 x 10 mL). The combined organic extracts were

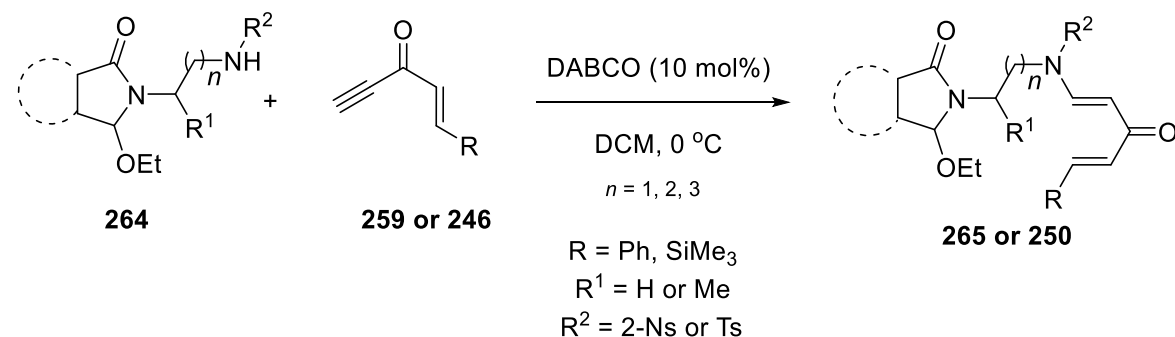
¹⁶⁹ a) Koseki, Y.; Fujino, K.; Takeshita, A.; Sato, H.; Nagasaka, T. *Tetrahedron: Asymmetry*. **2007**, *18*, 1533. b) Abdel, M. S.; Kim, M. R.; El-Gamal, M. I.; Gamal El-Din, M. M.; Tae, J. H.; Choi, S.; Lee, K. T.; Yoo, K. H.; Oh, C. H. *Eur. J. Med. Chem.* **2015**, *95*, 453.

dried (Na_2SO_4), concentrated under reduce pressure (15 mbar, 25 °C). The remaining crude residue was then dissolved in ethanol (0.3 M) and *p*-TsOH (0.1 mmol, 0.1 equiv) was added at room temperature. After completion, the mixture was concentrated under reduce pressure (15 mbar, 25 °C) and retaken with sat. NaHCO_3 (10 mL). The aqueous layer was extracted with EtOAc (3 x 10 mL). The combined organic extracts were dried (Na_2SO_4), purified by column chromatography on silica gel using a mixture of CH_2Cl_2 /acetone as eluent to afford the desired product **264**.

Compound 264c: *N*-(2-(1-ethoxy-3-oxo-1,3,3a,4,7,7a-hexahydro-2*H*-isoindol-2-yl)ethyl)-4-methylbenzenesulfonamide

Detailed procedure for 264c: To a solution of **264c** (1 mmol, 348.4 mg, 1 equiv) in $\text{MeOH}/\text{CH}_2\text{Cl}_2$ (1:1, *v/v*, 0.1 M) at 0 °C was added NaBH_4 (4 mmol, 151, 32 mg, 4 equiv). Reaction was monitored by TLC and after 2 hours 4 equivalents (4 mmol, 151, 32 mg) of NaBH_4 were added. After 2 more hours, the mixture was concentrated under reduce pressure (15 mbar, 25 °C) and retaken with sat. NaHCO_3 (10 mL). The aqueous layer was extracted with EtOAc (3 x 10 mL). The combined organic extracts were dried (Na_2SO_4), concentrated under reduce pressure (15 mbar, 25 °C). The remaining crude residue was then dissolved in ethanol (0.3 M) and *p*-TsOH (0.1 mmol, 19 mg, 0.1 equiv) was added at room temperature. After completion, the mixture was concentrated under reduce pressure (15 mbar, 25 °C) and retaken with sat. NaHCO_3 (10 mL). The aqueous layer was extracted with EtOAc (3 x 10 mL). The combined organic extracts were dried (Na_2SO_4), purified by column chromatography on silica gel using a mixture of CH_2Cl_2 /acetone as eluent to afford the desired product **264c** as a white solid (65%, 0.65 mmol, 246.0 mg).

5. Experimental procedure for **265** and **250**



General procedure:¹⁷⁰ To a solution of **264** (0.4 mmol, 1 equiv) in dry CH_2Cl_2 (0.04 M) at 0 °C were added DABCO (0.04 mmol, 0.1 equiv) and then dropwise **246** or **259** (0.44 mmol, 1.1 equiv). After 30 minutes at 0 °C, the reaction mixture was quenched with brine and the aqueous layer was extracted with CH_2Cl_2 (15 mL). The combined organic extracts were dried (Na_2SO_4), concentrated under reduce pressure (15 mbar, 25 °C) and purified by column chromatography on silica gel using a mixture of CH_2Cl_2 /acetone as eluent to afford the desired product **250**.

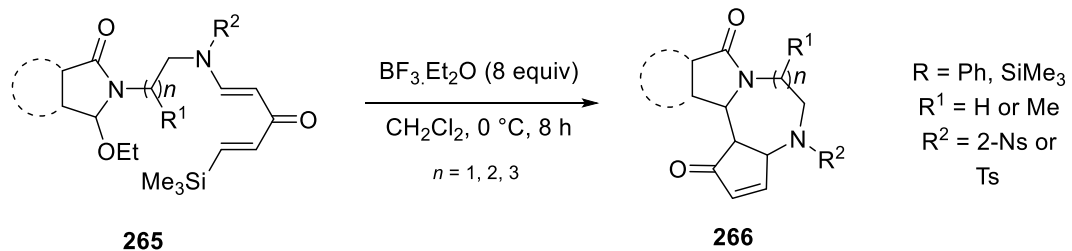
Compound 265c: *N*-(2-(1-ethoxy-3-oxo-1,3,3a,4,7,7a-hexahydro-2*H*-isoindol-2-yl)ethyl)-4-methyl-*N*-(1*E*,4*E*)-3-oxo-5-phenylpenta-1,4-dien-1-yl)benzenesulfonamide

Detailed procedure for 265c, performed on larger scale (1 mmol): To a solution of **264c** (1 mmol, 378.49 mg, 1 equiv) in dry CH_2Cl_2 (0.04 M, 2.5 mL) at 0 °C were added DABCO (0.1 mmol, 11.27 mg, 0.1 equiv) and then dropwise **259** (1.1 mmol, 171.8 mg, 1.1 equiv). After 30 minutes at 0 °C, the

¹⁷⁰ Ghpure, S. J.; Prasath, V.; Kumar, V. *Chem. Commun.* **2015**, 51, 13623.

reaction mixture was quenched with brine and the aqueous layer was extracted with CH_2Cl_2 (30 mL). The combined organic extracts were dried (Na_2SO_4), concentrated under reduced pressure (15 mbar, 25 °C) and purified by column chromatography on silica gel using a mixture of CH_2Cl_2 /acetone as eluent to afford the desired product **265c** as a colorless oil (95%, 0.95 mmol, 507.5 mg).

6. Experimental procedure for **266**



General procedure: To a solution of **265** (0.2 mmol, 1 equiv) was dissolved in dry CH_2Cl_2 (0.04 M), dropwise $\text{BF}_3\cdot\text{Et}_2\text{O}$ (8 equiv) at 0 °C and stirred for 8 h, reaction was monitored by TLC. Added sat. NaHCO_3 , the aqueous layer was extracted with CH_2Cl_2 (1 x 15 mL). The combined organic extracts were dried (Na_2SO_4), concentrated under reduced pressure (15 mbar, 25 °C) and purified by column chromatography on silica gel using a mixture of petroleum CH_2Cl_2 /acetone as eluent to afford the desired product **266**.

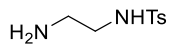
Compound 266c: 4-tosyl-3a,4,5,6,8a,9,12,12a-octahydrocyclopenta[5,6][1,4]diazepino[7,1-a]isoindole-1,8(12bH,12cH)-dione

Detailed procedure for **266c, performed on larger scale (1 mmol):** To a solution of **265c** (1 mmol, 530.23 mg, 1 equiv) was dissolved in dry CH_2Cl_2 (0.04 M, 25 mL), dropwise $\text{BF}_3\cdot\text{Et}_2\text{O}$ (8 mmol, 1.13 g, 8 equiv) at 0 °C and stirred for 8 h, reaction was monitored by TLC. A saturated solution of NaHCO_3 was added and the aqueous layer was extracted with CH_2Cl_2 (1 x 50 mL). The combined organic extracts were dried (Na_2SO_4), concentrated under reduced pressure (15 mbar, 25 °C) and purified by column chromatography on silica gel using a mixture of petroleum CH_2Cl_2 /acetone as eluent to afford the desired product **266c** as a white solid (85%, 0.85 mmol, 350.3 mg).

Characterization data

1. Characterization data for 241a-241e

Compound 241a : *N*-(2-aminoethyl)-4-methylbenzenesulfonamide

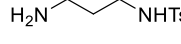
	C ₉ H ₁₄ N ₂ O ₂ S
	MW : 214.28 g.mol ⁻¹
	White solid
	81% (2.60 g, 12.15 mmol)

Characterization data match those of the literature.¹⁷¹

¹H NMR (500 MHz, CDCl₃): δ = 7.68 (d, , J = 8.2 Hz, 2H), 7.23 (d, J = 8.2 Hz, 2H), 3.09 (br, 3H), 2.89 (t, J = 5.6 Hz, 2H), 2.73 (t, J = 5.6 Hz, 2H), 2.34 (s, 3H) ppm.

R_f: 0.17 (CH₂Cl₂/MeOH, 90:10 v/v, UV, ninhydrin stain)

Compound 241b : *N*-(3-aminopropyl)-4-methylbenzenesulfonamide

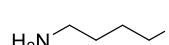
	C ₁₀ H ₁₆ N ₂ O ₂ S
	MW : 228.31 g.mol ⁻¹
	White solid
	81% (2.77 g, 12.15 mmol)

Characterization data match those of the literature.¹⁷¹

¹H NMR (500 MHz, CDCl₃): δ = 7.74 (d, J = 8.2 Hz, 2H), 7.29 (d, J = 8.2 Hz, 2H), 3.04 (t, J = 6.2 Hz, 2H), 2.77 (t, J = 6.2 Hz, 2H), 2.41 (s, 3H), 1.57 (m, 2H) ppm.

R_f: 0.10 (CH₂Cl₂/MeOH 90:10 v/v, UV, ninhydrin stain)

Compound 241c : *N*-(4-aminobutyl)-4-methylbenzenesulfonamide

	C ₁₁ H ₁₈ N ₂ O ₂ S
	MW : 242.34 g.mol ⁻¹
	White solid
	60% (2.18 g, 9 mmol)

Characterization data match those of the literature.¹⁷²

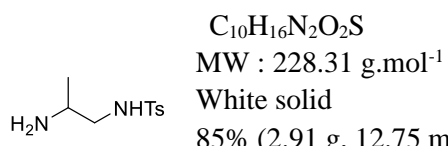
¹H NMR (500 MHz, CDCl₃): δ = 7.73 (d, J = 8.2 Hz, 2H), 7.28 (d, J = 8.2 Hz, 2H), 2.89 (t, J = 6.6 Hz, 2H), 2.65 (t, J = 6.6 Hz, 2H), 2.40 (s, 3H), 1.56 – 1.48 (m, 2H), 1.46 - 1.39 (m, 2H) ppm.

R_f: 0.25 (CH₂Cl₂/MeOH 90:10 v/v, UV, ninhydrin stain)

¹⁷¹ Abdel-Maksoud, M. S.; Kim, M.-I.; El-Gamal, M.; Gamal El-Din, M. M.; Tae, J.; Choi; H. S.; Lee, K-T.; Yoo, K. H.; Oh, C-H. *Eur. J. Med. Chem.* **2015**, 95, 453.

¹⁷² Khanjin, N. A.; Hesse, M. *Helv. Chim. Acta*. **2003**, 86, 2028.

Compound 241d : *N*-(2-aminopropyl)-4-methylbenzenesulfonamide

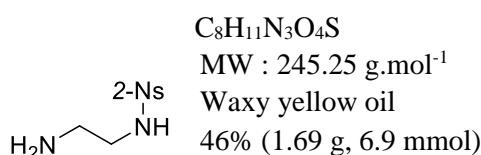


Characterization data match those of the literature.¹⁷³

¹H NMR (500 MHz, CDCl₃): δ = 7.75 (d, *J* = 8.2 Hz, 2H), 7.32 (d, *J* = 8.2 Hz, 2H), 3.00 – 2.93 (m, 2H), 2.72 – 2.51 (m, 1H), 2.44 (s, 3H), 1.04 – 1.01 (m, 3H) ppm.

R_f: 0.34 (CH₂Cl₂/MeOH 90:10 *v/v*, UV, ninhydrin stain)

Compound 241e : *N*-(2-aminoethyl)-2-nitrobenzenesulfonamide



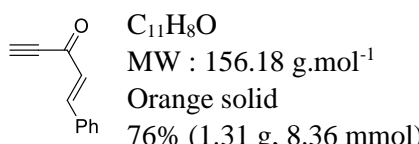
Characterization data match those of the literature.¹⁷⁴

¹H NMR (500 MHz, CDCl₃): δ = 8.12 – 8.10 (m, 1H), 7.84 – 7.82 (m, 1H), 7.74 – 7.72 (m, 2H), 3.13 – 3.10 (m, 2H), 2.94 (s, 3H), 2.86 – 2.83 (m, 2H) ppm.

R_f: 0.16 (CH₂Cl₂/MeOH, 90:10 *v/v*, UV, ninhydrin stain)

2. Characterization data for 246 and 259

Compound 246 : (*E*)-1-phenylpent-1-en-4-yn-3-one



The reaction was performed on 11 mmol scale. Characterization data match those of the literature.^{6b}

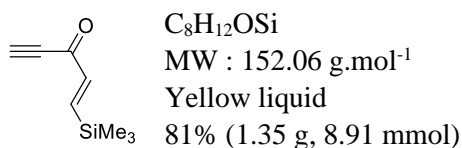
¹H NMR (300 MHz, CDCl₃): δ = 7.89 (d, *J* = 16.1 Hz, 1H), 7.62 – 7.55 (m, 2H), 7.47 – 7.39 (m, 3H), 6.81 (d, *J* = 16.1 Hz, 1H,), 3.32 (s, 1H) ppm.

R_f: 0.60 (CH₂Cl₂, UV)

¹⁷³ St John-Campbell, S.; White, A. J. P.; Bull, J. A. *Chem. Sci.* **2017**, 8, 4840.

¹⁷⁴ Stress, C. J.; Sauter, B.; Schneider, L. A.; Sharpe, T.; Gillingham, D. *Angew. Chem. Int. Ed.* **2019**, 58, 9570.

Compound 259 : (*E*)-1-(trimethylsilyl)pent-1-en-4-yn-3-one



¹H NMR (500 MHz, CDCl₃): δ = 7.52 (d, *J* = 19.0 Hz, 1H), 6.53 (d, *J* = 19.0 Hz, 1H), 3.29 (s, 1H), 0.18 (s, 9H) ppm.

¹³C NMR (125 MHz, CDCl₃): δ = 178.3, 155.6, 142.9, 80.4, 79.7, -1.8 (×3) ppm.

HRMS (ESI-TOF) m/z: [M+H]⁺ calcd for C₈H₁₃OSi 153.0736; Found 153.0751.

IR (neat): ν = 3251, 2958, 2873, 2094, 1647, 1248, 1169 cm⁻¹

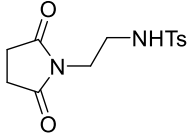
R_f: 0.75 (CH₂Cl₂, UV)

3. Characterization data for **263a – 263o**

Compound 263a : *N*-(2-(2,5-dioxopyrrolidin-1-yl)ethyl)-4-methylbenzenesulfonamide

C₁₃H₁₆N₂O₄S

MW : 296.34 g.mol⁻¹



White solid

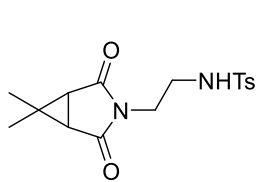
mp = 133 - 134 °C

73% (1.08 g, 3.65 mmol)

Characterization data match those of the literature.¹⁷⁵

¹H NMR (CDCl₃, 300 MHz): δ = 7.70 (d, 2 H, *J* = 8.2 Hz), 7.30 (d, 2 H, *J* = 8.2 Hz), 5.05 (t, 1H, *J* = 6.2 Hz, NH), 3.62 (t, 2 H, *J* = 5.7 Hz), 3.19 (dt, 2 H, *J* = 6.2 Hz, 5.7 Hz), 2.68 (s, 4 H), 2.42 (s, 3 H) ppm.

Compound 263b : *N*-(2-(6,6-dimethyl-2,4-dioxo-3-azabicyclo[3.1.0]hexan-3-yl)ethyl)-4-methylbenzenesulfonamide



C₁₆H₂₀N₂O₄S

MW: 336.41 g.mol⁻¹

White solid

mp = 152 – 154 °C

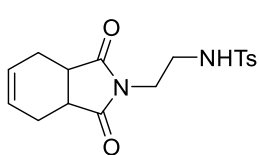
86% (1.45 g, 4.32 mmol)

263b was prepared according to method A, using **241a** and the appropriate anhydride. Characterization data match those of the literature.⁸

¹H NMR (500 MHz, CDCl₃): δ = 7.69 (d, *J* = 8.3 Hz, 2H), 7.27 (d, *J* = 8.3 Hz, 2H), 5.34 (t, *J* = 5.8 Hz, 1H), 3.46 (t, *J* = 5.8 Hz, 2H), 3.09 (dt, *J* = 5.8, 5.8 Hz, 2H), 2.38 (s, 3H), 2.28 (s, 2H), 1.20 (s, 3H), 1.14 (s, 3H) ppm.

Rf : 0.39 (Petroleum ether/EtOAc 50:50 v/v, UV, vanillin stain)

Compound 263c : *N*-(2-(1,3-dioxo-1,3,3a,4,7,7a-hexahydro-2*H*-isoindol-2-yl)ethyl)-4-methylbenzenesulfonamide



C₁₇H₂₀N₂O₄S

MW : 348.42 g.mol⁻¹

White solid

mp = 138 – 139 °C

80% (1.39 g, 3.99 mmol)

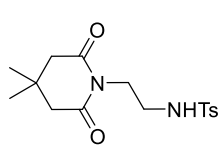
Characterization data match those of the literature.¹⁷⁶

¹H NMR (500 MHz, CDCl₃): δ = 7.69 (d, *J* = 8.1 Hz, 2H), 7.28 (d, *J* = 8.1 Hz, 2H), 5.86 (t, *J* = 3.0 Hz, 2H), 5.33 (t, *J* = 6.3 Hz, 1H), 3.57 (dt, *J* = 5.8, 3.0 Hz, 2H), 3.13 – 3.05 (m, 4H), 2.58 – 2.50 (m, 2H), 2.40 (s, 3H), 2.25 – 2.17 (m, 2H) ppm.

Rf : 0.55 (Petroleum ether/EtOAc 50:50 v/v, UV, ninhydrin stain)

¹⁷⁵ Andna, L.; Miesch, L. *Org. Lett.* **2018**, 20, 3430.

Compound 263d : *N*-(2-(4,4-dimethyl-2,6-dioxopiperidin-1-yl)ethyl)-4-methylbenzenesulfonamide



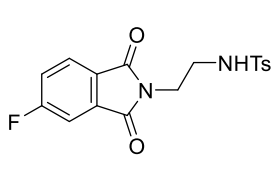
C₁₆H₂₂N₂O₄S
MW : 338.42 g.mol⁻¹
White solid
mp = 135 – 136 °C
60% (1.02 g, 3.02 mmol)

263d was prepared according to method A, using **241a** and the appropriate anhydride. Characterization data match those of the literature.⁸

¹H NMR (CDCl₃, 500 MHz): δ = 7.70 (d, *J* = 8.1 Hz, 2H), 7.29 (d, *J* = 8.1 Hz, 2H), 4.87 (t, *J* = 6.0 Hz, 1H), 3.90 (t, *J* = 5.9 Hz, 2H), 3.15 (dt, *J* = 6.0, 5.9 Hz, 2H), 2.47 (s, 4H), 2.41 (s, 3H), 1.05 (s, 6H) ppm.

R_f: 0.45 (Petroleum ether/EtOAc 50:50 *v/v*, UV, ninhydrin stain)

Compound 263e : *N*-(2-(5-fluoro-1,3-dioxoisindolin-2-yl)ethyl)-4-methylbenzenesulfonamide



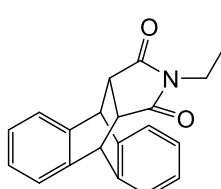
C₁₇H₁₅FN₂O₄S
MW: 362.38 g.mol⁻¹
White solid
mp = 143 – 144 °C
91% (1.65 g, 4.55 mmol)

263e was prepared according to method A, using **241a** and the appropriate anhydride. Characterization data match those of the literature.⁸

¹H NMR (500 MHz, CDCl₃): δ = 7.77 (dd, *J* = 8.2, 4.3 Hz 1H), 7.63 (d, *J* = 8.2 Hz, 2H), 7.42 (dd, *J* = 7.1, 2.2 Hz, 1H), 7.35 (td, *J* = 8.2, 2.2 Hz, 1H), 7.13 (d, *J* = 8.2 Hz, 2H), 5.32 (t, *J* = 6.2 Hz, 1H), 3.76 (t, *J* = 5.6 Hz, 2H), 3.29 (dt, *J* = 6.2 Hz, 5.6 Hz, 2H), 2.29 (s, 3H) ppm.

R_f: 0.65 (CH₂Cl₂/MeOH 90:10 *v/v*, UV, ninhydrin stain)

Compound 263f: *N*-(2-((9R,10S,11R,15S)-12,14-dioxo-9,10-dihydro-9,10-[3,4]epipyrroloanthracen-13-yl)ethyl)-4-methylbenzenesulfonamide



C₂₇H₂₄N₂O₄S
MW : 472.15 g.mol⁻¹
White solid
mp = 172 – 174 °C
75% (1.77 g, 3.75 mmol)

263f was prepared according to method B, using **241a** and the appropriate anhydride.

¹H NMR (500 MHz, CDCl₃): δ = 7.68 (d, *J* = 8.3 Hz, 2H), 7.37 (dd, *J* = 5.3, 3.3 Hz, 2H), 7.32 (d, *J* = 8.3 Hz, 2H), 7.26 (d, *J* = 2.8 Hz, 1H), 7.25 (d, *J* = 3.3 Hz, 1H), 7.18 (dd, *J* = 5.3, 3.2 Hz, 2H), 7.08 (dd, *J* = 5.4, 3.2 Hz, 2H), 4.77 (s, 2H), 4.03 (t, *J* = 6.4 Hz, 1H), 3.21 – 3.10 (m, 4H), 2.53 (dd, *J* = 11.6, 6.4 Hz, 2H), 2.43 (s, 3H) ppm.

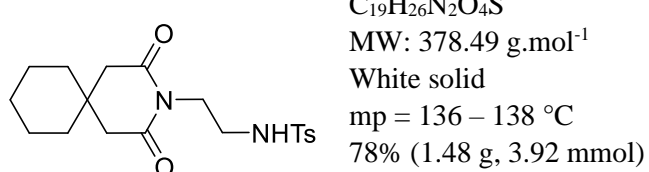
¹³C NMR (125 MHz, CDCl₃): δ = 177.0 (×2), 143.6, 141.2 (×2), 139.0 (×2), 137.3, 129.8 (×2), 127.3 (×2), 127.2 (×2), 127.0 (×2), 125.2 (×2), 124.4 (×2), 46.9 (×2), 45.6 (×2), 40.8, 38.6, 21.7 ppm.

HRMS (ESI-TOF) m/z: [M+Na]⁺ calcd for C₂₇H₂₄N₂O₄SNa 495.1350; Found 495.1338.

IR (neat): $\nu = 3214, 1691, 1332, 1158 \text{ cm}^{-1}$

R_f: 0.45 (CH₂Cl₂/MeOH 90:10 v/v, UV, ninhydrin stain)

Compound 263g : *N*-(2-(2,4-dioxo-3-azaspiro[5.5]undecan-3-yl)ethyl)-4-methylbenzenesulfonamide

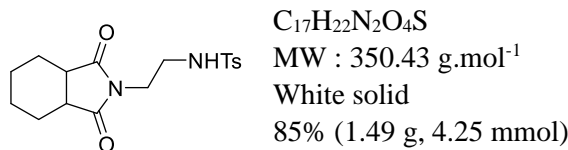


263g was prepared according to method A, using **241a** and the appropriate anhydride. Characterization data match those of the literature.⁸

¹H NMR (CDCl₃, 500 MHz): $\delta = 7.70$ (d, $J = 8.1$ Hz, 2H), 7.29 (d, $J = 8.1$ Hz, 2H), 4.86 (t, $J = 5.9$ Hz, 1H), 3.88 (t, $J = 5.9$ Hz, 2H), 3.15 (dt, $J = 5.9, 5.9$ Hz, 2H), 2.51 (s, 4H), 2.41 (s, 3H), 1.50 – 1.39 (m, 6H), 1.38 – 1.33 (m, 4H) ppm.

R_f: 0.51 (Petroleum ether/EtOAc 50:50 v/v, UV, ninhydrin stain)

Compound 263h : *N*-(2-(1,3-dioxooctahydro-2H-isoindol-2-yl)ethyl)-4-methylbenzenesulfonamide

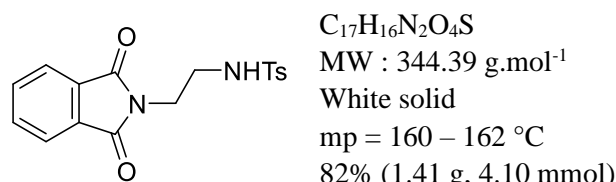


263h was prepared according to method A, using **241a** and the appropriate anhydride. Characterization data match those of the literature.⁷

¹H NMR (500 MHz, CDCl₃): $\delta = 7.71$ (d, $J = 7.9$ Hz, 2H), 7.31 – 7.24 (m, 2H), 5.03 (br, 1H), 3.60 (t, $J=5.8$ Hz, 2H), 3.16 (dd, $J=5.8, 10.8$ Hz, 2H), 2.81–2.86 (m, 2H), 2.41 (s, 3H), 1.73–1.86 (m, 4H), 1.42–1.45 (m, 4H) ppm.

R_f: 0.40 (CH₂Cl₂/acetone 90:10 v/v, UV)

Compound 263i : *N*-(2-(1,3-dioxoisindolin-2-yl)ethyl)-4-methylbenzenesulfonamide

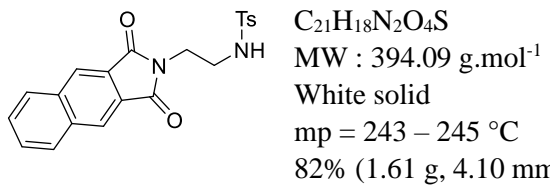


263i was prepared according to method A, using **241a** and the appropriate anhydride. Characterization data match those of the literature.⁷

¹H NMR (500 MHz, DMSO-d₆): $\delta = 7.83 – 7.77$ (m, 4H) 7.58 (d, $J = 8.2$ Hz, 2H), 7.29 (d, $J = 8.2$ Hz, 2H), 3.59 (dt, $J = 6.2, 5.7$ Hz, 2H), 3.00 (m, 2H), 2.30 (s, 3H) ppm.

R_f: 0.72 (CH₂Cl₂/MeOH 90:10 v/v, UV, ninhydrin stain)

Compound 263j : *N*-(2-(1,3-dioxo-1,3-dihydro-2H-benzo[f]isoindol-2-yl)ethyl)-4-methylbenzenesulfonamide



263j was prepared according to method B, using **241a** and the appropriate anhydride.

¹H NMR (500 MHz, CDCl₃): δ = 8.26 (s, 2H), 8.07 (dd, J = 6.1, 3.3 Hz, 2H), 7.73 (dd, J = 6.1, 3.3 Hz, 2H), 7.62 (d, J = 8.2 Hz, 2H), 6.97 (d, J = 8.2 Hz, 2H), 4.98 (t, J = 5.6 Hz, 1H), 3.87 – 3.77 (m, 2H), 3.39 (dd, J = 11.3, 5.6 Hz, 2H), 1.98 (s, 3H) ppm.

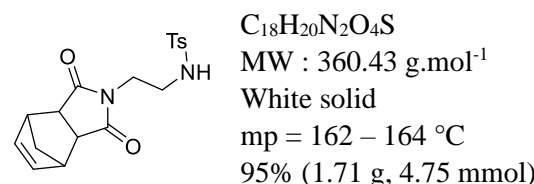
¹³C NMR (125 MHz, CDCl₃): δ = 168.0 ($\times 2$), 143.1, 136.9, 135.4 ($\times 2$), 130.3 ($\times 2$), 129.5 ($\times 2$), 129.5 ($\times 2$), 127.3 ($\times 2$), 126.8 ($\times 2$), 124.9 ($\times 2$), 42.4, 37.4, 21.1 ppm.

HRMS (ESI-TOF) m/z: [M+H]⁺ calcd for C₂₁H₁₉N₂O₄S 395.1060; Found 395.1060.

IR (neat): ν = 3225, 1693, 1333, 1148 cm⁻¹

R_f: 0.50 (CH₂Cl₂/acetone 90:10 v/v, UV)

Compound 263k : *N*-(2-(1,3-dioxo-1,3,3a,4,7,7a-hexahydro-2H-4,7-methanoisoindol-2-yl)ethyl)-4-methylbenzenesulfonamide



263k was prepared according to method A, using **241a** and the appropriate anhydride.

¹H NMR (500 MHz, CDCl₃): δ = 7.68 (d, J = 8.1 Hz, 2H), 7.29 – 7.25 (m, 2H), 6.25 (s, 2H), 5.39 (d, J = 6.1 Hz, 1H), 3.62 – 3.48 (m, 2H), 3.22 (s, 2H), 3.13 (dd, J = 11.4, 5.8 Hz, 2H), 2.65 (s, 2H), 2.38 (s, 3H), 1.46 (d, J = 9.9 Hz, 1H), 1.23 (d, J = 9.9 Hz, 1H) ppm.

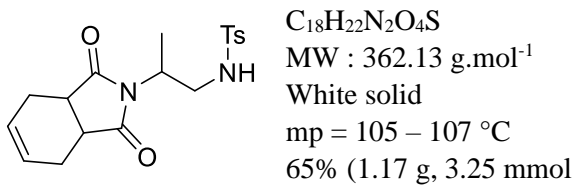
¹³C NMR (125 MHz, CDCl₃): δ = 178.4 ($\times 2$), 143.5, 137.8 ($\times 2$), 136.7, 129.8 ($\times 2$), 127.1 ($\times 2$), 48.0 ($\times 2$), 45.1 ($\times 2$), 42.9, 41.3, 37.8, 21.5 ppm.

HRMS (ESI-TOF) m/z: [M+Na]⁺ calcd for C₁₈H₂₀N₂O₄SnA 383.1036; Found 383.1028.

IR (neat): ν = 3157, 1684, 1373, 1159 cm⁻¹

R_f: 0.42 (CH₂Cl₂/acetone 90:10 v/v, UV)

Compound 263m : *N*-(2-(1,3-dioxo-1,3,3a,4,7,7a-hexahydro-2H-isoindol-2-yl)propyl)-methylbenzenesulfonamide



263m was prepared according to method A, using **241d** and the appropriate anhydride.

¹H NMR (500 MHz, CDCl₃): δ = 7.76 – 7.66 (m, 2H), 7.29 (dd, J = 10.3, 5.8 Hz, 2H), 5.93 – 5.84 (m, 2H), 5.46 – 5.26 (m, 1H), 4.27 and 3.63 – 3.47 (m and m, 2H), 3.31 and 3.10 – 2.98 (dd and m, J = 13.4, 3.6 Hz, 3H), 2.63 – 2.49 (m, 2H), 2.42 (d, J = 3.7 Hz, 3H), 2.29 – 2.14 (m, 2H), 1.25 and 0.99 (d, J = 7.0 Hz and J = 6.5 Hz, 3H) ppm.

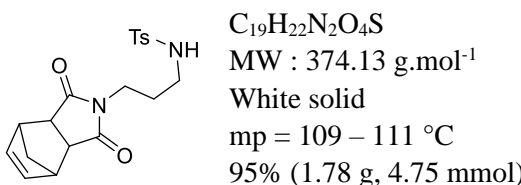
¹³C NMR (125 MHz, CDCl₃): δ = (181.0 and 180.8), (180.7 and 180.6), (143.5 and 143.3), (138.0 and 137.0), 129.8, 129.7, (127.9 and 127.9), 127.9, 127.1, 127.0, (48.2 and 47.8), (44.7 and 43.9), (39.3, and 39.0), (39.1 and 38.9), (23.7, and 23.7), 23.4, (21.6 and 21.6), (19.1 and 15.2) ppm.

HRMS (ESI-TOF) m/z: [M+K]⁺ calcd for C₁₈H₂₂N₂O₄SK 401.0932; Found 401.0917.

IR (neat): ν = 3272, 1686, 1329, 1157 cm⁻¹

R_f: 0.47 (CH₂Cl₂/acetone 90:10 v/v, UV)

Compound 263n: *N*-(3-(1,3-dioxo-1,3,3a,4,7,7a-hexahydro-2H-4,7-methanoisoindol-2-yl)propyl)-4-methylbenzenesulfonamide



263n was prepared according to method A, using **241b** and the appropriate anhydride.

¹H NMR (500 MHz, CDCl₃): δ = 7.71 (d, J = 7.9 Hz, 2H), 7.31 – 7.24 (m, 2H), 6.25 (s, 2H), 5.43 – 5.35 (m, 1H), 3.49 (t, J = 6.2 Hz, 2H), 3.18 (s, 2H), 2.83 (dd, J = 12.5, 6.2 Hz, 2H), 2.64 (s, 2H), 2.39 (s, 3H), 1.72 (dd, J = 12.5, 6.2 Hz, 2H), 1.43 (d, J = 9.8 Hz, 1H), 1.06 (d, J = 9.8 Hz, 1H) ppm.

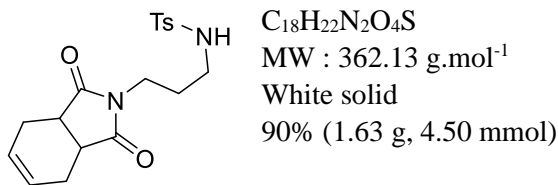
¹³C NMR (125 MHz, CDCl₃): δ = 178.5, 143.4, 137.8 ($\times 2$), 137.0, 137.0, 129.7 ($\times 2$), 127.1 ($\times 2$), 47.9 ($\times 2$), 45.1 ($\times 2$), 42.8, 40.2, 35.5, 27.9, 21.6 ppm.

HRMS (ESI-TOF) m/z: [M+K]⁺ calcd for C₁₉H₂₂N₂O₄SK 413.0932; Found 413.0905.

IR (neat): ν = 3287, 1678, 1156 cm⁻¹

R_f: 0.48 (CH₂Cl₂/acetone 90:10 v/v, UV)

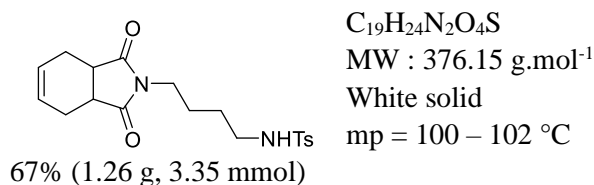
Compound 263o: *N*-(3-(1,3-dioxo-1,3,3a,4,7,7a-hexahydro-2H-isoindol-2-yl)propyl)-4-methylbenzenesulfonamide



¹H NMR (500 MHz, CDCl₃): δ = 7.70 (d, *J* = 8.2 Hz, 2H), 7.28 (d, *J* = 8.0 Hz, 2H), 5.70 – 5.59 (m, 2H), 5.41 (t, *J* = 6.8 Hz, 1H), 3.48 (t, *J* = 6.3 Hz, 2H), 3.04 (dd, *J* = 5.0, 2.3 Hz, 2H), 2.72 (q, *J* = 6.5 Hz, 2H), 2.49 (ddd, *J* = 16.0, 4.6, 2.2 Hz, 2H), 2.39 (s, 3H), 2.14 – 2.08 (m, 2H), 1.66 (p, *J* = 6.3 Hz, 2H) ppm.

¹³C NMR (125 MHz, CDCl₃): δ = 180.6 (×2), 143.3, 137.0, 129.6 (×2), 127.8 (×2), 127.1 (×2), 39.6, 39.1 (×2), 35.6, 27.6, 23.6 (×2), 21.5 ppm.

Compound 263p : *N*-(4-(1,3-dioxo-1,3,3a,4,7,7a-hexahydro-2H-isoindol-2-yl)butyl)-4-methylbenzenesulfonamide



263p was prepared according to method A, using **241c** and the appropriate anhydride.

¹H NMR (500 MHz, CDCl₃): δ = 7.68 (d, *J* = 8.2 Hz, 2H), 7.25 (d, *J* = 8.2 Hz, 2H), 5.87 – 5.69 (m, 2H), 5.27 (t, *J* = 6.1 Hz, 1H), 3.36 (t, *J* = 7.0 Hz, 2H), 3.08 – 2.97 (m, 2H), 2.84 (dd, *J* = 13.2, 6.1 Hz, 2H), 2.60 – 2.45 (m, 2H), 2.37 (s, 3H), 2.14 (dd, *J* = 12.0, 7.6 Hz, 2H), 1.53 – 1.41 (m, 2H), 1.41 – 1.31 (m, 2H) ppm.

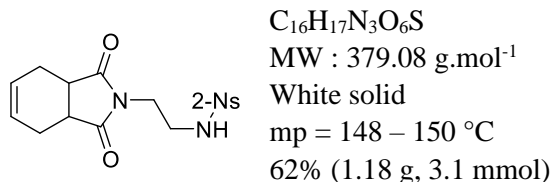
¹³C NMR (126 MHz, CDCl₃): δ = 180.3 (×2), 143.3, 136.9, 129.7 (×2), 127.8 (×2), 127.0 (×2), 42.5, 39.0 (×2), 38.1, 26.5, 24.7, 23.5 (×2), 21.5 ppm.

HRMS (ESI-TOF) m/z: [M+H]⁺ calcd for C₁₉H₂₅N₂O₄S 377.1529; Found 377.1523.

IR (neat): ν = 3132, 1682, 1328, 1156 cm⁻¹

R_f: 0.37 (CH₂Cl₂/acetone 90:10 v/v, UV)

Compound 263q : *N*-(2-(1,3-dioxo-1,3,3a,4,7,7a-hexahydro-2H-isoindol-2-yl)ethyl)-2-nitrobenzenesulfonamide



263q was prepared according to method A, using **241e** and the appropriate anhydride.

¹H NMR (500 MHz, CDCl₃): δ = 8.08 (dd, *J* = 5.8, 3.4 Hz, 1H), 7.84 (dd, *J* = 5.9, 3.3 Hz, 1H), 7.77 – 7.69 (m, 2H), 5.87 (d, *J* = 2.6 Hz, 2H), 5.75 (t, *J* = 6.0 Hz, 1H), 3.63 (t, *J* = 5.7 Hz, 2H), 3.31 (dd, *J* = 11.6, 6.0 Hz, 2H), 3.14 – 3.06 (m, 2H), 2.57 (d, *J* = 15.4 Hz, 2H), 2.22 (d, *J* = 13.2 Hz, 2H) ppm.

¹³C NMR (125 MHz, CDCl₃): δ = 180.4 (×2), 147.9, 133.7, 133.6, 132.9, 130.9, 127.8 (×2), 125.4, 41.3, 39.1 (×2), 38.3, 23.4 (×2) ppm.

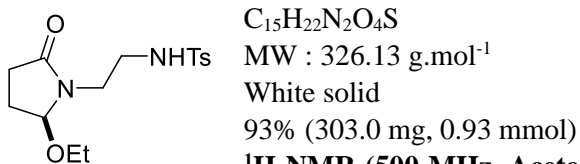
HRMS (ESI-TOF) m/z: [M+Na]⁺ calcd for C₁₆H₁₇N₃O₆SNa 402.0730; Found 402.0726.

IR (neat): ν = 3214, 1692, 1340, 1159 cm⁻¹

R_f: 0.48 (CH₂Cl₂/acetone 90:10 *v/v*, UV)

Characterization data for 264

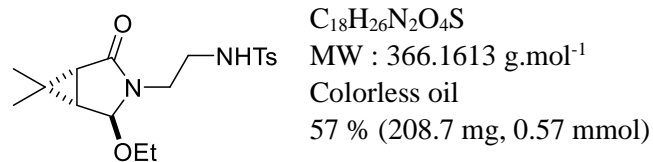
Compound 264a : (*S*)-*N*-(2-(2-ethoxy-5-oxopyrrolidin-1-yl)ethyl)-4-methylbenzenesulfonamide



¹H NMR (500 MHz, Acetone): δ 7.73 (d, *J* = 8.3 Hz, 2H), 7.40 (d, *J* = 8.1 Hz, 2H), 6.55 (d, *J* = 5.9 Hz, 1H), 4.99 – 4.90 (m, 1H), 3.48 (q, *J* = 7.0 Hz, 2H), 3.34 (t, *J* = 6.3 Hz, 2H), 3.10 – 2.99 (m, 2H), 2.42 (s, 3H), 2.34 – 2.25 (m, 1H), 2.15 – 2.08 (m, 2H), 1.95 – 1.85 (m, 1H), 1.14 (s, 3H). ppm.

¹³C NMR (126 MHz, Acetone): δ = 174.6, 142.9, 137.9, 129.5 (×2), 126.9 (×2), 89.8, 61.4, 41.3, 40.7, 28.1, 24.6, 20.5, 14.7. ppm.

Compound 264b : *N*-(2-(2-ethoxy-6,6-dimethyl-4-oxo-3-azabicyclo[3.1.0]hexan-3-yl)ethyl)-4-methylbenzenesulfonamide



¹H NMR (500 MHz, Acetone-*d*₆): δ = 7.69 (d, *J* = 8.3 Hz, 2H), 7.36 (d, *J* = 8.3 Hz, 2H), 6.52 (t, *J* = 5.4 Hz, 1H), 4.68 (d, *J* = 1.7 Hz, 1H), 3.54 – 3.44 (m, 2H), 3.37 – 3.37 (m, 1H), 3.20 – 3.12 (m, 1H), 2.98 – 2.94 (m, 2H), 2.38 (s, 3H), 1.74 – 1.69 (m, 2H), 1.13 (t, *J* = 7.2 Hz, 3H), 1.06 (s, 3H), 0.93 (s, 3H). ppm.

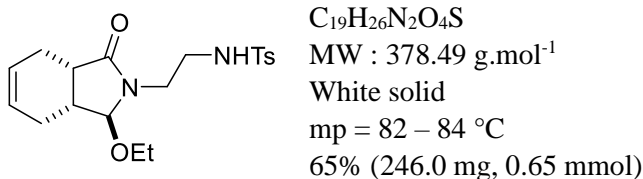
¹³C NMR (125 MHz, Acetone-*d*₆): δ = 173.0, 143.9, 138.5, 130.4 (×2), 127.8 (×2), 88.6, 60.7, 42.8, 41.2, 32.3, 31.2, 26.0, 25.0, 21.4, 15.6, 14.6. ppm.

HRMS (ESI-TOF) m/z: [M+Na]⁺ calcd for C₁₈H₂₆N₂O₄SNa 389.1505; Found 389.1497.

IR (neat): ν = 3218, 2932, 1687, 1334, 1158 cm⁻¹

R_f: 0.40 (CH₂Cl₂/acetone 90:10 v/v, UV)

Compound 264c : *N*-(2-(1-ethoxy-3-oxo-1,3,3a,4,7,7a-hexahydro-2H-isoindol-2-yl)ethyl)-4-methylbenzenesulfonamide



¹H NMR (500 MHz, CDCl₃): δ = 7.72 (d, J = 7.9 Hz, 2H), 7.40 (d, J = 7.9 Hz, 2H), 6.53 (t, J = 5.4 Hz, 1H), 5.67 (d, J = 2.6 Hz, 2H), 4.55 (s, 1H), 3.65 – 3.52 (m, 2H), 3.43 (dt, J = 14.0, 5.4 Hz, 1H), 3.38 – 3.31 (m, 1H), 3.09 – 2.96 (m, 2H), 2.80 – 2.73 (m, 1H), 2.44 – 2.39 (m, 4H), 2.35 (dd, J = 17.4, 2.3 Hz, 1H), 2.23 – 2.14 (m, 2H), 1.72 – 1.69 (m, 1H), 1.19 (t, J = 7.0 Hz, 3H) ppm.

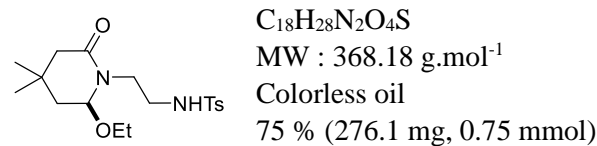
¹³C NMR (125 MHz, CDCl₃): δ = 177.3, 143.9, 138.6, 130.5 ($\times 2$), 127.8 ($\times 2$), 126.8, 125.9, 95.7, 63.6, 42.4, 42.1, 37.3, 35.2, 25.2, 22.3, 21.4, 15.6 ppm.

HRMS (ESI-TOF) m/z: [M+K]⁺ calcd for C₁₉H₂₆N₂O₄SK 417.1250; Found 417.1236.

IR (neat): ν = 3115, 2895, 1682, 1156 cm⁻¹

R_f: 0.47 (CH₂Cl₂/acetone 90:10 v/v, UV)

Compound 264d : *N*-(2-(2-ethoxy-4,4-dimethyl-6-oxopiperidin-1-yl)ethyl)-4-methylbenzenesulfonamide



¹H NMR (500 MHz, Acetone-*d*₆): δ = 7.73 (d, J = 7.9 Hz, 2H), 7.40 (d, J = 7.9 Hz, 2H), 6.59 (t, J = 5.3 Hz, 1H), 4.68 (t, J = 5.3 Hz, 1H), 3.58 – 3.46 (m, 3H), 3.37 – 3.30 (m, 1H), 3.11 – 3.07 (m, 2H), 2.42 (s, 3H), 2.09 (d, J = 15.6 Hz, 1H), 2.00 (t, J = 15.6 Hz, 1H), 1.84 (ddd, J = 13.8, 5.3, 1.5 Hz, 1H), 1.66 (dd, J = 13.4, 5.3 Hz, 1H), 1.17 (t, J = 7.0 Hz, 3H), 1.01 (s, 3H), 0.93 (s, 3H) ppm.

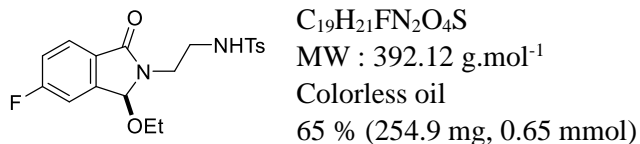
¹³C NMR (125 MHz, Acetone-*d*₆): δ = 170.4, 143.7, 138.9, 130.4 ($\times 2$), 127.8 ($\times 2$), 88.3, 63.4, 46.5, 45.2, 42.6, 40.5, 30.1, 29.3, 28.2, 21.4, 15.6 ppm.

HRMS (ESI-TOF) m/z: [M+Na]⁺ calcd for C₁₈H₂₈N₂O₄SNa 391.1662; Found 391.1676.

IR (neat): ν = 3174, 2872, 1634, 1334, 1160 cm⁻¹

R_f: 0.50 (CH₂Cl₂/acetone 90:10 v/v, UV)

Compound 264e : *N*-(2-(3-ethoxy-5-fluoro-1-oxoisoindolin-2-yl)ethyl)-4-methylbenzenesulfonamide



¹H NMR (500 MHz, Acetone-*d*₆): δ = 7.73 (dd, *J* = 8.3, 5.0 Hz, 1H), 7.70 (d, *J* = 8.3 Hz, 2H), 7.40 – 7.32 (m, 2H), 7.30 (d, *J* = 8.0 Hz, 2H), 6.64 (t, *J* = 5.0 Hz, 1H), 5.87 (s, 1H), 3.76 – 3.73 (m, 1H), 3.47 – 3.38 (m, 1H), 3.31 – 3.19 (m, 3H), 3.17 – 3.08 (m, 1H), 2.36 (s, 3H), 1.10 (t, *J* = 7.0 Hz, 3H) ppm.

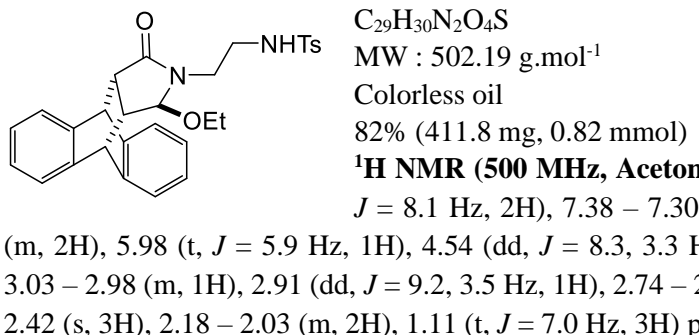
¹³C NMR (125 MHz, Acetone-*d*₆): δ = 167.2 (d, *J* = 250.0 Hz), 167.0, 145.6 (d, *J* = 9.5 Hz), 143.8, 138.8, 130.4 (×2), 129.5 (d, *J* = 2.2 Hz), 127.6 (×2), 125.9 (d, *J* = 9.6 Hz), 117.8 (d, *J* = 2.4 Hz), 111.8 (d, *J* = 2.4 Hz), 86.9 (d, *J* = 2.5 Hz), 59.8, 42.4, 40.3, 21.3, 15.4 ppm.

HRMS (ESI-TOF) m/z: [M+K]⁺ calcd for C₁₉H₂₁FN₂O₄SK 431.0838; Found 431.0832.

IR (neat): ν = 3266, 2977, 1692, 1331, 1158 cm⁻¹

R_f: 0.37 (CH₂Cl₂/acetone 90:10 v/v, UV)

Compound 264f : *N*-(2-((9*R*,10*S*,11*S*,15*R*)-12-ethoxy-14-oxo-11,12,14,15-tetrahydro-9*H*-9,10-[3,4]epipyrroloanthracen-13(10*H*)-yl)ethyl)-4-methylbenzenesulfonamide



¹H NMR (500 MHz, Acetone-*d*₆): δ = 7.66 (d, *J* = 8.2 Hz, 2H), 7.43 (d, *J* = 8.1 Hz, 2H), 7.38 – 7.30 (m, 3H), 7.11 – 7.08 (m, 3H), 6.95 – 6.88 (m, 2H), 5.98 (t, *J* = 5.9 Hz, 1H), 4.54 (dd, *J* = 8.3, 3.3 Hz, 2H), 4.35 (s, 1H), 3.52 – 3.42 (m, 2H), 3.03 – 2.98 (m, 1H), 2.91 (dd, *J* = 9.2, 3.5 Hz, 1H), 2.74 – 2.65 (m, 1H), 2.54 (dd, *J* = 9.2, 2.3 Hz, 1H), 2.42 (s, 3H), 2.18 – 2.03 (m, 2H), 1.11 (t, *J* = 7.0 Hz, 3H) ppm.

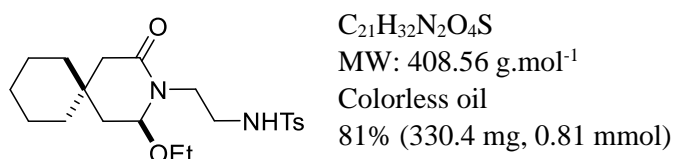
¹³C NMR (125 MHz, Acetone-*d*₆): δ = 173.7, 143.9, 143.7, 142.9, 141.7, 140.4, 138.7, 130.4 (×2), 127.8 (×2), 126.9 (×2), 126.9, 126.9, 125.6, 125.5, 124.8, 124.5, 92.1, 61.5, 48.8, 47.7, 46.5, 44.7, 40.4, 40.3, 21.4, 15.5 ppm.

HRMS (ESI-TOF) m/z: [M+Na]⁺ calcd for C₂₉H₃₀N₂O₄SNa 525.1818; Found 525.1850.

IR (neat): ν = 3201, 2872, 1676, 1328, 1156 cm⁻¹

R_f: 0.46 (CH₂Cl₂/acetone 90:10 v/v, UV)

Compound 264g : *N*-(2-(2-ethoxy-4-oxo-3-azaspiro[5.5]undecan-3-yl)ethyl)-4-methylbenzenesulfonamide



¹H NMR (500 MHz, Acetone-*d*₆): δ = 7.72 (d, *J* = 8.2 Hz, 2H), 7.39 (d, *J* = 8.0 Hz, 2H), 6.60 (t, *J* = 5.2 Hz, 1H), 4.67 (t, *J* = 4.9 Hz, 1H), 3.59 – 3.50 (m, 2H), 3.46 – 3.40 (m, 1H), 3.37 – 3.28 (m, 1H), 3.12 – 3.05 (m, 2H), 2.41 (s, 3H), 2.12 – 2.07 (m, 2H), 2.02 – 1.95 (m, 1H), 1.81 – 1.78 (m, 2H), 1.56 – 1.45 (m, 8H), 1.22 (dd, *J* = 11.3, 6.2 Hz, 1H), 1.18 (t, *J* = 7.0 Hz, 3H) ppm.

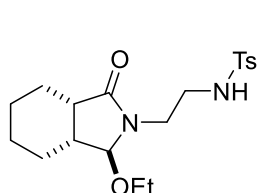
¹³C NMR (125 MHz, Acetone-*d*₆): δ = 170.4, 143.7, 138.9, 130.4 (×2), 127.8 (×2), 88.2, 63.6, 45.5, 44.9, 42.7, 40.8, 37.8, 37.4, 33.1, 26.8, 22.4, 22.3, 21.4, 15.6 ppm.

HRMS (ESI-TOF) m/z: [M+Na]⁺ calcd for C₂₁H₃₂N₂O₄SnA 431.1949; Found 431.1975.

IR (neat): ν = 3200, 2926, 1651, 1336, 1161 cm⁻¹

R_f: 0.40 (CH₂Cl₂/acetone 90:10 v/v, UV)

Compound 264h: *N*-(2-(1-ethoxy-3-oxohexahydro-1*H*-isoindol-2(3*H*)-yl)ethyl)-4-methylbenzenesulfonamide



C₁₉H₂₈N₂O₄S

MW : 380.18 g.mol⁻¹

Colorless oil

92 % (349.8 mg, 0.92 mmol)

¹H NMR (500 MHz, Acetone-*d*₆): δ = 7.73 (d, *J* = 8.2 Hz, 2H), 7.40 (d, *J* = 8.2 Hz, 2H), 6.52 (s, 1H), 4.43 (s, 1H), 3.59 – 3.51 (m, 2H), 3.48 – 3.40 (m, 1H), 3.38 – 3.30 (m, 1H), 3.08 – 2.97 (m, 2H), 2.57 (t, *J* = 6.0 Hz, 1H), 2.41 (s, 3H), 2.32 – 2.27 (m, 1H), 2.03 – 2.00 (m, 1H), 1.79 – 1.69 (m, 1H), 1.57 – 1.50 (m, 1H), 1.50 – 1.38 (m, 2H), 1.23 – 1.10 (m, 4H), 0.99 – 0.86 (m, 2H) ppm.

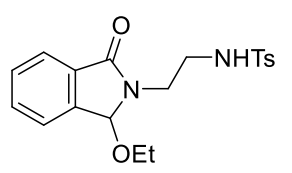
¹³C NMR (125 MHz, Acetone-*d*₆): δ = 175.9, 143.0, 137.8, 129.6 (×2), 126.9 (×2), 94.0, 62.8, 41.7, 41.3, 38.1, 37.4, 26.7, 23.3, 22.6, 22.5, 20.5, 14.8 ppm.

HRMS (ESI-TOF) m/z: [M+Na]⁺ calcd for C₁₉H₂₈N₂O₄SnA 403.1662; Found 403.1657.

IR (neat): ν = 3216, 2932, 1685, 1334, 1161 cm⁻¹

R_f: 0.46 (CH₂Cl₂/acetone 90:10 v/v, UV)

Compound 264i : *N*-(2-(1-ethoxy-3-oxoisoindolin-2-yl)ethyl)-4-methylbenzenesulfonamide



C₁₉H₂₂N₂O₄S

MW : 374.46 g.mol⁻¹

White solid

mp = 55 – 56 °C

65% (243.4 mg, 0.65 mmol)

¹H NMR (500 MHz, CDCl₃): δ = 7.73 – 7.68 (m, 3H), 7.65 (td, *J* = 7.4, 1.1 Hz, 1H), 7.59 – 7.57 m, 2H), 7.29 (d, *J* = 7.9 Hz, 2H), 6.69 (t, *J* = 5.8 Hz, 1H), 5.87 (s, 1H), 3.76 (dt, *J* = 14.0, 6.4 Hz, 1H), 3.44 – 3.42 (m, 1H), 3.29 – 3.17 (m, 3H), 3.09 – 3.06 (m, 1H), 2.34 (s, 3H), 1.08 (t, *J* = 7.0 Hz, 3H) ppm.

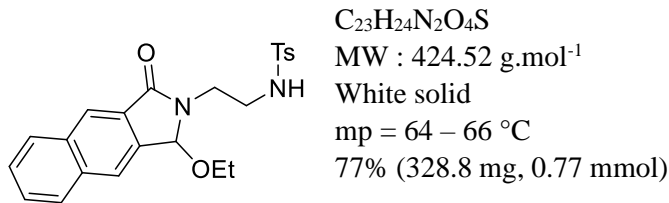
¹³C NMR (125 MHz, CDCl₃): δ = 168.1, 143.8, 142.8, 138.7, 133.3, 132.9, 130.5, 130.4 (×2), 127.7 (×2), 124.4, 123.6, 87.4, 59.4, 42.5, 40.2, 21.4, 15.4 ppm.

HRMS (ESI-TOF) m/z: [M+ Na]⁺ calcd for C₁₉H₂₂N₂O₄SNa 397.1192; Found 397.1185

IR (neat): $\nu = 3217, 2882, 1683, 1327, 1152 \text{ cm}^{-1}$

R_f: 0.49 (CH₂Cl₂/acetone 90:10 v/v, UV)

Compound 264j : N-(2-(1-ethoxy-3-oxo-1,3-dihydro-2H-benzo[f]isoindol-2-yl)ethyl)-4-methylbenzenesulfonamide



¹H NMR (500 MHz, CDCl₃): $\delta = 8.26$ (s, 1H), 8.14 (d, $J = 7.9$ Hz, 1H), 8.08 (s, 1H), 8.09 (d, $J = 7.9$ Hz, 1H), 7.71 – 7.70 (m, 2H), 7.68 – 7.62 (m, 2H), 7.23 (d, $J = 7.9$ Hz, 2H), 6.71 (t, $J = 5.8$ Hz, 1H), 6.00 (s, 1H), 3.87 – 3.78 (m, 1H), 3.50 (dt, $J = 14.2, 5.8$ Hz, 1H), 3.34 – 3.24 (m, 3H), 3.19 – 3.10 (m, 1H), 2.23 (s, 3H), 1.10 (t, $J = 7.0$ Hz, 3H) ppm.

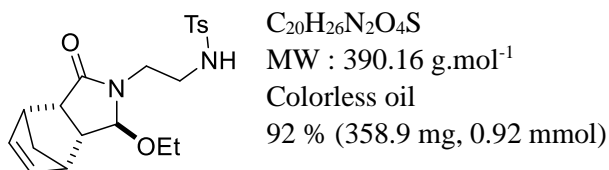
¹³C NMR (125 MHz, CDCl₃): $\delta = 167.9, 143.7, 138.8, 137.8, 136.1, 134.6, 130.9, 130.3 (\times 3), 129.5, 128.8, 127.9 (\times 2), 127.6, 124.0, 123.8, 87.4, 59.3, 42.5, 40.4, 21.2, 15.5$ ppm.

HRMS (ESI-TOF) m/z: [M+K]⁺ calcd for C₂₃H₂₄N₂O₄SK 463.1088; Found 463.1076.

IR (neat): $\nu = 3193, 2975, 1680, 1325, 1154 \text{ cm}^{-1}$

R_f: 0.46 (CH₂Cl₂/acetone 90:10 v/v, UV)

Compound 264k : N-(2-(1-ethoxy-3-oxo-3a,4,7,7a-tetrahydro-1H-4,7-methanoisoindol-2(3H)-yl)ethyl)-4-methylbenzenesulfonamide



¹H NMR (500 MHz, Acetone-d₆): $\delta = 7.73$ (d, $J = 7.9$ Hz, 2H), 7.40 (d, $J = 7.9$ Hz, 2H), 6.59 (t, $J = 5.6$ Hz, 1H), 6.19 – 6.18 (m, 2H), 4.66 (s, 1H), 3.53 (q, $J = 6.9$ Hz, 2H), 3.38 – 3.30 (m, 2H), 3.07 – 3.02 (m, 2H), 2.93 – 2.89 (m, 2H), 2.41 (s, 3H), 2.37 (d, $J = 7.8$ Hz, 1H), 2.05 – 2.03 (m, 1H), 1.27 – 1.21 (m, 2H), 1.18 (t, $J = 7.0$ Hz, 3H) ppm.

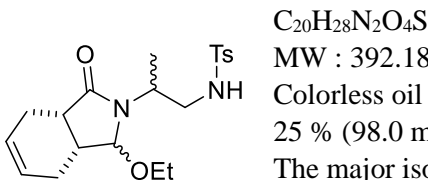
¹³C NMR (125 MHz, Acetone-d₆): $\delta = 175.2, 143.8, 138.5, 138.3, 138.0, 130.4 (\times 2), 127.7 (\times 2), 93.3, 61.7, 49.4, 46.8, 46.1, 45.3, 43.4, 42.1, 41.2, 21.3, 15.5$ ppm.

HRMS (ESI-TOF) m/z: [M+Na]⁺ calcd for C₂₀H₂₆N₂O₄SNa 413.1505; Found 413.1534

IR (neat): $\nu = 3179, 2974, 1673, 1330, 1160 \text{ cm}^{-1}$

R_f: 0.40 (CH₂Cl₂/acetone 90:10 v/v, UV)

Compound 264m: *N*-(2-(1-ethoxy-3-oxo-1,3,3a,4,7,7a-hexahydro-2H-isoindol-2-yl)propyl)-4-methylbenzenesulfonamide



C₂₀H₂₈N₂O₄S

MW : 392.18 g.mol⁻¹

Colorless oil

25 % (98.0 mg, 0.25 mmol)

The major isomer **264m** has been isolated out of **264** isomers for further steps.

¹H NMR (500 MHz, Acetone-d₆): δ = 7.70 (d, *J* = 8.0 Hz, 2H), 7.39 (d, *J* = 8.0 Hz, 2H), 6.31 (t, *J* = 6.1 Hz, 1H), 5.66 – 5.65 (m, 2H), 4.53 (s, 1H), 4.12 – 4.08 (m, 1H), 3.66 – 3.57 (m, 1H), 3.57 – 3.51 (m, 1H), 3.02 (t, *J* = 6.3 Hz, 2H), 2.85 – 2.78 (m, 1H), 2.47 – 2.35 (m, 2H), 2.41 (s, 3H), 2.24 – 2.13 (m, 2H), 1.64 – 1.57 (m, 1H), 1.23 – 1.11 (m, 6H) ppm.

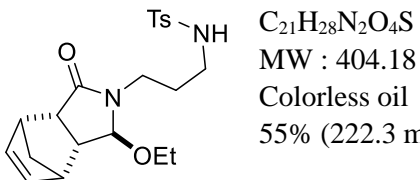
¹³C NMR (125 MHz, Acetone-d₆): δ = 176.8, 143.8, 138.7, 130.4 (×2), 127.7 (×2), 126.7, 125.5, 92.9, 63.1, 48.4, 47.3, 37.4, 34.7, 25.0, 22.0, 21.4, 15.6, 15.5 ppm.

HRMS (ESI-TOF) m/z: [M+Na]⁺ calcd for C₂₀H₂₈N₂O₄SNa 415.1662; Found 415.1650.

IR (neat): ν = 3215, 2917, 1696, 1330, 1157 cm⁻¹

R_f: 0.70 (CH₂Cl₂/acetone 90:10 v/v, UV)

Compound 264n: *N*-(3-(1-ethoxy-3-oxo-1,3,3a,4,7,7a-hexahydro-2H-4,7-methanoisoindol-2-yl)propyl)-4-methylbenzenesulfonamide



C₂₁H₂₈N₂O₄S

MW : 404.18 g.mol⁻¹

Colorless oil

55% (222.3 mg, 0.55 mmol)

¹H NMR (500 MHz, Acetone-d₆): δ = 7.75 (d, *J* = 8.0 Hz, 2H), 7.42 (d, *J* = 8.0 Hz, 2H), 6.55 (t, *J* = 6.2 Hz, 1H), 6.19 – 6.18 (m, 2H), 4.60 (s, 1H), 3.49 (q, *J* = 7.0 Hz, 2H), 3.37 – 3.32 (m, 1H), 3.24 – 3.15 (m, 1H), 2.91 – 2.89 (m, 2H), 2.78 (m, 1H), 2.44 – 2.34 (m, 4H), 2.06 – 2.01 (m, 2H), 1.75 – 1.68 (m, 2H), 1.22 (d, *J* = 9.2 Hz, 1H), 1.15 (t, *J* = 6.7 Hz, 3H), 1.02 (d, *J* = 9.2 Hz, 1H) ppm.

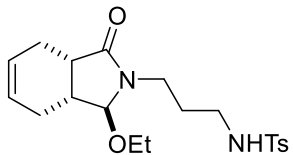
¹³C NMR (125 MHz, Acetone-d₆): δ = 175.3, 143.7, 138.8, 138.3, 138.0, 130.4 (×2), 127.8 (×2), 92.7, 61.5, 49.5, 46.8, 46.1, 45.4, 43.4, 41.4, 38.1, 28.2, 21.4, 15.6 ppm.

HRMS (ESI-TOF) m/z: [M+Na]⁺ calcd for C₂₁H₂₈N₂O₄SNa 427.1662; Found 427.1641.

IR (neat): ν = 3200, 2926, 1677, 1327, 1156 cm⁻¹

R_f: 0.40 (CH₂Cl₂/acetone 90:10 v/v, UV)

Compound 264o : *N*-(3-((1*S*,3*a**S*,7*a**R*)-1-ethoxy-3-oxo-1,3,3*a*,4,7,7*a*-hexahydro-2*H*-isoindol-2-yl)propyl)-4-methylbenzenesulfonamide

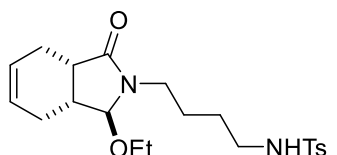


C₂₀H₂₈N₂O₄S
MW : 392.18 g.mol⁻¹
Colorless oil
55 % (215.6 mg, 0.55 mmol)

¹H NMR (500 MHz, Acetone-d₆): δ = 7.71 (d, *J* = 8.3 Hz, 2H), 7.39 (d, *J* = 7.9 Hz, 2H), 6.49 (t, *J* = 6.1 Hz, 1H), 5.68 – 5.57 (m, 2H), 4.49 (s, 1H), 3.59 – 3.50 (m, 2H), 3.40 (ddd, *J* = 14.2, 7.9, 6.3 Hz, 1H), 3.20 (dt, *J* = 14.1, 6.0 Hz, 1H), 2.89 (dt, *J* = 13.4, 6.6 Hz, 1H), 2.83 – 2.69 (m, 2H), 2.41 (s, 4H), 2.38 – 2.30 (m, 1H), 2.23 – 2.11 (m, 2H), 1.75 – 1.65 (m, 3H), 1.15 (t, *J* = 7.0 Hz, 3H). ppm.

¹³C NMR (125 MHz, Acetone-d₆): δ = 176.6, 142.8, 138.0, 129.5 (×2), 126.9 (×2), 126.3, 125.2, 94.2, 62.5, 40.2, 37.5, 36.9, 34.9, 27.6, 24.6, 21.7, 20.5, 14.8. ppm.

Compound 264p : *N*-(4-(1-ethoxy-3-oxo-1,3,3*a*,4,7,7*a*-hexahydro-2*H*-isoindol-2-yl)butyl)-4-methylbenzenesulfonamide



C₂₁H₃₀N₂O₄S
MW : 406.19 g.mol⁻¹
Colorless oil
90 % (365.6 mg, 0.90 mmol)

¹H NMR (500 MHz, Acetone-d₆): δ = 7.73 (d, *J* = 8.2 Hz, 2H), 7.38 (d, *J* = 8.2 Hz, 2H), 6.45 (t, *J* = 5.3 Hz, 1H), 5.73 – 5.65 (m, 2H), 4.50 (s, 1H), 3.60 – 3.52 (m, 2H), 3.38 (dt, *J* = 14.3, 7.3 Hz, 1H), 3.13 – 3.02 (m, 1H), 2.93 – 2.89 (m, 2H), 2.82 – 2.75 (m, 1H), 2.45 – 2.35 (m, 2H), 2.41 (s, 3H), 2.25 – 2.14 (m, 2H), 1.71 – 1.63 (m, 1H), 1.61 – 1.48 (m, 2H), 1.47 – 1.41 (m, 2H), 1.16 (t, *J* = 7.0 Hz, 3H) ppm.

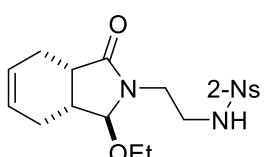
¹³C NMR (125 MHz, Acetone-d₆): δ = 176.7, 143.6, 139.1, 130.3 (×2), 127.7 (×2), 127.1, 126.0, 94.8, 63.3, 43.5, 40.7, 37.7, 35.7, 27.6, 25.6, 25.4, 22.5, 21.4, 15.7 ppm.

HRMS (ESI-TOF) m/z: [M+Na]⁺ calcd for C₂₁H₃₀N₂O₄SNa 429.1818; Found 429.1838.

IR (neat): ν = 3210, 2872, 1678, 1325, 1155 cm⁻¹

R_f: 0.30 (CH₂Cl₂/acetone 90:10 v/v, UV)

Compound 264q : *N*-(2-(1-ethoxy-3-oxo-3*a*,4,7,7*a*-tetrahydro-1*H*-isoindol-2(3*H*)-yl)ethyl)-2-nitrobenzenesulfonamide



C₁₈H₂₃N₃O₆S
MW : 409.13 g.mol⁻¹
Colorless oil
83 % (339.6 mg, 0.83 mmol)

¹H NMR (500 MHz, Acetone-d₆): δ = 8.14 – 8.09 (m, 1H), 7.99 – 7.94 (m, 1H), 7.94 – 7.87 (m, 2H), 6.79 (s, 1H), 5.66 – 5.65 (m, 2H), 4.58 (s, 1H), 3.67 – 3.57 (m, 2H), 3.55 (d, *J* = 14.1 Hz, 1H), 3.46 –

3.36 (m, 1H), 3.28 – 3.25 (m, 2H), 2.82 – 2.78 (m, 1H), 2.44 (dd, J = 15.8, 7.3 Hz, 1H), 2.36 (dd, J = 17.4, 2.3 Hz, 1H), 2.25 – 2.14 (m, 2H), 1.71 – 1.65 (m, 1H), 1.19 (t, J = 7.3 Hz, 3H) ppm.

^{13}C NMR (125 MHz, Acetone-*d*₆): δ = 177.3, 149.2, 134.9, 133.9, 133.6, 131.5, 126.8, 125.9 ($\times 2$), 95.7, 63.6, 42.8, 42.2, 37.3, 35.5, 25.2, 22.3, 15.6 ppm.

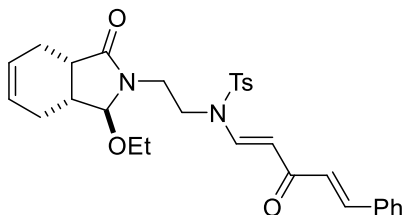
HRMS (ESI-TOF) m/z: [M+K]⁺ calcd for C₁₈H₂₃N₃O₆SK 432.1200; Found 432.1238.

IR (neat): ν = 3198, 2895, 1694, 1341, 1163 cm⁻¹

R_f: 0.40 (CH₂Cl₂/acetone 90:10 v/v, UV)

Characterization data for 250, 265

Compound 250 : *N*-(2-(1-ethoxy-3-oxo-1,3,3a,4,7,7a-hexahydro-2*H*-isoindol-2-yl)ethyl)-4-methyl-*N*-((1*E*,4*E*)-3-oxo-5-phenylpenta-1,4-dien-1-yl)benzenesulfonamide



C₃₀H₃₄N₂O₅S
MW : 534.22 g.mol⁻¹
colorless oil
95% (203.0 mg, 0.38 mmol)

¹H NMR (500 MHz, Acetone-*d*₆): δ = 8.11 (d, *J* = 13.8 Hz, 1H), 7.89 (d, *J* = 16.3 Hz, 1H), 7.85 (d, *J* = 8.4 Hz, 2H), 7.72 (dd, *J* = 7.7, 1.5 Hz, 2H), 7.51 (d, *J* = 8.0 Hz, 2H), 7.46 – 7.36 (m, 3H), 6.90 (d, *J* = 16.3 Hz, 1H), 6.64 (d, *J* = 13.8 Hz, 1H), 5.75 – 5.66 (m, 2H), 4.64 (s, 1H), 3.76 – 3.71 (m, 2H), 3.70 – 3.64 (m, 2H), 3.61 – 3.54 (m, 1H), 3.47 – 3.39 (m, 1H), 2.87 (dd, *J* = 11.9, 3.8 Hz, 1H), 2.45 (m, 5H), 2.30 – 2.25 (m, 2H), 1.84 – 1.75 (m, 1H), 1.24 (t, *J* = 7.0 Hz, 3H) ppm.

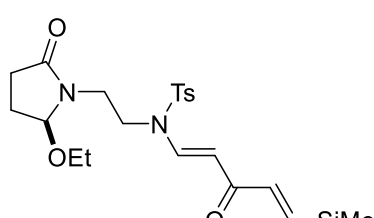
¹³C NMR (125 MHz, Acetone-*d*₆): δ = 187.9, 177.7, 146.2, 142.9, 140.9, 136.1, 136.1, 131.3 (×2), 131.0, 129.8 (×2), 129.1 (×2), 128.4, 128.1 (×2), 126.9, 126.2, 106.2, 96.3, 63.7, 44.6, 39.4, 37.7, 36.0, 25.4, 22.5, 21.5, 15.8 ppm.

HRMS (ESI-TOF) m/z: [M+Na]⁺ calcd for C₃₀H₃₄N₂O₅SnA 557.2081; Found 557.2045.

IR (neat): ν = 3322, 2898, 1675, 1576, 1164 cm⁻¹

R_f: 0.55 (CH₂Cl₂/acetone 95:5 v/v, UV)

Compound 265a : *N*-(2-((S)-2-ethoxy-5-oxopyrrolidin-1-yl)ethyl)-4-methyl-*N*-((1*E*,4*E*)-3-oxo-5-(trimethylsilyl)penta-1,4-dien-1-yl)benzenesulfonamide

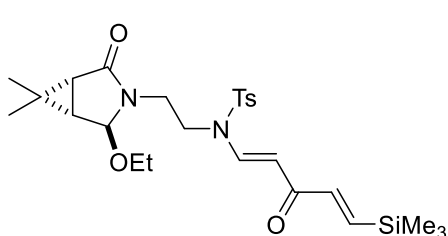


C₂₃H₃₄N₂O₅SSi
MW : 478.2 g.mol⁻¹
Colorless oil
78% (172.1 mg, 0.36 mmol)

¹H NMR (500 MHz, CDCl₃): δ = 8.16 (d, *J* = 13.8 Hz, 1H), 7.70 (d, *J* = 8.2 Hz, 2H), 7.32 (d, *J* = 8.2 Hz, 2H), 7.18 (d, *J* = 19.0 Hz, 1H), 6.59 (d, *J* = 19.0 Hz, 1H), 6.16 (d, *J* = 13.8 Hz, 1H), 4.93 (d, *J* = 5.4 Hz, 1H), 3.70 – 3.64 (m, 1H), 3.59 (td, *J* = 13.1, 6.0 Hz, 2H), 3.52 (q, *J* = 7.0 Hz, 2H), 3.48 – 3.43 (m, 1H), 2.49 (dt, *J* = 17.2, 9.0 Hz, 1H), 2.42 (s, 3H), 2.28 (ddd, *J* = 17.0, 9.9, 3.0 Hz, 1H), 2.22 – 2.12 (m, 1H), 1.96 (t, *J* = 10.7 Hz, 1H), 1.24 (t, *J* = 7.0 Hz, 3H), 0.14 (s, 9H) ppm.

¹³C NMR (125 MHz, CDCl₃): δ = 187.7, 175.5, 146.6, 145.1, 142.5, 141.7, 134.8, 130.2 (×2), 127.3 (×2), 104.6, 90.8, 62.6, 43.8, 38.8, 28.6, 25.3, 21.6, 15.4, -1.7 (×3) ppm.

Compound 265b : N-(2-(2-ethoxy-6,6-dimethyl-4-oxo-3-azabicyclo[3.1.0]hexan-3-yl)ethyl)-4-methyl-N-((1E,4E)-3-oxo-5-(trimethylsilyl)penta-1,4-dien-1-yl)benzenesulfonamide



C₂₆H₃₈N₂O₅SSi
MW : 518.23 g.mol⁻¹
Colorless oil
65% (134.7 mg, 0.26 mmol)

¹H NMR (500 MHz, CDCl₃): δ = 8.14 (d, *J* = 13.8 Hz, 1H), 7.70 (d, *J* = 8.3 Hz, 2H), 7.32 (d, *J* = 8.3 Hz, 2H), 7.21 (d, *J* = 19.0 Hz, 1H), 6.61 (d, *J* = 19.0 Hz, 1H), 6.30 (d, *J* = 13.8 Hz, 1H), 4.58 (d, *J* = 1.7 Hz, 1H), 3.67 – 3.49 (m, 5H), 3.14 (dd, *J* = 17.1, 6.0 Hz, 1H), 2.42 (s, 3H), 1.86 (dd, *J* = 6.0, 1.7 Hz, 1H), 1.71 (d, *J* = 6.0 Hz, 1H), 1.28 (t, *J* = 7.0 Hz, 3H), 1.13 (s, 3H), 1.00 (s, 3H), 0.16 (d, *J* = 14.2 Hz, 9H) ppm.

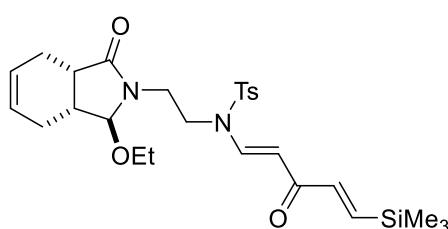
¹³C NMR (125 MHz, CDCl₃): δ = 187.9, 172.9, 146.7, 145.1, 142.8, 141.5, 135.0, 130.3 (×2), 127.4 (×2), 105.1, 89.0, 61.4, 43.8, 38.5, 32.1, 31.2, 26.0, 25.1, 21.8, 15.5, 14.4, -1.6 (×3) ppm.

HRMS (ESI-TOF) m/z: [M+K]⁺ calcd for C₂₆H₃₈N₂O₅SSiK 557.1902; Found 557.1910.

IR (neat): ν = 2956, 1689, 1571, 1361, 1167 cm⁻¹

R_f: 0.53 (CH₂Cl₂/acetone 95:5 v/v, UV)

Compound 265c : N-(2-(1-ethoxy-3-oxo-3a,4,7,7a-tetrahydro-1H-isoindol-2(3H)-yl)ethyl)-4-methyl-N-((1E,4E)-3-oxo-5-(trimethylsilyl)penta-1,4-dien-1-yl)benzenesulfonamide



C₂₇H₃₈N₂O₅SSi
MW : 530.23 g.mol⁻¹
Colorless oil
95% (201.5 mg, 0.38 mmol)

¹H NMR (500 MHz, CDCl₃): δ = 8.12 (d, *J* = 13.8 Hz, 1H), 7.69 (d, *J* = 8.3 Hz, 2H), 7.31 (d, *J* = 8.1 Hz, 2H), 7.20 (d, *J* = 19.0 Hz, 1H), 6.56 (d, *J* = 19.0 Hz, 1H), 6.24 (d, *J* = 13.8 Hz, 1H), 5.70 (dd, *J* = 17.8, 1.7 Hz, 2H), 4.42 (s, 1H), 3.69 – 3.53 (m, 5H), 3.43 – 3.34 (m, 1H), 2.90 – 2.81 (m, 1H), 2.44 – 2.41 (m, 5H), 2.28 – 2.18 (m, 2H), 1.77 – 1.69 (m, 1H), 1.26 (t, *J* = 7.0 Hz, 3H), 0.13 (s, 9H) ppm.

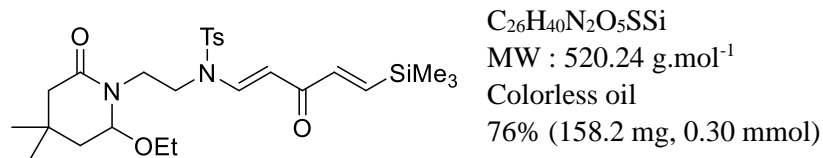
¹³C NMR (125 MHz, CDCl₃): δ = 187.9, 177.5, 146.5, 145.0, 142.8, 141.7, 134.8, 130.2 (×2), 127.2 (×2), 126.6, 125.1, 104.7, 96.4, 63.5, 43.8, 39.8, 37.2, 35.5, 25.1, 21.8, 21.6, 15.5, -1.7 (×3) ppm.

HRMS (ESI-TOF) m/z: [M+Na]⁺ calcd for C₂₇H₃₈N₂O₅SSiNa 553.2168; Found 553.2166.

IR (neat): ν = 2954, 1701, 1573, 1364, 1168 cm⁻¹

R_f: 0.65 (CH₂Cl₂/acetone 95:5 v/v, UV)

Compound 265d: *N*-(3-(2-ethoxy-4,4-dimethyl-6-oxopiperidin-1-yl)propyl)-4-methyl-*N*-((1*E*,4*E*)-3-oxo-5-(trimethylsilyl)penta-1,4-dien-1-yl)benzenesulfonamide



¹H NMR (500 MHz, Acetone-*d*₆): δ = 8.08 (d, *J* = 13.8 Hz, 1H), 7.79 (d, *J* = 8.4 Hz, 2H), 7.50 (d, *J* = 8.4 Hz, 2H), 7.30 (d, *J* = 19.2 Hz, 1H), 6.77 (d, *J* = 13.8 Hz, 1H), 6.60 (d, *J* = 19.2 Hz, 1H), 4.74 (t, *J* = 5.3 Hz, 1H), 3.84 – 3.73 (m, 2H), 3.67 – 3.52 (m, 3H), 3.27 – 3.19 (m, 1H), 2.44 (s, 3H), 2.14 (dt, *J* = 16.7, 9.0 Hz, 2H), 1.92 (m, 1H), 1.72 (dd, *J* = 13.8, 5.3 Hz, 1H), 1.27 (t, *J* = 7.0 Hz, 3H), 1.06 (s, 3H), 0.97 (s, 3H), 0.16 (d, *J* = 3.3 Hz, 9H) ppm.

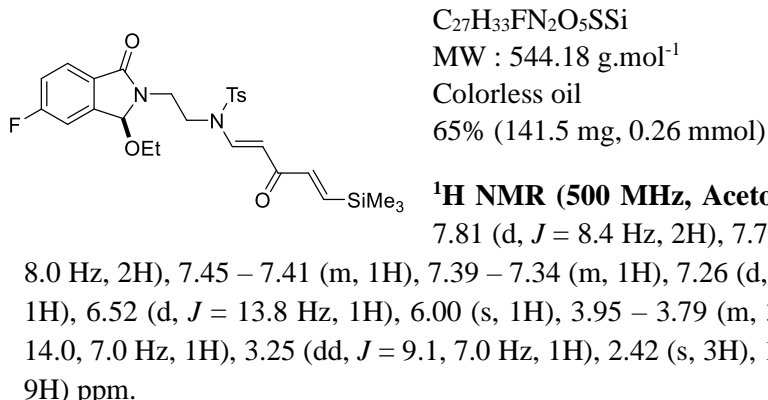
¹³C NMR (125 MHz, Acetone-*d*₆): δ = 187.8, 170.2, 146.2, 146.1, 144.2, 141.8, 136.3, 131.2 (×2), 128.0 (×2), 105.4, 88.8, 63.8, 46.6, 44.7, 42.8, 40.7, 29.1, 28.1, 21.5, 15.8, -1.7 (×3) ppm.

HRMS (ESI-TOF) m/z: [M+Na]⁺ calcd for C₂₆H₄₀N₂O₅SSiNa 543.2319; Found 543.2282.

IR (neat): ν = 2955, 1651, 1570, 1361, 1166 cm⁻¹

R_f: 0.50 (CH₂Cl₂/acetone 95:5 v/v, UV)

Compound 265e: *N*-(2-(3-ethoxy-5-fluoro-1-oxoisoindolin-2-yl)ethyl)-4-methyl-*N*-((1*E*,4*E*)-3-oxo-5-(trimethylsilyl)penta-1,4-dien-1-yl)benzenesulfonamide



¹H NMR (500 MHz, Acetone-*d*₆): δ = 8.10 (d, *J* = 13.8 Hz, 1H), 7.81 (d, *J* = 8.4 Hz, 2H), 7.77 (dd, *J* = 8.4, 4.9 Hz, 1H), 7.47 (d, *J* = 8.0 Hz, 2H), 7.45 – 7.41 (m, 1H), 7.39 – 7.34 (m, 1H), 7.26 (d, *J* = 19.1 Hz, 1H), 6.61 (d, *J* = 19.1 Hz, 1H), 6.52 (d, *J* = 13.8 Hz, 1H), 6.00 (s, 1H), 3.95 – 3.79 (m, 3H), 3.62 – 3.56 (m, 1H), 3.37 (dt, *J* = 14.0, 7.0 Hz, 1H), 3.25 (dd, *J* = 9.1, 7.0 Hz, 1H), 2.42 (s, 3H), 1.17 (t, *J* = 7.0 Hz, 3H), 0.20 – 0.12 (m, 9H) ppm.

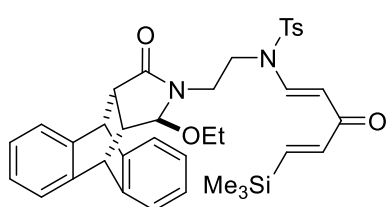
¹³C NMR (125 MHz, Acetone-*d*₆): δ = 187.4, 167.3 (d, *J* = 250.0 Hz), 165.3, 146.2 (d, *J* = 4.5 Hz) (×2), 145.7 (d, *J* = 9.7 Hz), 144.0, 141.6, 136.0, 131.3 (×2), 129.4 (d, *J* = 2.1 Hz), 128.1 (×2), 126.1 (d, *J* = 9.7 Hz), 117.9 (d, *J* = 23.5 Hz), 111.9 (d, *J* = 24.2 Hz), 105.3, 87.1 (d, *J* = 2.5 Hz), 60.2, 44.6, 37.5, 21.5, 15.6, -1.7 (×3) ppm.

HRMS (ESI-TOF) m/z: [M+Na]⁺ calcd for C₂₇H₃₃FN₂O₅SSiNa 567.1756; Found 567.1738.

IR (neat): ν = 2955, 1704, 1670, 1361, 1165 cm⁻¹

R_f: 0.59 (CH₂Cl₂/acetone 95:5 v/v, UV)

Compound 265f: *N*-(2-((9*R*,10*S*,11*S*,15*R*)-12-ethoxy-14-oxo-11,12,14,15-tetrahydro-9*H*-9,10-[3,4]epipyrroloanthracen-13(10*H*)-yl)ethyl)-4-methyl-*N*-((1*E*,4*E*)-3-oxo-5-(trimethylsilyl)penta-1,4-dien-1-yl)benzenesulfonamide



C₃₇H₄₂N₂O₅SSi
MW : 654.26 g.mol⁻¹
colorless oil
45% (117.8 mg, 0.18 mmol)

¹H NMR (500 MHz, Acetone-*d*₆): δ = 7.97 (d, *J* = 13.8 Hz, 1H), 7.75 (d, *J* = 8.4 Hz, 2H), 7.60 (d, *J* = 8.4 Hz, 2H), 7.47 – 7.39 (m, 3H), 7.31 (d, *J* = 19.2 Hz, 1H), 7.22 – 7.14 (m, 3H), 6.96 – 6.89 (m, 2H), 6.63 (d, *J* = 19.2 Hz, 1H), 6.27 (d, *J* = 13.8 Hz, 1H), 4.65 (dd, *J* = 17.1, 3.3 Hz, 2H), 4.54 (s, 1H), 3.57 (dd, *J* = 7.0, 2.6 Hz, 2H), 3.31 – 3.18 (m, 1H), 3.07 – 3.02 (m, 1H), 2.76 (m, 2H), 2.69 – 2.63 (m, 1H), 2.52 (s, 3H), 2.36 – 2.27 (m, 1H), 1.20 (t, *J* = 7.0 Hz, 3H), 0.25 (s, 9H) ppm.

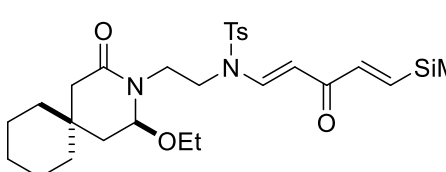
¹³C NMR (125 MHz, Acetone-*d*₆): δ = 187.5, 174.1, 146.4, 146.3, 144.0, 143.7, 142.7, 142.0, 141.1, 140.5, 135.8, 131.3 (×2), 128.1 (×2), 127.0, 127.0, 127.0, 126.9, 125.9, 125.6, 124.9, 124.6, 105.0, 92.0, 61.5, 48.7, 47.8, 46.7, 44.8, 42.6, 36.8, 21.5, 15.7, -1.6 (×3) ppm.

HRMS (ESI-TOF) m/z: [M+Na]⁺ calcd for C₃₇H₄₂N₂O₅SSiNa 677.2481; Found 677.2470.

IR (neat): ν = 2955, 1696, 1571, 1362, 1167 cm⁻¹

R_f: 0.66 (CH₂Cl₂/acetone 95:5 v/v, UV)

Compound 265g: *N*-(2-(2-ethoxy-4-oxo-3-azaspiro[5.5]undecan-3-yl)ethyl)-4-methyl-*N*-((1*E*,4*E*)-3-oxo-5-(trimethylsilyl)penta-1,4-dien-1-yl)benzenesulfonamide



C₂₆H₄₀N₂O₅SSi
MW : 560.27 g.mol⁻¹
Colorless oil
40% (89.6 mg, 0.16 mmol)

¹H NMR (500 MHz, Acetone-*d*₆): δ = 8.09 (d, *J* = 13.8 Hz, 1H), 7.84 – 7.78 (m, 2H), 7.52 (d, *J* = 8.0 Hz, 2H), 7.32 (d, *J* = 19.2 Hz, 1H), 6.77 (d, *J* = 13.8 Hz, 1H), 6.62 (d, *J* = 19.2 Hz, 1H), 4.75 (t, *J* = 5.0 Hz, 1H), 3.88 – 3.73 (m, 2H), 3.71 – 3.57 (m, 3H), 3.29 – 3.20 (m, 1H), 2.47 (s, 3H), 2.21 (q, *J* = 16.8 Hz, 2H), 1.97 – 1.85 (m, 2H), 1.59 (d, *J* = 7.8 Hz, 1H), 1.48 (m, 5H), 1.42 – 1.35 (m, 3H), 1.33 – 1.25 (m, 4H), 0.22 – 0.12 (m, 9H) ppm.

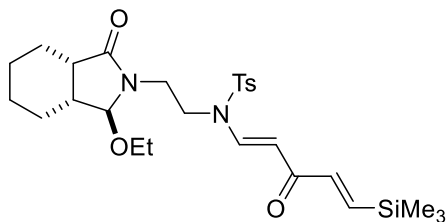
¹³C NMR (125 MHz, Acetone-*d*₆): δ = 187.7, 170.1, 146.1, 146.1, 144.2, 141.8, 136.3, 131.2 (×2), 128.0 (×2), 105.4, 88.6, 63.9, 44.7 (×2), 42.9 (×2), 37.6, 37.2, 33.1, 26.8, 22.4, 22.3, 21.5, 15.8, -1.7 (×3) ppm.

HRMS (ESI-TOF) m/z: [M+Na]⁺ calcd for C₂₆H₄₀N₂O₅SSiNa 583.2632; Found 583.2593.

IR (neat): ν = 2926, 1651, 1572, 1363, 1167 cm⁻¹

R_f: 0.60 (CH₂Cl₂/acetone 95:5 v/v, UV)

Compound 265h : *N*-(2-(1-ethoxy-3-oxohexahydro-1*H*-isoindol-2(3*H*)-yl)ethyl)-4-methyl-*N*-((1*E*,4*E*)-3-oxo-5-(trimethylsilyl)penta-1,4-dien-1-yl)benzenesulfonamide



C₂₇H₄₀N₂O₅SSi
MW : 532.24 g.mol⁻¹
Colorless oil
65% (138.4 mg, 0.26 mmol)

¹H NMR (500 MHz, Acetone-*d*₆): δ = 8.06 (d, *J* = 13.8 Hz, 1H), 7.81 (d, *J* = 8.3 Hz, 2H), 7.51 (d, *J* = 8.3 Hz, 2H), 7.29 (d, *J* = 19.2 Hz, 1H), 6.57 (dd, *J* = 29.7, 16.5 Hz, 2H), 4.51 (s, 1H), 3.70 (dd, *J* = 9.8, 5.5 Hz, 2H), 3.64 – 3.51 (m, 3H), 3.44 – 3.37 (m, 1H), 2.62 (t, *J* = 5.5 Hz, 1H), 2.45 (s, 3H), 2.36 – 2.28 (m, 1H), 2.08 (d, *J* = 5.5 Hz, 1H), 1.84 – 1.76 (m, 1H), 1.55 (d, *J* = 12.9 Hz, 1H), 1.47 (m, 2H), 1.23 – 1.13 (m, 4H), 1.00 (m, 2H), 0.16 (s, 9H) ppm.

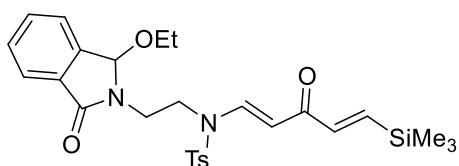
¹³C NMR (125 MHz, Acetone-*d*₆): δ = 187.6, 177.0, 146.3, 146.2, 144.1, 141.6, 136.1, 131.3 (×2), 128.1 (×2), 105.3, 95.3, 63.7, 44.6, 39.6, 39.0, 38.4, 27.6, 24.2, 23.5, 23.4, 21.5, 15.9, -1.7 (×3) ppm.

HRMS (ESI-TOF) m/z: [M+Na]⁺ calcd for C₂₇H₄₀N₂O₅SSiNa 555.2319; Found 555.2296.

IR (neat): ν = 2932, 1698, 1571, 1362, 1166 cm⁻¹

R_f: 0.56 (CH₂Cl₂/acetone 95:5 v/v, UV)

Compound 265i : *N*-(2-(1-ethoxy-3-oxo-3*a*,4,7,7*a*-tetrahydro-1*H*-4,7-methanoisoindol-2(3*H*)-yl)ethyl)-4-methyl-*N*-((1*E*,4*E*)-3-oxo-5-(trimethylsilyl)penta-1,4-dien-1-yl)benzenesulfonamide



C₂₇H₃₄N₂O₅SSi
MW : 526.19 g.mol⁻¹
Colorless oil
90% (189.4 mg, 0.36 mmol)

¹H NMR (500 MHz, CDCl₃): δ = 8.18 (d, *J* = 13.8 Hz, 1H), 7.78 (d, *J* = 7.4 Hz, 1H), 7.72 (d, *J* = 8.3 Hz, 2H), 7.58 (d, *J* = 7.3 Hz, 1H), 7.55 – 7.48 (m, 2H), 7.31 (d, *J* = 8.1 Hz, 2H), 7.21 (d, *J* = 19.0 Hz, 1H), 6.56 (d, *J* = 19.0 Hz, 1H), 6.27 (d, *J* = 13.8 Hz, 1H), 5.84 (s, 1H), 3.80 (d, *J* = 9.4 Hz, 2H), 3.69 – 3.60 (m, 2H), 3.27 – 3.12 (m, 2H), 2.40 (s, 3H), 1.16 (t, *J* = 7.0 Hz, 3H), 0.19 – 0.09 (m, 9H) ppm.

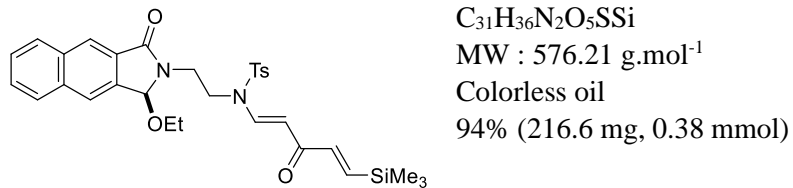
¹³C NMR (125 MHz, CDCl₃): δ = 187.8, 168.1, 146.6, 145.1, 142.6, 141.6, 141.4, 134.8, 132.3, 132.1, 130.3, 130.0 (×2), 127.3 (×2), 123.5, 123.4, 104.6, 87.2, 59.1, 43.9, 37.3, 21.6, 15.2, -1.7 (×3) ppm.

HRMS (ESI-TOF) m/z: [M+Na]⁺ calcd for C₂₇H₃₄N₂O₅SSiNa 549.1850; Found 549.1835.

IR (neat): ν = 2955, 1699, 1569, 1360, 1151 cm⁻¹

R_f: 0.65 (CH₂Cl₂/acetone 95:5 v/v, UV)

Compound 265j : *N*-(2-(1-ethoxy-3-oxo-1*H*-benzo[f]isoindol-2(3*H*)-yl)ethyl)-4-methyl-N-((1*E*,4*E*)-3-oxo-5-(trimethylsilyl)pent-1,4-dien-1-yl)benzenesulfonamide



¹H NMR (500 MHz, CDCl₃): δ = 8.30 (s, 1H), 8.20 (d, J = 13.8 Hz, 1H), 8.01 (d, J = 7.9 Hz, 1H), 7.95 (d, J = 11.5 Hz, 2H), 7.73 (d, J = 8.3 Hz, 2H), 7.65 – 7.56 (m, 2H), 7.30 (d, J = 8.3 Hz, 2H), 7.21 (d, J = 19.0 Hz, 1H), 6.57 (d, J = 19.0 Hz, 1H), 6.30 (d, J = 13.8 Hz, 1H), 6.00 (s, 1H), 3.88 (t, J = 7.3 Hz, 2H), 3.76 – 3.69 (m, 2H), 3.33 – 3.14 (m, 2H), 2.38 (s, 3H), 1.18 (t, J = 7.0 Hz, 3H), 0.15 (s, 9H) ppm.

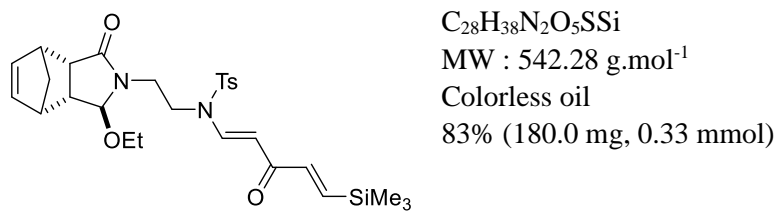
¹³C NMR (125 MHz, CDCl₃): δ = 187.8, 168.0, 146.6, 145.1, 142.6, 141.6, 136.2, 135.2, 134.8, 133.8, 130.3 ($\times 2$), 129.7, 129.4, 128.6, 128.2, 127.3 ($\times 2$), 127.2, 123.2, 123.1, 104.7, 87.2, 59.0, 43.9, 37.5, 21.6, 15.2, -1.7 ($\times 3$) ppm.

HRMS (ESI-TOF) m/z: [M+K]⁺ calcd for C₃₁H₃₆N₂O₅SSiK 615.1746; Found 615.1748.

IR (neat): ν = 2954, 1700, 1569, 1360, 1163 cm⁻¹

R_f: 0.65 (CH₂Cl₂/acetone 95:5 v/v, UV)

Compound 265k: *N*-(2-(1-ethoxy-3-oxoisooindolin-2-yl)ethyl)-4-methyl-N-((1*E*,4*E*)-3-oxo-5-(trimethylsilyl)pent-1,4-dien-1-yl)benzenesulfonamide



¹H NMR (500 MHz, CDCl₃): δ = 8.14 (d, J = 13.8 Hz, 1H), 7.69 (d, J = 8.3 Hz, 2H), 7.31 (d, J = 8.3 Hz, 2H), 7.22 (d, J = 19.0 Hz, 1H), 6.60 (d, J = 19.0 Hz, 1H), 6.30 (d, J = 13.8 Hz, 1H), 6.17 (m, 2H), 4.49 (s, 1H), 3.65 (d, J = 8.8 Hz, 2H), 3.61 – 3.53 (m, 3H), 3.30 – 3.18 (m, 1H), 3.09 (s, 1H), 2.86 (s, 1H), 2.51 (d, J = 7.8 Hz, 1H), 2.41 (s, 3H), 2.10 (d, J = 7.8 Hz, 1H), 1.41 (d, J = 9.5 Hz, 1H), 1.28 (t, J = 7.0 Hz, 3H), 1.16 (d, J = 9.5 Hz, 1H), 0.14 (s, 9H) ppm.

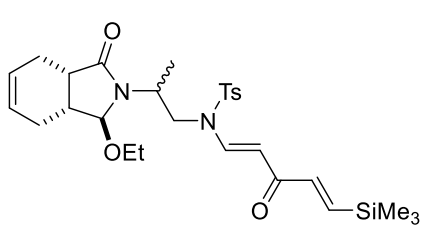
¹³C NMR (125 MHz, CDCl₃): δ = 187.8, 175.2, 146.6, 145.0, 142.6, 141.4, 137.6, 137.2, 134.9, 130.2 ($\times 2$), 127.2 ($\times 2$), 104.9, 93.9, 62.1, 49.1, 46.2, 46.1, 44.6, 43.5, 43.1, 38.8, 21.6, 15.4, -1.7 ($\times 3$) ppm.

HRMS (ESI-TOF) m/z: [M+Na]⁺ calcd for C₂₈H₃₈N₂O₅SSiNa 565.2163; Found 565.2142.

IR (neat): ν = 2975, 1684, 1559, 1360, 1162 cm⁻¹

R_f: 0.56 (CH₂Cl₂/acetone 95:5 v/v, UV)

Compound 265m: *N*-(2-(1-ethoxy-3-oxo-1,3,3a,4,7,7a-hexahydro-2*H*-isoindol-2-yl)propyl)-4-methyl-*N*-((1*E*,4*E*)-3-oxo-5-(trimethylsilyl)penta-1,4-dien-1-yl)benzenesulfonamide



C₂₈H₄₀N₂O₅SSi
MW : 544.24 g.mol⁻¹
Colorless oil
67% (145.9 mg, 0.27 mmol)

¹H NMR (500 MHz, Acetone-*d*₆): δ = 8.02 (dd, *J* = 13.9, 0.7 Hz, 1H), 7.74 (d, *J* = 8.4 Hz, 2H), 7.49 (d, *J* = 8.0 Hz, 2H), 7.33 (d, *J* = 19.3 Hz, 1H), 6.70 (d, *J* = 13.9 Hz, 1H), 6.53 (d, *J* = 19.3 Hz, 1H), 5.64 (d, *J* = 1.0 Hz, 2H), 4.59 (s, 1H), 4.41 – 4.26 (m, 1H), 3.76 (m, 1H), 3.63 (m, 2H), 3.39 (dd, *J* = 14.3, 4.9 Hz, 1H), 2.88 – 2.85 (m, 1H), 2.49 – 2.38 (m, 5H), 2.22 (m, 2H), 1.69 (m, 1H), 1.34 (d, *J* = 7.0 Hz, 3H), 1.25 (t, *J* = 7.0 Hz, 3H), 0.16 (s, 9H) ppm.

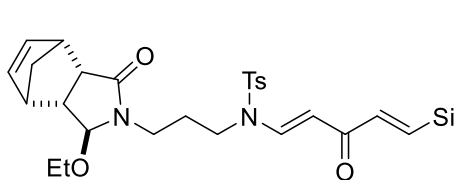
¹³C NMR (126 MHz, Acetone-*d*₆): δ = 187.8, 177.4, 146.4, 146.1, 144.4, 142.0, 136.0, 131.2 (×2), 127.9 (×2), 126.7, 125.9, 105.8, 94.1, 63.2, 50.7, 46.2, 37.9, 34.8, 25.3, 22.1, 21.5, 15.9, 15.3, -1.7 (×3) ppm.

HRMS (ESI-TOF) m/z: [M+Na]⁺ calcd for C₂₈H₄₀N₂O₅SSiNa 567.2319; Found 567.2310.

IR (neat): ν = 2954, 1697, 1573, 1362, 1169 cm⁻¹

R_f: 0.65 (CH₂Cl₂/acetone 95:5 v/v, UV)

Compound 265n: *N*-(3-(1-ethoxy-3-oxo-3a,4,7,7a-tetrahydro-1*H*-isoindol-2(3*H*)-yl)propyl)-4-methyl-*N*-((1*E*,4*E*)-3-oxo-5-(trimethylsilyl)penta-1,4-dien-1-yl)benzenesulfonamide



C₂₉H₄₀N₂O₅SSi
MW : 556.24 g.mol⁻¹
Colorless oil
90 % (200.2 mg, 0.36 mmol)

¹H NMR (500 MHz, Acetone-*d*₆): δ = 8.14 (d, *J* = 13.8 Hz, 1H), 7.66 (d, *J* = 8.3 Hz, 2H), 7.31 (d, *J* = 8.1 Hz, 2H), 7.08 (d, *J* = 18.9 Hz, 1H), 6.58 (d, *J* = 18.9 Hz, 1H), 6.18 (m, 2H), 5.74 (d, *J* = 13.8 Hz, 1H), 4.52 (s, 1H), 3.49 (m, 3H), 3.42 – 3.28 (m, 3H), 3.11 (s, 1H), 2.88 (s, 1H), 2.53 (d, *J* = 7.7 Hz, 1H), 2.41 (s, 3H), 2.10 (d, *J* = 7.8 Hz, 1H), 1.92 (m, 2H), 1.42 (d, *J* = 9.3 Hz, 1H), 1.20 (t, *J* = 7.0 Hz, 3H), 1.14 (d, *J* = 9.3 Hz, 1H), 0.13 (s, 9H).

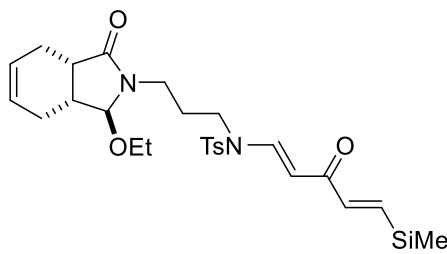
¹³C NMR (125 MHz, Acetone-*d*₆): δ = 187.6, 175.2, 146.2, 145.1, 142.2, 142.0, 137.7, 137.4, 135.1, 130.3 (×2), 127.3 (×2), 104.6, 92.8, 61.4, 49.3, 46.3, 45.5, 44.9, 44.6, 43.1, 38.5, 25.9, 21.7, 15.4, -1.6 (×3) ppm.

HRMS (ESI-TOF) m/z: [M+K]⁺ calcd for C₂₉H₄₀N₂O₅SSiK 595.2064; Found 595.2059.

IR (neat): ν = 2960, 1689, 1570, 1363, 1167 cm⁻¹

R_f: 0.39 (CH₂Cl₂/acetone 95:5 v/v, UV)

Compound 265o: *N*-(3-((1*S*,3*aS*,7*aR*)-1-ethoxy-3-oxo-1,3,3*a*,4,7,7*a*-hexahydro-2*H*-isoindol-2-yl)propyl)-4-methyl-*N*-((1*E*,4*E*)-3-oxo-5-(trimethylsilyl)penta-1,4-dien-1-yl)benzenesulfonamide

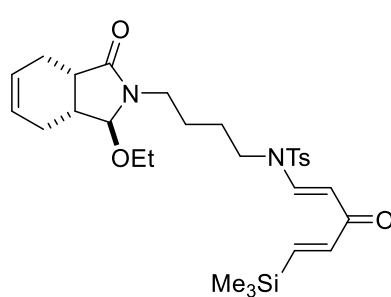


C₂₈H₄₀N₂O₅SSi
MW : 540.26 g.mol⁻¹
Colorless oil
63% (170.1 mg, 0.32 mmol)

¹H NMR (500 MHz, Acetone-*d*₆): δ = 8.10 (d, *J* = 13.8 Hz, 1H), 7.77 (d, *J* = 8.3 Hz, 2H), 7.48 (d, *J* = 8.1 Hz, 2H), 7.14 (d, *J* = 19.0 Hz, 1H), 6.65 (d, *J* = 19.0 Hz, 1H), 6.11 (d, *J* = 13.8 Hz, 1H), 5.72 (s, 2H), 4.54 (s, 1H), 3.65 – 3.54 (m, 3H), 3.49 (dt, *J* = 9.4, 4.9 Hz, 1H), 3.35 (ddd, *J* = 26.8, 14.1, 7.2 Hz, 2H), 2.88 – 2.82 (m, 1H), 2.53 – 2.38 (m, 5H), 2.33 – 2.14 (m, 2H), 2.01 – 1.90 (m, 1H), 1.88 – 1.72 (m, 2H), 1.16 (t, *J* = 7.0 Hz, 3H), 0.14 (s, 9H) ppm.

¹³C NMR (125 MHz, Acetone-*d*₆): δ = 187.1, 176.9, 146.0, 145.5, 143.8, 141.9, 136.2, 131.2 (×2), 128.0 (×2), 127.0, 126.0, 105.3, 95.6, 63.6, 45.1, 39.5, 37.6, 35.7, 26.7, 25.3, 22.5, 21.5, 15.7, -1.7 (×3) ppm.

Compound 265p: *N*-(4-(1-ethoxy-3-oxo-1,3,3a,4,7,7a-hexahydro-2H-isoindol-2-yl)butyl)-4-methyl-*N*-(*(1E,4E)*-3-oxo-5-(trimethylsilyl)penta-1,4-dien-1-yl)benzenesulfonamide



C₂₉H₄₂N₂O₅SSi
MW : 558.26 g.mol⁻¹
Colorless oil
92% (205.4 mg, 0.37 mmol)

¹H NMR (500 MHz, Acetone-*d*₆): δ = 8.09 (d, *J* = 13.8 Hz, 1H), 7.79 (d, *J* = 8.4 Hz, 2H), 7.48 (d, *J* = 8.4 Hz, 2H), 7.14 (d, *J* = 18.9 Hz, 1H), 6.70 (d, *J* = 18.9 Hz, 1H), 6.12 (d, *J* = 13.8 Hz, 1H), 5.66 (d, *J* = 1.3 Hz, 2H), 4.53 (s, 1H), 3.62 – 3.53 (m, 4H), 3.48 – 3.41 (m, 1H), 3.17 (d, *J* = 13.8 Hz, 1H), 2.81 (s, 1H), 2.42 (d, *J* = 20.3 Hz, 5H), 2.20 (dd, *J* = 7.9, 5.6 Hz, 2H), 1.75 – 1.66 (m, 1H), 1.61 (s, 4H), 1.18 (t, *J* = 7.0 Hz, 3H), 0.14 (s, 9H) ppm.

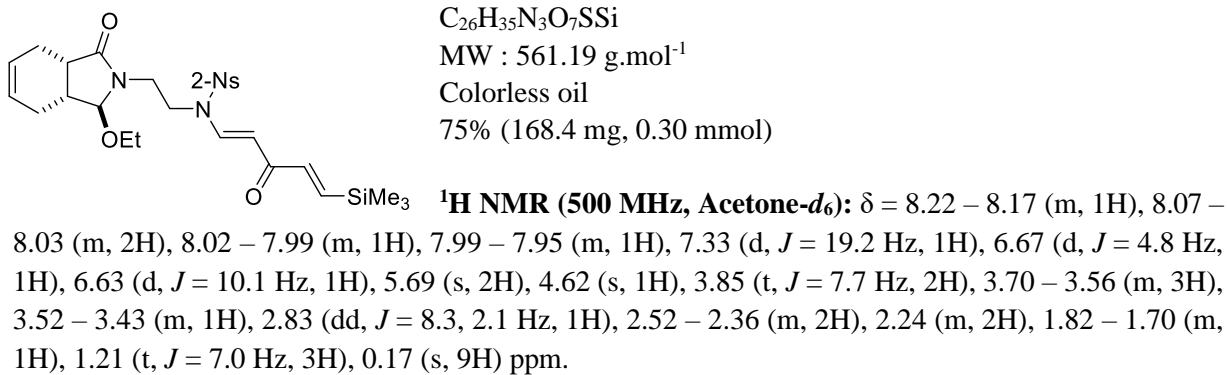
¹³C NMR (125 MHz, Acetone-*d*₆): δ = 187.1, 176.8, 145.9, 145.4, 145.4, 143.8, 142.1, 136.4, 131.2 (×2), 128.0 (×2), 127.2, 126.1, 105.8, 94.8, 63.3, 46.6, 40.3, 37.8, 35.7, 25.6, 25.5, 24.9, 22.6, 21.5, 15.8, -1.7 (×3) ppm.

HRMS (ESI-TOF) m/z: [M+Na]⁺ calcd for C₂₉H₄₂N₂O₅SSiNa 581.2476; Found 581.2464.

IR (neat): ν = 2953, 1696, 1569, 1363, 1166 cm⁻¹

R_f: 0.40 (CH₂Cl₂/acetone 95:5 v/v, UV)

Compound 265q: *N*-(2-(1-ethoxy-3-oxo-3*a*,4,7,7*a*-tetrahydro-1*H*-isoindol-2(3*H*)-yl)ethyl)-2-nitro-*N*-((1*E*,4*E*)-3-oxo-5-(trimethylsilyl)penta-1,4-dien-1-yl)benzenesulfonamide



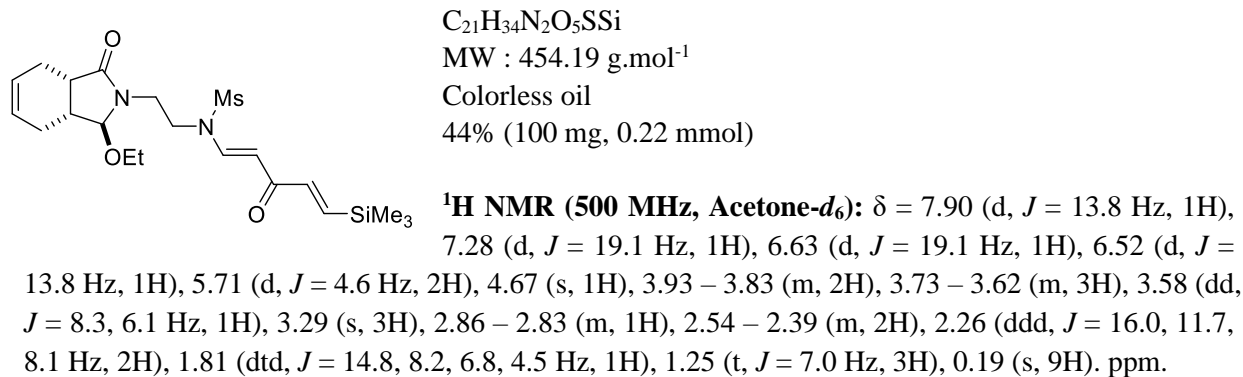
¹³C NMR (125 MHz, Acetone-*d*₆): $\delta = 187.6, 177.6, 148.9, 146.6, 143.8, 141.1, 136.8, 133.9, 131.9, 131.0, 126.9, 126.1, 126.1, 106.0, 96.2, 63.6, 44.7, 39.4, 37.5, 35.8, 25.4, 22.4, 15.8, -1.7 (\times 3)$ ppm.

HRMS (ESI-TOF) m/z: [M+Na]⁺ calcd for $C_{26}H_{35}N_3O_7SSiNa$ 584.1857; Found 584.1846.

IR (neat): $\nu = 3359, 2954, 1698, 1544, 1371, 1171$ cm⁻¹

R_f: 0.40 (CH₂Cl₂/acetone 95:5 v/v, UV)

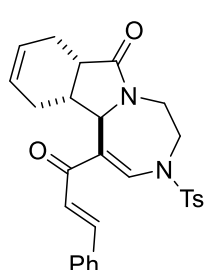
Compound 265r: *N*-(2-((1*S*,3*a*S,7*a*R)-1-ethoxy-3-oxo-1,3*a*,4,7,7*a*-hexahydro-2*H*-isoindol-2-yl)ethyl)-*N*-((1*E*,4*E*)-3-oxo-5-(trimethylsilyl)penta-1,4-dien-1-yl)methanesulfonamide



¹³C NMR (125 MHz, Acetone-*d*₆): $\delta = 187.6, 177.5, 145.8, 144.0, 142.1, 126.9, 126.1, 104.7, 96.3, 63.7, 44.8, 40.4, 39.9, 37.6, 35.9, 25.4, 22.4, 15.8, -1.7 (\times 3)$ ppm.

Characterization data for 251 and 269

Compound 251: 1-cinnamoyl-3-tosyl-3,4,5,7a,8,11,11a,11b-octahydro-7H-[1,4]diazepino[7,1-a]isoindol-7-one



C₂₈H₂₈N₂O₄S
MW : 488.18 g.mol⁻¹
Colorless oil
65% (126.9 mg, 0.26 mmol)

¹H NMR (500 MHz, CDCl₃): δ = 7.82 (s, 1H), 7.68 (d, J = 8.2 Hz, 2H), 7.65 – 7.54 (m, 3H), 7.46 – 7.40 (m, 3H), 7.35 (d, J = 8.2 Hz, 2H), 7.05 (d, J = 15.6 Hz, 1H), 5.72 – 5.68 (m, 2H), 4.41 (s, 1H), 4.29 – 4.18 (m, 1H), 4.05 – 3.96 (m, 1H), 3.61 – 3.55 (m, 1H), 3.02 – 3.0 (m, 1H), 2.53 – 2.36 (m, 1H), 2.47 (s, 3H), 2.19 – 2.15 (m, 1H), 1.86 – 1.82 (m, 1H) ppm.

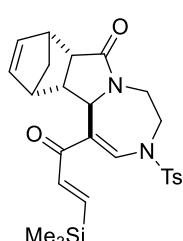
¹³C NMR (125 MHz, CDCl₃): δ = 191.4, 176.0, 145.3, 144.1, 138.8, 134.6, 134.4, 130.7, 130.4 (×2), 129.0 (×2), 128.4 (×2), 127.2 (×2), 126.0, 125.4, 124.7, 122.0, 63.2, 47.9, 41.2, 37.8, 35.6, 26.9, 21.9, 21.7 ppm.

HRMS (ESI-TOF) m/z: [M+Na]⁺ calcd for C₂₈H₂₈N₂O₄SNa 511.1662; Found 511.1636.

IR (neat): ν = 2920, 2248, 1690, 1594, 1163 cm⁻¹

R_f: 0.43 (CH₂Cl₂/acetone 95:5 v/v, UV)

Compound 269: (7aS,11aR)-3-tosyl-1-((E)-3-(trimethylsilyl)acryloyl)-3,4,5,7a,8,11,11a,11b-octahydro-7H-[1,4]diazepino[7,1-a]isoindol-7-one



C₂₆H₃₂N₂O₄SSi
MW : 496.19 g.mol⁻¹
Colorless oil
61% (121 mg, 0.24 mmol)

¹H NMR (500 MHz, CDCl₃): δ = 7.94 (s, 1H), 7.66 (d, J = 8.2 Hz, 2H), 7.36 (d, J = 8.2 Hz, 2H), 7.00 (d, J = 18.8 Hz, 1H), 6.80 (d, J = 18.8 Hz, 1H), 6.12 (s, 2H), 4.34 (s, 1H), 4.18 (m, 1H), 3.92 – 3.83 (m, 1H), 3.63 – 3.50 (m, 1H), 3.26 (s, 1H), 3.11 (s, 1H), 2.97 – 2.87 (m, 1H), 2.45 (s, 3H), 2.33 (d, J = 8.2 Hz, 1H), 1.85 (d, J = 7.4 Hz, 1H), 1.44 (d, J = 9.3 Hz, 1H), 1.29 (d, J = 9.3 Hz, 1H), 0.20 (s, 9H) ppm.

¹³C NMR (125 MHz, CDCl₃): δ = 192.3, 174.4, 147.6, 145.6, 138.9, 137.9, 137.8, 137.4, 134.3, 130.5 (×2), 127.3 (×2), 123.4, 63.6, 49.2, 49.2, 49.0, 46.7, 46.0, 43.0, 40.4, 21.8, -1.6 (×3) ppm.

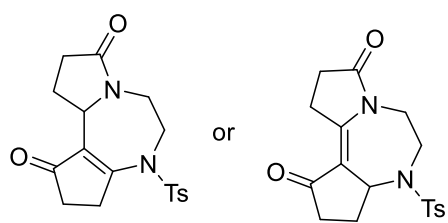
HRMS (ESI-TOF) m/z: [M+Na]⁺ calcd for C₂₆H₃₂N₂O₄SSiNa 519.1744; Found 519.1714.

IR (neat): ν = 2956, 2875, 1678, 1613, 1357, 1249, 1164. cm⁻¹

R_f: 0.45 (CH₂Cl₂/acetone 95:5 v/v, UV)

Characterization data for 266

Compound 266a:

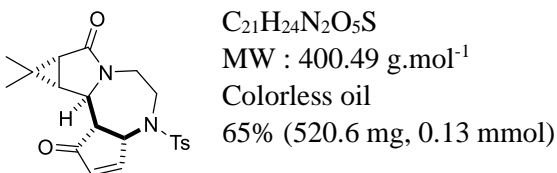


C₁₈H₂₀N₂O₄S
MW : 360.11 g.mol⁻¹
44% (31.0 mg, 0.088 mmol)

¹H NMR (500 MHz, CDCl₃): δ = 7.72 (d, J = 8.3 Hz, 2H), 7.35 (d, J = 8.0 Hz, 2H), 4.58 (dq, J = 5.9, 2.0 Hz, 1H), 4.43 – 4.23 (m, 2H), 3.65 (ddd, J = 14.3, 12.4, 3.8 Hz, 1H), 3.13 – 3.04 (m, 1H), 3.04 – 2.93 (m, 1H), 2.76 (ddt, J = 18.2, 5.7, 2.8 Hz, 1H), 2.47 – 2.38 (m, 6H), 2.26 (dtd, J = 17.2, 9.1, 4.8 Hz, 2H), 2.15 – 2.06 (m, 1H) ppm.

¹³C NMR (125 MHz, CDCl₃): δ = 203.8, 175.6, 169.3, 145.3, 135.9, 130.3 (×2), 127.4 (×2), 126.9, 55.1, 50.1, 42.2, 34.6, 29.3, 28.6, 23.8, 21.7 ppm.

Compound 266b: (8aR,9aS,9bR)-9,9-dimethyl-4-tosyl-3a,5,6,8a,9,9a,9b,9c-octahydro-1H-cyclopenta[f]cyclopropa[3,4]pyrrolo[1,2-d][1,4]diazepine-1,8(4H)-dione



C₂₁H₂₄N₂O₅S
MW : 400.49 g.mol⁻¹
Colorless oil
65% (520.6 mg, 0.13 mmol)

¹H NMR (500 MHz, CDCl₃): δ = 7.68 (d, J = 8.3 Hz, 2H), 7.32 (d, J = 8.3 Hz, 2H), 7.22 (dd, J = 5.8, 2.4 Hz, 1H), 6.31 (dd, J = 5.8, 2.5 Hz, 1H), 4.87 (dd, J = 3.9, 2.5 Hz, 1H), 4.08 – 4.05 (m, 1H), 3.61 – 3.59 (m, 2H), 3.50 (dd, J = 10.0, 1.0 Hz, 1H), 2.85 (dt, J = 14.0, 5.2 Hz, 1H), 2.62 (dd, J = 10.0, 6.5 Hz, 1H), 2.44 (s, 3H), 2.23 (d, J = 6.0 Hz, 1H), 1.79 (dd, J = 6.0, 1.5 Hz, 1H), 1.12 (s, 3H), 0.89 (s, 3H) ppm.

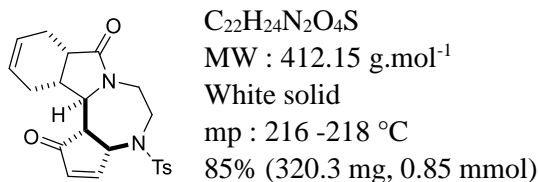
¹³C NMR (125 MHz, CDCl₃): δ = 203.3, 174.5, 158.5, 144.3, 138.1, 136.3, 130.2 (×2), 127.3 (×2), 62.6, 56.2, 55.7, 48.1, 43.7, 31.6, 28.1, 25.8, 22.7, 21.7, 14.8 ppm.

HRMS (ESI-TOF) m/z: [M+Na]⁺ calcd for C₂₁H₂₄N₂O₅SNa 423.1349; Found 423.1307.

IR (neat): ν = 2925, 1682, 1334, 1158 cm⁻¹

R_f: 0.35 (CH₂Cl₂/acetone 90:10 v/v, UV)

Compound 266c: 4-tosyl-3a,4,5,6,8a,9,12,12a-octahydrocyclopenta[5,6][1,4]diazepino[7,1-a]isoindole-1,8(12bH,12cH)-dione



¹H NMR (500 MHz, CDCl₃): δ = 7.67 (d, *J* = 8.2 Hz, 2H), 7.32 (d, *J* = 8.2 Hz, 2H), 7.22 (dd, *J* = 5.8, 2.3 Hz, 1H), 6.32 (dd, *J* = 5.8, 2.3 Hz, 1H), 5.73 – 5.58 (m, 2H), 5.00 – 4.99 (m, 1H), 4.27 – 4.22 (m, 1H), 3.80 – 3.77 (m, 1H), 3.30-3.29 (m, 2H), 2.89 – 2.82 (m, 2H), 2.66 – 2.59 (m, 2H), 2.51 – 2.47 (m, 1H), 2.43 (s, 3H), 2.27 – 2.26 (m, 2H), 1.66 – 1.57 (m, 1H) ppm.

¹³C NMR (125 MHz, CDCl₃): δ = 203.6, 176.5, 159.2, 144.1, 137.6, 136.1, 130.1 (×2), 127.2 (×2), 125.7, 124.5, 62.0, 61.5, 50.5, 46.1, 43.1, 36.3, 34.0, 25.9, 21.6, 21.6 ppm.

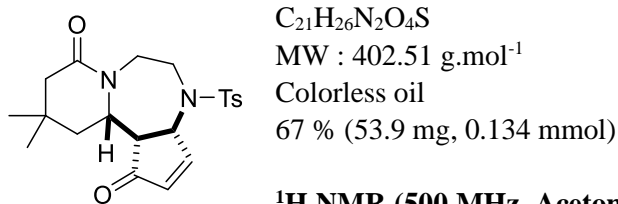
HRMS (ESI-TOF) m/z: [M+H]⁺ calcd for C₂₂H₂₅N₂O₄S 413.1535; Found 413.1529.

IR (neat): ν = 1678, 1330, 1152 cm⁻¹

R_f: 0.60 (CH₂Cl₂/acetone 90:10 v/v, UV)

CCDC 1831780 (266c) contains the supplementary crystallographic data for this paper. These data can be obtained free of charge from The Cambridge Crystallographic Data Centre.

Compound 266d: (11aR)-10,10-dimethyl-4-tosyl-3a,5,6,9,10,11,11a,11b-octahydro-1H-cyclopenta[f]pyrido[1,2-d][1,4]diazepine-1,8(4H)-dione



¹H NMR (500 MHz, Acetone-d₆): δ = 7.72 (d, *J* = 8.3 Hz, 2H), 7.34 (d, *J* = 8.3 Hz, 2H), 7.19 (dd, *J* = 5.9, 2.9 Hz, 1H), 6.41 (dd, *J* = 5.9, 1.7 Hz, 1H), 5.65 – 5.62 (m, 1H), 4.42 (dd, *J* = 12.7, 4.0 Hz, 1H), 4.32 (dd, *J* = 14.8, 8.5 Hz, 1H), 4.12 – 4.06 (m, 1H), 2.61 (dd, *J* = 12.7, 5.9 Hz, 1H), 2.44 (s, 3H), 2.39 (d, *J* = 7.5 Hz, 1H), 2.18 – 2.10 (m, 2H), 1.97 (d, *J* = 17.2 Hz, 1H), 1.80 (t, *J* = 12.8 Hz, 1H), 1.52 – 1.48 (m, 1H), 1.06 (s, 3H), 0.97 (s, 3H) ppm.

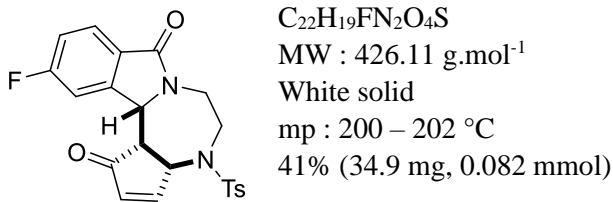
¹³C NMR (125 MHz, Acetone-d₆): δ = 205.5, 170.3, 159.5, 144.0, 137.5, 136.1, 130.2 (×2), 127.1 (×2), 57.7, 52.7, 50.2, 45.1, 43.6, 42.3, 39.7, 31.0, 29.7, 26.4, 21.7 ppm.

HRMS (ESI-TOF) m/z: [M+Na]⁺ calcd for C₂₁H₂₆N₂O₄SNa 425.1505; Found 425.1493.

IR (neat): ν = 2957, 1714, 1633, 1333, 1157, 1089 cm⁻¹

R_f: 0.45 (CH₂Cl₂/acetone 95:5 v/v, UV)

Compound 266e: 11-fluoro-4-tosyl-3a,4,5,6-tetrahydrocyclopenta[5,6][1,4]diazepino[7,1-a]isoindole-1,8(12bH,12cH)-dione



¹H NMR (500 MHz, CDCl₃): δ = 7.78 (dd, *J* = 8.2, 5.1 Hz, 1H), 7.67 (d, *J* = 8.2 Hz, 2H), 7.62 (dd, *J* = 5.8, 1.9 Hz, 1H), 7.33 (d, *J* = 8.1 Hz, 2H), 7.23 – 7.19 (m, 1H), 7.14 (td, *J* = 8.1, 1.9 Hz, 1H), 6.16 (dd, *J* = 5.8, 2.2 Hz, 1H), 5.17 (d, *J* = 8.1 Hz, 1H), 4.39 (d, *J* = 14.7 Hz, 1H), 3.97 (d, *J* = 14.7 Hz, 1H), 3.66 – 3.65 (m, 1H), 3.61 – 3.59 (dd, *J* = 8.1, 4.0 Hz, 1H), 3.49 – 3.29 (m, 2H), 2.45 (s, 3H) ppm.

¹³C NMR (125 MHz, CDCl₃): δ = 202.3, 167.8, 166.3 (d, *J* = 250.0 Hz), 161.2, 144.5, 143.8 (d, *J* = 10.2 Hz), 137.6, 132.3, 130.2 (×2), 127.1 (×2), 125.5 (d, *J* = 11.0 Hz), 117.1 (d, *J* = 23.8 Hz), 113.5 (d, *J* = 25.0 Hz), 61.4, 57.7(d, *J* = 2.6 Hz), 55.2, 49.7, 43.2, 21.6 ppm.

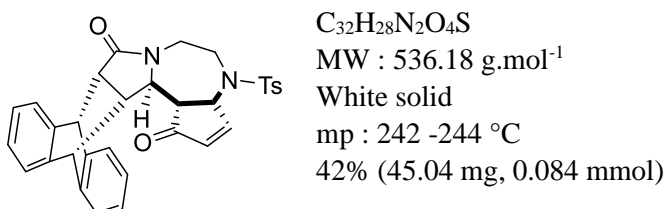
HRMS (ESI-TOF) m/z: [M+K]⁺ calcd for C₂₂H₁₉FN₂O₄SK 465.0681; Found 465.0657.

IR (neat): ν = 1674, 1401, 1347, 1145 cm⁻¹

R_f: 0.35 (CH₂Cl₂/acetone 95:5 v/v, UV)

CCDC 2001081 (**266e**) contains the supplementary crystallographic data for this paper. These data can be obtained free of charge from The Cambridge Crystallographic Data Centre.

Compound 266f: (6bS,7S,12R,12aR)-4-tosyl-4,5,6,6a,6b,7,12,12a-octahydro-7,12-[1,2]benzenobenzo[f]cyclopenta[2,3][1,4]diazepino[7,1-a]isoindole-1,13(3aH,14aH)-dione



¹H NMR (500 MHz, CDCl₃): δ = 7.61 (d, *J* = 8.2 Hz, 2H), 7.38 (dd, *J* = 5.2, 3.0 Hz, 1H), 7.33 (dd, *J* = 5.2, 3.0 Hz, 1H), 7.30 – 7.27 (m, 3H), 7.23 (dd, *J* = 5.2, 3.0 Hz, 1H), 7.17 – 7.12 (m, 3H), 7.09 (dd, *J* = 5.5, 3.0 Hz, 2H), 6.34 (dd, *J* = 5.8, 2.4 Hz, 1H), 4.78 (dd, *J* = 4.0, 2.4 Hz, 1H), 4.68 (s, 1H), 4.32 (s, 1H), 3.70 – 3.65 (m, 1H), 3.44 – 3.38 (m, 1H), 3.33 – 3.26 (m, 1H), 3.18 (d, *J* = 10.0 Hz, 1H), 3.03 (s, 2H), 2.47 (s, 3H), 2.49 – 2.39 (m, 1H), 1.82 – 1.78 (m, 1H) ppm.

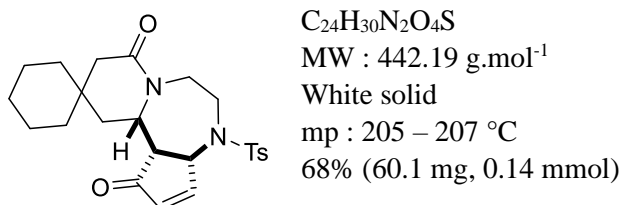
¹³C NMR (125 MHz, CDCl₃): δ = 203.4, 174.8, 158.5, 144.1, 142.6, 141.3, 140.3, 138.9, 137.8, 136.0, 130.0 (×2), 127.2 (×2), 126.5, 126.3, 126.3, 126.3, 125.1, 124.5, 124.1, 124.0, 62.1, 59.9, 56.4, 48.3, 48.1, 47.2, 46.2, 43.8, 43.3, 21.6 ppm.

HRMS (ESI-TOF) m/z: [M+Na]⁺ calcd for C₃₂H₂₈N₂O₄SNa 559.1662; Found 559.1679.

IR (neat): ν = 1687, 1401, 1347, 1145 cm⁻¹

R_f: 0.61 (CH₂Cl₂/acetone 90:10 v/v, UV)

Compound 266g: 4'-tosyl-3a',5',6',11',11a',11b'-hexahydrospiro[cyclohexane-1,10'-cyclopenta[f]pyrido[1,2-d][1,4]diazepine]-1',8'(4'H,9'H)-dione



¹H NMR (500 MHz, CDCl₃): δ = 7.72 (d, *J* = 8.2 Hz, 2H), 7.34 (d, *J* = 8.2 Hz, 2H), 7.14 (dd, *J* = 5.9, 2.7 Hz, 1H), 6.39 (dd, *J* = 5.9, 1.5 Hz, 1H), 5.64 (d, *J* = 7.4 Hz, 1H), 4.40 (dd, *J* = 12.5, 3.8 Hz, 1H), 4.33 (dd, *J* = 14.9, 8.0 Hz, 1H), 4.05 (td, *J* = 12.0, 8.7 Hz, 1H), 2.60 (dd, *J* = 12.7, 5.7 Hz, 1H), 2.44 – 2.43 (s, 3H), 2.44 – 2.43 (m, 1H), 2.34 (d, *J* = 16.8 Hz, 1H), 2.17 – 2.11 (m, 1H), 1.92 (d, *J* = 16.8 Hz, 1H), 1.80 (t, *J* = 12.9 Hz, 1H), 1.67 – 1.62 (m, 1H), 1.45 – 1.39 (m, 8H), 1.29 – 1.24 (m, 2H) ppm.

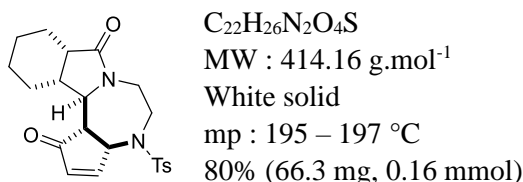
¹³C NMR (125 MHz, CDCl₃): δ = 205.2, 170.4, 159.3, 143.9, 137.2, 136.2, 130.1 (×2), 127.0 (×2), 57.7, 51.6, 50.0, 43.0, 42.5, 41.1, 39.5, 39.4, 34.9, 32.4, 26.0, 21.7, 21.6, 21.5 ppm.

HRMS (ESI-TOF) m/z: [M+Na]⁺ calcd for C₂₄H₃₀N₂O₄SNa 465.1818; Found 465.1788.

IR (neat): ν = 2924, 1715, 1636, 1334, 1162 cm⁻¹

R_f: 0.33 (CH₂Cl₂/acetone 90:10 v/v, UV)

Compound 266h: 4-tosyl-3a,4,5,6,8a,9,10,11,12,12a-decahydrocyclopenta[5,6][1,4]diazepino[7,1-a]isoindole-1,8(12bH,12cH)-dione



¹H NMR (500 MHz, CDCl₃): δ = 7.66 (d, *J* = 8.3 Hz, 2H), 7.31 (d, *J* = 8.3 Hz, 2H), 7.23 (dd, *J* = 5.8, 2.3 Hz, 1H), 6.30 (dd, *J* = 5.8, 2.3 Hz, 1H), 4.97 – 4.96 (m, 1H), 4.27 – 4.22 (m, 1H), 3.88 – 3.74 (m, 1H), 3.30 (m, 1H), 3.15 (d, *J* = 9.8 Hz, 1H), 2.87 (dt, *J* = 13.5, 4.4 Hz, 1H), 2.74 – 2.65 (m, 1H), 2.54 (dd, *J* = 9.8, 6.5 Hz, 1H), 2.46 – 2.40 (m, 1H), 2.42 (s, 3H), 2.11 – 2.05 (m, 1H), 1.72 – 1.69 (m, 1H), 1.59 – 1.41 (m, 3H), 1.22 – 1.06 (m, 2H), 1.02 – 0.90 (m, 1H) ppm.

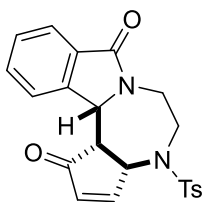
¹³C NMR (125 MHz, CDCl₃): δ = 203.6, 175.8, 159.4, 144.1, 137.5, 136.1, 130.0 (×2), 127.2 (×2), 61.6, 61.0, 50.5, 45.9, 43.2, 38.4, 37.3, 28.4, 23.8, 22.9, 22.8, 21.6 ppm.

HRMS (ESI-TOF) m/z: [M+Na]⁺ calcd for C₂₂H₂₆N₂O₄SNa 437.1486; Found 427.1505.

IR (neat): ν = 1679, 1431, 1335, 1156 cm⁻¹

R_f: 0.42 (CH₂Cl₂/acetone 90:10 v/v, UV)

Compound 266i: (3aS,12bS,12cS)-4-tosyl-3a,4,5,6,12b,12c-hexahydrocyclopenta[5,6][1,4]diazepino[7,1-a]isoindole-1,8-dione



C₂₂H₂₀N₂O₄S
MW : 408.47 g.mol⁻¹
White solid
mp : 205 - 207 °C
50% (40.8 mg, 0.10 mmol)

¹H NMR (500 MHz, CDCl₃): δ = 7.79 (d, *J* = 6.6 Hz, 1H), 7.66 (d, *J* = 8.0 Hz, 2H), 7.60 (dd, *J* = 5.8, 2.4 Hz, 1H), 7.50 – 7.41 (m, 3H), 7.33 (d, *J* = 8.0 Hz, 2H), 6.13 (dd, *J* = 5.8, 2.4 Hz, 1H), 5.19 (d, *J* = 8.0 Hz, 1H), 4.41 (dd, *J* = 14.6, 2.0 Hz, 1H), 3.98 (dd, *J* = 14.6, 2.2 Hz, 1H), 3.64 – 3.62 (m, 1H), 3.57 – 3.54 (dd, *J* = 8.0, 6.5 Hz, 1H), 3.47 – 3.32 (m, 2H), 2.44 (s, 3H) ppm.

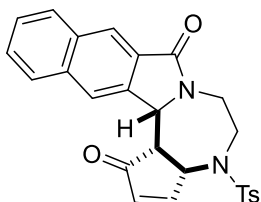
¹³C NMR (125 MHz, CDCl₃): δ = 202.7, 169.0, 161.4, 144.6, 141.5, 137.8, 133.3, 132.5, 132.3, 130.3 (×2), 129.2, 127.2 (×2), 125.9, 123.6, 61.5, 58.1, 55.2, 49.8, 43.2, 21.7 ppm.

HRMS (ESI-TOF) m/z: [M+Na]⁺ calcd for C₂₂H₂₀N₂O₄SnA 431.1036; Found 431.1021.

IR (neat): ν = 1672, 1345, 1142 cm⁻¹

R_f: 0.38 (CH₂Cl₂/acetone 95:5 v/v, UV)

Compound 266j: 4-tosyl-3a,4,5,6-tetrahydrobenzo[f]cyclopenta[5,6][1,4]diazepino[7,1-a]isoindole-1,8(14bH,14cH)-dione



C₂₆H₂₂N₂O₄S
MW : 458.13 g.mol⁻¹
White solid
mp : 220 - 222 °C
55% (50.4 mg, 0.11 mmol)

¹H NMR (500 MHz, CDCl₃): δ = 8.33 (s, 1H), 7.96 (d, *J* = 7.8 Hz, 1H), 7.94 (s, 1H), 7.89 (d, *J* = 7.8 Hz, 1H), 7.68 (d, *J* = 8.1 Hz, 2H), 7.60 – 7.54 (m, 3H), 7.34 (d, *J* = 8.1 Hz, 2H), 6.16 (dd, *J* = 5.8, 2.2 Hz, 1H), 5.37 (d, *J* = 7.9 Hz, 1H), 4.52 – 4.44 (m, 1H), 4.06 – 3.98 (m, 1H), 3.71 – 3.69 (m, 1H), 3.65 – 3.63 (m, 1H), 3.45 (m, 2H), 2.45 (s, 3H) ppm.

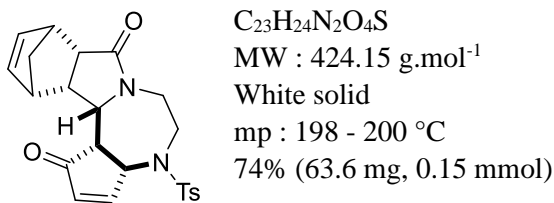
¹³C NMR (125 MHz, CDCl₃): δ = 202.9, 168.8, 161.4, 144.6, 137.8, 136.1, 135.5, 133.1, 132.5, 130.6 (×2), 130.3, 129.4, 128.9, 128.1, 127.2 (×2), 127.2, 125.5, 124.0, 61.8, 58.0, 56.0, 49.9, 43.4, 21.8 ppm.

HRMS (ESI-TOF) m/z: [M+H]⁺ calcd for C₂₆H₂₃N₂O₄S 459.1373; Found 459.1366.

IR (neat): ν = 1677, 1411, 1345, 1188 cm⁻¹

R_f: 0.39 (CH₂Cl₂/acetone 95:5 v/v, UV)

Compound 266k: 4-tosyl-3a,4,5,6,8a,9,12,12a-octahydro-9,12-methanocyclopenta[5,6][1,4]diazepino[7,1-a]isoindole-1,8(12bH,12cH)-dione



¹H NMR (500 MHz, CDCl₃): δ = 7.67 (d, *J* = 8.3 Hz, 2H), 7.32 (d, *J* = 8.3 Hz, 2H), 7.19 (dd, *J* = 5.9, 2.5 Hz, 1H), 6.30 (dd, *J* = 5.9, 2.5 Hz, 1H), 6.22 – 6.15 (m, 2H), 4.88 – 4.87 (m, 1H), 4.23 – 4.17 (m, 1H), 3.67 – 3.54 (m, 2H), 3.37 (d, *J* = 9.4 Hz, 1H), 3.19 (s, 1H), 2.97 – 2.92 (m, 1H), 2.80 (s, 1H), 2.53 (dd, *J* = 9.5, 6.5 Hz, 1H), 2.48 (s, 2H), 2.43 (s, 3H), 1.35 (d, *J* = 9.4 Hz, 1H), 1.06 (d, *J* = 9.4 Hz, 1H) ppm.

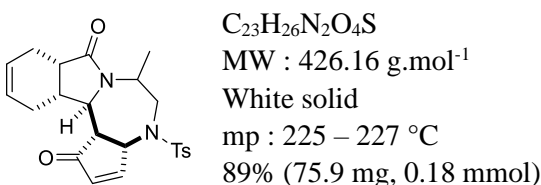
¹³C NMR (126 MHz, CDCl₃): δ = 203.3, 176.6, 158.1, 144.2, 138.0, 137.8, 137.1, 136.1, 130.0 (×2), 127.2 (×2), 62.1, 61.1, 56.8, 48.5, 48.2, 47.3, 46.5, 44.2, 44.2, 42.8, 21.6 ppm.

HRMS (ESI-TOF) m/z: [M+Na]⁺ calcd for C₂₃H₂₄N₂O₄SNa 447.1349; Found 447.1324.

IR (neat): ν = 1672, 1326, 1511 cm⁻¹

R_f: 0.41 (CH₂Cl₂/acetone 90:10 v/v, UV)

Compound 266m: 6-methyl-4-tosyl-3a,4,5,6,8a,9,12,12a,12b,12c-deahydrocyclopenta[5,6][1,4]diazepino[7,1-a]isoindole-1,8-dione



¹H NMR (500 MHz, CDCl₃): δ = 7.69 (d, *J* = 8.3 Hz, 2H), 7.32 – 7.30 (m, 3H), 6.31 (dd, *J* = 5.8, 2.5 Hz, 1H), 5.70 – 5.54 (m, 2H), 5.10 (d, *J* = 5.8 Hz, 1H), 4.47 – 4.42 (m, 1H), 4.02 (dd, *J* = 15.6, 4.8 Hz, 1H), 2.98 (d, *J* = 10.6 Hz, 1H), 2.74 (dt, *J* = 9.7, 6.7 Hz, 1H), 2.62 – 2.49 (m, 4H), 2.42 (s, 3H), 2.25 – 2.14 (m, 1H), 2.10 – 2.07 (m, 1H), 1.51 – 1.48 (m, 1H), 0.93 (d, *J* = 6.7 Hz, 3H) ppm.

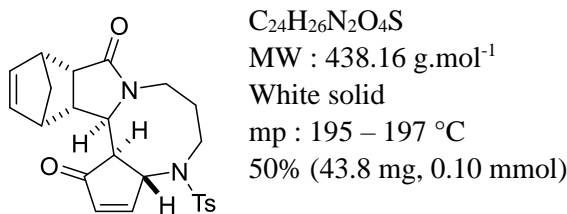
¹³C NMR (125 MHz, CDCl₃): δ = 203.1, 175.8, 161.4, 144.2, 136.7, 135.9, 130.1 (×2), 127.3 (×2), 125.9, 124.1, 60.0, 58.4, 50.2, 48.3, 48.2, 36.0, 33.7, 25.9, 21.6, 21.2, 14.8 ppm.

HRMS (ESI-TOF) m/z: [M+Na]⁺ calcd for C₂₃H₂₆N₂O₄SNa 449.1504; Found 449.1505.

IR (neat): ν = 1688, 1342, 1161 cm⁻¹

R_f: 0.48 (CH₂Cl₂/acetone 90:10 v/v, UV)

Compound 266n: 4-tosyl-4,5,6,7,9a,10,13,13a,13b,13c-decahydro-1H-10,13-methanocyclopenta[3,4][1,5]diazocino[2,1-a]isoindole-1,9(3aH)-dione



¹H NMR (500 MHz, CDCl₃): δ = 7.67 (d, *J* = 8.3 Hz, 2H), 7.56 (dd, *J* = 5.8, 2.1 Hz, 1H), 7.32 (d, *J* = 8.3 Hz, 2H), 6.21 (dd, *J* = 5.8, 2.1 Hz, 1H), 6.13 (dd, *J* = 5.6, 3.0 Hz, 1H), 6.02 (dd, *J* = 5.6, 3.0 Hz, 1H), 4.13 – 4.11 (m, 1H), 3.84 – 3.74 (m, 3H), 3.33 (dd, *J* = 5.5, 4.2 Hz, 1H), 3.17 (s, 1H), 3.14 – 3.09 (m, 1H), 2.92 (s, 1H), 2.85 – 2.79 (m, 1H), 2.44 (s, 3H), 2.35 – 2.29 (m, 2H), 2.00 – 1.93 (m, 1H), 1.49 – 1.45 (m, 2H), 1.33 (d, *J* = 9.6 Hz, 1H) ppm.

¹³C NMR (125 MHz, CDCl₃): δ = 203.5, 174.5, 161.8, 144.1, 138.2, 137.8, 137.0, 133.5, 130.0 (×2), 127.0 (×2), 64.0, 61.7, 56.5, 50.0, 49.3, 47.8, 45.7, 43.2, 41.6, 39.0, 26.2, 21.6 ppm.

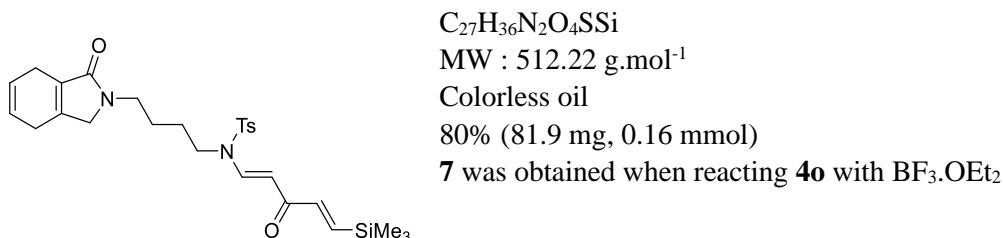
HRMS (ESI-TOF) m/z: [M+Na]⁺ calcd for C₂₄H₂₆N₂O₄SnA 461.1505; Found 461.1487.

IR (neat): ν = 2933, 1701, 1658, 1331, 1147 cm⁻¹

R_f: 0.36 (CH₂Cl₂/acetone 90:10 v/v, UV)

CCDC 2001082 (**266n**) contains the supplementary crystallographic data for this paper. These data can be obtained free of charge from The Cambridge Crystallographic Data Centre.

Compound 266p: 4-methyl-N-(4-(1-oxo-1,3,4,7-tetrahydro-2H-isoindol-2-yl)butyl)-N-((1*E*,4*E*)-3-oxo-5-(trimethylsilyl)penta-1,4-dien-1-yl)benzenesulfonamide



¹H NMR (500 MHz, CDCl₃): δ = 8.13 (d, *J* = 13.8 Hz, 1H), 7.67 (d, *J* = 8.3 Hz, 2H), 7.30 (d, *J* = 8.3 Hz, 2H), 7.09 (d, *J* = 18.9 Hz, 1H), 6.62 (d, *J* = 18.9 Hz, 1H), 5.73 (d, *J* = 13.8 Hz, 3H), 3.78 (s, 2H), 3.47 – 3.44 (m, 4H), 2.95 – 2.88 (m, 4H), 2.40 (s, 3H), 1.71 – 1.57 (m, 4H), 0.13 (s, 9H) ppm.

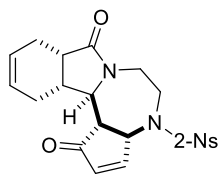
¹³C NMR (125 MHz, CDCl₃): δ = 187.6, 171.5, 146.7, 146.2, 145.0, 142.1, 142.0, 135.2, 130.3 (×2), 129.7, 127.2 (×2), 124.6, 122.6, 105.3, 52.9, 45.8, 41.0, 25.9, 25.8, 23.9, 22.4, 21.7, -1.6 (×3) ppm.

HRMS (ESI-TOF) m/z: [M+Na]⁺ calcd for C₂₇H₃₆N₂O₄SSiNa 535.2036; Found 535.2057.

IR (neat): ν = 2955, 1665, 1568, 1360, 1165 cm⁻¹

R_f: 0.30 (CH₂Cl₂/acetone 95:5 v/v, UV)

Compound 266q: (8aS,12aR,12bR)-4-((2-nitrophenyl)sulfonyl)-3a,4,5,6,8a,9,12,12a,12b,12c-deahydrocyclopenta[5,6][1,4]diazepino[7,1-a]isoindole-1,8-dione



C₂₁H₂₁N₃O₆S

MW : 443.47 g.mol⁻¹

Colorless oil

51 % (45.2 mg, 0.102 mmol)

¹H NMR (500 MHz, Acetone-*d*₆): δ = 8.12 (dd, *J* = 7.5, 1.4 Hz, 1H), 7.82 – 7.67 (m, 3H), 7.33 (dd, *J* = 5.6, 1.9 Hz, 1H), 6.39 (dd, *J* = 5.8, 2.2 Hz, 1H), 5.72 – 5.60 (m, 2H), 5.34 (d, *J* = 5.8 Hz, 1H), 4.06 – 3.96 (m, 1H), 3.88 – 3.85 (m, 1H), 3.37 (d, *J* = 8.0 Hz, 1H), 3.30 (m, 1H), 2.99 (dd, *J* = 9.0, 6.8 Hz, 1H), 2.81 – 2.87 (m, 1H), 2.82 – 2.79 (m, 1H), 2.73 (dt, *J* = 13.8, 4.5 Hz, 1H), 2.43 (d, *J* = 18.6 Hz, 1H), 2.32 – 2.22 (m, 2H), 1.67 – 1.63 (m, 1H) ppm.

¹³C NMR (125 MHz, Acetone-*d*₆): δ = 204.1, 176.6, 147.7, 136.7, 134.5, 134.1, 132.6, 131.6 (×2), 125.9, 125.0, 124.6, 62.1, 53.6, 50.0, 42.3, 36.4, 35.0, 29.9, 25.9, 21.8 ppm.

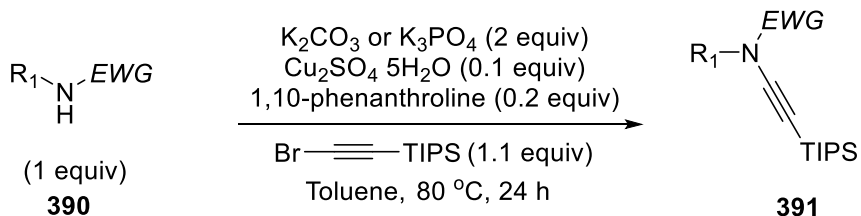
HRMS (ESI-TOF) m/z: [M+K]⁺ calcd for C₂₁H₂₁N₃O₆K 482.0783; Found 482.0812.

IR (neat): ν = 2923, 1689, 1542, 1369, 1162 cm⁻¹

R_f: 0.35 (CH₂Cl₂/acetone 90:10 v/v, UV)

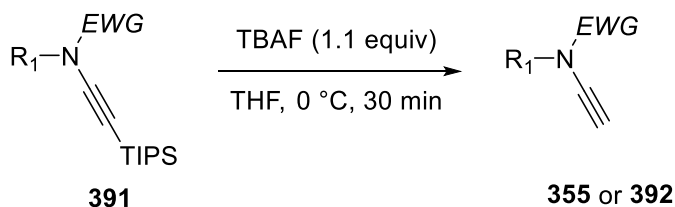
Chapter 2

1. Experimental procedure for **391**



General procedure for **391:**¹⁷⁷ To a mixture of an amide (1.0 equiv), K_3PO_4 or K_2CO_3 (2.0 equiv), $\text{CuSO}_4 \cdot 5\text{H}_2\text{O}$ (0.10 equiv), and 1,10-phenanthroline (0.20 equiv) in a reaction vial was added a solution of a respective 1-bromoalkyne (1.1 equiv, 1.0 M) in toluene. The reaction mixture was capped and heated in an oil bath at 80 °C for 24 h while being monitored with TLC analysis. Upon completion, the reaction mixture was cooled to rt and diluted with EtOAc and filtered, and the filtrate was concentrated under reduce pressure (15 mbar, 25 °C) and purified by column chromatography on silica gel using a mixture of petroleum ether/EtOAc as eluent to afford the desired product **391**.

2. Experimental procedure for **355** and **392**



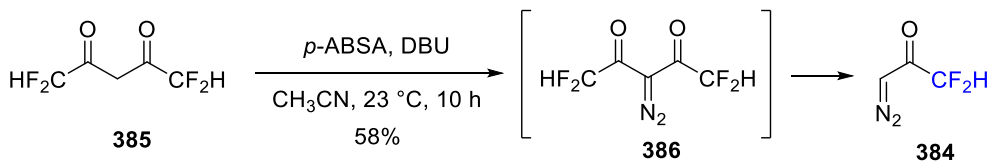
General procedure for **355 and **392**:**¹⁷⁸ To a solution of TIPS protected ynamide (1mmol, 1.0 equiv) in anhydrous 5 mL THF stirring at 0 °C was added TBAF (1.1 mmol, 1.1 equiv, 1M solution in THF) via syringe over a period of 5 minutes. The resulting solution was stirred at 0 °C. After TLC indicated that the starting material was completely consumed, the solution was concentrated in vacuo, purified by column chromatography on silica gel using a mixture of petroleum ether/EtOAc as eluent to afford the desired product **355** or **392** (or the reaction was quenched with water (5 mL) and extracted with ether 3 times. The combined organic extracts were dried (Na_2SO_4), concentrated under reduce pressure (15 mbar, 25 °C) and recrystallized with ether and petroleum ether).

3. Experimental procedure for compound **3**¹⁷⁹:

¹⁷⁷ Zhang, Y. S.; Hsung, R. P.; Tracey, M. R.; Kurtz, K. C. M.; Vera, E. L. *Org. Lett.*, **2004**, *6*, 1151 - 1154.

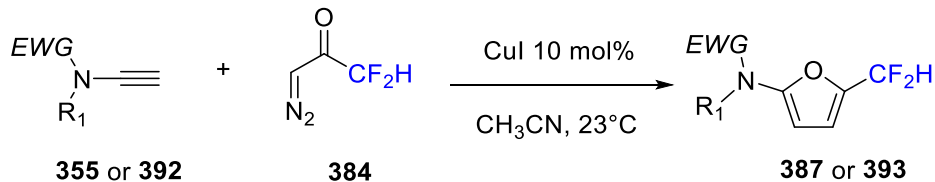
¹⁷⁸ Zhang, X. J.; Hsung, R. P.; Li, H. Y.; Zhang, Y.; Johnson, W. L.; Figueroa, R. *Org. Lett.*, **2008**, *10*, 3477 - 3479.

¹⁷⁹ Zakharova, V. M.; Hennig, L.; Nikolaev, V. A. *Synthesis* **2005**, 2871-2874.



To a stirring solution of **385** (1 mmol, 1 equiv, 172 mg), *p*-ABSA (1.1 mmol, 1.1 equiv, 264 mg) in anhydrous MeCN (2 mL) at 0 °C, DBU (1.1 mmol, 1.1 equiv, 167 mg, in 1 mL MeCN) was added via syringe over a period of 5 minutes. The resulting solution was stirred at 0 °C while being monitored with TLC analysis. Upon completion, DBU (1.1 mmol, 1.1 equiv, 167 mg, in 1 mL MeCN) was added again. The reaction mixture was stirred at room temperature for 10 h, concentrated under reduced pressure, purified quickly by column chromatography on silica gel using a mixture of ether/pentane as eluent to afford difluoro-diazoacetone **384** (stored in an ether solution, 0.5 mol/L).

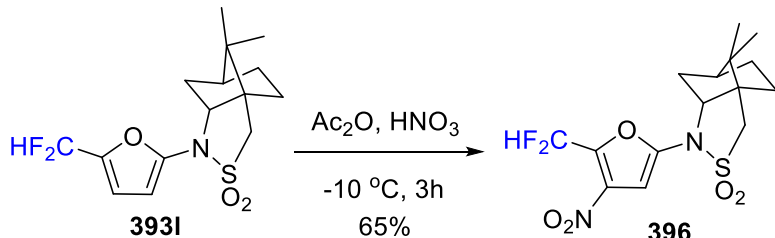
4. Experimental procedure for compounds **387** and **393**:



General procedure A: To a solution of **355** or **392** (0.2 mmol, 1 equiv) and CuI (10 mol %, 4 mg) in MeCN (2 mL) at 23 °C, difluoro-diazoacetone **384** (0.3 mmol, 1.5 equiv, 0.6 mL) was added dropwise while being monitored with TLC analysis. Upon completion, the mixture was concentrated under reduced pressure (15 mbar, 25 °C), purified by column chromatography on silica gel using a mixture of EtOAc/pentane as eluent to afford the desired products **387** or **393**.

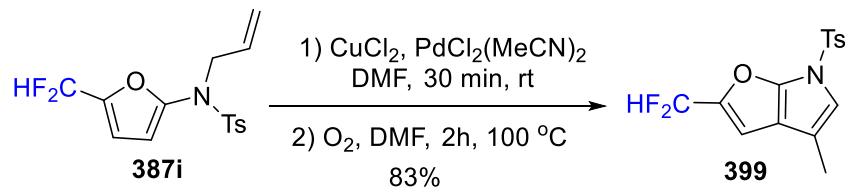
General procedure for **387p, **393f** and **393j**:** To a solution of TIPS protected ynamide (1 mmol, 1.0 equiv) in anhydrous 5 mL THF stirring at 0 °C was added TBAF (1.1 mmol, 1.1 equiv, 1M solution in THF) via syringe over a period of 5 minutes. The resulting solution was stirred at 0 °C. After TLC indicated that the starting material was completely consumed, the reaction was quenched with water (5 mL) and extracted with ether 3 times. The combined organic extracts were dried (Na₂SO₄), concentrated under reduced pressure afford the desired crude product **355p**, **392f**, **392j**. Then To a solution of **355p** or **392f** or **392j** (0.2 mmol, 1 equiv) and CuI (10 mol %, 4 mg) in MeCN (2 mL) at 23 °C, difluoro-diazoacetone **3** (0.3 mmol, 1.5 equiv, 0.6 mL) was added dropwise while being monitored with TLC analysis. Upon completion, the mixture was concentrated under reduced pressure (15 mbar, 25 °C), purified by column chromatography on silica gel using a mixture of EtOAc/pentane as eluent to afford the desired products **387p**, **393f**, **393j**.

5. Experimental procedure for **396**⁴



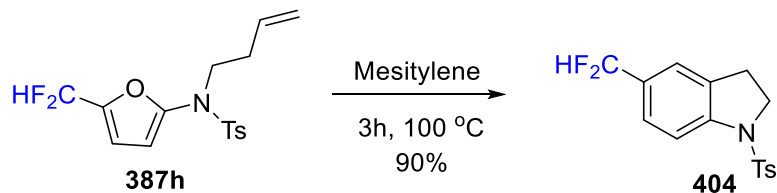
Acetic anhydride (0.5 mL) was added to compound **393l** (0.1 mmol, 1 equiv, 33 mg). After cooling the reaction mixture to -10 °C, fuming nitric acid (0.05 mL) was slowly added. The reaction mixture was stirred at -10°C for 1 h and then poured onto an ice/water mixture (5 mL). Organic layer was extracted with EtOAc (3 x 5 mL), washed with a saturated NaHCO₃ solution (5 mL), dried on Na₂SO₄, filtered and concentrated. Purification by column chromatography on silica gel using a mixture of EtOAc/pentane as eluent afforded the desired product **396** (0.065 mmol, 25 mg).

6. Experimental procedure for **399**¹⁸⁰



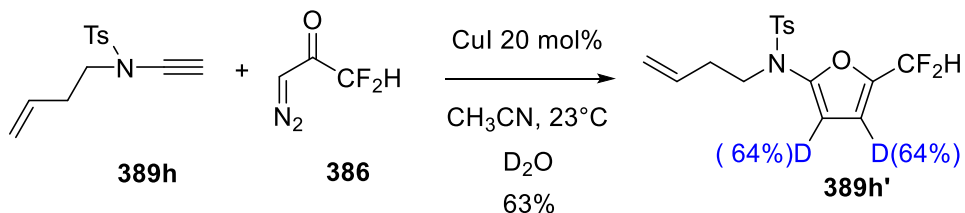
A mixture of PdCl₂(MeCN)₂ (15 mol %, 4 mg) and CuCl₂ (15 mol %, 2 mg) in DMF (1 mL) was stirred at room temperature for 30 min under oxygen atmosphere. After addition of a solution of **387i** (0.1 mmol, 1equiv, 33 mg) in DMF (1 mL), the mixture was heated in an oil bath at 100 °C for 2 h under an O₂ atmosphere. The mixture was washed with brine and extracted with Et₂O (2 × 10 mL). The organic layer was dried over Na₂SO₄ and the solvent removed under reduced pressure. Purification by column chromatography on silica gel using a mixture of EtOAc/pentane as eluent to afford the desired product **399** (0.083 mmol, 27 mg).

7. Experimental procedure for **404**¹⁸¹



A mixture of **387h** (0.1 mmol, 1equiv, 34 mg) in mesitylene (1 mL) was stirred in an oil bath at 100 °C for 3h. The mixture was concentrated under reduce pressure (15 mbar, 25 °C) purified by column chromatography on silica gel using a mixture of EtOAc/pentane as eluent to afford the desired product **404** (0.09 mmol, 29 mg).

8. Experimental procedure for **5h'**:



To a solution of **389h** (0.2 mmol, 1 equiv, 50 mg) and CuI (20 mol%, 8 mg) in MeCN (2 mL) and D₂O (0.1 mL) at 23 °C difluorinated diazoacetone **386** (0.3 mmol, 1.5 equiv, 0.6 mL) was added while

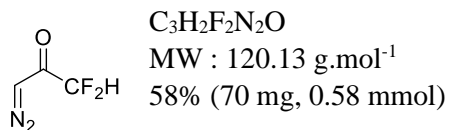
¹⁸⁰ Beccalli, E. M.; Borsini, E.; Broggini, G.; Rigamonti, M.; Sottocor-nola, S. *Synlett* **2008**, 1053-1057

¹⁸¹ Flick, A. C.; Pawda, A. *Advances in Heterocyclic Chemistry*, **2013**, 110, 1-41.

being monitored with TLC analysis. Upon completion, the mixture was concentrated under reduce pressure (15 mbar, 25 °C) purified by column chromatography on silica gel using a mixture of EtOAc/pentane as eluent to afford the desired product **389h'**.

Characterization data

Compound 384 : 3-diazo-1,1-difluoropropan-2-one



¹H NMR (500 MHz, CDCl₃): δ = 5.82 (t, J = 54.1 Hz, 1H), 5.76 (s, 1H) ppm.

¹³C NMR (125 MHz, CDCl₃) δ = 183.5 (q, J = 26.3 Hz), 109.5 (q, J = 251.9 Hz), 54.7 ppm

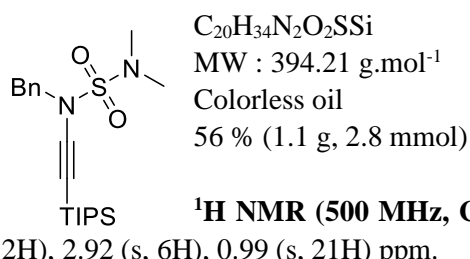
¹⁹F NMR (282 MHz, CDCl₃) δ = -126.18 ppm.

IR (neat): ν = 2119, 1660, 725 cm⁻¹

R_f: 0.41 (Petroleum ether / Ethyl acetate 5:1 v/v, UV)

Spectral data was in accordance with those reported in the literature: 391p¹⁸², 355a¹⁸³, 355b⁶, 355c⁶, 355d⁶, 355e¹⁸⁴, 355f⁷, 355g¹⁸⁵, 355h⁶, 355i¹⁸⁶, 355j¹⁸⁷, 355k⁷, 392a¹⁸⁸, 392b⁷, 392d⁹, 392e⁹

Compound 391f :



¹H NMR (500 MHz, CDCl₃): δ = 7.45 – 7.38 (m, 2H), 7.38 – 7.29 (m, 3H), 4.58 (s, 2H), 2.92 (s, 6H), 0.99 (s, 21H) ppm.

¹³C NMR (125 MHz, CDCl₃) δ = 135.4, 128.9 (×2), 128.5 (×2), 128.3, 97.3, 69.5, 56.8, 38.9 (×2), 18.6 (×6), 11.3 (×3) ppm.

HRMS (ESI-TOF) m/z: [M+Na]⁺ calcd for C₂₀H₃₄N₂NaO₂SSI 417.2008; Found 417.2017.

IR (neat): ν = 2941, 2864, 2159, 1457, 1365, 1161 cm⁻¹

R_f: 0.70 (Petroleum ether / Ethyl acetate 9:1 v/v, UV)

¹⁸² Beltran, F.; Andna, L.; Miesch, L. *Org. Chem. Front.*, **2019**, 6, 373-376.

¹⁸³ Zeng, X. Z.; Tu, Y. L.; Zhang, Z. M.; You, C. M.; Wu, J.; Ye, Z. Y.; Zhao, J. F. *J. Org. Chem.* **2019**, 84, 4458-4466.

¹⁸⁴ Zhao, L.; Yang, H. Y.; Li, R. K.; Tao, Y.; Guo, X. F.; Anderson, E. A.; Whiting, A.; Wu, N. *J. Org. Chem.* **2021**, 86, 1938-1947.

¹⁸⁵ Marion, F.; Coulomb, J.; Courillon, C.; Fensterbank, L.; Malacria, M. *Org. Lett.* **2004**, 6, 1509-1511

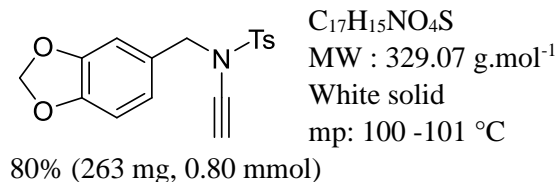
¹⁸⁶ Clavier, H.; Lepronier, A.; Bengobesse-Mintsa, N.; Gatineau, D.; Pellissier, H.; Giordano, L.; Tenaglia, A.; Buono, G. *Adv. Synth. Catal.* **2013**, 355, 403-408.

¹⁸⁷ Garcia, P.; Evanno, Y.; George, P.; Sevrin, M.; Ricci, G.; Malacria, M.; Aubert, C.; Gandon, V.; *Org. Lett.* **2011**, 13, 2030-2033.

¹⁸⁸ Tu, Y. L.; Zeng, X. Z.; Wang, H.; Zhao, J. F. *Org. Lett.* **2018**, 20, 280–283.

Compound 355l

N-(benzo[d][1,3]dioxol-5-ylmethyl)-*N*-ethynyl-4-methylbenzenesulfonamide



¹H NMR (300 MHz, CDCl₃): δ = 7.76 (d, *J* = 8.3 Hz, 2H), 7.32 (d, *J* = 7.9 Hz, 2H), 6.80 – 6.70 (m, 3H), 5.94 (s, 2H), 4.39 (s, 2H), 2.70 (s, 1H), 2.45 (s, 3H). ppm.

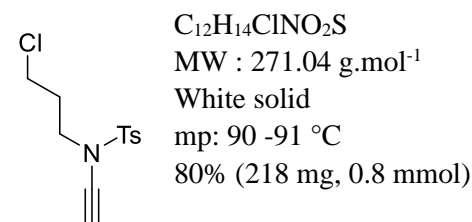
¹³C NMR (125 MHz, CDCl₃) δ = 147.8, 147.8, 144.8, 134.7, 129.8 (×2), 127.9, 127.7 (×2), 122.7, 109.1, 108.1, 101.2, 76.2, 59.8, 55.2, 21.7 ppm.

HRMS (ESI-TOF) m/z: [M+Na]⁺ calcd for C₁₇H₁₅NNaO₄S 352.0614; Found 352.0611.

IR (neat): ν = 3277, 2892, 2132, 1168 cm⁻¹

R_f: 0.41(Petroleum ether / Ethyl acetate 5:1 v/v, UV)

Compound 355m : *N*-(3-chloropropyl)-*N*-ethynyl-4-methylbenzenesulfonamide



¹H NMR (500 MHz, CDCl₃): δ = 7.81 (d, *J* = 8.4 Hz, 2H), 7.37 (d, *J* = 8.0 Hz, 2H), 3.57 (t, *J* = 6.3 Hz, 2H), 3.49 (t, *J* = 6.7 Hz, 2H), 2.76 (s, 1H), 2.46 (s, 3H), 2.12 (p, *J* = 6.5 Hz, 2H) ppm.

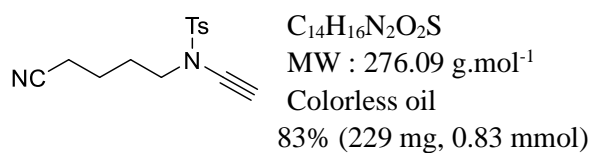
¹³C NMR (125 MHz, CDCl₃) δ = 145.0, 134.2, 129.9 (×2), 127.7 (×2), 75.7, 59.5, 48.5, 41.3, 30.8, 21.7 ppm.

HRMS (ESI-TOF) m/z: [M+H]⁺ calcd for C₁₂H₁₅ClNO₂S 272.0507; Found 272.0492.

IR (neat): ν = 3273, 2942, 2137, 1593, 1442, 1352 cm⁻¹

R_f: 0.52 (Petroleum ether / Ethyl acetate 5:1 v/v, UV)

Compound 355n: *N*-(4-cyanobutyl)-*N*-ethynyl-4-methylbenzenesulfonamide



¹H NMR (500 MHz, CDCl₃): δ = 7.79 (d, *J* = 8.1 Hz, 2H), 7.36 (d, *J* = 8.1 Hz, 2H), 3.34 (t, *J* = 6.5 Hz, 2H), 2.75 (s, 1H), 2.45 (s, 3H), 2.40 (t, *J* = 6.9 Hz, 2H), 1.86 – 1.79 (m, 2H), 1.77 – 1.70 (m, 2H) ppm.

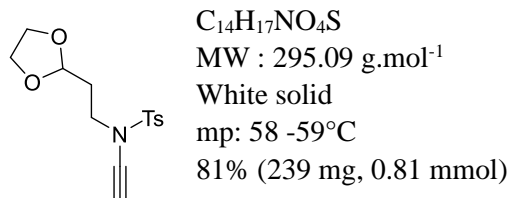
¹³C NMR (125 MHz, CDCl₃) δ = 145.1, 134.2, 129.9 (×2), 127.6 (×2), 119.1, 75.5, 59.6, 50.0, 26.4, 22.0, 21.7, 16.6 ppm.

HRMS (ESI-TOF) m/z: [M+Na]⁺ calcd for C₁₄H₁₆NNaO₂S 299.0830; Found 299.0841.

IR (neat): ν = 2941, 2362, 1352 cm⁻¹

R_f: 0.30 (Petroleum ether / Ethyl acetate 3:1 v/v, UV)

Compound 355o : *N*-(2-(1,3-dioxolan-2-yl)ethyl)-*N*-ethynyl-4-methylbenzenesulfonamide



¹H NMR (500 MHz, CDCl₃): δ = 7.81 (d, *J* = 8.4 Hz, 2H), 7.35 (d, *J* = 7.9 Hz, 2H), 4.89 (t, *J* = 4.4 Hz, 1H), 3.98 – 3.90 (m, 2H), 3.87 – 3.78 (m, 2H), 3.51 – 3.42 (m, 2H), 2.75 (s, 1H), 2.45 (s, 3H), 2.04 – 1.98 (m, 2H) ppm.

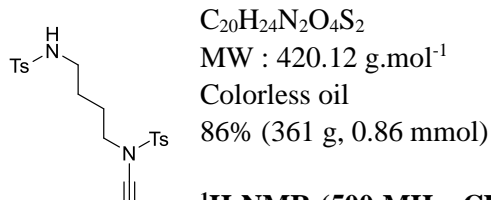
¹³C NMR (125 MHz, CDCl₃) δ = 144.8, 134.4, 129.8 (×2), 127.7 (×2), 101.7, 75.8, 65.0 (×2), 59.4, 46.5, 31.9, 21.7 ppm.

IR (neat): ν = 3246, 2961, 2936, 2855, 2126, 1594, 1364, 900 cm⁻¹

HRMS (ESI-TOF) m/z: [M+Na]⁺ calcd for C₁₄H₁₇NNaO₄S 318.0774; Found 318.0770.

R_f: 0.51 (Petroleum ether / Ethyl acetate 3:1 v/v, UV)

Compound 355q: *N*-ethynyl-4-methyl-*N*-(4-((4-methylphenyl)sulfonamido)butyl)benzenesulfonamide



¹H NMR (500 MHz, CDCl₃): δ = 7.77 (d, *J* = 8.3 Hz, 2H), 7.73 (d, *J* = 8.2 Hz, 2H), 7.35 (d, *J* = 8.1 Hz, 2H), 7.31 (d, *J* = 8.0 Hz, 2H), 4.58 (m, 1H), 3.25 (t, *J* = 6.8 Hz, 2H), 2.94 (q, *J* = 6.7 Hz, 2H), 2.71 (s, 1H), 2.45 (s, 3H), 2.42 (s, 3H), 1.64 – 1.68 (m, 2H), 1.58 – 1.46 (m, 2H) ppm.

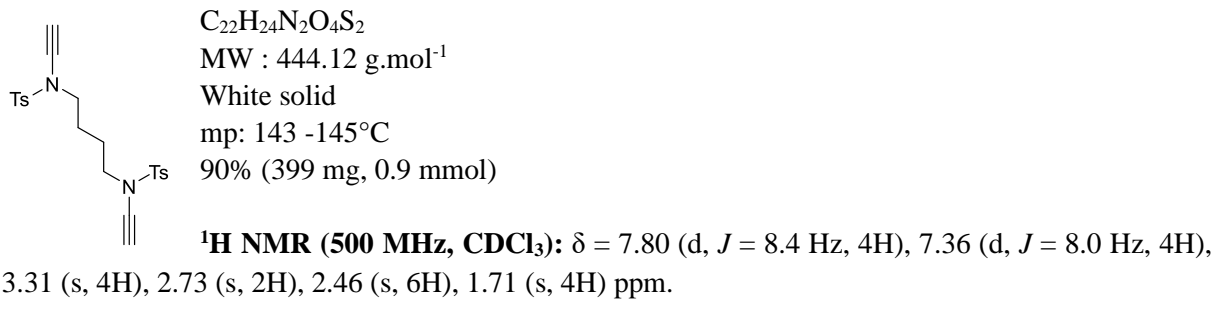
¹³C NMR (125 MHz, CDCl₃) δ = 144.9, 143.5, 136.7, 134.2, 129.9 (×2), 129.8 (×2), 127.6 (×2), 127.1 (×2), 75.7, 59.3, 50.5, 42.5, 26.0, 24.6, 21.7, 21.6 ppm.

HRMS (ESI-TOF) m/z: [M+K]⁺ calcd for C₂₀H₂₄KN₂O₄S₂ 459.0809; Found 459.0808.

IR (neat): ν = 3282, 2929, 2131, 1597, 1324, 1155 cm⁻¹

R_f: 0.20 (Petroleum ether / Ethyl acetate 3:1 v/v, UV)

Compound 355r: *N,N'*-(butane-1,4-diyl)bis(*N*-ethynyl-4-methylbenzenesulfonamide)



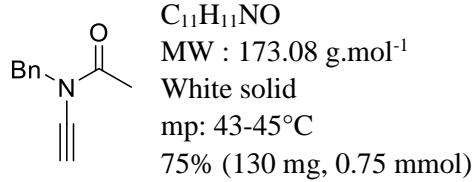
^{13}C NMR (125 MHz, CDCl₃) δ = 144.9 ($\times 2$), 144.9 ($\times 2$), 129.9 ($\times 4$), 127.7 ($\times 4$), 75.7 ($\times 2$), 59.3 ($\times 2$), 50.3 ($\times 2$), 24.1 ($\times 2$), 21.7 ($\times 2$) ppm.

HRMS (ESI-TOF) m/z: [M+Na]⁺ calcd for C₂₂H₂₄N₂NaO₄S₂ 467.1070; Found 467.1066.

IR (neat): ν = 3299, 2127, 1595, 1352, 1165 cm⁻¹

R_f: 0.20 (Petroleum ether / Ethyl acetate 5:1 v/v, UV)

Compound 393c : *N*-benzyl-*N*-ethynylacetamide



^1H NMR (500 MHz, CDCl₃): δ = 7.38 – 7.28 (m, 5H), 4.67 (s, 2H), 2.96 (s, 1H), 2.36 (s, 3H) ppm.

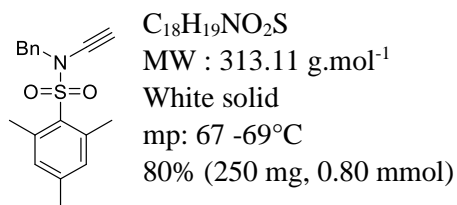
^{13}C NMR (125 MHz, CDCl₃) δ = 172.0, 135.9, 128.6 ($\times 2$), 128.6 ($\times 2$), 128.0, 78.1, 61.8, 51.0, 22.3.

HRMS (ESI-TOF) m/z: [M+Na]⁺ calcd for C₁₁H₁₁NNaO 197.0732; Found 197.0733.

IR (neat): ν = 3248, 3068, 3028, 2951, 2139, 1679, 1351, 1246 cm⁻¹

R_f: 0.50 (Petroleum ether / Ethyl acetate 9:1 v/v, UV)

Compound 393g: *N*-benzyl-*N*-ethynyl-2,4,6-trimethylbenzenesulfonamide



^1H NMR (300 MHz, CDCl₃): δ = 7.32 (m, 5H), 6.98 (s, 2H), 4.57 (s, 2H), 2.68 (s, 1H), 2.65 (s, 6H), 2.33 (s, 3H) ppm.

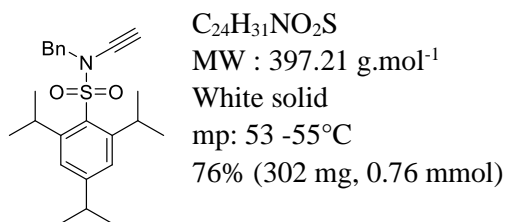
^{13}C NMR (125 MHz, CDCl₃) δ 143.8, 140.9 ($\times 2$), 134.5, 132.1 ($\times 2$), 131.5, 128.7 ($\times 2$), 128.6 ($\times 2$), 128.3, 75.7, 61.0, 53.9, 23.1 ($\times 2$), 21.1 ppm.

HRMS (ESI-TOF) m/z: [M+K]⁺ calcd for C₁₈H₁₉KNO₂S 352.0760; Found 352.0768.

IR (neat): ν = 3282, 2136, 1602, 1455, 1156 cm⁻¹

R_f: 0.67 (Petroleum ether / Ethyl acetate 5:1 v/v, UV)

Compound 393h : *N*-benzyl-*N*-ethynyl-2,4,6-triisopropylbenzenesulfonamide



¹H NMR (300 MHz, CDCl₃): δ = 7.33 (m, 5H), 7.19 (s, 2H), 4.61 (s, 2H), 4.13 (h, *J* = 6.8 Hz, 2H), 2.91 (h, *J* = 6.9 Hz, 1H), 2.68 (s, 1H), 1.27 (d, *J* = 6.9 Hz, 6H), 1.24 (d, *J* = 6.8 Hz, 12H) ppm.

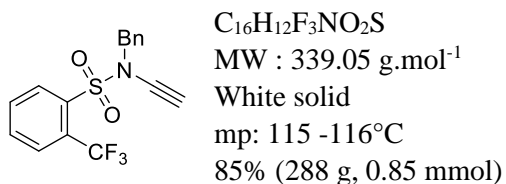
¹³C NMR (125 MHz, CDCl₃) δ = 154.2, 152.0 (×2), 134.6, 130.3, 129.0 (×2), 128.5 (×2), 128.3, 124.0 (×2), 75.8, 61.3, 53.3, 34.2, 29.8 (×2), 24.8 (×4), 23.6 (×2) ppm.

HRMS (ESI-TOF) m/z: [M+K]⁺ calcd for C₂₄H₃₁KNO₂S 436.1688; Found 436.1707.

IR (neat): ν = 3277, 2132, 1601, 1166 cm⁻¹

R_f: 0.81 (Petroleum ether / Ethyl acetate 5:1 v/v, UV)

Compound 393i: *N*-benzyl-*N*-ethynyl-2-(trifluoromethyl)benzenesulfonamide



¹H NMR (500 MHz, CDCl₃): δ = 8.25 (d, *J* = 7.8 Hz, 1H), 7.94 (d, *J* = 7.8 Hz, 1H), 7.79 – 7.70 (m, 2H), 7.41 – 7.29 (m, 5H), 4.68 (s, 2H), 2.67 (s, 1H) ppm.

¹³C NMR (125 MHz, CDCl₃) δ = 136.6, 134.4, 133.7, 132.9, 132.2, 128.7 (×2), 128.7 (×2), 128.5 (q, *J* = 6.3 Hz), 128.5, 128.1 (q, *J* = 33.3 Hz), 122.3 (q, *J* = 272.4 Hz), 75.0, 60.9, 55.3 ppm.

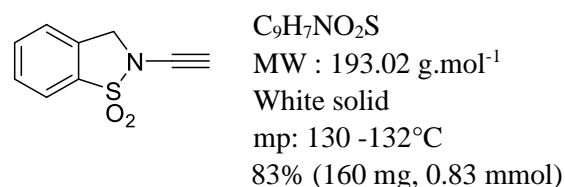
¹⁹F NMR (282 MHz, CDCl₃) δ = -57.68 ppm.

HRMS (ESI-TOF) m/z: [M+Na]⁺ calcd for C₁₆H₁₂F₃NNaO₂S 362.0438; Found 362.0433.

IR (neat): ν = 3271, 2913, 1365, 1310, 1167, 1115 cm⁻¹

R_f: 0.30 (Petroleum ether / Ethyl acetate 5:1 v/v, UV)

Compound 393k : 2-ethynyl-2,3-dihydrobenzo[d]isothiazole 1,1-dioxide



¹H NMR (300 MHz, CDCl₃): δ = 7.84 (m, 1H), 7.69 (td, *J* = 7.6, 1.3 Hz, 1H), 7.61 (m, 1H), 7.43 (m, 1H), 4.81 (s, 2H), 2.98 (s, 1H) ppm.

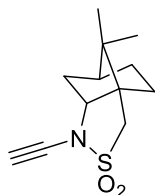
¹³C NMR (125 MHz, CDCl₃) δ = 133.8, 132.7, 131.4, 129.8, 124.6, 122.0, 71.6, 61.6, 52.3 ppm.

HRMS (ESI-TOF) m/z: [M+Na]⁺ calcd for C₉H₇NNaO₂S 216.0090; Found 216.0087.

IR (neat): ν = 3280, 2137, 1466, 1301, 1158 cm⁻¹

R_f: 0.19 (Petroleum ether / Ethyl acetate 5:1 *v/v*, UV)

Compound 393l: (3aS,6S)-1-ethynyl-8,8-dimethylhexahydro-3H-3a,6-methanobenzo[c]isothiazole 2,2-dioxide



C₁₂H₁₇NO₂S

MW : 239.10 g.mol⁻¹

White solid

mp: 170 -172°C

92% (220 mg, 0.92 mmol)

¹H NMR (300 MHz, CDCl₃): δ = 3.60 (dd, *J* = 8.1, 4.2 Hz, 1H), 3.25 (s, 2H), 2.81 (s, 1H), 2.27 – 2.18 (m, 1H), 2.00 – 1.94 (m, 1H), 1.94 – 1.83 (m, 2H), 1.78 (dd, *J* = 13.4, 8.2 Hz, 1H), 1.48 – 1.28 (m, 2H), 1.10 (s, 3H), 0.94 (s, 3H) ppm.

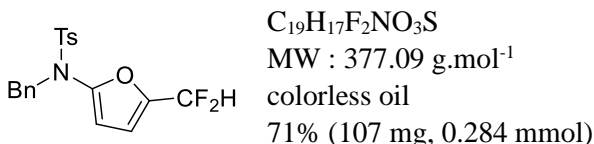
¹³C NMR (125 MHz, CDCl₃) δ = 70.8, 66.8, 61.3, 51.3, 49.8, 48.0, 44.4, 34.3, 31.6, 27.0, 20.1, 20.0 ppm.

HRMS (ESI-TOF) m/z: [M+K]⁺ calcd for C₁₂H₁₇KNO₂S 278.0612; Found 278.0609.

IR (neat): ν = 3255, 2952, 2895, 1315, 1163 cm⁻¹

R_f: 0.35 (Petroleum ether / Ethyl acetate 5:1 *v/v*, UV)

Compound 387a: *N*-benzyl-*N*-(5-(difluoromethyl)furan-2-yl)-4-methylbenzenesulfonamide



¹H NMR (500 MHz, C₆D₆): δ = δ 7.63 (d, *J* = 8.1 Hz, 2H), 7.19 (d, *J* = 7.2 Hz, 2H), 7.01 (t, *J* = 7.4 Hz, 2H), 6.97 (d, *J* = 7.2 Hz, 1H), 6.75 (d, *J* = 7.9 Hz, 2H), 5.90 (d, *J* = 3.4 Hz, 1H), 5.87 (d, *J* = 2.7 Hz, 1H), 5.70 (t, *J* = 54.0 Hz, 1H), 4.53 (s, 2H), 1.85 (s, 3H) ppm.

¹³C NMR (125 MHz, C₆D₆) δ = 147.8 (t, *J* = 2.3 Hz), 144.2, 143.9 (t, *J* = 28.4 Hz), 136.6, 135.8, 130.0 (×2), 129.1 (×2), 128.9 (×2), 128.5, 128.2 (×2), 112.3 (t, *J* = 5.0 Hz), 108.6 (t, *J* = 233.4 Hz), 108.3, 53.8, 21.3 ppm.

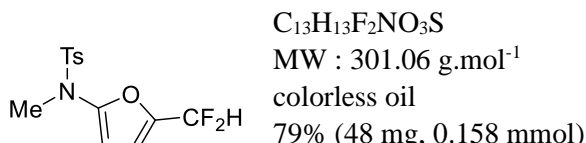
¹⁹F NMR (282 MHz, C₆D₆) δ = -114.56 ppm.

HRMS (ESI-TOF) m/z: [M+Na]⁺ calcd for C₁₉H₁₇F₂NNaO₃S 400.0787; Found 400.0789.

IR (neat): ν = 2925, 2853, 1701, 1558, 1352, 1164, 1089 cm⁻¹

R_f: 0.50 (Petroleum ether / Ethyl acetate 5:1 *v/v*, UV)

Compound 387b: *N*-(5-(difluoromethyl)furan-2-yl)-*N*,4-dimethylbenzenesulfonamide



¹H NMR (500 MHz, C₆D₆): δ = 7.52 (d, *J* = 8.3 Hz, 2H), 6.70 (d, *J* = 7.7 Hz, 2H), 6.06 (m, 1H), 6.02 (d, *J* = 3.4 Hz, 1H), 5.78 (t, *J* = 54.0 Hz, 1H), 2.75 (s, 3H), 1.81 (s, 3H) ppm.

¹³C NMR (125 MHz, C₆D₆) δ = 149.2 (t, *J* = 2.2 Hz), 143.7, 142.9 (t, *J* = 28.7 Hz), 134.6, 129.4 (×2), 127.6 (×2), 111.8 (t, *J* = 4.8 Hz), 108.1 (t, *J* = 233.2 Hz), 104.4, 35.7, 20.8 ppm.

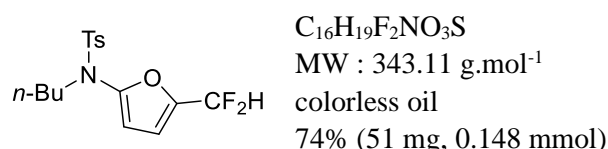
¹⁹F NMR (282 MHz, C₆D₆) δ = -114.32 ppm.

HRMS (ESI-TOF) m/z: [M+Na]⁺ calcd for C₁₃H₁₃F₂NNaO₃S 324.0473; Found 324.0476.

IR (neat): ν = 2946, 1558, 1357, 1159, 1016, 667 cm⁻¹

R_f: 0.46 (Petroleum ether / Ethyl acetate 5:1 *v/v*, UV)

Compound 387c: *N*-butyl-*N*-(5-(difluoromethyl)furan-2-yl)-4-methylbenzenesulfonamide



¹H NMR (500 MHz, C₆D₆): δ = 7.62 (d, *J* = 8.3 Hz, 2H), 6.75 (d, *J* = 8.0 Hz, 2H), 6.11 – 6.09 (m, 1H), 6.08 (d, *J* = 3.4 Hz, 1H), 5.81 (t, *J* = 54.0 Hz, 1H), 3.40 (t, *J* = 7.1 Hz, 2H), 1.85 (s, 3H), 1.33 – 1.26 (m, 2H), 1.13 (m, 2H), 0.71 (t, *J* = 7.3 Hz, 3H) ppm.

¹³C NMR (125 MHz, C₆D₆) δ = 147.8 (t, *J* = 2.3 Hz), 143.6 (t, *J* = 28.7 Hz), 143.5, 136.1, 129.4 (×2), 127.5 (×2), 111.7 (t, *J* = 4.9 Hz), 108.1 (t, *J* = 233.4 Hz), 107.4, 49.1, 30.2, 20.8, 19.3, 13.3 ppm.

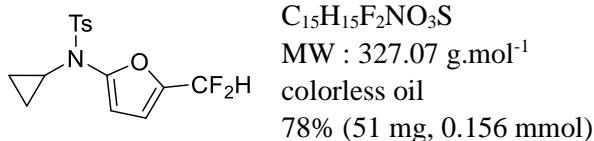
¹⁹F NMR (282 MHz, C₆D₆) δ = -114.53 ppm.

HRMS (ESI-TOF) m/z: [M+Na]⁺ calcd for C₁₆H₁₉F₂NNaO₃S 366.0958; Found 366.0946.

IR (neat): ν = 2934, 1558, 1352, 1167, 1018, 750, 668 cm⁻¹

R_f: 0.60 (Petroleum ether / Ethyl acetate 5:1 v/v, UV)

Compound 387d: *N*-cyclopropyl-*N*-(5-(difluoromethyl)furan-2-yl)-4-methylbenzenesulfonamide



¹H NMR (500 MHz, C₆D₆): δ = 7.72 (d, *J* = 8.3 Hz, 2H), 6.78 (d, *J* = 7.9 Hz, 2H), 6.11 – 6.08 (m, 1H), 5.92 (d, *J* = 3.4 Hz, 1H), 5.78 (d, *J* = 54.0 Hz, 1H), 2.40 – 2.36 (m, 1H), 1.87 (s, 3H), 0.76 – 0.71 (m, 2H), 0.36 – 0.29 (m, 2H) ppm.

¹³C NMR (125 MHz, C₆D₆) δ = 149.2 (t, *J* = 2.3 Hz), 143.8, 143.6 (t, *J* = 28.8 Hz), 135.2, 129.4 (×2), 128.1 (×2), 111.5 (t, *J* = 4.8 Hz), 108.2 (t, *J* = 233.4 Hz), 106.5, 31.0, 20.8, 7.5 (×2) ppm.

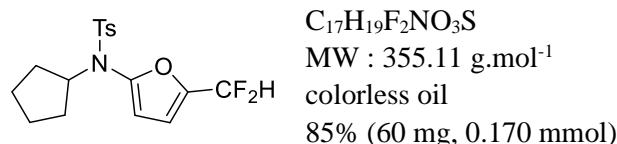
¹⁹F NMR (282 MHz, C₆D₆) δ = -114.61 ppm.

HRMS (ESI-TOF) m/z: [M+Na]⁺ calcd for C₁₅H₁₅F₂NNaO₃S 350.0626; Found 350.0633.

IR (neat): ν = 1558, 1355, 1167, 1089, 1008 cm⁻¹

R_f: 0.50 (Petroleum ether / Ethyl acetate 5:1 v/v, UV)

Compound 387e: *N*-cyclopentyl-*N*-(5-(difluoromethyl)furan-2-yl)-4-methylbenzenesulfonamide



¹H NMR (500 MHz, C₆D₆): δ = 7.77 (d, *J* = 8.3 Hz, 2H), 6.78 (d, *J* = 8.0 Hz, 2H), 6.13 – 6.11 (m, 1H), 5.95 (d, *J* = 3.3 Hz, 1H), 5.86 (t, *J* = 54.1 Hz, 1H), 4.46 (p, *J* = 8.1 Hz, 1H), 1.87 (s, 3H), 1.69 – 1.64 (m, 2H), 1.33 – 1.25 (m, 2H), 1.17 – 1.04 (m, 4H) ppm.

¹³C NMR (125 MHz, C₆D₆) δ = 145.9 (t, *J* = 2.4 Hz), 144.6 (t, *J* = 28.9 Hz), 143.3, 137.53, 129.4 (×2), 127.8 (×2), 111.3 (t, *J* = 4.8 Hz), 110.6, 108.2 (t, *J* = 233.7 Hz), 60.8, 30.6 (×2), 23.1 (×2), 20.8 ppm.

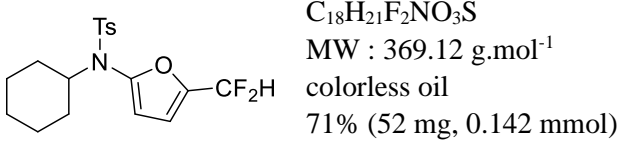
¹⁹F NMR (282 MHz, C₆D₆) δ = -115.00 ppm.

HRMS (ESI-TOF) m/z: [M+Na]⁺ calcd for C₁₇H₁₉F₂NNaO₃S 378.0957; Found 378.0946.

IR (neat): ν = 2959, 2873, 1556, 1349, 1161, 1017, 666 cm⁻¹

R_f: 0.48 (Petroleum ether / Ethyl acetate 5:1 v/v, UV)

Compound 387f: *N*-cyclohexyl-*N*-(5-(difluoromethyl)furan-2-yl)-4-methylbenzenesulfonamide



¹H NMR (500 MHz, C₆D₆): δ = 7.82 (d, J = 8.2 Hz, 2H), 6.77 (d, J = 8.0 Hz, 2H), 6.16 (q, J = 2.5 Hz, 1H), 5.96 (d, J = 3.3 Hz, 1H), 5.89 (t, J = 54.2 Hz, 1H), 4.07 – 4.01 (m, 1H), 1.85 (s, 3H), 1.85 – 1.80 (m, 2H), 1.42 – 1.35 (m, 2H), 1.25 – 1.18 (m, 1H), 1.06 – 0.95 (m, 4H), 0.62 – 0.52 (m, 1H) ppm.

¹³C NMR (125 MHz, C₆D₆) δ = 145.6 (t, J = 2.3 Hz), 144.7 (t, J = 29.1 Hz), 143.2, 138.2, 129.4 ($\times 2$), 127.5 ($\times 2$), 111.2 (t, J = 4.7 Hz), 110.6, 108.3 (t, J = 234.0 Hz), 59.6, 32.3 ($\times 2$), 25.5 ($\times 2$), 24.7, 20.8 ppm.

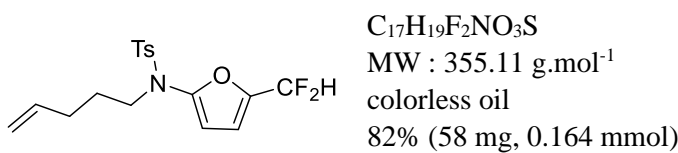
¹⁹F NMR (282 MHz, C₆D₆) δ = -115.04 ppm.

HRMS (ESI-TOF) m/z: [M+Na]⁺ calcd for C₁₈H₂₁F₂NNaO₃S 392.1092; Found 392.1102.

IR (neat): ν = 2935, 2858, 1557, 1353, 1168, 667 cm⁻¹

R_f: 0.58 (Petroleum ether / Ethyl acetate 5:1 v/v, UV)

Compound 387g: N -(5-(difluoromethyl)furan-2-yl)-4-methyl-N-(pent-4-en-1-yl)benzenesulfonamide



¹H NMR (500 MHz, C₆D₆): δ = 7.61 (d, J = 8.3 Hz, 2H), 6.76 (d, J = 7.9 Hz, 2H), 6.11 (q, J = 2.5 Hz, 1H), 6.06 (d, J = 3.4 Hz, 1H), 5.84 (t, J = 54.0 Hz, 1H), 5.61 – 5.53 (m, 1H), 4.95 – 4.87 (m, 2H), 3.38 (t, J = 7.1 Hz, 2H), 1.89 – 1.82 (m, 2H), 1.86 (s, 3H), 1.41 (p, J = 7.3 Hz, 2H) ppm.

¹³C NMR (125 MHz, C₆D₆) δ = 147.6 (t, J = 2.3 Hz), 143.7 (t, J = 28.7 Hz), 143.6, 137.1, 136.0, 129.5 ($\times 2$), 127.5 ($\times 2$), 115.2, 111.7 (t, J = 4.8 Hz), 110.0, 107.5 (t, J = 233.4 Hz), 48.9, 30.2, 27.5, 20.8 ppm.

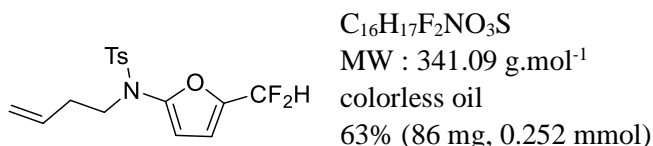
¹⁹F NMR (282 MHz, C₆D₆) δ = -114.59 ppm.

HRMS (ESI-TOF) m/z: [M+Na]⁺ calcd for C₁₇H₁₉F₂NNaO₃S 378.0936; Found 378.0946.

IR (neat): ν = 2934, 1558, 1352, 1165, 1016, 765, 661 cm⁻¹

R_f: 0.60 (Petroleum ether / Ethyl acetate 5:1 v/v, UV)

Compound 387h: *N*-(but-3-en-1-yl)-*N*-(5-(difluoromethyl)furan-2-yl)-4-methylbenzenesulfonamide



¹H NMR (500 MHz, C₆D₆): δ = 7.60 (d, *J* = 8.4 Hz, 2H), 6.74 (d, *J* = 8.0 Hz, 2H), 6.10 – 6.09 (m, 1H), 6.05 (d, *J* = 3.4 Hz, 1H), 5.82 (t, *J* = 54.0 Hz, 1H), 5.55 – 5.47 (m, 1H), 4.93 – 4.86 (m, 2H), 3.43 (t, *J* = 7.2 Hz, 2H), 2.10 – 2.03 (m, 2H), 1.85 (s, 3H) ppm.

¹³C NMR (125 MHz, C₆D₆) δ = 147.5 (t, *J* = 2.3 Hz), 143.7 (t, *J* = 28.7 Hz), 143.6, 136.0, 133.9, 129.4 (×2), 127.5 (×2), 116.9, 111.7 (t, *J* = 4.9 Hz), 108.1 (t, *J* = 233.5 Hz), 107.7, 48.9, 32.7, 20.8 ppm.

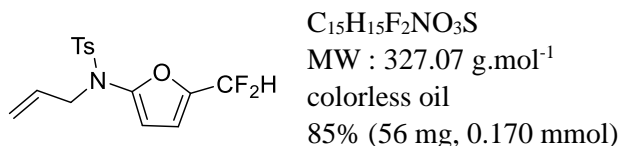
¹⁹F NMR (282 MHz, C₆D₆) δ = -114.58 ppm.

HRMS (ESI-TOF) m/z: [M+Na]⁺ calcd for C₁₆H₁₇F₂NNaO₃S 364.0770; Found 364.0789.

IR (neat): ν = 2982, 1558, 1352, 1165, 1016, 666 cm⁻¹

R_f: 0.59 (Petroleum ether / Ethyl acetate 5:1 *v/v*, UV)

Compound 387i: *N*-allyl-*N*-(5-(difluoromethyl)furan-2-yl)-4-methylbenzenesulfonamide



¹H NMR (500 MHz, C₆D₆): δ = 7.60 (d, *J* = 8.4 Hz, 2H), 6.74 (d, *J* = 7.9 Hz, 2H), 6.07 – 6.05 (m, 1H), 6.04 (d, *J* = 3.3 Hz, 1H), 5.80 (t, *J* = 54.0 Hz, 1H), 5.63 – 5.55 (m, 1H), 4.94 – 4.79 (m, 2H), 3.95 (dt, *J* = 6.4, 1.3 Hz, 2H), 1.85 (s, 3H) ppm.

¹³C NMR (125 MHz, C₆D₆) δ = 147.6 (t, *J* = 2.3 Hz), 143.7, 143.5 (t, *J* = 28.7 Hz), 136.0, 131.9, 129.4 (×2), 127.6 (×2), 119.0, 111.6 (t, *J* = 4.9 Hz), 108.1 (t, *J* = 233.4 Hz), 107.3, 52.2, 20.8 ppm.

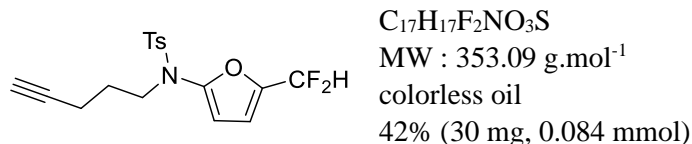
¹⁹F NMR (282 MHz, C₆D₆) δ = -114.55 ppm.

HRMS (ESI-TOF) m/z: [M+Na]⁺ calcd for C₁₅H₁₅F₂NNaO₃S 350.0618; Found 350.0633.

IR (neat): ν = 2988, 2927, 1558, 1355, 1017, 750, 666 cm⁻¹

R_f: 0.58 (Petroleum ether / Ethyl acetate 5:1 *v/v*, UV)

Compound 387j: *N*-(5-(difluoromethyl)furan-2-yl)-4-methyl-*N*-(pent-4-yn-1-yl)benzenesulfonamide



¹H NMR (500 MHz, C₆D₆): δ = 7.60 (d, *J* = 7.9 Hz, 2H), 6.72 (d, *J* = 7.9 Hz, 2H), 6.04 – 6.05 (m, 1H), 5.98 (d, *J* = 3.3 Hz, 1H), 5.77 (t, *J* = 54.1 Hz, 1H), 3.43 (t, *J* = 7.0 Hz, 2H), 1.89 – 1.86 (m, 2H), 1.83 (s, 3H), 1.70 (s, 1H), 1.45 (p, *J* = 7.1 Hz, 2H) ppm.

¹³C NMR (125 MHz, C₆D₆) δ = 147.6 (t, *J* = 2.3 Hz), 143.8 (t, *J* = 28.9 Hz), 143.7, 136.0, 129.5 (×2), 127.6 (×2), 111.7 (t, *J* = 4.8 Hz), 108.1 (t, *J* = 233.5 Hz), 107.6, 82.5, 69.4, 48.5, 27.4, 20.8, 15.3 ppm.

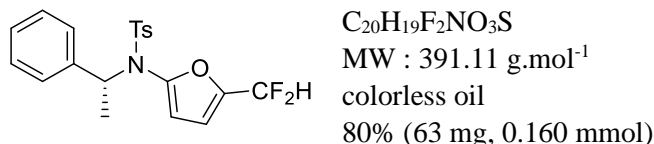
¹⁹F NMR (282 MHz, C₆D₆) δ = -114.65 ppm.

HRMS (ESI-TOF) m/z: [M+Na]⁺ calcd for C₁₇H₁₇F₂NNaO₃S 376.0786; Found 376.0789.

IR (neat): ν = 3303, 2926, 1559, 1357, 1164, 754, 666 cm⁻¹

R_f: 0.57 (Petroleum ether / Ethyl acetate 5:1 v/v, UV)

Compound 387k: (*R*)-*N*-(5-(difluoromethyl)furan-2-yl)-4-methyl-*N*-(1-phenylethyl)benzenesulfonamide



¹H NMR (500 MHz, C₆D₆): δ = 7.73 (d, *J* = 8.0 Hz, 2H), 7.15 – 7.10 (m, 2H), 7.05 – 6.98 (m, 3H), 6.75 (d, *J* = 8.0 Hz, 2H), 5.98 – 5.98. (m, 1H), 5.79 (t, *J* = 54.2 Hz, 1H), 5.67 (d, *J* = 3.4 Hz, 1H), 5.43 (q, *J* = 7.1 Hz, 1H), 1.86 (s, 3H), 1.22 (d, *J* = 7.1 Hz, 3H) ppm.

¹³C NMR (125 MHz, C₆D₆) δ = 145.3 (t, *J* = 2.4 Hz), 144.5 (t, *J* = 29.0 Hz), 143.3, 139.8, 137.8, 129.3 (×2), 128.2 (×2), 127.7, 127.7 (×2), 127.5 (×2), 111.1 (t, *J* = 4.7 Hz), 110.9, 108.1 (t, *J* = 233.7 Hz), 58.7, 20.8, 18.3 ppm.

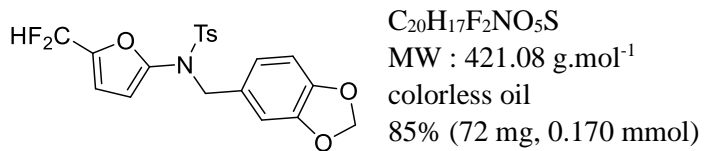
¹⁹F NMR (282 MHz, C₆D₆) δ = -115.08, -115.03 ppm.

HRMS (ESI-TOF) m/z: [M+Na]⁺ calcd for C₂₀H₁₉F₂NNaO₃S 414.0936; Found 414.0946.

IR (neat): ν = 2926, 2360, 1556, 1350, 1164, 751, 666, 547 cm⁻¹

R_f: 0.64 (Petroleum ether / Ethyl acetate 5:1 v/v, UV)

Compound 387l: *N*-(benzo[d][1,3]dioxol-5-ylmethyl)-*N*-(5-(difluoromethyl)furan-2-yl)-4-methylbenzenesulfonamide



¹H NMR (500 MHz, C₆D₆): δ = 7.62 (d, *J* = 8.0 Hz, 2H), 6.83 (s, 1H), 6.76 (d, *J* = 8.0 Hz, 2H), 6.55 (d, *J* = 7.9 Hz, 1H), 6.47 (d, *J* = 7.9 Hz, 1H), 5.93 (d, *J* = 3.5 Hz, 1H), 5.91 – 5.92 (m, 1H), 5.73 (t, *J* = 53.9 Hz, 1H), 5.19 (s, 2H), 4.44 (s, 2H), 1.86 (s, 3H) ppm.

¹³C NMR (125 MHz, C₆D₆) δ = 148.0, 147.6, 147.2 (t, *J* = 2.3 Hz), 143.7, 143.4 (t, *J* = 28.3 Hz), 136.1, 129.5 (×2), 128.9, 127.6 (×2), 122.4, 111.8 (t, *J* = 5.0 Hz), 109.0, 108.0 (t, *J* = 233.4 Hz), 108.0, 107.9, 100.7, 53.1, 20.8 ppm.

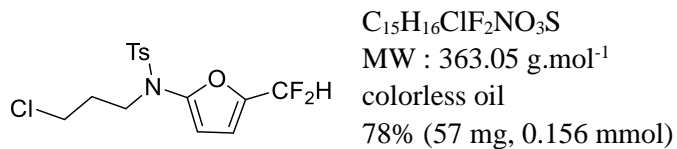
¹⁹F NMR (282 MHz, C₆D₆) δ = -114.48 ppm.

HRMS (ESI-TOF) m/z: [M+Na]⁺ calcd for C₂₀H₁₇F₂NNaO₅S 444.0666; Found 444.0688.

IR (neat): ν = 2989, 1559, 1354, 1166, 1037, 750, 666 cm⁻¹

R_f: 0.40 (Petroleum ether / Ethyl acetate 5:1 v/v, UV)

Compound 387m: *N*-(3-chloropropyl)-*N*-(5-(difluoromethyl)furan-2-yl)-4-methylbenzenesulfonamide



¹H NMR (500 MHz, C₆D₆): δ = 7.58 (d, *J* = 8.0 Hz, 2H), 6.73 (d, *J* = 8.0 Hz, 2H), 6.06 – 6.06 (m, 1H), 5.97 (d, *J* = 3.4 Hz, 1H), 5.79 (t, *J* = 54.0 Hz, 1H), 3.41 (t, *J* = 6.7 Hz, 2H), 3.05 (t, *J* = 6.3 Hz, 2H), 1.84 (s, 3H), 1.55 (p, *J* = 6.5 Hz, 2H) ppm.

¹³C NMR (125 MHz, C₆D₆) δ = 147.4 (t, *J* = 2.3 Hz), 143.8 (t, *J* = 29.0 Hz), 143.8, 135.6, 129.5 (×2), 127.6 (×2), 111.7 (t, *J* = 4.8 Hz), 108.0 (t, *J* = 233.6 Hz), 107.5, 46.9, 41.1, 31.3, 20.8 ppm.

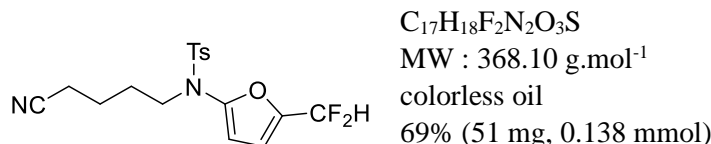
¹⁹F NMR (282 MHz, C₆D₆) δ = -114.60 ppm.

HRMS (ESI-TOF) m/z: [M+Na]⁺ calcd for C₁₅H₁₆ClF₂NNaO₃S 386.0378; Found 386.0400.

IR (neat): ν = 2964, 1558, 1352, 1162, 1016, 764, 666, 544 cm⁻¹

R_f: 0.50 (Petroleum ether / Ethyl acetate 5:1 v/v, UV)

Compound 387n: *N*-(4-cyanobutyl)-*N*-(5-(difluoromethyl)furan-2-yl)-4-methylbenzenesulfonamide



¹H NMR (500 MHz, C₆D₆): δ = 7.58 (d, *J* = 8.3 Hz, 2H), 6.77 (d, *J* = 8.0 Hz, 2H), 6.09 – 6.07 (m, 1H), 6.03 (d, *J* = 3.5 Hz, 1H), 5.84 (t, *J* = 53.9 Hz, 1H), 3.16 (t, *J* = 6.6 Hz, 2H), 1.86 (s, 3H), 1.36 (t, *J* = 7.0 Hz, 2H), 1.14 – 1.06 (m, 2H), 1.03 – 0.95 (m, 2H) ppm.

¹³C NMR (125 MHz, C₆D₆) δ = 147.2 (t, *J* = 2.3 Hz), 143.9, 143.8 (t, *J* = 28.4 Hz), 135.7, 129.5 (×2), 127.5 (×2), 118.7, 111.9 (t, *J* = 4.9 Hz), 108.1 (t, *J* = 233.6 Hz), 107.6, 48.3, 26.7, 21.7, 20.8, 15.6 ppm.

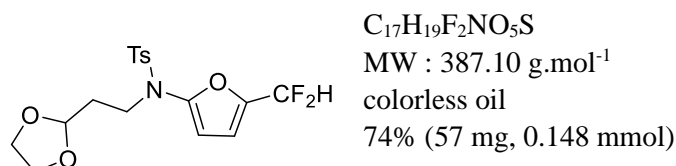
¹⁹F NMR (282 MHz, C₆D₆) δ = -114.58 ppm.

HRMS (ESI-TOF) m/z: [M+Na]⁺ calcd for C₁₇H₁₈F₂N₂NaO₃S 391.0887; Found 391.0898.

IR (neat): ν = 2943, 2874, 2360, 1560, 1354, 1165, 1018, 750, 669, 549 cm⁻¹

R_f: 0.30 (Petroleum ether / Ethyl acetate 3:1 v/v, UV)

Compound 387o: *N*-(2-(1,3-dioxolan-2-yl)ethyl)-*N*-(5-(difluoromethyl)furan-2-yl)-4-methylbenzenesulfonamide



¹H NMR (500 MHz, C₆D₆): δ = 7.62 (d, *J* = 8.3 Hz, 2H), 6.70 (d, *J* = 8.0 Hz, 2H), 6.07 – 1.89 (m, 1H), 6.05 (d, *J* = 3.4 Hz, 1H), 5.76 (t, *J* = 54.1 Hz, 1H), 4.71 (t, *J* = 4.5 Hz, 1H), 3.81 – 3.71 (m, 2H), 3.46 – 3.36 (m, 2H), 3.28 – 3.20 (m, 2H), 1.96 – 1.89 (m, 2H), 1.82 (s, 3H) ppm.

¹³C NMR (125 MHz, C₆D₆) δ = 147.5 (t, *J* = 2.3 Hz), 143.8 (t, *J* = 29.2 Hz), 143.5, 135.9, 129.4 (×2), 127.6 (×2), 111.5 (t, *J* = 4.7 Hz), 108.1 (t, *J* = 233.6 Hz), 107.7, 101.70, 64.5 (×2), 45.3 32.9, 20.8 ppm.

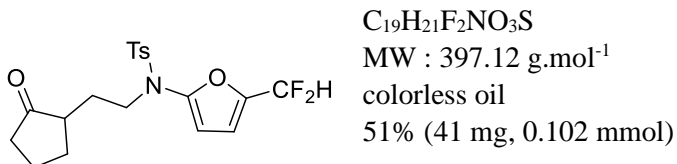
¹⁹F NMR (282 MHz, C₆D₆) δ = -114.81 ppm.

HRMS (ESI-TOF) m/z: [M+Na]⁺ calcd for C₁₇H₁₉F₂NNaO₅S 410.0825; Found 410.0844.

IR (neat): ν = 2958, 2886, 1558, 1353, 1164, 1016, 765, 666, 549 cm⁻¹

R_f: 0.16 (Petroleum ether / Ethyl acetate 5:1 v/v, UV)

Compound 387p: *N*-(5-(difluoromethyl)furan-2-yl)-4-methyl-*N*-(2-(2-oxocyclopentyl)ethyl)benzenesulfonamide



¹H NMR (500 MHz, C₆D₆): δ = 7.64 (d, *J* = 8.4 Hz, 2H), 6.75 (d, *J* = 8.0 Hz, 2H), 6.12 – 6.07 (m, 2H), 5.81 (t, *J* = 54.0 Hz, 1H), 3.62 – 3.56 (m, 1H), 3.51 – 3.46 (m, 1H), 1.97 – 1.91 (m, 1H), 1.88 – 1.82 (m, 2H), 1.84 (s, 3H), 1.81 – 1.76 (m, 1H), 1.64 – 1.56 (m, 1H), 1.41 – 1.35 (m, 1H), 1.26 – 1.14 (m, 2H), 0.98 – 0.90 (m, 1H) ppm.

¹³C NMR (125 MHz, C₆D₆) δ = 217.5, 147.4 (t, *J* = 2.3 Hz), 143.8 (t, *J* = 28.8 Hz), 143.7, 135.9, 129.5 (×2), 127.6 (×2), 111.7 (t, *J* = 4.8 Hz), 108.1 (t, *J* = 233.6 Hz), 107.7, 48.0, 45.8, 37.1, 29.3, 28.6, 20.8, 20.3 ppm.

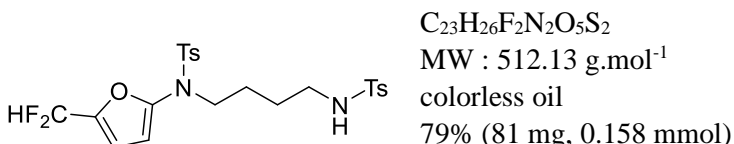
¹⁹F NMR (282 MHz, C₆D₆) δ = -114.68 ppm.

HRMS (ESI-TOF) m/z: [M+H]⁺ calcd for C₁₉H₂₂F₂NO₃S 398.1218; Found 398.1232.

IR (neat): ν = 2963, 2874, 1733, 1353, 1164, 1016, 759, 667, 545 cm⁻¹

R_f: 0.24 (Petroleum ether / Ethyl acetate 5:1 *v/v*, UV)

Compound 387q: *N*-(5-(difluoromethyl)furan-2-yl)-4-methyl-*N*-(4-((4-methylphenyl)sulfonamido)butyl)benzenesulfonamide



¹H NMR (500 MHz, C₆D₆): δ = 7.86 (d, *J* = 7.9 Hz, 2H), 7.65 (d, *J* = 8.0 Hz, 2H), 6.90 (d, *J* = 7.9 Hz, 2H), 6.81 (d, *J* = 7.9 Hz, 2H), 6.16 (d, *J* = 2.8 Hz, 1H), 6.09 (d, *J* = 3.4 Hz, 1H), 5.92 (t, *J* = 54.0 Hz, 1H), 4.83 (m, 1H), 3.36 – 3.27 (m, 2H), 2.73 – 2.67 (m, 2H), 1.96 (s, 3H), 1.87 (s, 3H), 1.25 (t, *J* = 3.6 Hz, 4H) ppm.

¹³C NMR (125 MHz, C₆D₆) δ = 147.4 (t, *J* = 2.3 Hz), 143.8 (t, *J* = 28.9 Hz), 143.8, 142.6, 137.9, 135.7, 129.5 (×2), 129.5 (×2), 127.6 (×2), 127.1 (×2), 111.7 (t, *J* = 4.8 Hz), 108.2 (t, *J* = 233.5 Hz), 107.6, 48.9, 42.3, 25.8, 25.0, 20.8 (×2) ppm.

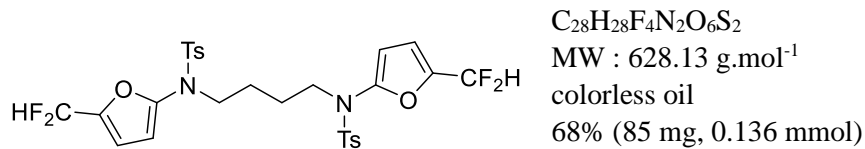
¹⁹F NMR (282 MHz, C₆D₆) δ = -114.66 ppm.

HRMS (ESI-TOF) m/z: [M+Na]⁺ calcd for C₂₃H₂₆F₂N₂NaO₅S₂ 535.1118; Found 535.1143.

IR (neat): ν = 3288, 2927, 2872, 2359, 1559, 1352, 1159, 1090, 750, 666, 549 cm⁻¹

R_f: 0.20 (Petroleum ether / Ethyl acetate 3:1 *v/v*, UV)

Compound 387r: *N*-(5-(difluoromethyl)furan-2-yl)-*N*-(4-((*N*-(5-(difluoromethyl)furan-2-yl)-4-methylphenyl)sulfonamido)butyl)-4-methylbenzenesulfonamide



¹H NMR (500 MHz, C₆D₆): δ = 7.64 (d, *J* = 8.0 Hz, 4H), 6.79 (d, *J* = 8.0 Hz, 4H), 6.15 – 6.13 (m, 2H), 6.05 (d, *J* = 3.5 Hz, 2H), 5.89 (t, *J* = 54.0 Hz, 2H), 3.38 (s, 4H), 1.87 (s, 6H), 1.35 (s, 4H) ppm.

¹³C NMR (125 MHz, C₆D₆) δ = 147.5 (t, *J* = 2.3 Hz) (×2), 143.8 (t, *J* = 28.9 Hz) (×2), 143.7 (×2), 135.8 (×2), 129.5 (×4), 127.6 (×4), 111.7 (t, *J* = 4.8 Hz) (×2), 108.1 (t, *J* = 233.4 Hz) (×2), 107.4 (×2), 48.5 (×2), 24.5 (×2), 20.8 (×2) ppm.

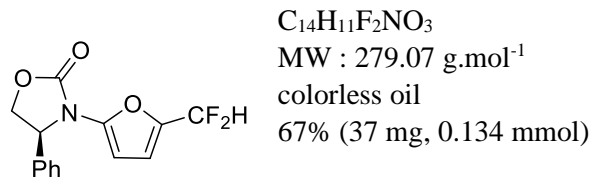
¹⁹F NMR (282 MHz, C₆D₆) δ = -114.64 ppm.

HRMS (ESI-TOF) m/z: [M+Na]⁺ calcd for C₂₈H₂₈F₄N₂NaO₆S₂ 651.1202; Found 651.1217.

IR (neat): ν = 2936, 1558, 1351, 1164, 666, 544 cm⁻¹

R_f: 0.19 (Petroleum ether / Ethyl acetate 5:1 *v/v*, UV)

Compound 393a: (*S*)-3-(5-(difluoromethyl)furan-2-yl)-4-phenyloxazolidin-2-one



¹H NMR (500 MHz, Acetone): δ = 7.47 – 7.30 (m, 5H), 6.77 – 6.76 (m, 1H), 6.74 (t, *J* = 53.3 Hz, 1H), 6.22 (d, *J* = 3.5 Hz, 1H), 5.63 – 5.57 (m, 1H), 4.97 (t, *J* = 8.7 Hz, 1H), 4.36 (dd, *J* = 8.8, 5.4 Hz, 1H) ppm.

¹³C NMR (125 MHz, Acetone) δ = 154.8, 147.4, 141.8 (t, *J* = 27.1 Hz), 139.4, 129.7(×2), 129.5, 127.4(×2), 113.9 (t, *J* = 5.5 Hz), 109.2 (t, *J* = 230.4 Hz), 99.0, 71.4, 60.7 ppm.

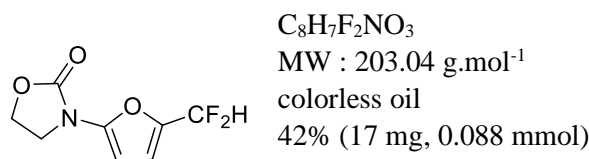
¹⁹F NMR (282 MHz, Acetone) δ = -109.82, -109.83 ppm.

HRMS (ESI-TOF) m/z: [M+Na]⁺ calcd for C₁₄H₁₁F₂NNaO₃ 302.0594; Found 302.0599.

IR (neat): ν = 1769, 1572, 1397, 1202, 787 cm⁻¹

R_f: 0.24 (Petroleum ether / Ethyl acetate 5:1 *v/v*, UV)

Compound 393b: 3-(5-(difluoromethyl)furan-2-yl)oxazolidin-2-one



¹H NMR (500 MHz, C₆D₆): δ = 6.37 (d, *J* = 3.4 Hz, 1H), 6.10 – 6.08 (m, 1H), 5.92 (t, *J* = 53.5 Hz, 1H), 3.08 – 3.02 (m, 2H), 2.63 – 2.56 (m, 2H). ppm.

¹³C NMR (125 MHz, C₆D₆) δ = 152.6, 147.9, 138.6 (t, J = 24.7 Hz), 113.9 (t, J = 5.6 Hz), 108.4 (t, J = 231.7 Hz), 92.4, 61.4, 42.3 ppm.

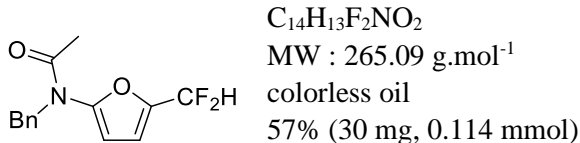
¹⁹F NMR (282 MHz, C₆D₆) δ = -112.21 ppm.

HRMS (ESI-TOF) m/z: [M+Na]⁺ calcd for C₈H₇F₂NNaO₃ 226.0285; Found 226.0286.

IR (neat): ν = 2925, 1751, 1590, 1139, 1001 cm⁻¹

R_f: 0.40 (Petroleum ether / Ethyl acetate 3:1 v/v, UV)

Compound 393c: *N*-benzyl-*N*-(5-(difluoromethyl)furan-2-yl)acetamide



¹H NMR (500 MHz, C₆D₆): δ = 7.15 – 6.99 (m, 5H), 5.92 (s, 1H), 5.84 (t, J = 54.1 Hz, 1H), 5.18 (s, 1H), 4.63 (s, 2H), 1.64 (s, 3H) ppm.

¹³C NMR (125 MHz, C₆D₆) δ = 169.4, 150.5, 143.4 (t, J = 28.9 Hz), 137.2, 128.3 (×2), 128.0, 127.6 (×2), 111.2, 108.1 (t, J = 233.6 Hz), 104.9, 50.9, 21.3 ppm.

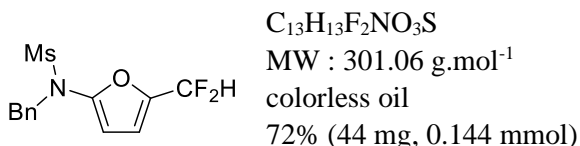
¹⁹F NMR (282 MHz, C₆D₆) δ = -114.61 ppm.

HRMS (ESI-TOF) m/z: [M+Na]⁺ calcd for C₁₄H₁₃F₂NNaO₂ 288.0803; Found 288.0807.

IR (neat): ν = 2933, 2366, 1685, 1564, 1379, 1276, 1015, 750 cm⁻¹

R_f: 0.30 (Petroleum ether / Ethyl acetate 5:1 v/v, UV)

Compound 393d: *N*-benzyl-*N*-(5-(difluoromethyl)furan-2-yl)methanesulfonamide



¹H NMR (500 MHz, C₆D₆): δ = 7.16 – 7.15 (m, 2H), 7.05 – 6.96 (m, 3H), 5.86 – 5.83 (m, 1H), 5.79 (t, J = 54.5 Hz, 1H), 5.72 (d, J = 3.5 Hz, 1H), 4.39 (s, 2H), 2.26 (s, 3H) ppm.

¹³C NMR (125 MHz, C₆D₆) δ = 147.3 (t, J = 2.3 Hz), 143.3 (t, J = 28.0 Hz), 135.4, 128.6 (×2), 128.5 (×2), 128.0, 112.0 (t, J = 5.1 Hz), 108.1 (t, J = 233.4 Hz), 107.2, 53.5, 38.7 ppm.

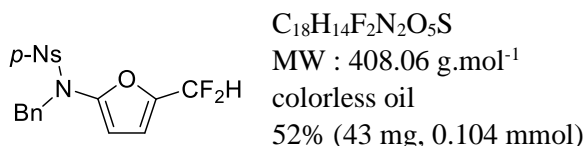
¹⁹F NMR (282 MHz, C₆D₆) δ = -114.44 ppm

HRMS (ESI-TOF) m/z: [M+Na]⁺ calcd for C₁₃H₁₃F₂NNaO₃S 324.0488; Found 324.0476.

IR (neat): ν = 2935, 1558, 1348, 1158, 1014, 752 cm⁻¹

R_f: 0.31 (Petroleum ether / Ethyl acetate 5:1 v/v, UV)

Compound 393e: *N*-benzyl-*N*-(5-(difluoromethyl)furan-2-yl)-4-nitrobenzenesulfonamide



¹H NMR (500 MHz, C₆D₆): δ = 7.55 (d, *J* = 8.9 Hz, 2H), 7.35 (d, *J* = 8.8 Hz, 2H), 7.12 (d, *J* = 6.5 Hz, 2H), 7.02 – 6.94 (m, 3H), 5.83 – 5.81 (m, 1H), 5.77 (d, *J* = 4.4 Hz, 1H), 5.66 (t, *J* = 53.7 Hz, 1H), 4.39 (s, 2H) ppm.

¹³C NMR (125 MHz, C₆D₆) δ = 149.9, 146.1 (t, *J* = 2.3 Hz), 143.9 (t, *J* = 28.1 Hz), 143.7, 134.4, 128.6 (×2), 128.5 (×2), 128.2 (×2), 128.0, 123.8 (×2), 111.8 (t, *J* = 5.0 Hz), 108.4, 107.8 (t, *J* = 233.7 Hz), 53.7 ppm.

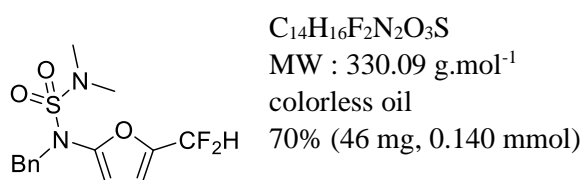
¹⁹F NMR (282 MHz, C₆D₆) δ = -114.70 ppm.

HRMS (ESI-TOF) m/z: [M+K]⁺ calcd for C₁₈H₁₄F₂KN₂O₅S 447.0200; Found 447.0223.

IR (neat): ν = 3105, 2927, 1525, 1349, 1169, 1029 cm⁻¹

R_f: 0.50 (Petroleum ether / Ethyl acetate 5:1 v/v, UV)

Compound 393f:



¹H NMR (500 MHz, CDCl₃): δ = 7.29 – 7.20 (m, 5H), 6.47 – 6.49 (m, 1H), 6.46 (t, *J* = 54.1 Hz, 1H), 6.03 (d, *J* = 3.5 Hz, 1H), 4.75 (s, 2H), 2.76 (s, 6H) ppm.

¹³C NMR (125 MHz, CDCl₃) δ = 147.8 (t, *J* = 2.3 Hz), 143.4 (t, *J* = 29.0 Hz), 135.7, 128.6 (×2), 128.5 (×2), 128.1, 111.9 (t, *J* = 4.9 Hz), 108.1 (t, *J* = 233.9 Hz), 107.3, 55.4, 38.1 (×2) ppm.

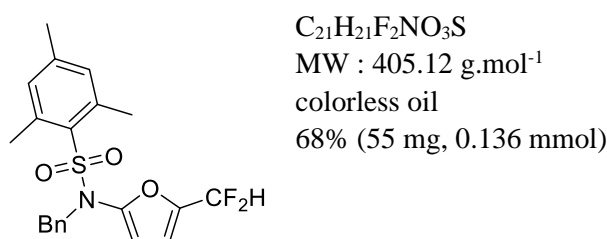
¹⁹F NMR (282 MHz, CDCl₃) δ = -114.90 ppm.

HRMS (ESI-TOF) m/z: [M+Na]⁺ calcd for C₁₄H₁₆F₂N₂NaO₃S 353.0738; Found 353.0742.

IR (neat): ν = 2929, 2361, 1558, 1350, 1155, 1014, 751, 699 cm⁻¹

R_f: 0.44(Petroleum ether / Ethyl acetate 5:1 v/v, UV)

Compound 393g: *N*-benzyl-*N*-(5-(difluoromethyl)furan-2-yl)-2,4,6-trimethylbenzenesulfonamide



¹H NMR (500 MHz, CDCl₃): δ = 7.31 – 7.16 (m, 5H), 6.96 (s, 2H), 6.44 – 6.43 (m, 1H), 6.40 (t, J = 54.3 Hz, 1H), 5.96 (d, J = 3.4 Hz, 1H), 4.78 (s, 2H), 2.57 (s, 6H), 2.32 (s, 3H) ppm.

¹³C NMR (125 MHz, CDCl₃) δ = 146.5 (t, J = 2.4 Hz), 143.9 (t, J = 29.8 Hz), 143.4, 140.6 (×2), 135.1, 132.1 (×2), 131.9, 128.7 (×2), 128.5 (×2), 128.0, 111.3 (t, J = 4.4 Hz), 108.0 (t, J = 234.0 Hz), 107.7, 52.8, 22.9 (×2), 21.0 ppm.

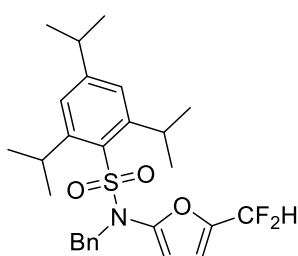
¹⁹F NMR (282 MHz, CDCl₃) δ = -115.43 ppm.

HRMS (ESI-TOF) m/z: [M+Na]⁺ calcd for C₂₁H₂₁F₂NNaO₃S 428.1082; Found 428.1102.

IR (neat): ν = 2941, 2359, 1557, 1333, 1159, 1014, 752, 699, 658 cm⁻¹

R_f: 0.65 (Petroleum ether / Ethyl acetate 5:1 v/v, UV)

Compound 393h: *N*-benzyl-*N*-(5-(difluoromethyl)furan-2-yl)-2,4,6-trisopropylbenzenesulfonamide



C₂₇H₃₃F₂NO₃S
MW : 489.21 g.mol⁻¹
colorless oil
65% (64 mg, 0.130 mmol)

¹H NMR (500 MHz, CDCl₃): δ = 7.37 – 7.27 (m, 5H), 7.22 (s, 2H), 6.50 – 6.49 (m, 1H), 6.46 (t, J = 54.3 Hz, 1H), 5.99 (d, J = 3.5 Hz, 1H), 4.90 (s, 2H), 4.08 (p, J = 6.7 Hz, 2H), 2.98 (p, J = 6.9 Hz, 1H), 1.33 (d, J = 6.9 Hz, 6H), 1.27 (d, J = 6.8 Hz, 12H) ppm.

¹³C NMR (125 MHz, CDCl₃) δ = 153.9, 151.8 (×2), 146.6 (t, J = 2.4 Hz), 144.2 (t, J = 30.0 Hz), 135.1, 130.6, 128.9 (×2), 128.5 (×2), 128.0, 124.0 (×2), 111.1 (t, J = 4.4 Hz), 108.5, 108.0 (t, J = 234.2 Hz), 52.3, 34.2, 29.7 (×2), 24.8 (×4), 23.5 (×2) ppm.

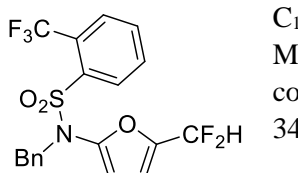
¹⁹F NMR (282 MHz, CDCl₃) δ = -115.52 ppm.

HRMS (ESI-TOF) m/z: [M+Na]⁺ calcd for C₂₇H₃₃F₂NNaO₃S 512.2027; Found 512.2041.

IR (neat): ν = 2960, 2870, 1558, 1164, 1036, 751, 663 cm⁻¹

R_f: 0.80 (Petroleum ether / Ethyl acetate 5:1 v/v, UV)

Compound 393i: *N*-benzyl-*N*-(5-(difluoromethyl)furan-2-yl)-2-(trifluoromethyl)benzenesulfonamide



C₁₉H₁₄F₅NO₃S
MW : 431.06 g.mol⁻¹
colorless oil
34% (28 mg, 0.068 mmol)

¹H NMR (500 MHz, CDCl₃): δ = 7.99 (d, J = 7.9 Hz, 1H), 7.92 (d, J = 8.0 Hz, 1H), 7.72 (t, J = 7.6 Hz, 1H), 7.64 (t, J = 7.7 Hz, 1H), 7.29 – 7.24 (m, 5H), 6.45 – 6.44 (m, 1H), 6.35 (t, J = 54.1 Hz, 1H), 6.07 (d, J = 3.5 Hz, 1H), 4.85 (s, 2H) ppm.

¹³C NMR (125 MHz, CDCl₃) δ = 145.6 (t, J = 2.3 Hz), 144.0 (t, J = 29.4 Hz), 137.8, 134.9, 133.3, 132.3, 132.1, 128.7 (×2), 128.6 (×2), 128.5 (q, J = 6.4 Hz), 128.2 (q, J = 33.2 Hz), 128.2, 122.4 (q, J = 272.4 Hz), 111.6 (t, J = 4.6 Hz), 108.8, 107.8 (t, J = 234.1 Hz), 54.2 ppm.

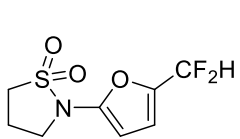
¹⁹F NMR (282 MHz, CDCl₃) δ = -115.50, -57.67 ppm.

HRMS (ESI-TOF) m/z: [M+Na]⁺ calcd for C₁₉H₁₄F₅NNaO₃S 454.0507; Found 454.0492.

IR (neat): ν = 1558, 1364, 1306, 1168, 1034 cm⁻¹

R_f: 0.30 (Petroleum ether / Ethyl acetate 5:1 v/v, UV)

Compound 393j: 2-(5-(difluoromethyl)furan-2-yl)isothiazolidine 1,1-dioxide



C₈H₉F₂NO₃S
MW : 237.03 g.mol⁻¹
colorless oil
70% (33 mg, 0.140 mmol)

¹H NMR (500 MHz, CDCl₃): δ = 6.67 – 6.60 (m, 1H), 6.45 (d, J = 54.3 Hz, 1H), 6.20 (d, J = 3.4 Hz, 1H), 3.84 (t, J = 6.8 Hz, 2H), 3.33 (t, J = 7.5 Hz, 2H), 2.54 (p, J = 7.0 Hz, 2H). ppm.

¹³C NMR (125 MHz, CDCl₃) δ = 145.3 (t, J = 2.3 Hz), 143.1 (t, J = 29.6 Hz), 112.2 (t, J = 4.6 Hz), 108.2 (t, J = 233.8 Hz), 101.6, 47.3, 47.0, 19.3 ppm.

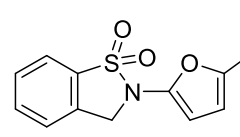
¹⁹F NMR (282 MHz, CDCl₃) δ = -114.85 ppm.

HRMS (ESI-TOF) m/z: [M+Na]⁺ calcd for C₈H₉F₂NNaO₃S 260.0163; Found 260.0163.

IR (neat): ν = 2964, 2360, 1560, 1275, 1142, 1014, 750 cm⁻¹

R_f: 0.40 (Petroleum ether / Ethyl acetate 1:1 v/v, UV)

Compound 393k: 2-(5-(difluoromethyl)furan-2-yl)-2,3-dihydrobenzo[d]isothiazole 1,1-dioxide



C₁₂H₉F₂NO₃S
MW : 285.03 g.mol⁻¹
colorless oil
81% (46 mg, 0.162 mmol)

¹H NMR (500 MHz, CDCl₃): δ = 7.86 (d, J = 7.8 Hz, 1H), 7.69 (t, J = 7.5 Hz, 1H), 7.61 (t, J = 7.6 Hz, 1H), 7.48 (d, J = 7.7 Hz, 1H), 6.72 – 6.71 (m, 1H), 6.57 (t, J = 54.2 Hz, 1H), 6.40 (d, J = 3.5 Hz, 1H), 4.94 (s, 2H) ppm.

¹³C NMR (125 MHz, CDCl₃) δ = 144.0 (t, J = 2.3 Hz), 143.6 (t, J = 29.6 Hz), 133.7, 133.5, 132.1, 129.7, 124.7, 121.9, 112.3 (t, J = 4.6 Hz), 108.1 (t, J = 233.9 Hz), 102.2, 50.5 ppm.

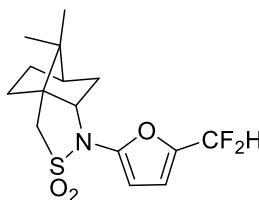
¹⁹F NMR (282 MHz, CDCl₃) δ = -114.99 ppm.

HRMS (ESI-TOF) m/z: [M+Na]⁺ calcd for C₁₂H₉F₂NNaO₃S 308.0163; Found 308.0171.

IR (neat): ν = 3122, 1561, 1304, 1005, 755, 706, 637 cm⁻¹

R_f: 0.20 (Petroleum ether / Ethyl acetate 5:1 v/v, UV)

Compound 393l: (3aR,6R)-1-(5-(difluoromethyl)furan-2-yl)-8,8-dimethylhexahydro-3H-3a,6-methanobenzo[c]isothiazole 2,2-dioxide



C₁₅H₁₉F₂NO₃S

MW : 331.11 g.mol⁻¹

colorless oil

91% (60 mg, 0.182 mmol)

¹H NMR (500 MHz, C₆D₆): δ = 6.10 – 6.08 (m, 1H), 6.07 (d, J = 3.5 Hz, 1H), 5.89 (t, J = 54.2 Hz, 1H), 3.49 (dd, J = 8.0, 4.4 Hz, 1H), 2.80 – 2.67 (m, 2H), 1.66 – 1.61 (m, 1H), 1.37 – 1.29 (m, 2H), 1.25 – 1.16 (m, 2H), 0.97 (s, 3H), 0.88 – 0.81 (m, 1H), 0.74 – 0.68 (m, 1H), 0.42 (s, 3H) ppm.

¹³C NMR (125 MHz, C₆D₆) δ = 144.8 (t, J = 2.2. Hz), 143.6 (t, J = 28.8 Hz), 112.0 (t, J = 4.8 Hz), 108.3 (t, J = 233.4 Hz), 102.4, 65.2, 49.6, 49.5, 47.4, 44.1, 34.5, 31.2, 26.5, 19.9, 19.3 ppm.

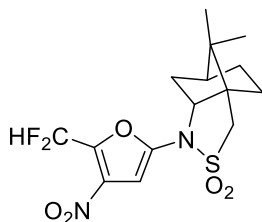
¹⁹F NMR (282 MHz, C₆D₆) δ = -114.56, -114.64 ppm.

HRMS (ESI-TOF) m/z: [M+Na]⁺ calcd for C₁₅H₁₉F₂NNaO₃S 354.0935; Found 354.0946.

IR (neat): ν = 2959, 2884, 1557, 1325, 1276, 1166, 1140, 1013, 783, 537 cm⁻¹

R_f: 0.34 (Petroleum ether / Ethyl acetate 5:1 v/v, UV)

Compound 396: (3aS,6S)-1-(5-(difluoromethyl)-4-nitrofuran-2-yl)-8,8-dimethylhexahydro-3H-3a,6-methanobenzo[c]isothiazole 2,2-dioxide



C₁₅H₁₈F₂N₂O₅S

MW : 376.09 g.mol⁻¹

colorless oil

65% (25 mg, 0.065 mmol)

¹H NMR (500 MHz, CDCl₃): δ = 7.22 (s, 1H), 6.57 (t, J = 53.8 Hz, 1H), 4.22 (dd, J = 8.0, 4.4 Hz, 1H), 3.50 – 3.39 (m, 2H), 2.03 – 1.86 (m, 4H), 1.74 (dd, J = 12.9, 8.1 Hz, 1H), 1.61 (m, 1H), 1.36 (m, 1H), 1.27 (s, 3H), 1.00 (s, 3H) ppm.

¹³C NMR (126 MHz, CDCl₃) δ = 143.5 (t, J = 32.1 Hz), 141.76, 132.45, 108.1 (t, J = 4.1 Hz), 107.1 (t, J = 237.1 Hz), 66.1, 51.0, 50.9, 48.1, 44.7, 35.0, 32.2, 26.8, 20.3, 20.2 ppm.

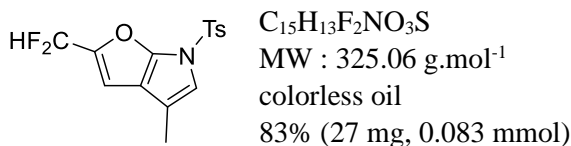
¹⁹F NMR (282 MHz, CDCl₃) δ = -117.63, -117.70 ppm.

HRMS (ESI-TOF) m/z: [M+Na]⁺ calcd for C₁₅H₁₈F₂N₂NaO₅S 399.0797; Found 399.0797.

IR (neat): ν = 3126, 2962, 2885, 2361, 1585, 1336, 1143, 1045, 751 cm⁻¹

R_f: 0.39 (Petroleum ether / Ethyl acetate 5:1 v/v, UV)

Compound 399: 2-(difluoromethyl)-4-methyl-6-tosyl-6H-furo[2,3-b]pyrrole



¹H NMR (500 MHz, CDCl₃): δ = 7.83 (d, *J* = 8.5 Hz, 2H), 7.29 (d, *J* = 8.0 Hz, 2H), 6.71 (t, *J* = 2.2 Hz, 1H), 6.67 (d, *J* = 1.4 Hz, 1H), 6.63 (t, *J* = 54.2 Hz, 1H), 2.39 (s, 3H), 2.08 (d, *J* = 1.4 Hz, 3H) ppm.

¹³C NMR (126 MHz, CDCl₃) δ = 147.3 (t, *J* = 2.3 Hz), 146.8 (t, *J* = 29.9 Hz), 145.5, 135.0, 130.1 (×2), 127.1 (×2), 117.8, 116.1, 114.3, 108.5 (t, *J* = 233.6 Hz), 105.9 (t, *J* = 4.7 Hz), 21.7, 11.5 ppm

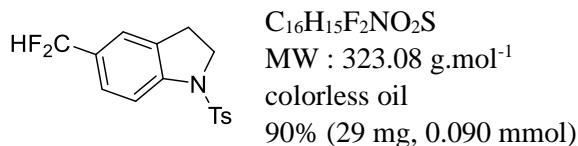
¹⁹F NMR (282 MHz, CDCl₃) δ = -113.46 ppm.

HRMS (ESI-TOF) m/z: [M+H]⁺ calcd for C₁₅H₁₄F₂NO₃S 326.0657; Found 326.0663.

IR (neat): ν = 2925, 2359, 2335, 1276, 1175, 750, 669 cm⁻¹

R_f: 0.59 (Petroleum ether / Ethyl acetate 5:1 *v/v*, UV)

Compound 404: 5-(difluoromethyl)-1-tosylindoline



¹H NMR (500 MHz, CDCl₃): δ = 7.69 (m, 3H), 7.31 (d, *J* = 8.3 Hz, 1H), 7.25 (m, 3H), 6.56 (t, *J* = 56.6 Hz, 1H), 4.00 – 3.91 (t, *J* = 14.5 Hz, 2H), 2.97 (t, *J* = 8.5 Hz, 2H), 2.38 (s, 3H) ppm.

¹³C NMR (126 MHz, CDCl₃) δ = 144.5, 144.2 (t, *J* = 1.9 Hz), 133.7, 132.2, 129.8 (×2), 127.3 (×2), 125.8 (t, *J* = 6.4 Hz), 122.4 (t, *J* = 5.6 Hz), 114.7 (t, *J* = 236.7 Hz), 114.3, 50.1, 27.6, 21.6 ppm.

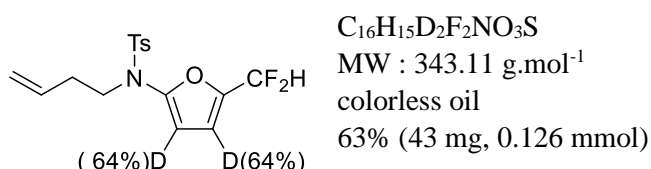
¹⁹F NMR (282 MHz, CDCl₃) δ = -108.87 ppm.

HRMS (ESI-TOF) m/z: [M+K]⁺ calcd for C₁₆H₁₅F₂KNO₂S 362.0423; Found 362.0425.

IR (neat): ν = 2988, 2359, 2358, 1355, 1166, 750, 664 cm⁻¹

R_f: 0.40 (Petroleum ether / Ethyl acetate 5:1 *v/v*, UV)

Compound 389h': *N*-(but-3-en-1-yl)-*N*-(5-(difluoromethyl)furan-2-yl-3,4-d2)-4-methylbenzenesulfonamide



¹H NMR (500 MHz, CDCl₃) δ = 7.59 (d, *J* = 8.3 Hz, 2H), 7.29 (d, *J* = 8.0 Hz, 2H), 6.63 (s, 0.36H), 6.46 (t, *J* = 54.3 Hz, 1H), 6.28 (s, 0.36H), 5.76 – 5.63 (m, 1H), 5.10 – 4.98 (m, 2H), 3.54 (t, *J* = 7.3 Hz, 2H), 2.44 (s, 3H), 2.24 (q, *J* = 7.2 Hz, 2H) ppm.

¹H NMR (500 MHz, C₆D₆) δ = 7.60 (d, *J* = 8.0 Hz, 2H), 6.71 (d, *J* = 8.0 Hz, 2H), 6.05 (s, 0.72H), 5.77 (t, *J* = 54.0 Hz, 1H), 5.56 – 5.46 (m, 1H), 4.95 – 4.80 (m, 2H), 3.44 (t, *J* = 7.2 Hz, 2H), 2.06 (q, *J* = 7.0 Hz, 2H), 1.82 (s, 3H) ppm.

¹³C NMR (125 MHz, C₆D₆) δ = 147.5, 143.5, 143.6, 136.1, 133.9, 129.4 (×2), 127.5 (×2), 116.9, 111.7, 108.1 (t, *J* = 233.5 Hz), 107.6, 48.8, 32.7, 20.8 ppm.

R_f: 0.59(Petroleum ether / Ethyl acetate 5:1 v/v, UV)

DFT calculations

Mechanistic study by means of DFT calculations

Based on previous literature report on copper-catalyzed coupling reactions with alkynes, we propose a multistep pathway, involving the formation of a copper ynamide intermediate (**D**) (Figure 1). In the presence of copper (I) salt, ynamide **A** leads to copper-ynamidyl **B**. The addition of difluorodiazoacetone allows the formation of the intermediate **C**, leading to the intermediate **D**, after the expulsion of N₂. At this point, depending on which carbon the proton of the HI acid attacks, two different possible pathways can be envisaged, leading to the amido-difluorinated furan (**J**), as detailed in Figure 1.

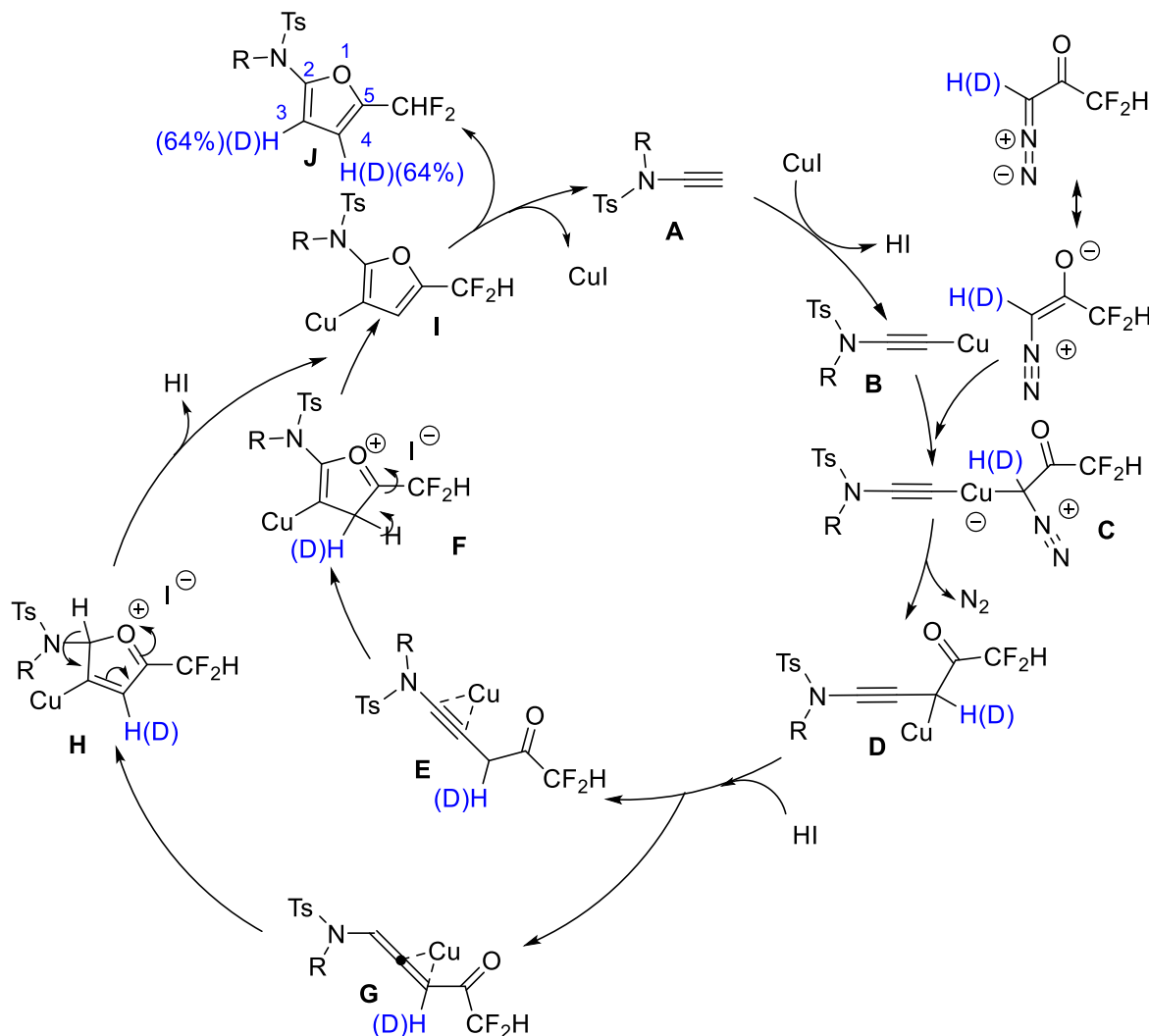


Figure 1 Hypothesized mechanism

In order to confirm the postulated reaction mechanism, we performed Density Functional Theory (DFT) calculations. Ground-state full structural optimizations have been performed by employing the PBE0 global hybrid exchange-correlation functional¹ containing the 25% of Hartree-Fock exchange as implemented in the Gaussian 16 package.² The triple zeta Pople all electron basis functions (6-311+G(d)³) for the lighter elements (C, H, O, N, S and F) and the LANL2 pseudo potential in combination with a double zeta basis set for I and Cu⁵ coupled with the Grimme's D3-BJ correction⁴ to include dispersion interactions were applied in all calculation. Solvent effects (here acetonitrile) were taken into account implicitly by resorting

to the conductor-like polarizable continuum model (CPCM).⁶ The analysis of the vibrational harmonic frequencies has been conducted to verify the nature of all stationary points found on the PES, namely local minima having all positive normal mode frequencies and saddle points corresponding to first-order transition states (TS) which feature an imaginary frequency. The resulting computed reaction paths together with the labelling scheme is reported in **Figures 2-4.**

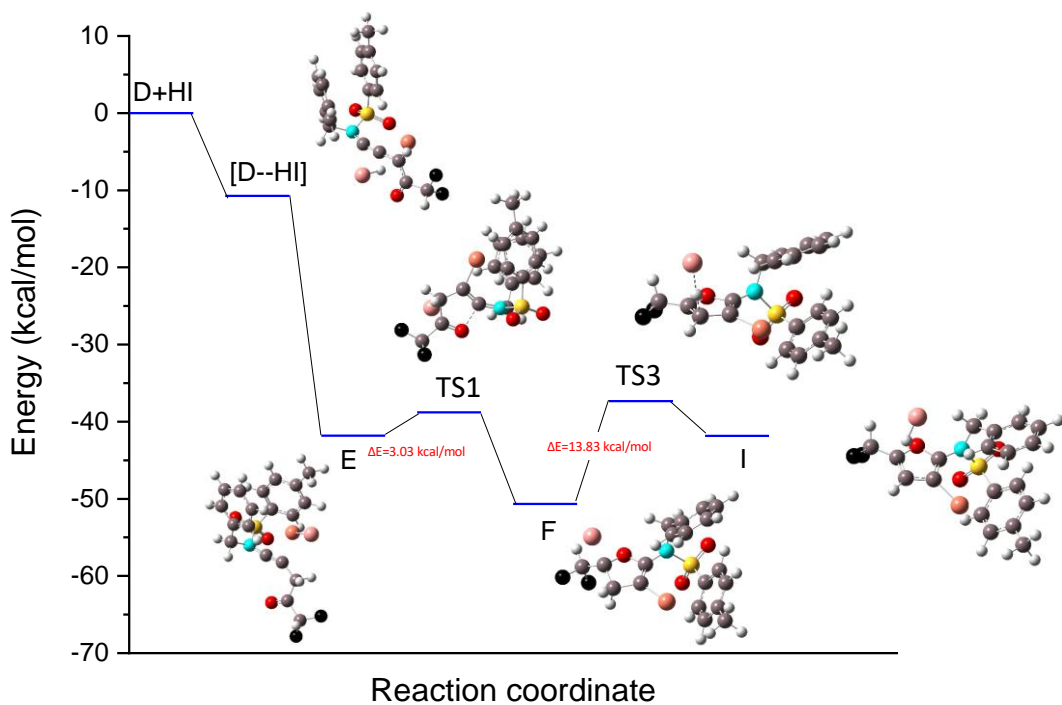


Figure 2 Computed reaction path leading from D to I, refer to Figure 1, together with the corresponding optimized structures.

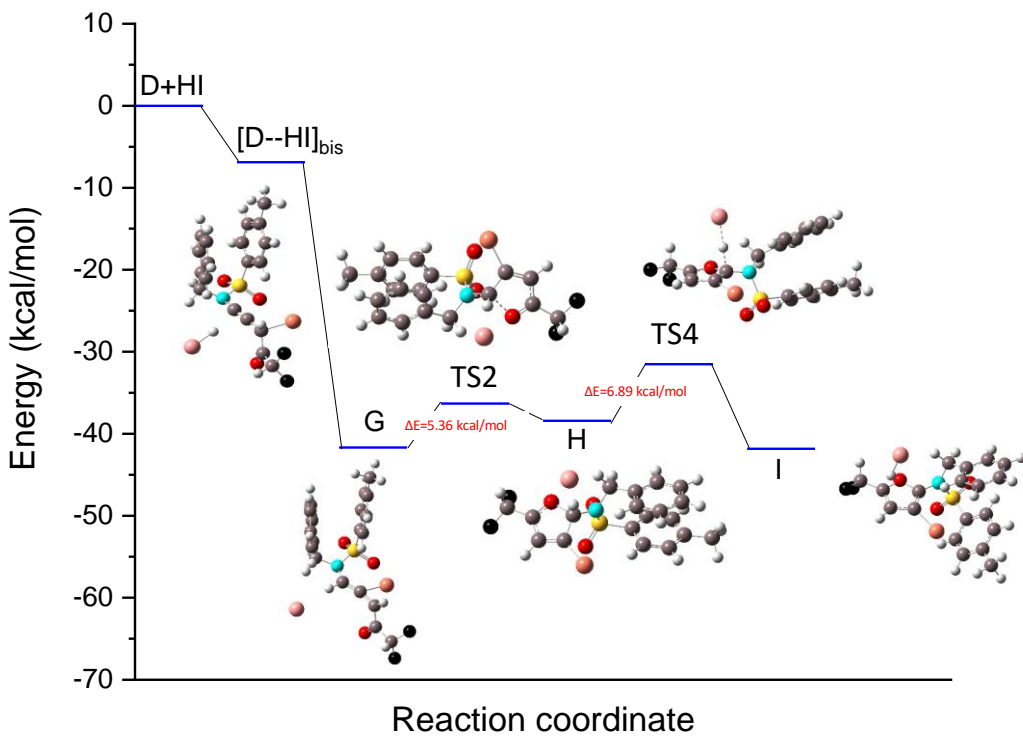


Figure 3 Computed reaction path together with the corresponding optimized structures.

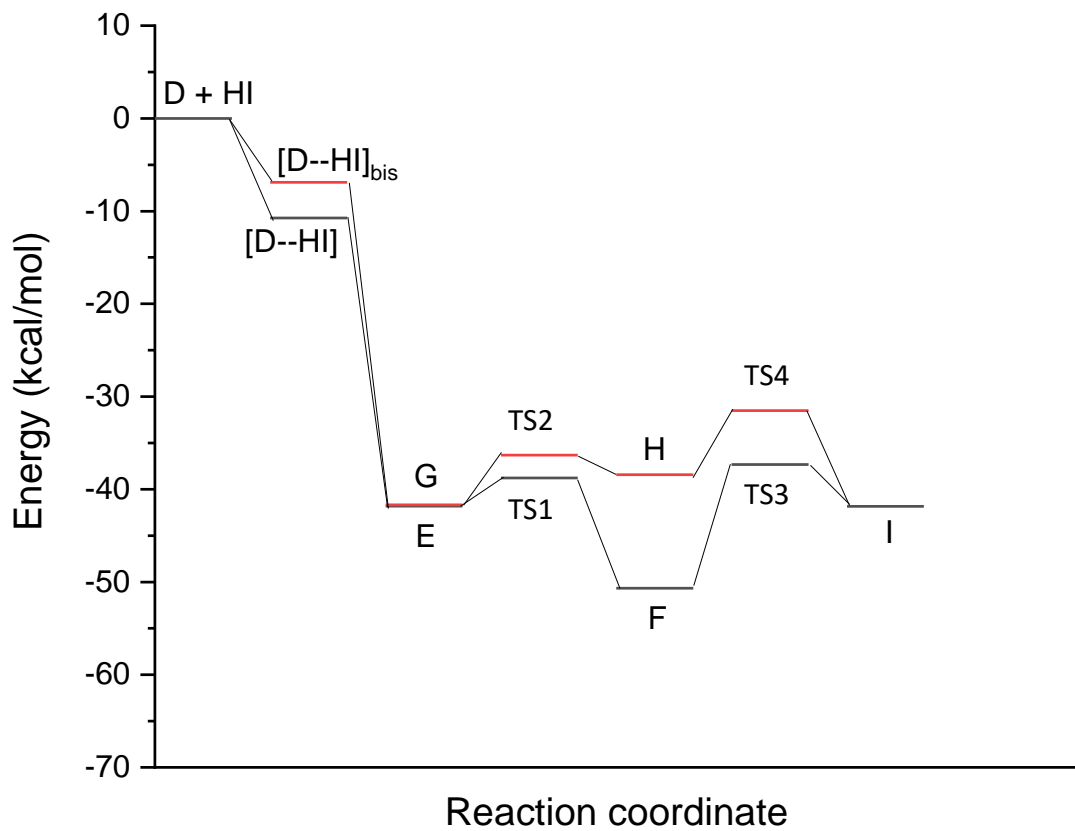


Figure 4 Computed reaction paths.

The reaction mechanism has been built by setting as zero-point energy the sum of the energy of the isolated Intermediate **D** and HI. The initial step corresponds to the proton transfer from the hydriodic acid, which can activate the ynamide **D** leading easily to the formation of

intermediates **E** or **G**, according if the protonation is in α or γ position with respect to the carbonyl- CF_2 moiety. Henceforth, we will indicate as $[\text{D} - \text{HI}]$ and $[\text{D} - \text{HI}]_{\text{bis}}$ the adducts formed by addition of the proton to the α or γ carbons of Intermediate **D**, respectively. However, for such proton transfer reactions the PES is usually extremely flat making it hard to find the corresponding TS structures. As a result, a coordinate scan of the PES along the C - H bond was conducted. The C - H bond length was kept fixed to a certain value ranging from 2.04 Å and 2.06 Å (correspond to the $[\text{D} - \text{HI}]$ and $[\text{D} - \text{HI}]_{\text{bis}}$ coordination distances) up to 1.10 Å, (the C - H equilibrium bond length in **E** and **G**), while all other parameters were allowed to relax. The graph in **Figure 5** shows the two hypothesized proton transfer pathways in terms of internal energy ΔE calculated for each step along the reaction coordinate. It is worth noticing the proton transfer reactions leading to **E** and **G** are thermodynamically favored, since the produced species (**E** and **G**) are more stable than the starting one (**D**), and furthermore barrierless (there is no activation barrier), meaning that the reactions occur without kinetic impediment.

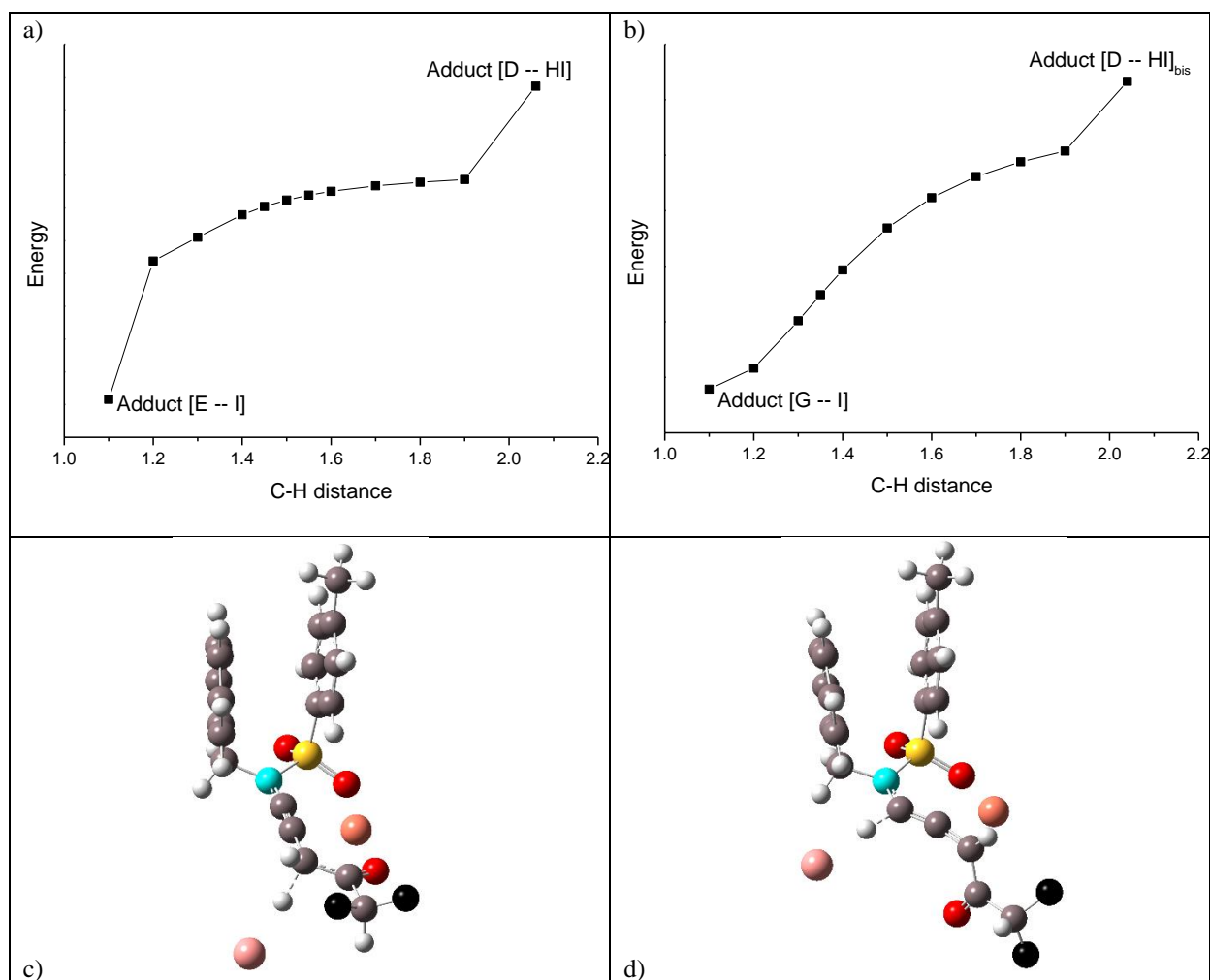


Figure 2 Reaction coordinate scan along the α C - H (a) and γ C - H (b) and corresponding molecular representation of Adducts $[\text{D} - \text{HI}]$ and $[\text{D} - \text{HI}]_{\text{bis}}$ (c and d respectively) as balls and sticks model with the investigated coordinates represented as dotted lines.

Later on, **E** and **G** undergo a cyclization via the TS_1/TS_2 transition states: the carbonylic C-0 bond is elongated up to around 1.24 Å, while the distance between the carbonylic oxygen and the γ carbon decreases achieving a value of around 1.80-1.85 Å and suggesting the closure of

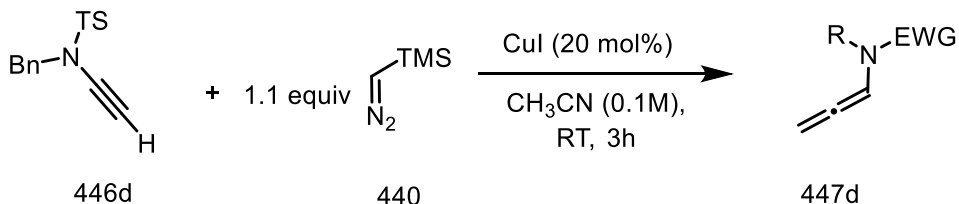
the furanic cycle. **TS₁** and **TS₂** lies at 3.03 kcal/mol and 5.36 kcal/mol, respectively, higher in energy with respect to the **E** and **G** and lead to the formation of intermediates **F** and **H**. For these last two, the C-O bond distance is about 1.40-1.50 Å, corresponding to a fully formed furanic cycle, with copper atom in position 3. Comparing the atomic (Mulliken) charges computed for the **TS₁** and the **F**, it is found that carbons in position 2 respectively of the furanic cycle becomes more electrophilic (from -0.28|e-|to 0.62|e-|), making the bonded proton more acidic (from 0.37|e-|to 0.43|e-|). This makes possible to envisage a proton transfer from carbons in 2 and 4 positions of **F/H** respectively towards the iodide anion present in the reaction environment. The energy barriers (13.33 and 6.89 kcal/mol) computed for these two proton transfers confirmed such hypothesis and both lead to the same resulting stable furanic specie **I**, with an energy of -41.85 kcal/mol, and formation of hydriodic acid. At this stage, the reaction terminates via a substitution of the copper atom with a proton coming from the hydriodic acid. The decupration regenerates the copper iodide and forms the desired amidodifluorinated furan **J**. In conclusion, the whole reaction results to be exergonic and thermodynamically driven by the formation of really stable product (-98.42 kcal/mol). The computed mechanism is in agreement with the experimental evidence that by adding D₂O to the reaction mixture, we obtain **5h'** with an equal deuterium incorporation at both positions 3 and 4 (Scheme 6, c in the main text), which actually are the reactive positions where the carbons exchanges with hydriodic acid-d.

References

1. C. Adamo, V. Barone, J. Chem. Phys. 1999, 110, 6158–6179.
2. Gaussian 16, Revision C.01, Frisch, M. J.; Trucks, G. W.; Schlegel, H. B.; Scuseria, G. E.; Robb, M. A.; Cheeseman, J. R.; Scalmani, G.; Barone, V.; Petersson, G. A.; Nakatsuji, H.; Li, X.; Caricato, M.; Marenich, A. V.; Bloino, J.; Janesko, B. G.; Gomperts, R.; Mennucci, B.; Hratchian, H. P.; Ortiz, J. V.; Izmaylov, A. F.; Sonnenberg, J. L.; Williams-Young, D.; Ding, F.; Lipparini, F.; Egidi, F.; Goings, J.; Peng, B.; Petrone, A.; Henderson, T.; Ranasinghe, D.; Zakrzewski, V. G.; Gao, J.; Rega, N.; Zheng, G.; Liang, W.; Hada, M.; Ehara, M.; Toyota, K.; Fukuda, R.; Hasegawa, J.; Ishida, M.; Nakajima, T.; Honda, Y.; Kitao, O.; Nakai, H.; Vreven, T.; Throssell, K.; Montgomery, J. A., Jr.; Peralta, J. E.; Ogliaro, F.; Bearpark, M. J.; Heyd, J. J.; Brothers, E. N.; Kudin, K. N.; Staroverov, V. N.; Keith, T. A.; Kobayashi, R.; Normand, J.; Raghavachari, K.; Rendell, A. P.; Burant, J. C.; Iyengar, S. S.; Tomasi, J.; Cossi, M.; Millam, J. M.; Klene, M.; Adamo, C.; Cammi, R.; Ochterski, J. W.; Martin, R. L.; Morokuma, K.; Farkas, O.; Foresman, J. B.; Fox, D. J. Gaussian, Inc., Wallingford CT, 2016
3. R. Krishnan, J. S. Binkley, R. Seeger, and J. A. Pople, J. Chem. Phys. 72, 650 (1980)
4. S. Grimme, S. Ehrlich, L. Goerigk, J. Comput. Chem. 2011, 32, 1456-1465.
5. T. H. Dunning Jr. and P. J. Hay, in Modern Theoretical Chemistry, Ed. H. F. Schaefer III, Vol. 3 (Plenum, New York, 1977) 1-28.
6. V. Barone and M. Cossi, J. Phys. Chem. (A) 1998, 102, 11, 1995-2001.

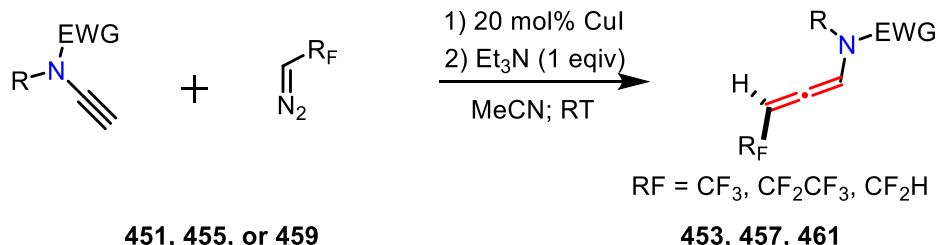
Chapter 3

Experimental procedure and characterization data for **447d**



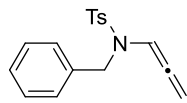
Ynamide **446d** (0.25 mmol, 1 equiv) was dissolved in dry acetonitrile (0.1 M). CuI (0.05 mmol, 0.2 equiv) was introduced and trimethylsilyldiazomethane (0.27 mmol, 2M in Et₂O, 1.1 equiv) was added dropwise. The reaction mixture was stirred at room temperature during 3h. After disappearance of starting material (indicated by TLC) a solution of TBAF (0.25 mmol, 1M in THF, 1 equiv) was added dropwise at 0°C. The reaction mixture was stirred for another 30 minutes. The reaction mixture was quenched by water, extracted two times with CH₂Cl₂ and Et₂O. The organic layers was washed with saturated NaCl solution. The organic layers was dried over Na₂SO₄, filtered and evaporated under reduce pressure. The crude material was purified by column chromatography on silica gel using a mixture petroleum ether/EtOAc, as eluent to afford the desired product **447d**

Experimental procedure and characterization data for **453**, **457**, **461**



Ynamide (0.21 mmol, 1 equiv) was dissolved in dry acetonitrile (0.1 M). CuI (0.04 mmol, 0.2 equiv) and trimethylamine (0.05 mmol, 1 equiv) was added and diazomethane derivative (0.62 mmol, 2M in Et₂O, 3 equiv) was added dropwise and the reaction was stirred for 3 h. The mixture was quenched by water, extracted two times with CH₂Cl₂. The organic layers was washed with saturated NaCl solution, dried over Na₂SO₄, filtered and evaporated under reduce pressure. The crude material was purified by column chromatography on silica gel using a mixture petroleum ether/EtOAc, as eluent to afford the desired product **453**, **457**, **461**

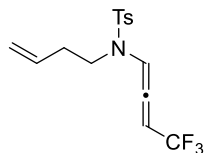
Compound 447d *N*-benzyl-4-methyl-*N*-(propa-1,2-dien-1-yl)benzenesulfonamide¹⁸⁹



C₁₇H₁₇NO₂S
MW : 299.388 g.mol⁻¹
Colorless oil
Yield : 66%

¹H NMR (300 MHz, CDCl₃): δ = 7.68 (d, *J* = 8.3 Hz, 2H), 7.30 – 7.20 (m, 7H), 6.79 (t, *J* = 6.2 Hz, 1H), 5.10 (d, *J* = 6.2 Hz, 2H), 4.26 (s, 2H), 2.41 (s, 3H) ppm.

Compound 453a *N*-(but-3-en-1-yl)-4-methyl-*N*-(4,4,4-trifluorobuta-1,2-dien-1-yl)benzenesulfonamide



C₁₅H₁₆F₃NO₂S
MW : 332.09 g.mol⁻¹
colorless oil
Yield: 95%

¹H NMR (500 MHz, C₆D₆): δ = 7.52 (d, *J* = 8.1 Hz, 2H), 7.31 – 7.29 (m, 1H), 6.70 (d, *J* = 8.0 Hz, 2H), 5.57 – 5.48 (m, 1H), 5.35 (p, *J* = 5.6 Hz, 1H), 5.00 – 4.85 (m, 2H), 3.07 – 2.95 (m, 2H), 2.24 – 2.07 (m, 2H), 1.82 (s, 3H) ppm.

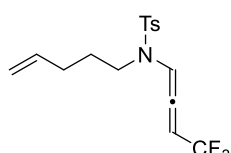
¹³C NMR (125 MHz, C₆D₆) δ = 198.5 (q, *J* = 5.9 Hz), 143.7, 135.8, 133.6, 129.6 (×2), 127.0 (×2), 121.6 (q, *J* = 270.0 Hz), 117.1, 107.1, 95.7 (q, *J* = 38.7 Hz), 46.5, 31.5, 20.7 ppm.

¹⁹F NMR (282 MHz, C₆D₆) δ = -62.18 ppm.

HRMS (ESI-TOF) m/z: [M+H]⁺ calcd for C₁₅H₁₇F₃NO₂S 332.0936; Found 332.0927.

IR (neat): ν = 3069, 3047, 2931, 1265, 1126 cm⁻¹

Compound 453b 4-methyl-*N*-(pent-4-en-1-yl)-*N*-(4,4,4-trifluorobuta-1,2-dien-1-yl)benzenesulfonamide



C₁₆H₁₈F₃NO₂S
MW : 345.10 g.mol⁻¹
colorless oil
Yield: 90%

¹H NMR (500 MHz, C₆D₆): δ = 7.55 (d, *J* = 8.3 Hz, 2H), 7.33 – 7.30 (m, 1H), 6.73 (d, *J* = 8.0 Hz, 2H), 5.65 – 5.57 (m, 1H), 5.36 (p, *J* = 5.6 Hz, 1H), 4.97 – 4.89 (m, 2H), 3.02 – 2.87 (m, 2H), 1.96 – 1.76 (m, 5H), 1.58 – 1.39 (m, 2H) ppm.

¹³C NMR (125 MHz, C₆D₆) δ = 198.5 (q, *J* = 5.9 Hz), 143.7, 137.0, 135.7, 129.6 (×2), 127.0 (×2), 121.7 (q, *J* = 270.0 Hz), 115.2, 107.2, 95.6 (q, *J* = 38.7 Hz), 46.6, 30.5, 26.1, 20.7 ppm.

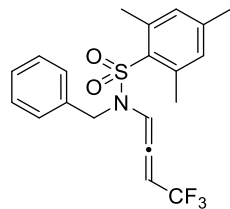
¹⁹F NMR (282 MHz, C₆D₆) δ = -62.21 ppm.

HRMS (ESI-TOF) m/z: [M+Na]⁺ calcd for C₁₆H₁₈F₃NNaO₂S 368.0908; Found 368.0903.

¹⁸⁹ R. Blieck, L. Perego, I. Ciofini, L. Grimaud, M. Taillefer, F. Monnier, *Synthesis* **2019**, *51*, 1225–1234.

IR (neat): $\nu = 3046, 2931, 2868, 1977, 1642, 1123 \text{ cm}^{-1}$

Compound 453c *N*-benzyl-2,4,6-trimethyl-*N*-(4,4,4-trifluorobuta-1,2-dien-1-yl)benzenesulfonamide



C₂₀H₂₀F₃NO₂S
MW : 395.12 g.mol⁻¹
colorless oil
Yield: 85%

¹H NMR (500 MHz, C₆D₆): $\delta = 7.40 - 7.37$ (m, 1H), $7.17 - 7.17$ (m, 2H), 7.04 (t, $J = 7.5$ Hz, 2H), 6.99 (t, $J = 7.3$ Hz, 1H), 6.51 (s, 2H), 5.21 (p, $J = 5.6$ Hz, 1H), 4.20 (d, $J = 16.0$ Hz, 1H), 3.96 (d, $J = 16.0$ Hz, 1H), 2.52 (s, 6H), 1.86 (s, 3H) ppm.

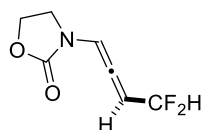
¹³C NMR (125 MHz, C₆D₆) $\delta = 197.8$ (q, $J = 6.0$ Hz), $143.0, 140.1$ ($\times 2$), $135.0, 132.5, 132.2$ ($\times 2$), 128.4 ($\times 2$), $127.6, 127.5$ ($\times 2$), 121.6 (q, $J = 270.0$ Hz), $106.8, 95.5$ (q, $J = 38.7$ Hz), $50.1, 22.9$ ($\times 2$), 20.3 ppm.

¹⁹F NMR (282 MHz, C₆D₆) $\delta = -62.69$ ppm.

HRMS (ESI-TOF) m/z: [M+Na]⁺ calcd for C₂₀H₂₀F₃NNaO₂S 418.1072; Found 418.1059.

IR (neat): $\nu = 3034, 2979, 2941, 1976, 1452, 1343, 1124 \text{ cm}^{-1}$

Compound 457a 3-(4,4-difluorobuta-1,2-dien-1-yl)oxazolidin-2-one



C₇H₇F₂NO₂
MW : 175.13 g.mol⁻¹
Colorless oil
Yield : 65%

¹H NMR (C₆D₆, 500 MHz): $\delta = 7.01$ (q, $J = 5.5$ Hz, 1H), $5.82 - 5.50$ (m, 2H), $3.27 - 3.14$ (m, 2H), $2.29 - 2.14$ (m, 2H) ppm.

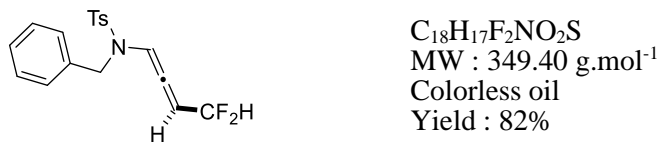
¹³C NMR (C₆D₆, 126 MHz): $\delta = 199.4, 199.3, 199.2, 154.2, 114.9, 113.0, 111.1, 101.6, 99.0, 98.8, 98.6, 61.4, 41.7$ ppm.

¹⁹F NMR (C C₆D₆, 471 MHz): $\delta = -109.79, -109.80$ ppm.

IR (neat): $\nu = 2981, 2931, 2858, 1738, 1677, 1580, 1135, 1099, 1046, 807, 518 \text{ cm}^{-1}$

HRMS (ESI-TOF) m/z: [M+H]⁺ calcd. for C₇H₇F₂NO₂ 176.0518; Found 176.0507.

Compound 457b *N*-benzyl-*N*-(4,4-difluorobuta-1,2-dien-1-yl)-4-methylbenzenesulfonamide



¹H NMR (CDCl₃, 500 MHz): δ = 7.76 (d, J = 8.3 Hz, 2H), 7.39 (d, J = 8.0 Hz, 2H), 7.35 – 7.26 (m, 5H), 7.23 (dd, J = 11.0, 5.7 Hz, 1H), 5.68 (p, J = 6.0 Hz, 1H), 5.39 (td, J = 56.0, 6.0 Hz, 1H), 4.48 (d, J = 15.1 Hz, 1H), 4.18 (d, J = 15.1 Hz, 1H), 2.49 (s, 3H) ppm.

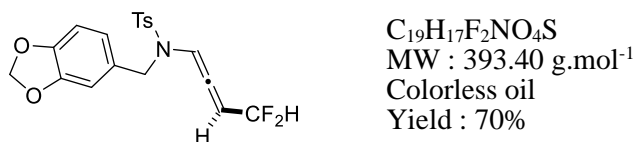
¹³C NMR (CDCl₃, 126 MHz): δ = 199.8, 199.7, 199.6, 144.4, 135.0, 134.9, 130.0, 128.5, 127.8, 127.7, 127.2, 115.0, 113.1, 111.2, 104.3, 104.3, 99.6, 99.4, 99.1, 50.6, 21.7 ppm.

¹⁹F NMR (CDCl₃, 471 MHz): δ = -108.91, -109.55, -110.10, -110.74 ppm.

IR (neat): ν = 3278, 3032, 1598, 1455, 1324, 1156, 1092, 812, 698, 663, 551 cm⁻¹

HRMS (ESI-TOF) m/z: [M+Na]⁺ calcd. for C₁₈H₁₇F₂NNaO₂S 372.0846; Found 372.0830.

Compound 457c (benzo[d][1,3]dioxol-5-ylmethyl)-*N*-(4,4-difluorobuta-1,2-dien-1-yl)-4-methylbenzenesulfonamide



¹H NMR (CDCl₃, 500 MHz): δ = 7.74 (d, J = 8.2 Hz, 2H), 7.38 (d, J = 8.2 Hz, 2H), 7.21 (dd, J = 11.1, 5.6 Hz, 1H), 6.84 (d, J = 0.9 Hz, 1H), 6.79 – 6.65 (m, 2H), 5.97 (d, J = 2.4 Hz, 2H), 5.79 – 5.45 (m, 2H), 4.33 (d, J = 14.9 Hz, 1H), 4.11 (d, J = 14.9 Hz, 1H), 2.49 (s, 3H) ppm.

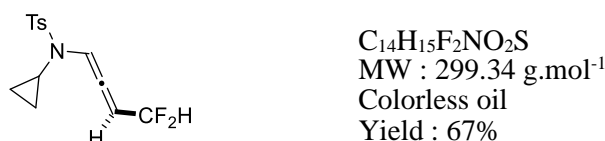
¹³C NMR (CDCl₃, 126 MHz): δ = 199.7, 199.6, 199.5, 148.0, 147.2, 144.4, 135.0, 130.0, 128.6, 127.2, 121.5, 115.1, 113.2, 111.3, 108.2, 108.0, 104.3, 101.2, 99.5, 99.3, 99.1, 50.4, 21.7 ppm.

¹⁹F NMR (CDCl₃, 282 MHz): δ = -108.65, -109.72, -109.98, -111.05, -116.54 ppm.

IR (neat): ν = 3280, 2922, 1597, 1454, 1324, 1155, 1091, 812, 697, 662, 550 cm⁻¹

HRMS (ESI-TOF) m/z: [M+Na]⁺ calcd. for C₁₉H₁₇F₂NNaO₄S 416.0744; Found 416.0748.

Compound 457d *N*-cyclopropyl-*N*-(4,4-difluorobuta-1,2-dien-1-yl)-4-methylbenzenesulfonamide



¹H NMR (CDCl₃, 500 MHz): δ = 7.76 (d, J = 8.3 Hz, 2H), 7.38 (d, J = 8.0 Hz, 2H), 7.19 (q, J = 5.5 Hz, 1H), 6.12 – 5.83 (m, 2H), 2.48 (s, 3H), 1.74 (tt, J = 6.9, 3.6 Hz, 1H), 1.06 (tdt, J = 6.6, 4.8, 3.5 Hz, 1H), 0.95 – 0.90 (m, 1H), 0.81 – 0.71 (m, 2H) ppm.

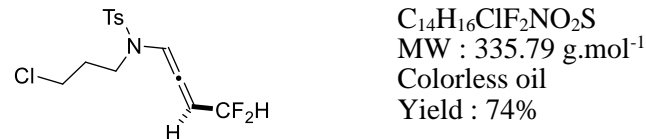
¹³C NMR (CDCl₃, 126 MHz): δ = 200.2, 200.1, 200.0, 144.4, 133.4, 129.8, 127.7, 115.2, 113.3, 111.4, 107.0, 98.3, 98.1, 97.8, 28.9, 21.6, 8.1, 7.6 ppm.

¹⁹F NMR (CDCl₃, 471 MHz): δ = -109.86 ppm.

IR (neat): ν = 3283, 3014, 2925, 2853, 1705, 1597, 1364, 1159, 1091, 877, 665, 550 cm⁻¹

HRMS (ESI-TOF) m/z: [M+H]⁺ calcd. for C₁₄H₁₅F₂NO₂S 300.0864; Found 300.0884.

Compound 457e *N*-(3-chloropropyl)-*N*-(4,4-difluorobuta-1,2-dien-1-yl)-4-methylbenzenesulfonamide



¹H NMR (CDCl₃, 300 MHz): δ = 7.72 (d, *J* = 8.3 Hz, 2H), 7.37 (d, *J* = 8.0 Hz, 2H), 7.31 – 7.25 (m, 1H), 6.24 – 5.83 (m, 2H), 3.58 (t, *J* = 6.3 Hz, 2H), 3.28 (td, *J* = 6.7, 1.4 Hz, 2H), 2.47 (s, 3H), 2.08 – 1.98 (m, 2H) ppm.

¹³C NMR (CDCl₃, 126 MHz): δ = 198.2, 198.1, 198.0, 144.5, 134.7, 130.2, 130.0, 127.3, 127.2, 114.6, 112.7, 110.7, 105.2, 100.0, 99.8, 99.6, 44.5, 41.8, 30.5, 21.6 ppm.

¹⁹F NMR (CDCl₃, 282 MHz): δ = -110.35, -110.45.

IR (neat): ν = 2984, 2941, 2910, 1736, 1447, 1372, 1234, 1043, 846, 607cm⁻¹

HRMS (ESI-TOF) m/z: [M+H]⁺ calcd. for C₁₄H₁₇ClF₂NO₂S 336.0631; Found 336.0620.

Compound 457f *N*-(2-(1,3-dioxolan-2-yl)ethyl)-*N*-(4,4-difluorobuta-1,2-dien-1-yl)-4-methylbenzenesulfonamide



¹H NMR (CDCl₃, 300 MHz): δ = 7.72 (d, *J* = 8.3 Hz, 2H), 7.39 – 7.31 (m, 2H), 7.28 – 7.21 (m, 1H), 6.23 – 5.81 (m, 2H), 4.89 (t, *J* = 4.6 Hz, 1H), 3.99 – 3.78 (m, 4H), 3.30 (td, *J* = 7.0, 3.6 Hz, 2H), 2.46 (s, 3H), 1.90 (ddd, *J* = 8.1, 7.0, 4.6 Hz, 2H) ppm.

¹³C NMR (CDCl₃, 126 MHz): δ = 198.4, 144.3, 135.1, 130.0, 127.2, 114.8, 112.9, 111.0, 104.9, 102.0, 99.8, 99.6, 99.4, 65.0, 65.0, 42.3, 31.7, 21.6 ppm.

¹⁹F NMR (CDCl₃, 282 MHz): δ = -110.22, -110.25 ppm.

IR (neat): ν = 3364, 2958, 2890, 1732, 1597, 1328, 1159, 815, 666, 550 cm⁻¹

HRMS (ESI-TOF) m/z: [M+H]⁺ calcd. for C₁₆H₉F₂NO₄S 360.1076; Found 360.1064.

Compound 457g *N*-(4,4-difluorobuta-1,2-dien-1-yl)-*N*-(4-((*N*-(*S*)-4,4-difluorobuta-1,2-dien-1-yl)-4-methylphenyl)sulfonamido)butyl)-4-methylbenzenesulfonamide



¹H NMR (C₆D₆, 300 MHz): δ 7.64 (dd, J = 8.3, 1.4 Hz, 2H), 7.18 (d, J = 5.6 Hz, 1H), 6.78 (d, J = 8.0 Hz, 2H), 5.80 – 5.34 (m, 2H), 3.07 (s, 2H), 1.85 (s, 3H), 1.46 (d, J = 4.9 Hz, 2H) ppm.

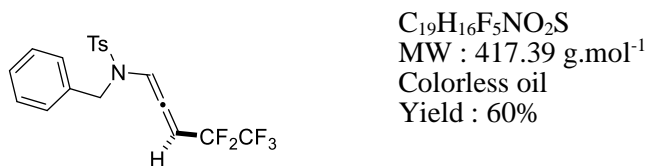
¹³C NMR (C₆D₆, 126 MHz): δ = 198.5, 198.5, 198.4, 198.4, 198.3, 198.3, 143.6, 135.6, 135.5, 129.6, 128.0, 127.1, 127.1, 114.9, 114.8, 113.0, 112.9, 111.1, 111.0, 104.9, 99.2, 99.0, 98.8, 45.9, 45.9, 23.5, 23.5, 20.8 ppm.

¹⁹F NMR (C₆D₆, 282 MHz): δ = -108.60, -108.68, -109.66, -109.74, -109.87, -109.93, -110.93, -110.98 ppm.

IR (neat): ν = 3049, 2926, 2872, 1597, 1435, 1349, 1164, 1087, 1021, 814, 666, 547 cm⁻¹

HRMS (ESI-TOF) m/z: [M+Na]⁺ calcd. for C₂₆H₂₈F₄N₂NaO₄S₂ 595.1319; Found 595.1316.

Compound 461a *N*-benzyl-4-methyl-*N*-(4,4,5,5,5-pentafluoropenta-1,2-dien-1-yl)benzenesulfonamide



¹H NMR (CDCl₃, 500 MHz): δ = 7.74 (d, J = 8.3 Hz, 2H), 7.48 (dd, J = 9.2, 4.4 Hz, 1H), 7.38 (d, J = 8.1 Hz, 2H), 7.30 (ddt, J = 13.1, 7.9, 4.4 Hz, 5H), 5.66 (td, J = 9.6, 5.9 Hz, 1H), 4.65 (d, J = 15.3 Hz, 1H), 3.95 (d, J = 15.3 Hz, 1H), 2.49 (s, 3H) ppm.

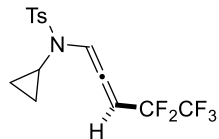
¹³C NMR (CDCl₃, 126 MHz): δ = 201.2, 201.1, 201.0, 144.6, 134.9, 134.7, 130.0, 128.5, 127.9, 127.5, 127.2, 107.0, 95.0, 94.7, 94.5, 50.8, 21.6 ppm.

¹⁹F NMR (CDCl₃, 471 MHz): δ = -84.50, -84.51, -84.51, -113.10, -113.10 ppm.

IR (neat): ν = 3281, 3033, 2924, 2852, 1598, 1455, 1328, 1204, 1093, 813, 664, 551 cm⁻¹

HRMS (ESI-TOF) m/z: [M+H]⁺ calcd. for C₁₉H₁₆F₅NO₂S 418.0895; Found 418.0870.

Compound 461b *N*-cyclopropyl-4-methyl-*N*-(4,4,5,5,5-pentafluoropenta-1,2-dien-1-yl)benzenesulfonamide



C₁₅H₁₄F₅NO₂S
MW : 367.33 g.mol⁻¹
Colorless oil
Yield : 64%

¹H NMR (C₆D₆, 500 MHz): δ = 7.63 (d, *J* = 8.2 Hz, 2H), 7.29 (dd, *J* = 9.9, 4.2 Hz, 1H), 6.78 (dd, *J* = 7.9, 4.1 Hz, 2H), 5.30 (tt, *J* = 9.8, 5.0 Hz, 1H), 1.85 (d, *J* = 3.5 Hz, 3H), 1.39 (dq, *J* = 10.2, 3.5 Hz, 1H), 1.01 – 0.94 (m, 1H), 0.75 – 0.68 (m, 1H), 0.35 (dq, *J* = 13.5, 6.3 Hz, 1H), 0.29 – 0.20 (m, 1H) ppm.

¹³C NMR (C₆D₆, 126 MHz): δ = 201.7, 201.6, 201.6, 143.9, 143.9, 133.9, 133.9, 129.4, 127.9, 127.7, 127.6, 127.5, 109.3, 92.8, 92.6, 92.4, 28.7, 20.8, 7.7, 7.5 ppm.

¹⁹F NMR (C₆D₆, 282 MHz): δ = -84.66, -84.67, -84.67, -84.67, -84.68, -84.69, -112.61, -112.62, -112.68, -112.69 ppm.

IR (neat): ν = 3295, 3053, 2925, 1598, 1365, 1199, 1110, 1019, 994, 879, 663, 550 cm⁻¹

HRMS (ESI-TOF) m/z: [M+Na]⁺ calcd. for C₁₅H₁₄F₅NNaO₂S 390.0558; Found 390.0543

Des énamides et des ynamides pour la synthèse d'hétérocycles fonctionnalisés

Résumé

Les travaux décrits dans ce manuscrit de thèse ont porté dans un premier temps sur le développement d'une réaction domino au départ de *N*-imides équipés de diénones croisées. Dans un second temps, la réactivité des ynamides vis-à-vis de composés diazo a été étudiée pour accéder d'une part à des amido-furanes difluorés et d'autre part à une nouvelle synthèse de *N*-allénamides.

Des énamides tertiaires intégrés dans des diénones croisées ont conduit à une réaction domino impliquant une cyclisation intramoléculaire sur un ion *N*-acyliminium suivie d'une réaction de Nazarov avec un stéréocontrôle total. Des diazépines comportant une cyclopentènone, sous structure de composés psychotropes ont ainsi été obtenues avec de très bon rendements.

Une addition cupro-catalysée de diazoacétone difluoré sur des ynamides a permis de mettre au point une nouvelle synthèse d'amido-furanes difluorés, des composés très prisés en chimie médicinale et en phytochimie. Ces composés ont ensuite été utilisés comme plateforme pour réaliser la synthèse d'hétérocycles plus complexes.

La réactivité particulière des ynamides vis-à-vis de composés diazo nous a permis de mettre au point une nouvelle synthèse de *N*-allénamides terminaux. En utilisant des composés diazo judicieusement fonctionnalisés, nous avons obtenus des *N*-allénamides push-pull substitués en position γ par un groupement CF_3 , CF_2H ou CF_3CF_2 .

Mots clés : ènesulfonamides tertiaires, diazépines, ynamides, furanes difluorés, *N*-allénamides, composés diazo

Résumé en anglais

The work described in this thesis manuscript focused first on the development of a domino reaction from *N*-imides equipped enamidyl vinyl ketones. Secondly, the reactivity of ynamides towards diazo compounds was studied to access, on one hand, to difluorinated amido-furans and on the other hand to a new synthesis of *N*-allenamides.

Tertiary enamides integrated into cross-conjugated dienones underwent a domino-reaction involving *N*-acyliminium ion trapping followed by a Nazarov cyclization. Psychoactive substructures *i.e.* diazepines fused with cyclopentenones were thus obtained with very good yields.

A copper-catalyzed addition of difluorinated diazoacetone to ynamides made it possible to develop a new synthesis of difluorinated amidofurans highly valued in medicinal chemistry and phytochemistry. These compounds were then used as platforms to achieve the synthesis of more complex heterocycles.

The particular reactivity of ynamides towards diazo compounds has enabled us to develop a new synthesis of terminal *N*-allenamides. By using judiciously functionalized diazo compounds, we obtained push-pull *N*-allenamides substituted in position γ by a CF_3 , CF_2H or a CF_3CF_2 moiety.

Keywords : tertiary enesulfonamides, diazepines, ynamides, difluorinated-furans, *N*-allenamides, diazo-compounds.